SYNTHETIC RECEPTORS IN MOLECULAR RECOGNITION

Edited by
Volodymyr I. Rybachenko

Donetsk 2007

Видавниче підприємство „Східний видавничий дім”
(Державне свідоцтво № ДК 697 від 30.11. 2001)
Вул. Артема 45, 83086 м. Донецьк, Україна
тел/факс (+380 62) 338-06-97, 337-04-80

Publishing house „Schidnyj wydawnyczyj dim”

ISBN 978-966-317-013-8

Contents

Preference

Molecular recognition is a one of fundamental processes in nature. It may be defined by Ball, P. in Designing the Molecular World: Chemistry at the Frontier. Princeton University Press, 1994. p. 145-185 is the "...specific recognition of (and interaction with) one molecule by another". The term molecular recognition refers to the specific interaction between two or more molecules through non covalent bonding such as including hydrogen bonding, metal coordination, hydrophobic forces, van der Waals forces, π-π interactions, and/or electrostatic effects. The host and guest involved in molecular recognition exhibit molecular complementarity. Molecular recognition plays an important role in biological systems and is observed in between receptor-ligand, antigen-antibody, DNA-protein, sugar-lectin, RNA-ribosome etc.. The molecular recognition and application of formed supermolecules will be presented here. I hope that book have very interesting review papers and helpful for not only researchers working in science, in particular in chemistry, but also for students.

Prof. V. I. Rybachenko

List of Contributors

Agnieszka Adamczyk-Woźniak
Faculty of Chemistry, Warsaw University of Technology,
Noakowskiego 3, 00-664 Warsaw, Poland

Zbigniew Brzózka
Warsaw University of Technology, Department of Analytical Chemistry,
Noakowskiego 3, 00-664 Warsaw, Poland

Alicja Filipowicz-Szymańska
Warsaw University of Technology, Department of Analytical Chemistry,
Noakowskiego 3, 00-664 Warsaw, Poland

Waldemar Iwanek
Institute of Chemistry, Pedagogical University,
Chęcińska 5, 25020 Kielce, Poland

Joanna Kurczewska
Faculty of Chemistry, A. Mickiewicz University,
Grunwaldzka 6, 60-780 Poznań, Poland

Bogusława Łęska
Faculty of Chemistry, Adam Mickiewicz University,
Grunwaldzka 6, 60-780 Poznań, Poland

Joanna Łojewska
Faculty of Chemistry, Jagiellonian University,
Ingardena 3, 30-060 Kraków, Poland

Kamilla Małek
Faculty of Chemistry, Jagiellonian University,
Ingardena 3, 30-060 Kraków, Poland

Jan Milecki
Faculty of Chemistry, A. Mickiewicz University,
Grunwaldzka 6, 60-780 Poznań, Poland

Paweł Niedziałkowski
Faculty of Chemistry, University of Gdańsk,
Sobieskiego 18/19, 80-952 Gdańsk, Poland

Izabela Nowak
Faculty of Chemistry, Adam Mickiewicz University,
Grunwaldzka 6, 60-780 Poznan, Poland

Tadeusz Ossowski
Faculty of Chemistry, University of Gdańsk,
Sobieskiego 18/19, 80-952 Gdańsk, Poland

Radosław Pankiewicz
Faculty of Chemistry, Adam Mickiewicz University,
Grunwaldzka 6, 60-780 Poznań, Poland

Leonard M. Proniewicz
Faculty of Chemistry, Jagiellonian University,
Ingardena 3, 30-060 Kraków, Poland

Grzegorz Schroeder
Faculty of Chemistry, A. Mickiewicz University,
Grunwaldzka 6, 60-780 Poznań, Poland

Andrzej Sporzyński
Faculty of Chemistry, Warsaw University of Technology,
Noakowskiego 3, 00-664 Warsaw, Poland

Mariusz Walkowiak
Institute of Non-Ferrous Metals, branch in Poznan,
Central Laboratory of Batteries and Cells,
Forteczna 12, 61-362 Poznań, Poland

Alicja Wzorek
Institute of Chemistry, Pedagogical University,
Chęcińska 5, 25020 Kielce, Poland

Dorota Zarzeczańska
Faculty of Chemistry, University of Gdańsk
Sobieskiego 18/19, 80-952 Gdańsk, Poland

Anna Żubrowska
Faculty of Chemistry, Warsaw University of Technology,
Noakowskiego 3, 00-664 Warsaw, Poland

Chapter 1

Synthesis and complexing ability of 1,4,7,10-tetraazacyclododecane derivatives

Paweł Niedziałkowski[1], Tadeusz Ossowski[1], Dorota Zarzeczańska[1], Joanna Kurczewska[2] and Grzegorz Schroeder[2]

[1]*Faculty of Chemistry, University of Gdańsk Sobieskiego 18/19, 80-952 Gdańsk, Poland*

[2]*Faculty of Chemistry, A. Mickiewicz University, Grunwaldzka 6, 60-780 Poznań, Poland*

Introduction:

Gadolinium (III) has become commonly used element in medical diagnostic in the course of a decade. The specific magnetic properties of its ion induce to use gadolinium (III) chelates as magnetic resonance imaging (MRI) contrast agents. Signal intensity in MRI usually comes from the local value of the longitudinal relaxation rate of water protons, $1/T_1$, and the transverse rate $1/T_2$. Generally, signal increases with $1/T_1$ increasing and it decreases with $1/T_2$ increasing. However, all contrast agents increase both $1/T_1$ and $1/T_2$. In case of gadolinium (III), the percentage change in longitudinal relaxation rate in tissue dominates significantly over that in transverse rate, and such agents are favored in MRI [1]. On the other hand Gd^{3+} ion itself is toxic at the concentrations used in MRI and it has to be injected as a thermodynamically and kinetically inert chelate to ensure a rapid excretion from the body and reaching a high acute intravenous tolerance [2]. It stimulates searching of such ligands that remain gadolinium chelated in the body and the chelates are excreted intact.

The first generation of contrast agents consisted of nonspecific ones that were carried by blood circulation out to tumors. New paramagnetic lanthanide chelates are

constantly being synthesized in hopes of reaching the largest possible reduction of the longitudinal proton relaxation time T_1 *in vivo* and thus the best contrast in magnetic resonance images. Contrast agents must fulfill strict requirements concerning toxicity, biodistribution, and relaxivity (relaxation rate $1/T_1$ in s^{-1} and per mmol of Gd^{3+}). The toxicity of the Gd^{3+} ion itself has been drastically reduced by encapsulating this ion into polyamino polycarboxylic cages, most of which are derived from DOTA skeletons [3], which are derivatives of 1,4,7,10-tetraazacyclododecane. Recently, a research is devoted to the synthesis of new effective chelating agents based on 1,4,7,10-tetraazacyclododecane skeleton.

Synthesis of derivatives 1,4,7,10-tetraazacyclododecane

N_4-donor macrocyclic ligand cyclen (1,4,7,10-tetraazacyclododecane) is characterized by the presence of four equivalent nitrogen atoms, which makes difficult the selective substitution of discussed cyclic polyamine. In order to eliminate that problem, protected cyclen is applied in N-alkylation reactions. The most popular protecting groups, which are easily incorporated into cyclen structure, are p-toluenesulfonyl (tosyl; Ts) [4] and butoxycarbonyl (Boc) ones [5]. Also formamide group is often used to protect nitrogen atoms in cyclen [6]. The selective substitution of cyclen by the direct alkylation is economically unfavourable because it demands the utilization of expensive cyclen in significant excess.

Some compounds form triprotected cyclen derivatives that are used in monosubstitution reaction of 1,4,7,10-tetraazacyclododecane. Nitrogen atom that doesn't participate in bounding, allows then nucleophilic attack. Therefore, different compounds are applied: chromium and molybdenum [7], phosphorus [8], boron [9] and silicon compounds [10]. Another method of selective monosubstitution is based on the bridging of adjacent nitrogen atoms [11].

In general, N-derivatization has been accomplished by following two approaches: direct derivatization and protection - derivatization - deprotection. Literature reports on mono-, bis-, and tri-derivatization by either approach are known [12]. However, bis-derivatization procedures are scarce and particular interest is given to the possibility of obtaining either symmetrical or unsymmetrical N- trans and N- cis

polyaza macrocyclic derivatives. The protection-functionalization-deprotection based methods have two disadvantages: first, the low to moderate overall yields (from 48-78%) for the final functionalized cyclen derivative and second, the harsh conditions required for the removal of some of the suggested protecting groups. Therefore, direct functionalization methods are often preferred. Luis M. De Leon- Rodriguez and his co-workers show efficient methodology to prepare di – functionalized cyclen (**1**) derivatives using several reagents commonly used in peptide synthesis – *tert*-butoxycarbonyl and benzyloxycarbonyl protecting group **Scheme 1.**

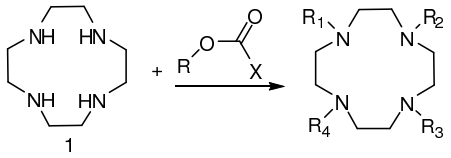

$R_1 = R_2 = R_3 = H$ $R_4 = -CO_2R'$ N – mono

$R_1 = R_3 = -H$ $R_2 = R_4 = -CO_2R'$ N1,N7 – di

$R_1 = H$ $R_2 = R_3 = R_4 = -CO_2R'$ N – tri

$R_1 = R_2 = R_3 = R_4 = -CO_2R'$ N – tetra

Scheme 1. Regioselective N-protection of cyclen. Where R=bezyl or tert-butyl and X=chloride , -OCOBn or oxysucciimide.

They have found that N1, N7 diprotected product can be obtained in nearly quantitative yields when the corresponding (oxycarbonyloxy) succiimide reagents are used.

The protonation constant (pKa values) of the four amino groups are known from literature reports to be 10.5, 9.5, 1.6, 0.8 respectively [13]. Based on the knowledge of pKa values, it has been shown that cyclen can be N1, N7 diprotected with benyloxycarbonyl group in aqueous media with good yields (88%) by keeping pH between 2 and 3 during by slow addition of chloroformates [14]. The slow addition of

the chloroformate reagent is inconvenient, also this procedure is limited to non-acid labile protecting groups as the reaction is run in the fairy acid solution.

The X ray studies on cyclen show that it has two amino groups with freely available pair of electrons and therefore the addition of 2 equiv. of chloroformate reagent should give a N1, N7 diprotected product. Furthermore, if one or both of the non protected amino groups N4, N 10 are basic enough then the diprotected cyclen hydrochloride should be formed and precipitated from the reaction mixture in non polar solvent.

The good example of application of protection/functionalization/deproteciton method was described by J. Yoo et al. [15], an efficient synthetic way for different N-substituted cyclen isomers (**Scheme 2**). In general, cyclen's nitrogens were protected regioselectively. Then such species were reacted with 4-(*tert*-butyl)benzyl bromide to give the intermediate alkylated products and final products were obtained after deprotection step. A tri-protected cyclen derivative was synthesized in reaction with chloral hydrate. Then triformylcyclen was reacted with 4-(*tert*-butyl)benzyl bromide to give mono-alkylated intermediated product. Formyl groups were removed in acidic conditions. Afterwards *i*Pr$_2$NEt was applied to introduce *tert*-butyl bromoacetate and *tert*-butyl groups were deprotected by hydrochloric acid to give tri-acetate DO3A derivative. Disubstituted cyclen isomers (1,4- and 1,7-) were obtained using protecting groups such as diethyl oxalate and benzyl chloroformate to give cyclenoxamide and 1,7-dibenzyloxycarbonyl-cyclen. Finally, *cis* and *trans*-DO2A derivatives were prepared. A synthesis of trialkylated cyclen derivatives was more sophisticated. First, three nitrogens of cyclen were protected by the same group (formyl group), secondly all four nitrogens were protected by another group (benzyl carbamate group) which led to mono-protected cyclen – mono-*N*-Cbz-cyclen. Further synthetic steps, based on the same strategy as previously described, including 1st alkylation/deprotection/2nd alkylation/deprotection led to DO1A derivative.

The reaction with di *tert*-butylcarbonate gives the N-tri-protected product in high yield [16]. This reaction is poorly regioselective, yielding a mixture of N1, N7-di-, N-tri- and N-tetra protected products. This interesting difference in the observed regioselectivity is likely due to the intermolecular steric effect inherent in the

protecting group. This regioselective method for preparation can be useful for the synthesis of new class of cyclen derivatives which can be used in preparation of new compounds selectively substituted in position N1, N7 [12] **Scheme 3.**

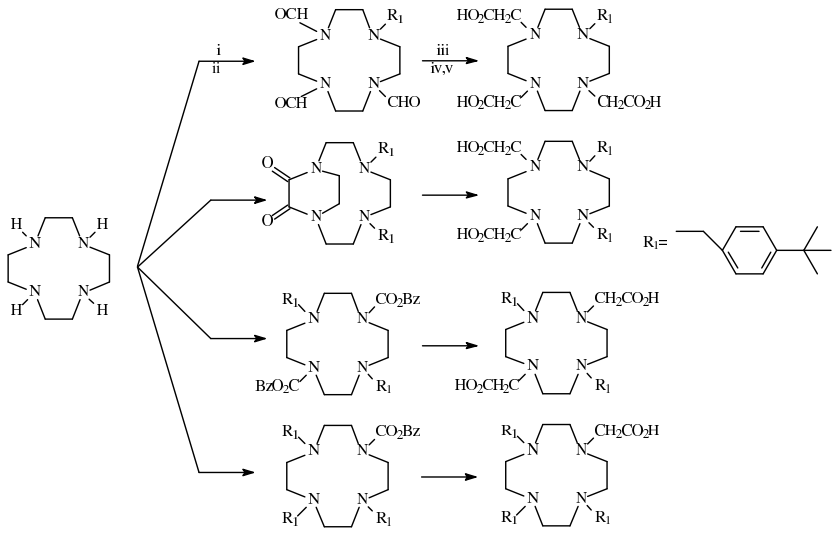

Scheme 2. A strategy of regioselective protection (i)/1st alkylation (ii)/deprotection(iii)/ 2nd alkylation (iv).

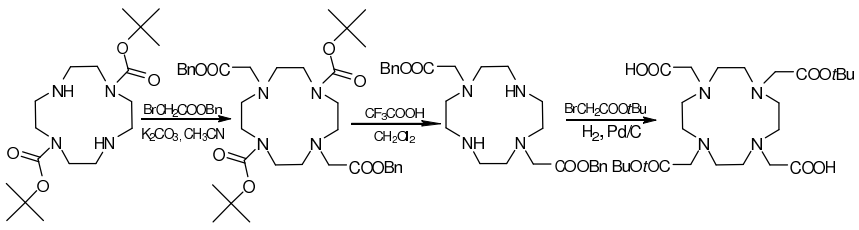

Scheme 3. Synthesis of cyclen derivatives.

A convenient procedure for directly including *tert*-butoxycarbonylmethyl groups to the two neighboring N-substituted positions of cyclen in high yield and with

excellent regioselectivity was described by Cong Li and Wing-Tak Wong [17]. Previously Kruper found that the regioselectivity of the alkylation of polyazamacrocycles was dependent on both the steric hindrance of electrophiles and solvent systems [18], so for this reason, the *tert*-butyl bromoacetate was used by Cong Li and Wing-Tak Wong to react with cyclen in the ratio 2 : 1 in the different conditions **Tabele 1**. At room temperature in the presence of 10 equiv of triethylamine, pyridine, or five equivalents of K_2CO_3 at room temperature from 6 to 8 h to obtain (**2**).

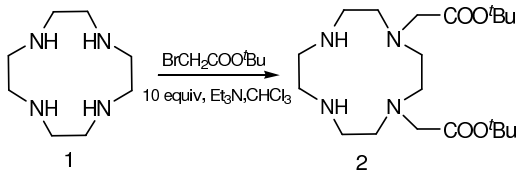

Scheme 4. Synthesis of 1,4-Bis(tert-butoxycarbonylmethyl)-1,4,7,10-tetraazacyclododecane.

Table 1.

entry	conditions	base	Yield %			1,4/1,7 bis substituted cyclen *
			tris	bis	mono	
1	$CHCl_3$	free	14	55	~8	>99*
2	$CHCl_3$	pyridine	11	63	~5	>99*
3	$CHCl_3$	K_2CO_3	15	57	~6	>99*
4	$CHCl_3$	triethylamine	6	84	~2	>99*
5	DMF	triethylamine	13	61	~8	4.3
6	MeOH	triethylamine	23	46	~7	4.2

- 1,7-Bis(*tert*butoxycarbonylmethyl) cyclen was not detected

Synthesis of Gd (III) complexes based on 1,4,7,10-tetraazacyclododecane.

Derivatives of 1,4,7,10-tetraazacyclododecane have also attracted interest because of the stability of their lanthanide complexes and the potential use as MRI agents [19].

The current generation of contrast argents is based predominantly on amino polyacetic acid chelates of Gd (III) (**3-5)** and function by promoting the relaxivity of protons on solvating water. Although magnetic resonance imaging (MRI) was initially envisioned as completely noninvasive technique, intravenously administered paramagnetic contrast agent (PCAs) can improve the overall quality and detail of images and allow for the unambiguous identification of pathologies that would otherwise be undetected. Numerous reports demonstrate how contrast enhanced magnetic resonance imaging (CE-MR) images readily indicate the presence of lesions, tumors, and defects that are unobserved by conventional MRI technique [20].

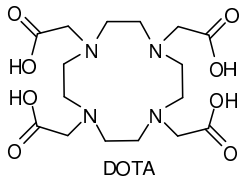

DOTA
3

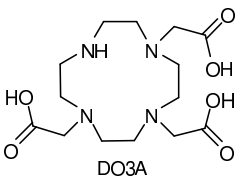

DO3A
4

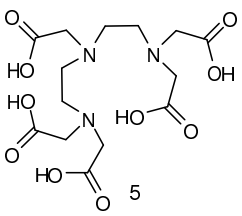

5

Ideally, ligand that posses substantial liophilic character should serve as more efficient carriers for the transport of the paramagnetic gadolinium ion across cell membranes. Increased hydrophobicity of the ligand lead to plasma protein binding and some degree of hepatobinary excretion, thereby creating the potential for liver targeting [21].

William C. Baker and his co-workers [21] reported new synthesis methodology of tetraazacyclododecane derivatives, which allows selective monoalkylation of cyclen using slight excess of alkyl halide in excellent yield. They have prepared a series of new lipophilic Gd (III) complexes (**Scheme 5**) for use as paramagnetic contrast argents (PCAs) and reported that the lipophicity could be increased by substituting one of the carboxylate arms of DOTA (1). This synthesis of compounds with varying lengths of

alkyl side chains has resulted in the creation of potential paramagnetic contrast argent with a tunable lipophilicity (**Table 2**).

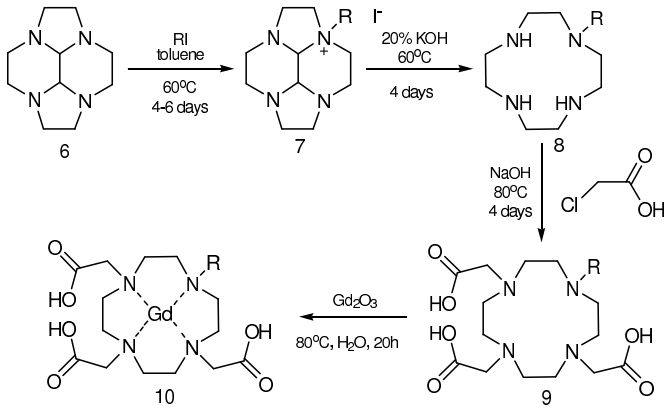

Scheme 5. Synthesis of cyclen comlex.

Table 2. Synthesis of alkylated DO3A analogues (% yield).

R	7	8	9	10
C_2H_5	92	92	88	100
C_3H_7	91	95	81	100
C_4H_9	84	100	87	100
C_5H_{11}	76	100	78	100
C_6H_{13}	79	84	83	100
C_8H_{17}	77	79	90	100
$C_{10}H_{21}$	72	75	86	100
$C_{12}H_{25}$	85	82	89	100
$C_{14}H_{29}$	94	85	80	100
$C_{16}H_{33}$	74	84	77	100
$C_{18}H_{37}$	77	78	75	100
C_2H_2	94	0	-	-

Lowe et al. employed a toluene sulfonamide as pH labile lightning group in a Eu and Gd complexes of the (DO3A) (**11**) chelate [22], as the pH of a solution is

reduced, the sulfonamide becomes protonated and dissociates from a metal center. These authors also reported that careful consideration must be given to the ligating ability and pKa labile ligand to observe this effect.

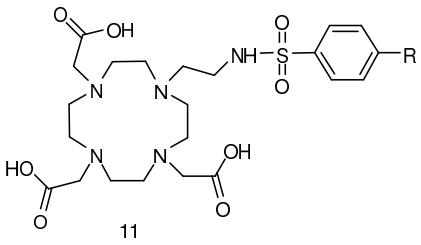

11

R= OMe

R= Me

R= CF_3

Woods et al. observed a similar pH-sensitive dissociation in complexes with one

p- nitrophenolic ligating group [23] in derivatives of cyclen. The results of these studies are performed on the lanthanides (III) (Gd, Ln, Dy, Tb) complexes of two ligands, the triacetate (NP-DO3A) (**12**) and triamide (NP-DO3AM) (**13**). The synthesis of ligand (NP-DO3A) and (NP-DO3AM) was synthesized according to route shown on **Scheme 6.** For Gd(NP-DO3A) complex the pH range over which this pendant arm dissociates from the central lanthanide ion renders it ideal as a basic of pH responsive contrast media for MRI. Substitution of amide pendant arms for acetates has several deleterious effects on the complex. The reduced electron-donating capacity of the amide ligathing groups renders the central lanthanide ion too electron deficient to release the nitrophenol. In consequence, complex of Gd (NP-DO3AM) becomes protonated at lower pH.

Aime et al. focused on some ligands for lanthanide ions that were based on H3DO3A structure [24] and were bearing one N-sulfonylacetamide arm (R). Such systems were obtained following the pathway outlined in the **Scheme 7.** The Gd^{3+} complexes were prepared by addition of gadolinium chloride to a ligand solution and

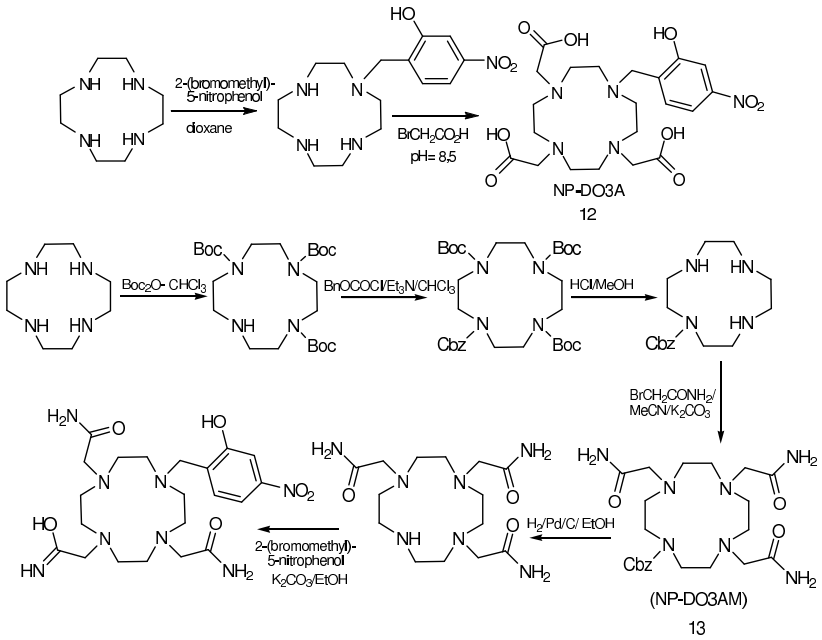

Scheme 6. Synthesis of ligand (NP-DO3A) and (NP-DO3AM).

monitored by measuring the solvent proton relaxation rate. They synthesized such systems that potentially could interact with serum protein – HSA (human serum albumin). It is well known, that the higher relaxation rates the better MRI contrast agent is. The increased relaxation rates could be obtained by increasing the rotational correlation time of Gd^{3+} complexes, which is possible due to binding of Gd^{3+} chelates to macromolecules like HSA. Moreover, strong interaction between contrast agent and HSA contributes in longer resistance lifetime in the bloodstream.

Shin Aoki [25] and co-workers synthesized and characterized doubly functionalized cyclen with three carbamoylmethyl groups and one dansylaminoethyl to design useful fluorescent sensors for La^{3+} and other relevant M^{3+}. The compound (**14**) with incorporated three carbamoylmethyl pendants was synthesized as show in **Scheme 8**. The three carbamoyl pendants affect the microenvironment surrounding the fluorescent dansyl pendant arm.

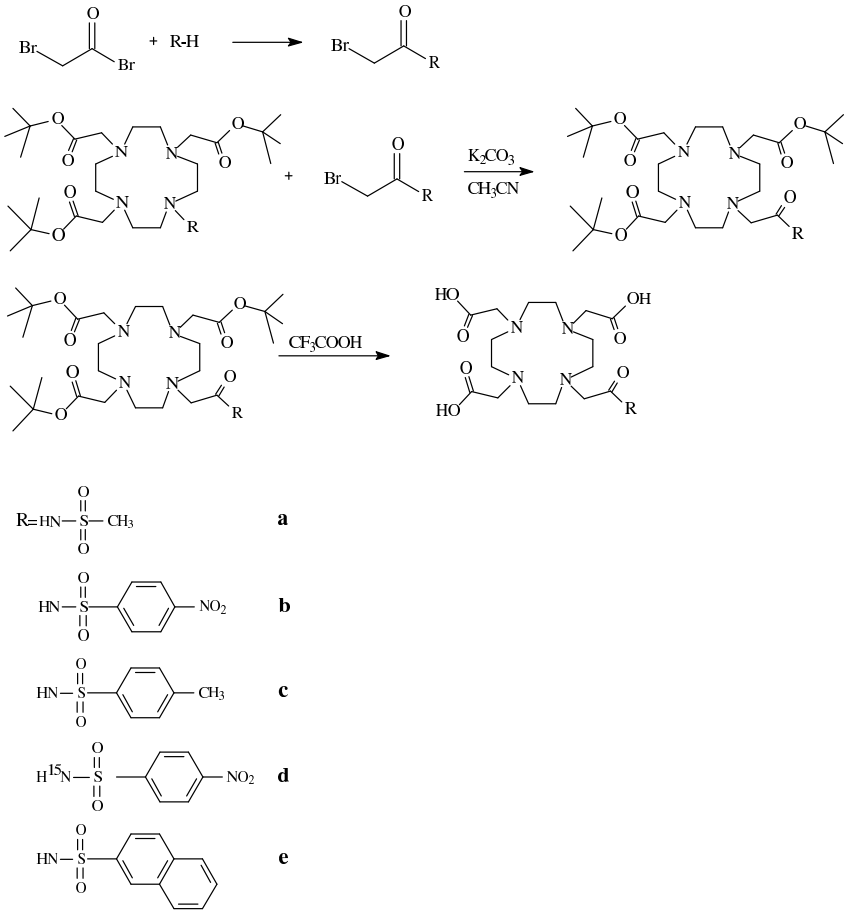

Scheme 7. Synthesis of N-sulfonylacetamide derivatives of H4DOTA.

The double functionalization of a cyclen with a dansyl group and three carbamoylmethyl moieties, **14**, dramatically expanded the fluorescence behaviors of a cyclen in comparison with a cyclen without carbamoylmethyl groups. The three-carbamoyl functionalization provided the hydrogenbonding donors to facilitate the nearby dansyl deprotonation to accompany strong fluorescent emission in the excited state **Scheme 9**.

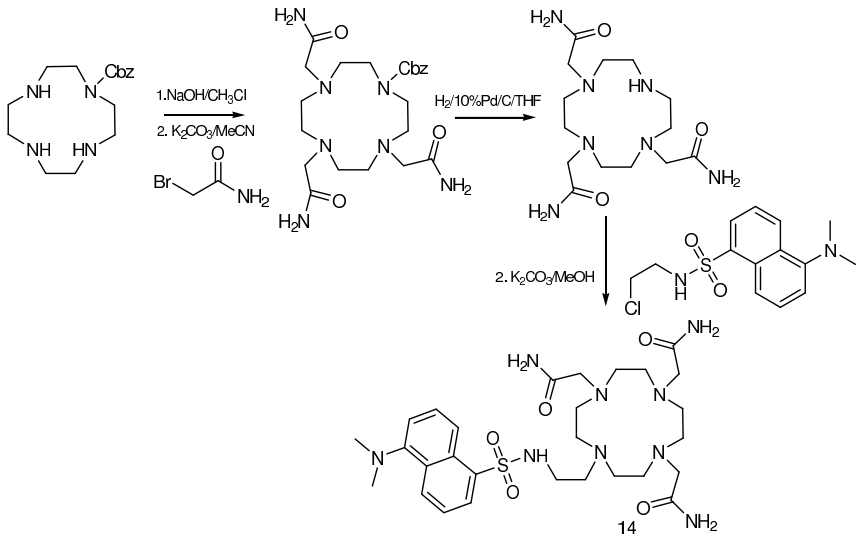

Scheme 8. Synthesis of cyclen with three carbamoylmethyl groups and one dansylaminoethyl.

The appended three carbamoyls stabilized yttrium(III)- and lanthanum(III)-cyclen complexes to permit selective and efficient signaling from the deprotonated dansyl group. Cyclen derivatives such as **14** may be a convenient and selective sensor for qualitative and quantitative assays of micromolar concentrations of Y^{3+} and La^{3+} ions in water solutions. This compound could be useful in radioimmunotherapy [26].

The application of dansyl unit in macrocyclic polyamine derivatives is quite common. However the number of Zn^{2+} selective fluorophores is small compared to those for other important divalent ions. Such ligand, containing one dansylamidoethyl pendant arm, was synthesized by Kimura and co-workers [27]. They used dioxocyclen as starting material and final product was obtained after several steps in low yield (~17 %), **Scheme 10**. In the consequence of mentioned reason, Xue et al. searched for such dansylamidoethyl polyamine derivatives that would be easily synthesized in high yield. After all they elaboreted one-step procedure for macrocyclic polyamines containing two dansylamidoethyl side arms [28]. This strategy is based on ring-

opening of N-dansyl aziridine (**Scheme 11**). The obtained macrocyclic system is potential zinc fluoroionophore.

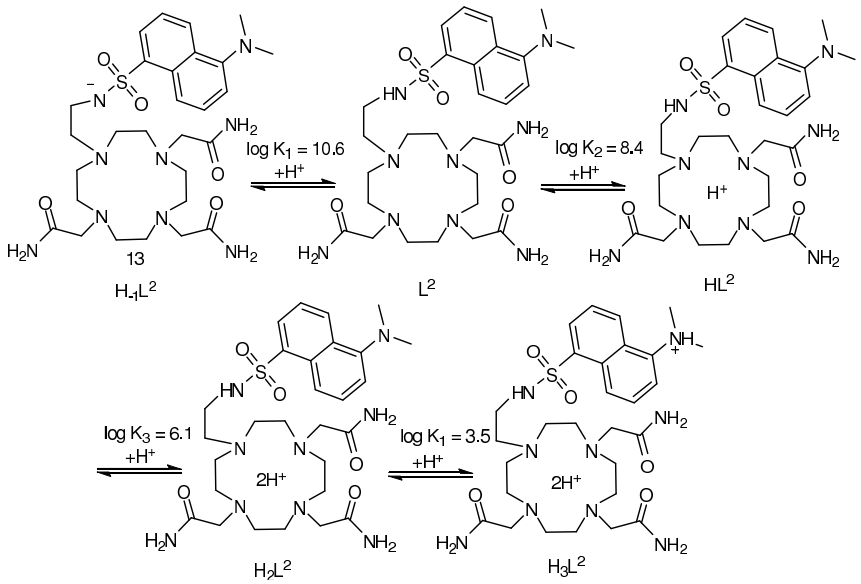

Scheme 9. The assignment of the four protonation.

Another two-component ligand system (**15**) containing 1,4,7,10-tetraazacyclododecane-1,4,7-triacetic acid (DO3A) as the hosting unit for the lanthanide cations and an appended asymmetrically functionalized 1,10-phenanthroline as the chromophore was synthesized by Silvio Quici et. al [29], **Scheme 12.** (DO3A) is the thermodynamic and kinetic stable Ln-chelating subunit which in water coordinate lanthanide cations with log K_{ML} > 20 [30]. In complexes of ligand **(15)** with lanthanide ions, the phenanthroline subunit directly participates to the coordination of the metal ion. Furthermore, the rigidity and spatial arrangement of this chromophore prevent the access of any water molecule into the first coordination sphere of the metal ion. This feature has been exploited to achieve Eu^{3+} and Tb^{3+} complexes, which are characterized by high luminescence efficiencies in water.

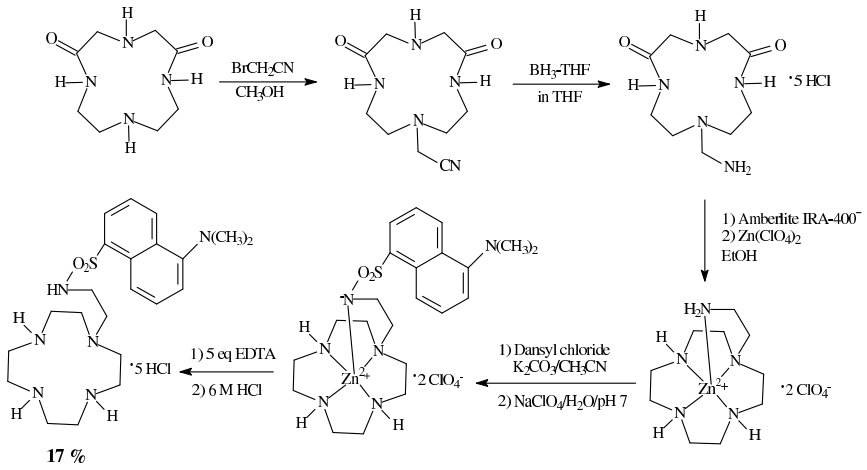

Scheme 10. Synthesis of monodansylamidoethylcyclen.

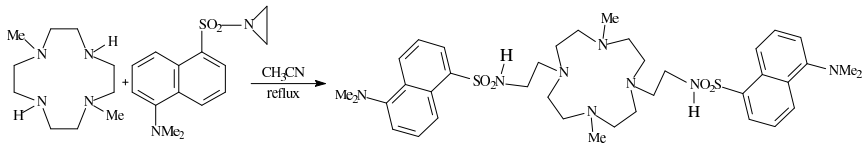

Scheme 11. Synthesis of cyclen derivative with two dansylamidoethyl side arms.

Paris [31] showed new class of tetraazacyclododecane unit substituted by three acetate arms and one by 6-hydroxy-5,6-dihydro-1,10-phenanthroline group (PhenHDO3A) **16.** This ligand was specially designed to obtain highly stable heteropolymetallic assemblies. (PhenHDO3A) has been prepared starting from phenanthroline epoxide and either a triprotected tetraazacyclododecane or tert-butyl triester of N,N',N''-tetraazacyclododecanetriacetic acid, **Scheme 13**.

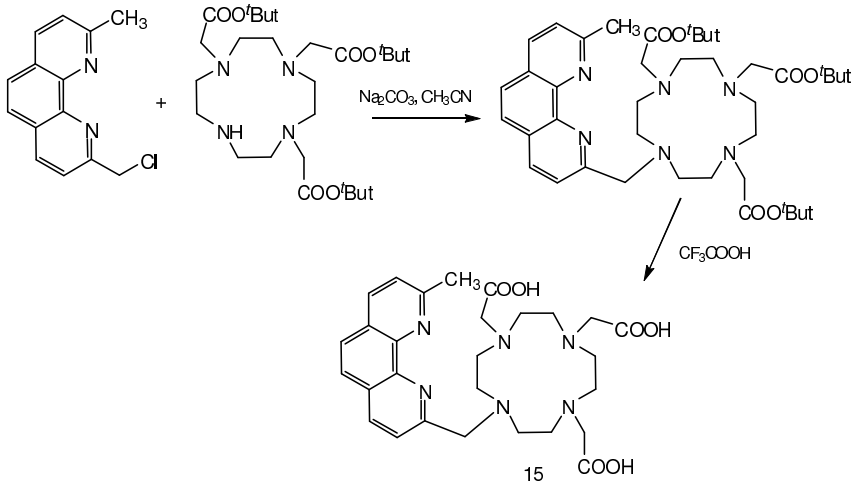

Scheme 12. Synthesis of (DO3A) and 1,10-phenanthroline derivatives.

PhenHDO3A **16** forms kinetically stable lanthanide complexes. The alcohol group of the dihydro-phenanthroline unit remains coordinated to the encapsulated metal ion despite the steric crowding brought about by this group. Furthermore these complexes are monohydrated, what is shown by luminescence lifetime measurements on EuPhenHDO3A solutions. The complex GdPhenHDO3A is available for the spontaneous formation of highly stable tris complexes with the Fe^{2+} and Ni^{2+} ions. It is multimetallic structures that are formed by the selfassociation process illustrated in **Scheme 14.**

Davide Maffeo, J.A.Gareth Williams [32] show synthesis of new tetraazamacrocylic ligands in which one of the four nitrogens bears an 8-benzyloxyquinoline group, bound either via a simple methylene unit (-CH_2-) (**17**), or through amide linker (-$CH_2C(O)N(Me)CH_2$-) (**18**), in both cases at the 2-position is the chromophore. The other three nitrogens of the macrocycle are functionalized with

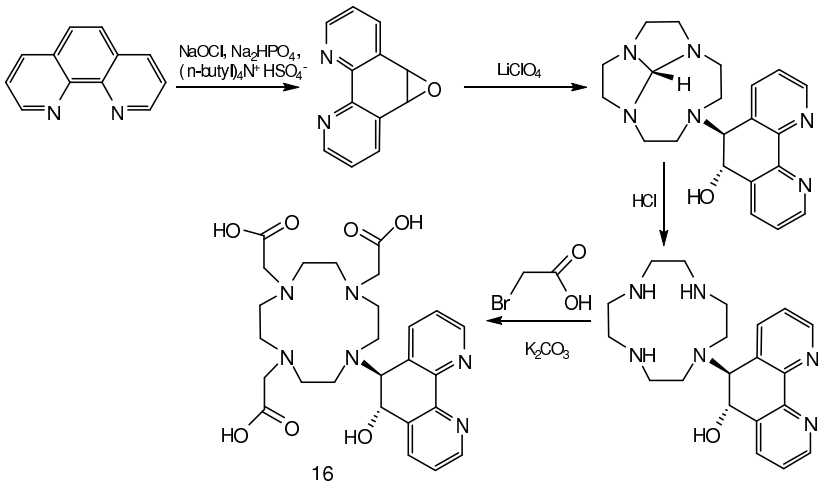

Scheme 13. Synthetic pathways to obtain PhenHDO3A.

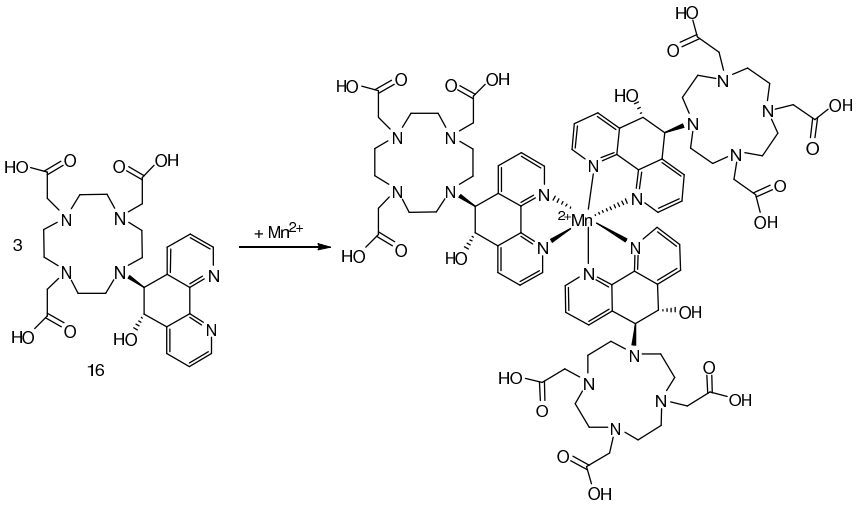

Scheme 14. The formation of tris complexes around Fe- (II) or Ni(II).

acetate donors, leading to a (DO3A) -type ligand suitable for complexation of lanthanide ions. The authors reported how to eliminate the single remaining water molecule from the ninth coordination site of the metal ion in such complexes based on N-functionalised (DO3A). Their approach was to attach an 8-benzyloxyquinoline unit to the macrocycle, via a methylene linker at the C-2 position of the aromatic group **Scheme 15**. In this way, the quinoline nitrogen should be suitably positioned to bind to the lanthanide, at the same time forcing the benzyloxy group into the position normally adopted by the water molecule and expelling it from the coordination sphere of the metal ion, whilst maintaining the overall charge neutrality of the complex. The 8-benzyloxyquinoline group in (**17)** successfully blocks the coordination of a water molecule to the metal ion that is normally anticipated in such DO3A-based systems which is the most important in lanthanium complexes.

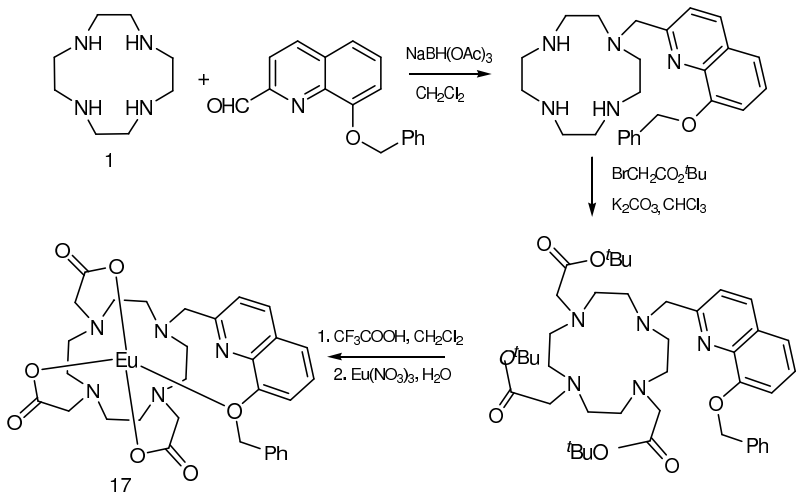

Scheme 15. Synthesis of ligand 17.

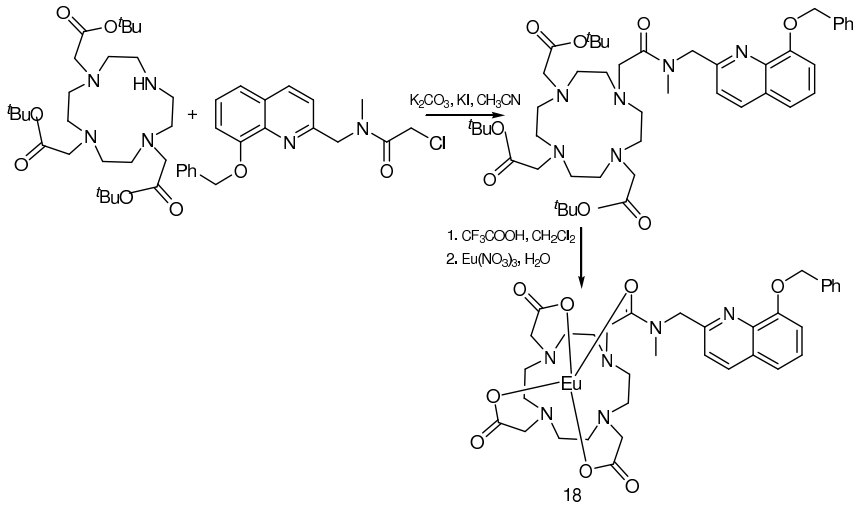

Scheme 16. Synthesis of ligand 18.

Synthesis of another fluorescent chemosensor consisting of cyclen and one **19** or two **20** (**Scheme 17**) anthrylmethyl groups for detection of pH and transition metal cations in aqueous solution was reported by Yasuhiro Shiraishi [33] and his co-workers. The fluorescent behavior and complexation properties of **20** in compare with that of a cyclen with a single anthrylmethyl group shows that **20** demonstrates fluorescence behavior similar to that of **19** but **20** show stronger fluorescence at a low-pH region (p*K*a) 8.4) and in the presence of Zn^{2+} and Cd^{2+} but showing weak fluorescence at a high-pH region and in the presence of Cu^{2+}. This is owing to the higher electron density of the cyclen nitrogen on H-**20** and metal-**20** complex and to the lower energy-transfer efficiency from the photoexcited anthracene to the coordinated metal cation. Compound **20** is very stable even left to stand under a humid atmosphere at least 30 days, whereas **19** was decomposed within one week, suggesting that **20** may be a potential effective fluorescent chemosensor for detection of pH and metal cations in aqueous solution.

Burkhard König [34] shows synthesis of cyclen derivatives with riboflavin. Cyclen with three selective protecting groups was used to the synthesis, such as Cbz (benzyloxycarbonyl) or Boc (*tert*-butoxycarbonyl). The free amino group was coupled

with 3-phenothiazin-10-ylpropionic acid using standard peptide procedures. The substituted azamacrocycle **21** was converted into zinc complex **2** by treatment with zinc perchlorate in refluxing methanol for 1 h (**Scheme 18**).

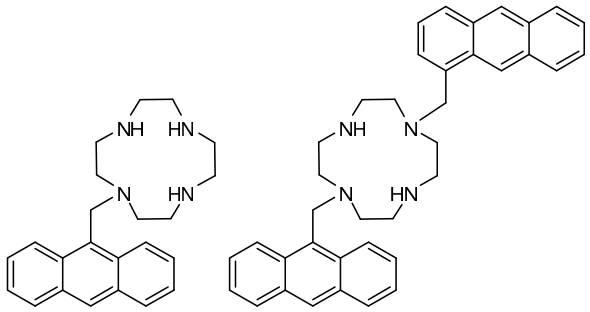

19 20

Scheme 17. Structure of fluorescent chemosensors.

The binding and protonation constants of **21** were performed by potentiometric titrations. The obtained data show that the acidity of complex **21** is similar to that of zinc(II) complex with 1,4,7,10-tetraazacyclododecane. p*K*a values of coordinated water is 8.0 for compound **21** and 7.9 for complex with tetraazacyclododecane. A similar ability of **21** and zinc complex of tetraazacyclododecane to coordinate the imide moiety of riboflavin are similar and were confirmed by titration of mixtures of **21** and riboflavin. The observed pH profile corresponds to the formation of a 1:1 complex with an association constant of log $K = 5.9$.

Pier Lucio Anelli [35] and his co-workers reported the synthesis of lipophilic gadolinium complexes that could be very useful agents for magnetic resonance angiography (MRA) when formulated as mixed micelles. Mixed micelles are multicomponent micelles containing a phospholipids a biocompatible nonionic surfactant and a lipophilic gadolinium complex, such as **23** or **24** (**Scheme 19**). In particular, compound **23** was found very interesting. The mixed micelles containing **23** show high relaxivities and long blood permanence in rats, two essential features for a

MRA agent. The only drawback of **23** is its elimination. In fact, 7 days after injection in rats of the formulation only 50% of injected dose is eliminated by the liver while the remaining is still present into the animal body. To increase the elimination, the compound **24** was synthesized contains two palmitic esters which should be hydrolyzed in vivo, giving rise to a small, hydrophilic gadolinium complex more easily eliminable. The gadolinium complex **of 24** is a promising component of mixed micelles for MRI coronarography.

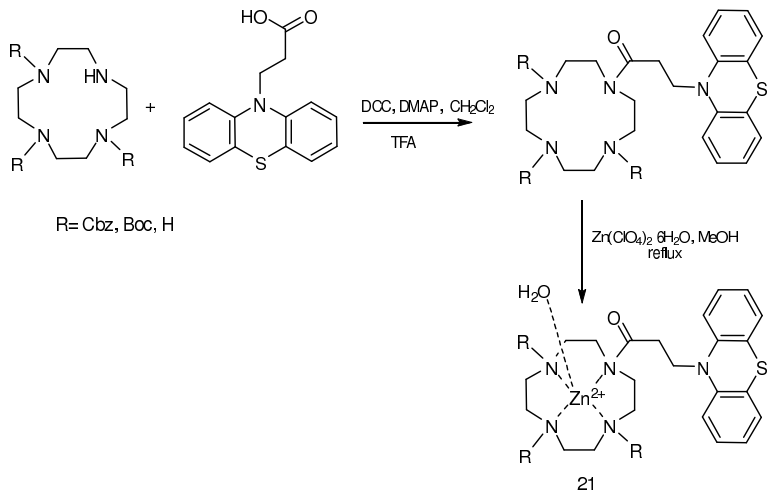

Scheme 18. Synthesis of 1,4,7,10-tetraazacyclododecane derivatives with riboflavin.

The compound **23** and **24** was formed from compound **25** **(Scheme 20**), which is very interesting, because it can be easily coupled to a variety of carriers bearing an amino group and then deprotected to DOTA monoamide under mild and neutral conditions by catalytic hydrogenolysis. This is a considerable advantage over compound **26** derivatives of cyclen, which requires acidic conditions for the deprotection.

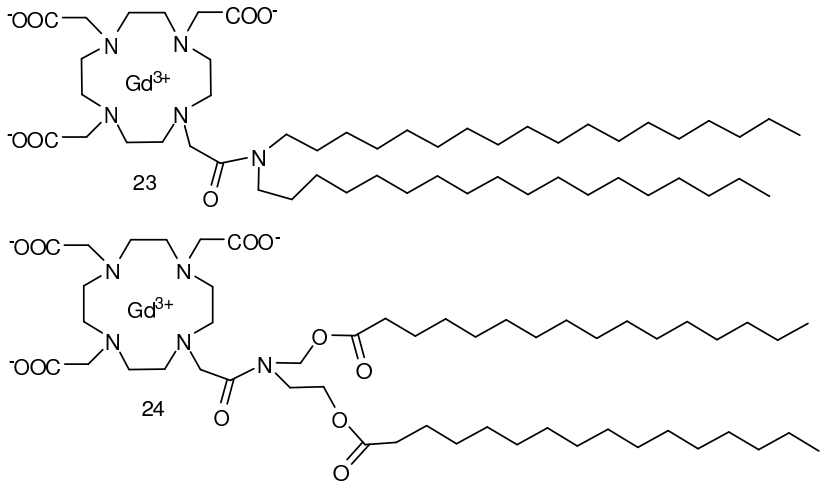

Scheme 19. Structures of the lipophilic gadolinium complexes 23 and 24.

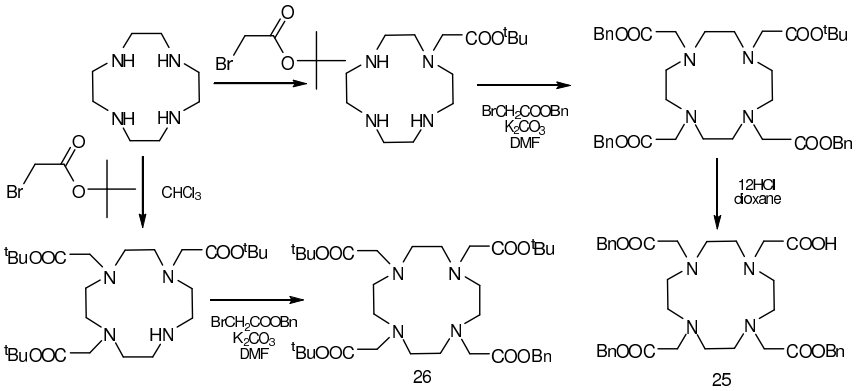

Scheme 20. Synthesis of DOTA esters 25, 26.

There are many ligands based on cyclen with varying types and numbers of pendant arms. Laszlo Burai [36] were prepared and characterized by two new 1,7-

disubstituted-1,4,7,10-tetraazacyclododecane ligands (**27, 28**) and their complexes with Mg^{2+}, Ca^{2+}, Sr^{2+}, Mn^{2+}, Zn^{2+} and Ln^{3+} (**Scheme 21**). The pH titration data shows that **27** and **28** both form 1:1 M:L complexes with all divalent and trivalent metal ions. Protonated complexes did not appear to form with **28**, but were evident for all of the metal ion-**27** complexes. The alkaline earth metal ion-**27** complexes formed both ML and MHL complexes while the lanthanide ion (Ln^{3+}), Zn^{2+} and Mn^{2+} complexes of **27** formed ML, MHL, and MH_2L species. Zn^{2+} formed the most stable complex with both ligands. Compound **27** forms an "in-cage" complex with Eu^{3+} using all four macrocyclic ring nitrogens and two phosphonate sidearms as ligands.

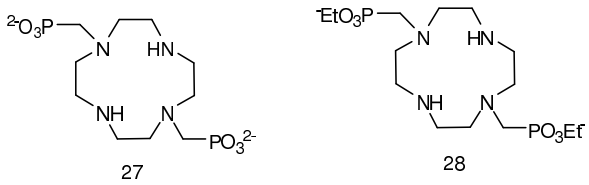

Scheme 21. The phosphorous pendant arm of cyclen.

Very effective gadolinium (III) complexing agents are represented by mono- and diethyl esters of monophosphonic acid analogue of DOTA [37]. Generally, commercial low-molecular-weight MRI contrast agents are characterized by slow water exchange rate, which could be optimized by increasing the negative charge of the complex (easier dissociation of the coordinated water molecule) or by introduction of the bulky groups near the water-binding site of the complex (increased exchange rate due to sterical reasons).

Ligands based on DOTA bind to lanthanide(III) ions via nitrogen and carboxylate oxygen atoms. Such complexes exist in solution in four isomeric forms. Tetrahedral phosphorus acid moieties are significantly more bulky compared to planar carboxylic group. A replacement of carboxylic group by phosphorous acid takes effect in enhanced overall exchange rate of the bound water molecules and total number of possible isomers increases to eight. New ligands containing phosphonate moieties (one mono- and one diester phosphonate group) were synthesized according to **Scheme 22**. The presence of phosphonate groups ensures faster water exchange rate.

Other example of macromolecular compound having phosphonic acid pendant arm is represented by lanthanide chelating ligand synthesized by Griffin and co-workers [38]. The obtained ligand is based on cyclen with a single carboxyl group for conjugation, two phosphonic acids for strong lanthanide complexation and 6-fluoroquinaldine light harvesting moiety for efficient lanthanide sensitization (**Scheme 23**). First 1,7-bis (methylene phosphonic acid diethyl ester)-1,4,7,10-tetraazacyclododecane; R=$CH_2PO(OC_2H_5)_2$) was used as starting material. However, disubstituted compound was the main product (R=$CH_2PO(OC_2H_5)_2$; R'=$CH_2C_9H_5NF$). After applying 1,7-bis(benzyloxycarbonyl)-1,4,7,10-tetraazacyclododecane (R=$COOCH_2Ph$), the desired product with the quinaldine light-harvesting moiety, was isolated in high yield (R=$COOCH_2Ph$; R'=H). Then remaining nitrogen was alkylated to give acetic acid conjugation unit and protecting benzylocarbonyl (BOC) groups were removed by hydrogenation. Finally bis methylene phosphonic acid arms were added and acid hydrolysis led to stable final product.

Small molecular gadolinium complexes, such as Gd-DOTA (Dotarem), and its derivatives, are widely used as magnetic resonance imaging (MRI) contrast agents (CAs) to aid the diagnosis of pathologies by enhancing the morphology and functionality of the tissue with the advantage of low inherent toxicity. Small complexes demonstrate relatively low relaxivity, so a high dosage is required to achieve a satisfactory signal enhancement. To overcome the problems, Gd^{3+} complexes were covalently bound to macromolecules, such as proteins, antibodies, dendrimers, and micellar aggregates because their large sizes not only lead to the confinement and a long circulation lifetime in the vasculature, but also improve the relaxivity by increasing their rotational correlation time [39]. Unfortunately, the increasing toxicity induced by the slow clearance rate and the inefficient delivery of these macromolecules to the targeting sites seriously limits their applications. Cong Li [40] reported the synthesis of connections between cyclen and crown ethers. The mono-crown alkylated cyclen was reacted with *tert*-butyl bromoacetate, following a deprotection step, the resulting ligands (**29**) were treated with $Ln_2(CO_3)_3$ to give the desired Gd^{3+}, Tb^{3+} and Eu^{3+} complexes The synthesis of **Ln29** is depicted in **Scheme**

24. Gd^{3+}-DO3A complex showing efficient MR signal enhancements, an extended excretion rate, and low acute cytotoxicity. The relaxometric and in vivo imaging studies demonstrate that crown ether moiety as a functional group is a potential choice to realize the compromise between the prolonged excretion rate and the low toxicity of MRI contrast agents.

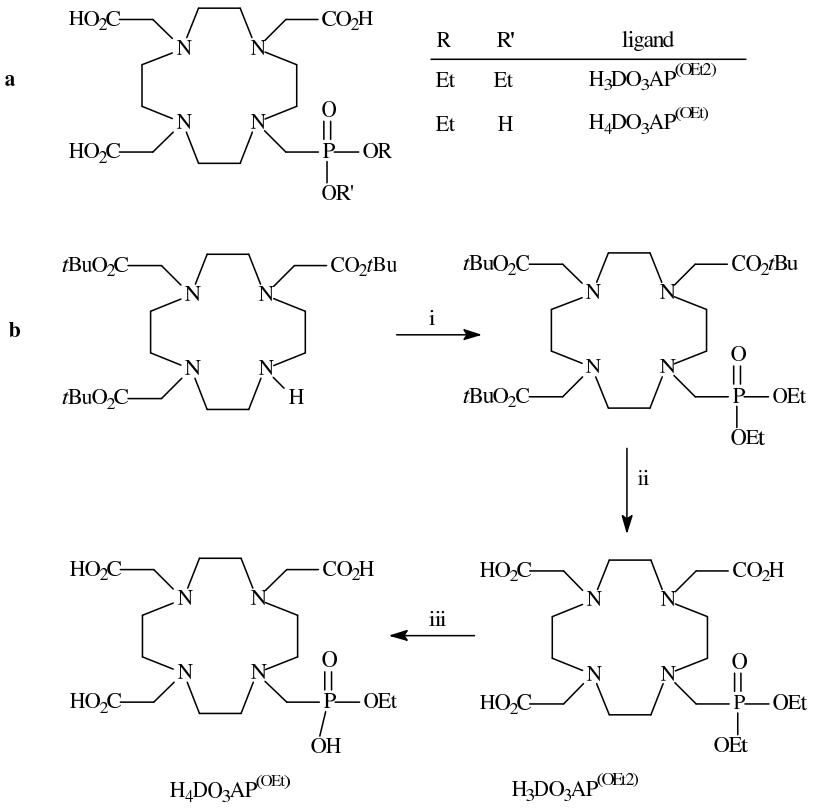

Scheme 22. a) Structures of monophosphonic acid derivatives; b) Ligand synthesis: i $P(OEt)_3$, $CHCl_3$, paraformaldehyde; ii CF_3COOH, CH_2Cl_2; iii KOH.

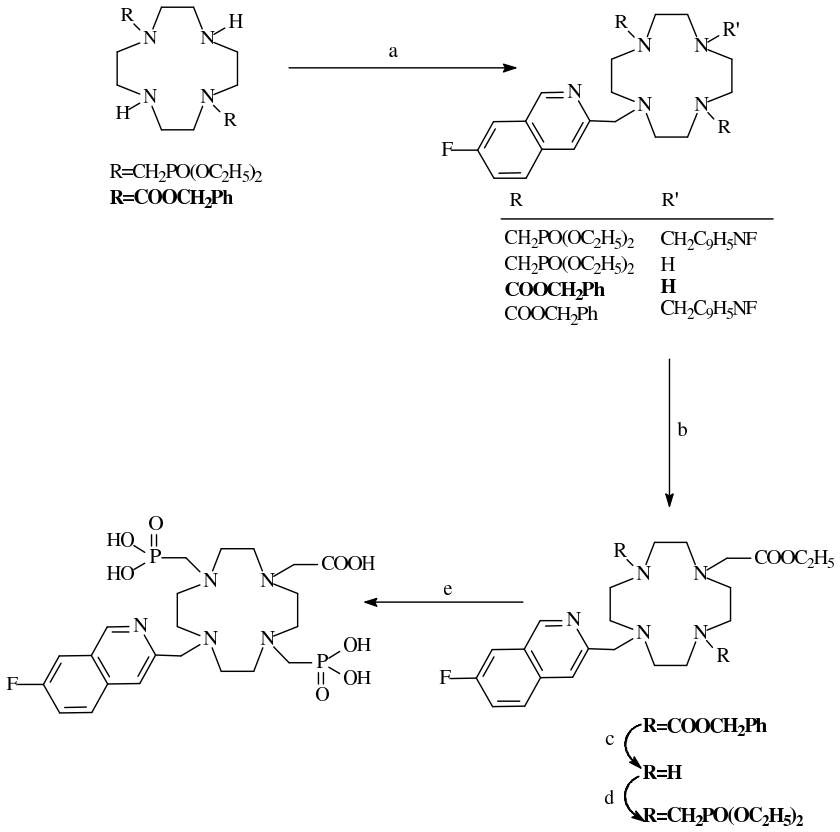

Scheme 23. Synthesis of trifunctional chelate. a) $ClCH_2C_9H_5NF$, CH_3CN, K_2CO_3; b) $BrCH_2COOC_2H_5$, CH_3CN, K_2CO_3; c) cyclohexane, Pd/C 5%, ethanol; d) paraformaldehyde, triethyl phosphite; e) 6 M HCl.

Using the Buchwald–Hartwig [41] coupling reaction as a synthetic tool for direct N-aryl connection. Václav Stastny [42] reported the synthesis of calix[4]arene derivatives constrained in the cone or 1,3-alternate conformations, bearing one or two

cyclen (1,4,7,10- tetraazacyclododecane) moieties directly connected to the upper rim (**Scheme 25).** The cyclen ligands were deprotected and converted into the bis-zinc(II) complexes (**30**), (**31**). Attempts to use the complexes to hydrolyze activated phosphodiester bonds were unfortunately unsuccessful.

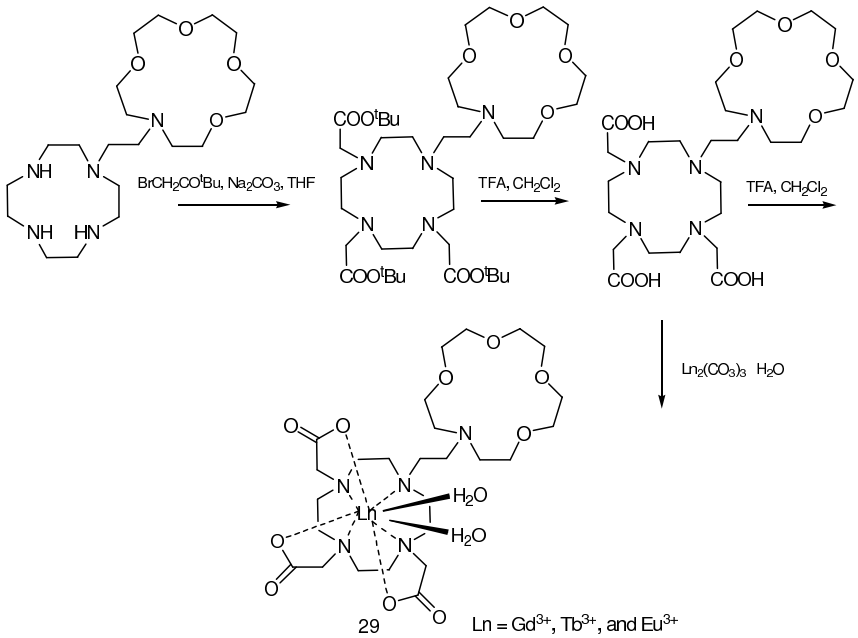

Scheme 24. Synthesis procedure of 29.

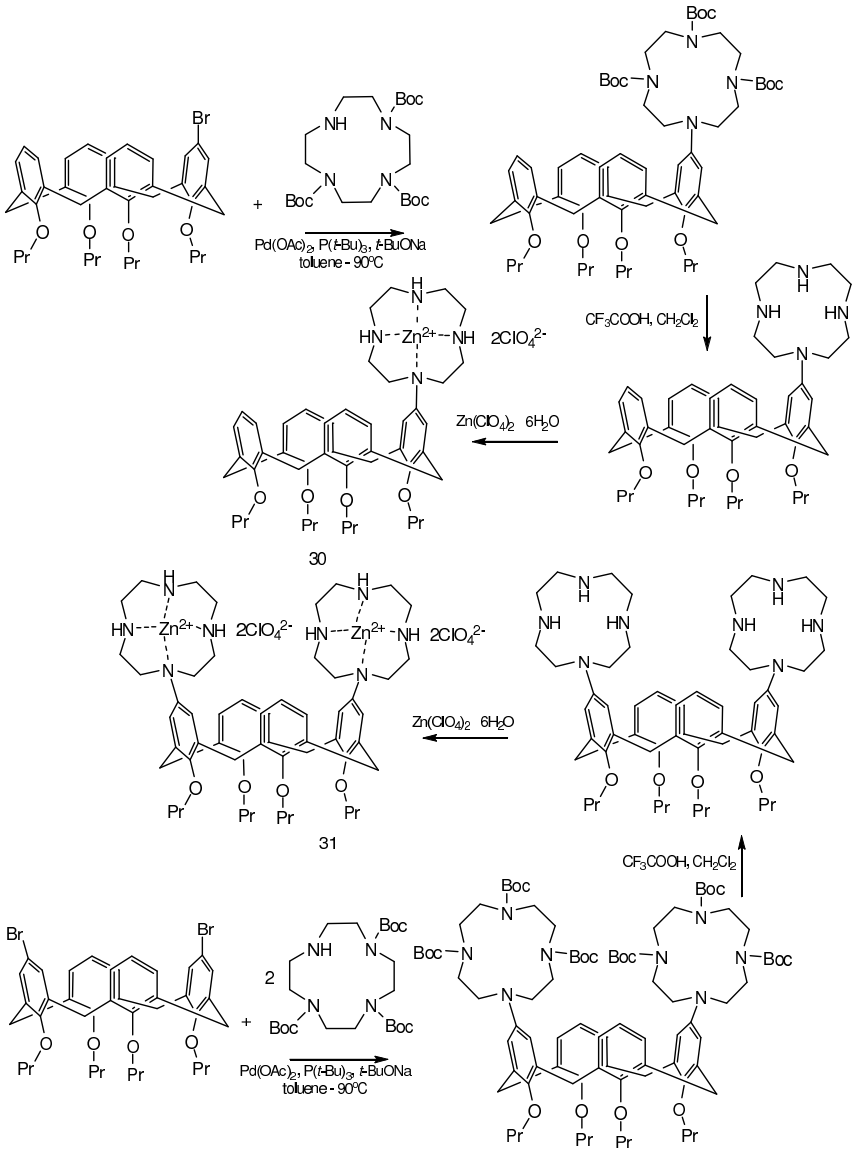

Scheme 25. Synthesis of derivatives of cyclen and calyx[4]arene.

Robert Trokowski [43] show new ligands based on tetramide derivatives of cyclen with phenylboronic acids groups as pendant arms and their Eu^{3+} complexes as glucose sensors using chemical exchange saturation transfer (CEST) MR imaging for detection. Trokowski presented the synthesis of two bis-phenylboronate complexes of Eu(**32**) and Eu(**33**), and a mono-phenylboronate complex (**Scheme 26**). Both the free ligands and their Eu^{3+} complexes bind to simple sugars, but their selectivity and binding affinities vary with sugar structure. The free ligands, **32** and **33**, are very interesting because they are selective for fructose over glucose, but this selectivity order switches in the respective Eu^{3+} complexes. The complex of Eu (32) shows the highest selectivity and binding affinity for glucose. Glucose acts as a "capping" moiety in the Eu (**32**) glucose binary complex and modulates water exchange between a single Eu^{3+} -bound water molecule and bulk water, an effect that can be detected by CEST imaging. Thus, Eu (**32**) represents a new class of metabolite-specific imaging agents that may allow mapping of metabolites by MRI of the bulk water signal.

Another supramolecular system that could be attached to cyclen is cyclodextrin. Akkaya presented the strategy for the synthesis of cobalt(III) complexes on the primary- and secondary sites of β-cyclodextrin [44], (**Scheme 27**). It is well known that cyclen-Co(III) is characterized by great ability to catalyze acyl- and phosphoryl-transfer reactions but it has not been used before in artificial metalloenzyme designing. New metalloenzyme (final product at Scheme 27A) is able to enhance metal-promoted ester hydrolysis due to the presence of CD binding site. However the properties of primary- and secondary-sites CD are different. In case of primary-side one, hydroxymethyl group takes part in chelation of metal ion.

Co(III)-complexes of cyclen-CD catalyze the hydrolysis of *p*-nitrophenyl phosphate by factors 2900- (primary side cyclen-CD) and 3700-fold (secondary side cyclen-CD) compared to uncatalyzed reaction. The complexes were prepared according to **Scheme 27**. Cyclen and *β*-CD monotosylate gave the primary-side cyclen-CD conjugate, while *β*-CD monoepoxide was converted to the secondary-side one.

Cyclodextrin derivative could also act as host molecule for cyclen. Edwards and co-workers obtained β-CD dimer that bound di-*tert*-butylbenzyl-Cu-cyclen [45] and

such dimer was designed as potential tumor pretargeting agent (**Scheme 28**). Di-*tert*-butylbenzyl- cyclen is a radiometal-binding macrocycle containing pendant hydrophobic groups with the appropriate geometry for inclusion into the cavity of CDs.

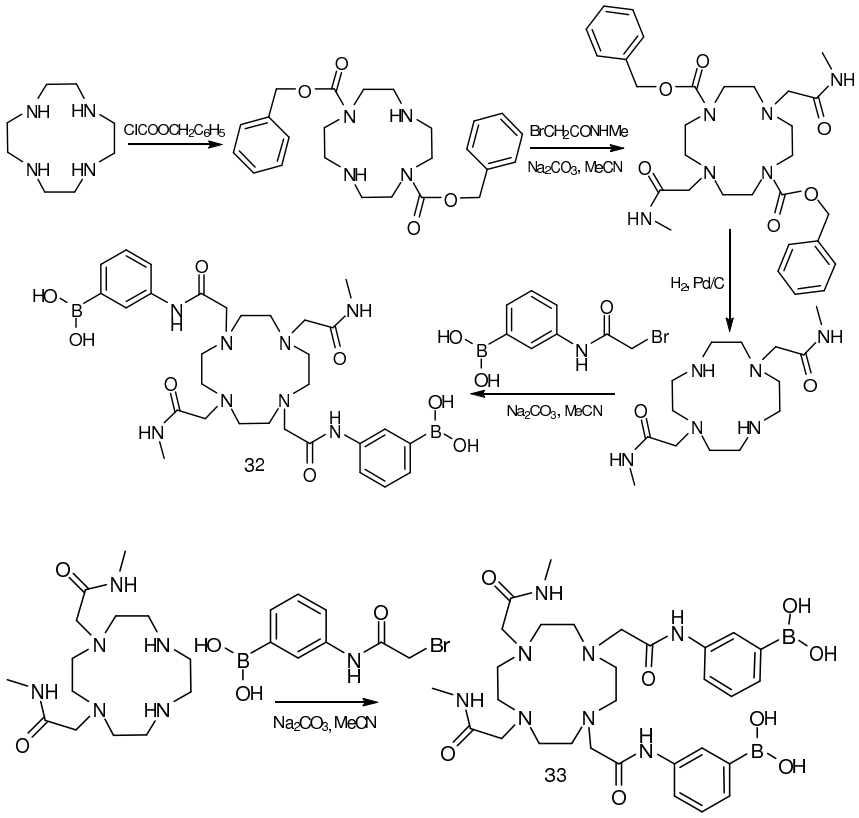

Scheme 26. Synthesis of sugar sensors based on cyclen.

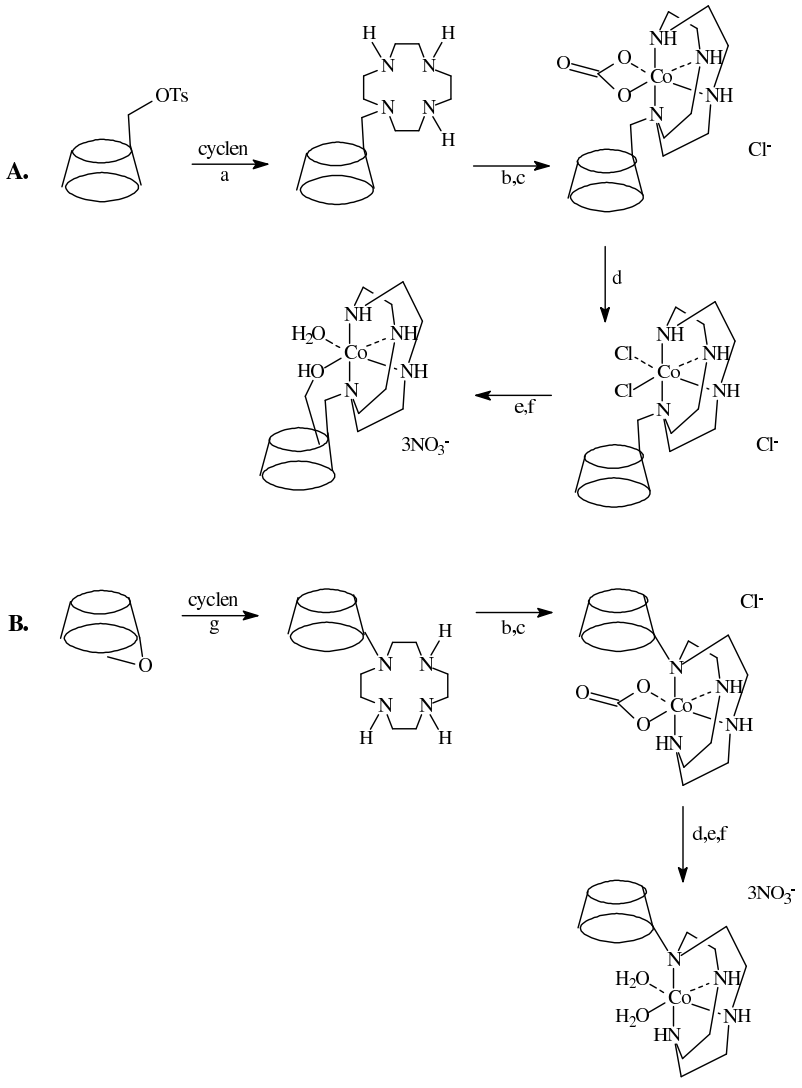

Scheme 27. Synthesis of complexes bearing primary- and secondary-side cyclodextrin binding sites: a) DMF; b) HCl; c) Na_3-$Co(CO_3)_3$; d) MeOH, HCl; e) QAE-Chromatorgaphy; f) HNO_3; g) DMF.

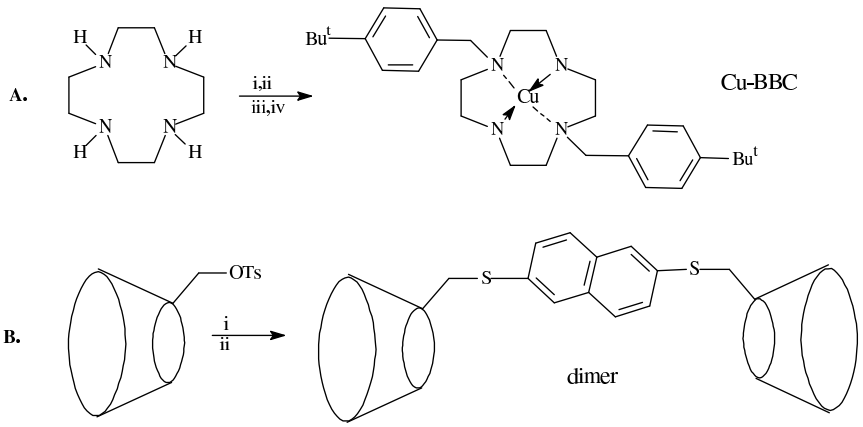

Scheme 28. A: i) chloroethylformate; ii) tert-butylbenzyl bromide; iii) hydrazine, ethylene glycol, KOH; iv) copper acetate. B: i) KI; ii) 2,6-naphthalenedithiol.

Whereas Carrera and coworkers [46] obtained new contrast agent responsive to thiol containing compounds, (**Scheme 29**). Such systems are very important in the detoxification of reactive oxygen species, in controlling the redox status of the cell surface and in regulating the activity of cell surface proteins. The thiol containing compounds are: glutathione (GSH), L-cysteine and L-cysteinyl-glycine (metabolite of glutathione).

New synthesized system, based on DO3A ligand, has a flexible linker ending with 2-pyridyl-dithio group, which can react with free thiols to form mixed disulfides. The conjugation of new ligand (Gd-DO3AS-Act) with GSH or other mentioned extracellular thiol compounds influences significantly water proton relaxation enhacement of the paramagnetic probe. Such covalent adduct with GSH decreases milimolar relaxivity to 4.1 $mM^{-1}s^{-1}$ (compared to 8.1 $mM^{-1}s^{-1}$ for Gd-DO3AS-Act) due to the formation of intramolecular bond between glutathionyl carboxyl group and Gd(III) centre.

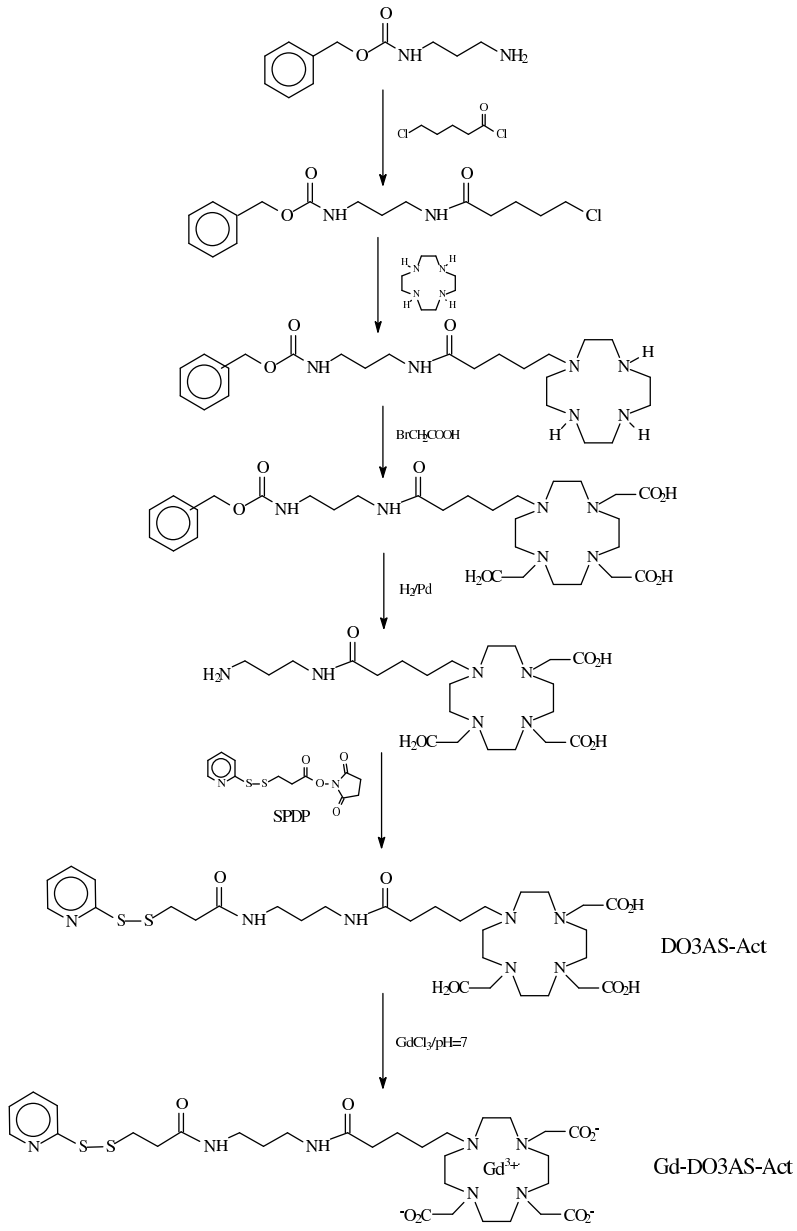

Scheme 29. Synthesis of Gd-DO3AS-Act.

The synthetic way for Gd-DO3AS-Apt is outlined in **Scheme 29.** N-benzyloxycarbonyl-1,3-diaminopropane was reacted with 5-chloropentanoyl chloride. Obtained product was added to the solution of cyclen to give 1-(5,11-dioxo-6,10-diaza-12-oxa-13-phenyltridecyl)-1,4,7,10-tetraazacyclododecane. Then it was reacted with bromoacetic acid to form polyaminocarboxylic cage. Afterwards, hydrogenation with Pd/C gave free primary amino groups on the spacer arm that was coupled with N-succinimidyl 3-(2-pyridyldithio) propionate (SPDP) to yield the desired product, DO3AS-Apt (1-[5,11-dioxo-6,10-diaza-13-(2-pyridyldithio)tridecyl]-1,4,7,10-tetraazacyclododecan-4,7,10-triacetic acid).

Radiolabelled (bio)molecules are potentially useful tools for tumor targeting in order to obtain diagnostic information (spread and localization of the disease) if they contain γ- emitting radiometals, such as ^{99m}Tc, ^{111}In or ^{67}Ga. They also can be used for selective internal radiotherapy when complexed with particle-emitting isotopes, such as the β-emitters ^{90}Y, ^{186}Re, etc. Among potential biomolecules, the regulatory peptides are of special interest because of the high expression of their receptors on different malignancies. Heppeler [47] show the synthesis of incorporation the tetraazacyclododecane derivatives into a peptide using solid-phase synthesis. A. Heppeler and his co-workers coupled the DOTA to the somatostatin analogue (**34**) (**Scheme 30**). This peptide modified with a chelator, was complexed with the radiometals $^{67}Ga^{3+}$, $^{111}In^{3+}$ and $^{90}Y^{3+}$. The three radiopeptides are very interesting because have high stability in human serum and high affinity to the somatostatin receptor: it is four to five times higher for ^{67}Ga-DOTATOC compared to ^{90}Y-DOTATOC and ^{111}In-DOTATOC.

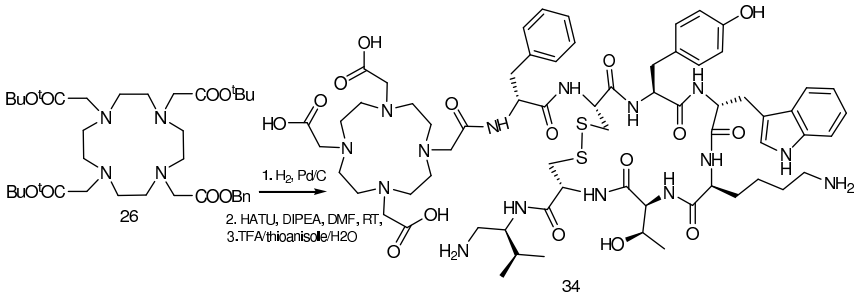

Scheme 30. Synthesis of incorporation cyclen to a somatostatin analoque.

Another convenient approach to the functionalization of peptides with the macrocyclic 1,4,7,10-tetraazacyclododecane- *N*,*N*',*N*'',*N*'''-tetraacetic acid (DOTA) moiety has been developed by James J. Peterson [48]. Protected tetraazacyclododecane by *tert*-butyl or *tert* butyloxycarbonyl groups can be attached to the peptide on the solid resin support. Deprotection and cleavage of the resin-bound DOTA-peptides can be performed in one step using a trifluoroacetic acid cleavage mixture to yield free DOTA-peptide amides. Functionalization of the amino terminus of the peptide- resin was provided through the use of the bifunctional bromoacetyl bromide or chloroacetyl chloride. Since the acyl halide functionality is much more reactive than the alkyl halide with respect to amine nucleophilic attack, acylation was the preferred reaction pathway (**Scheme 31**). These obtained DOTA-peptides in this way can be use in radioimmunoconjugates or targeted delivery vehicles for radioisotopes.

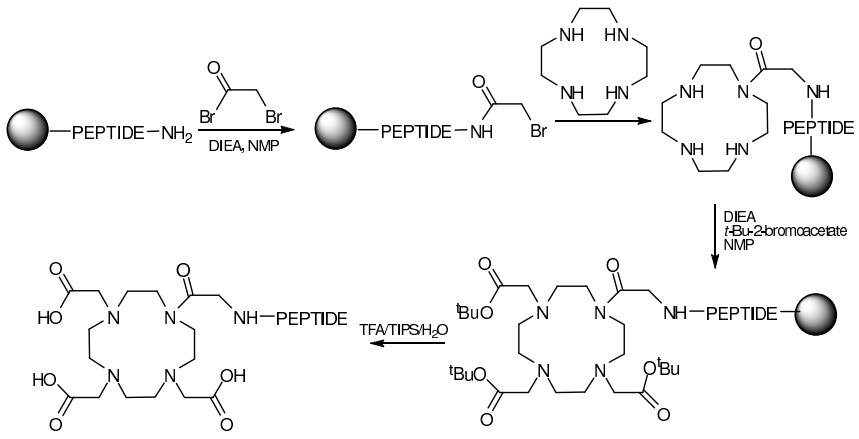

Scheme 31. Solid-Phase Synthesis of DOTA-Peptides.

Using solid-phase peptide synthesis (SPPS) Byunghee Yoo [49] reported a new method to couple DOTA to the C-terminus of a peptide and incorporate DOTA within the peptide sequence in order to synthesize peptidyl contrast agents for molecular imaging (**Scheme 32**).

Byunghee Yoo investigated a selective cleavage of CBz (benzyloxy carbonyl group) protecting groups in SPPS and optimized for the DOTA-loaded resin. The CBz

deprotection step and the step to load DOTA into the resin. The synthesized peptide-DOTA products by Byunghee Yoo (**35**) was used to chelate thulium to create imaging contrast agents that demonstrated good detection sensitivities at physiological conditions (**36**). This synthesis strategy provides great flexibility for coupling one or more peptides to DOTA to create peptide-DOTA imaging contrast agents for many molecular imaging applications.

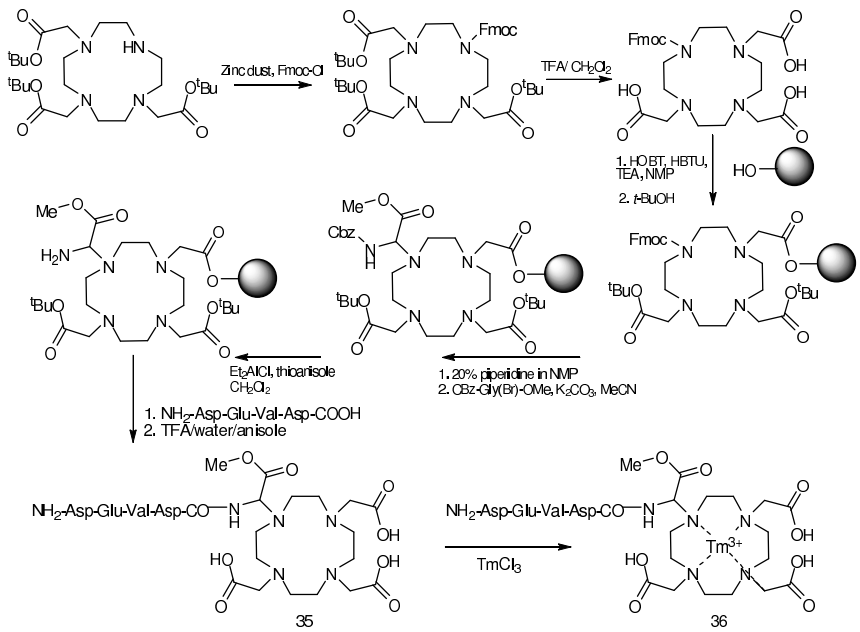

Scheme 32. Synthesis of Peptidyl Contrast argent.

Using a standard oligonucleotide synthesizer Lassi Jaakkola [50] used 1,4,7,10-tetraazacyclododecane-1,4,7,10-tetraacetic acid (DOTA) to synthetize oligonucleotides connected directly to cyclen (**37**) (**Scheme 33**).Upon completion of the syntheses, the conjugate was deprotected and converted to the corresponding gadolinium(III) chelate by treatment with gadolinium- (III) citrate (**38**) (**Scheme 34**). Since the metal was introduced after the chain assembly is completed, the molecule synthesized can be

used in various applications simply by changing the metal. Because of the synthetic strategy, the oligonucleotide conjugate is always free from unconjugated chelate. This is extremely important for in vivo applications.

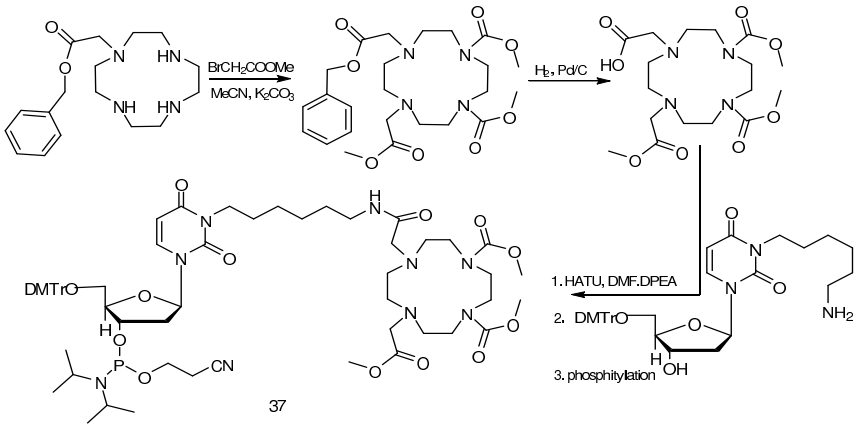

Scheme 33. Synthesis of the nucleosidic phosphoramidite building block.

The sensitivities of fluorescence and radionuclear methods are comparable, which enable the incorporation of antennae for both methods into a relatively small molecular mass (<6 kDa) single molecule in a 1:1 signaling ratio. This optical-radionuclear molecular construct would allow the use of a short-lived radioisotope component of the MOMIA (monomolecular multimodal imaging agent) to localize diseases in deep tissue without the depth limitation of optical methods. After mapping the region of interest, longitudinal monitoring of the diseased tissue can be conducted by optical methods outside radioactivity restricted areas. Optical imaging in the near-infrared (NIR) region minimizes light attenuation by endogenous chromophores and facilitates deep tissue imaging. Zongren Zhang [51] reported the synthesis of (NIR) light emitting dye-DOTA conjugates linked by alkyl or peptidyl units (**39**), (**40**) using solid phase synthesis method (**Scheme 35**) or synthesis in solution (**Scheme 36**). The MOMIAs unit (**39**), (**40**) are stable in serum up to 48 h postincubation at 37 °C. The biodistribution studies by optical and radionuclear methods show similar trends,

indicating that both fluorescence and γ-emissions emanated from the same source. These findings demonstrate the feasibility of using MOMIA strategy to image tissues by combined optical and nuclear methods.

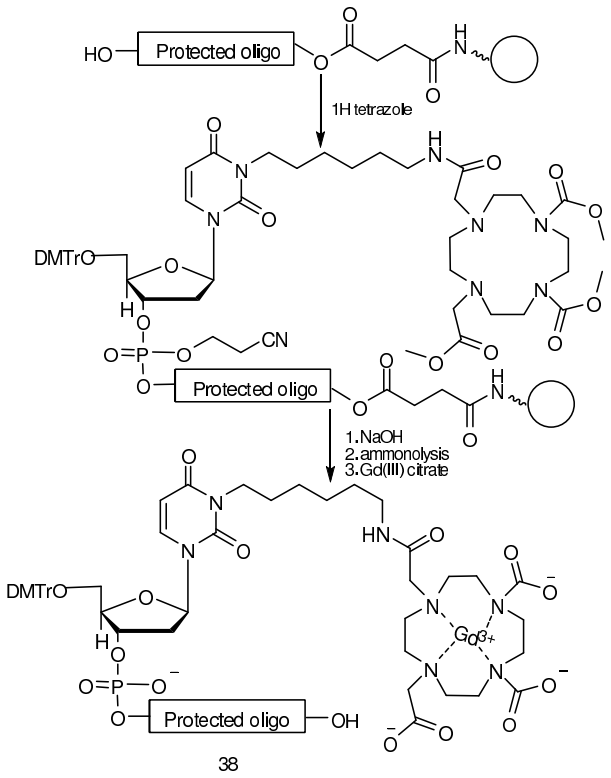

38

Scheme 34. Synthesis of gadolinium (III) complex of 38.

This review presents only a part of available cyclen derivatives. However it clearly proves how significant those systems are for industrial, environmental and clinical purpose, which stimulates interest in searching of new ligands based on 1,4,7,10-tetraazacyclododecane with potentially useful and desired applications. The

most current papers concentrate inter alia around host-guest assemblies involving cyclen and other species [52, 53], and around cyclen derivatives with thiol substituents that could not only complex transition metals but form monolayers as well [54].

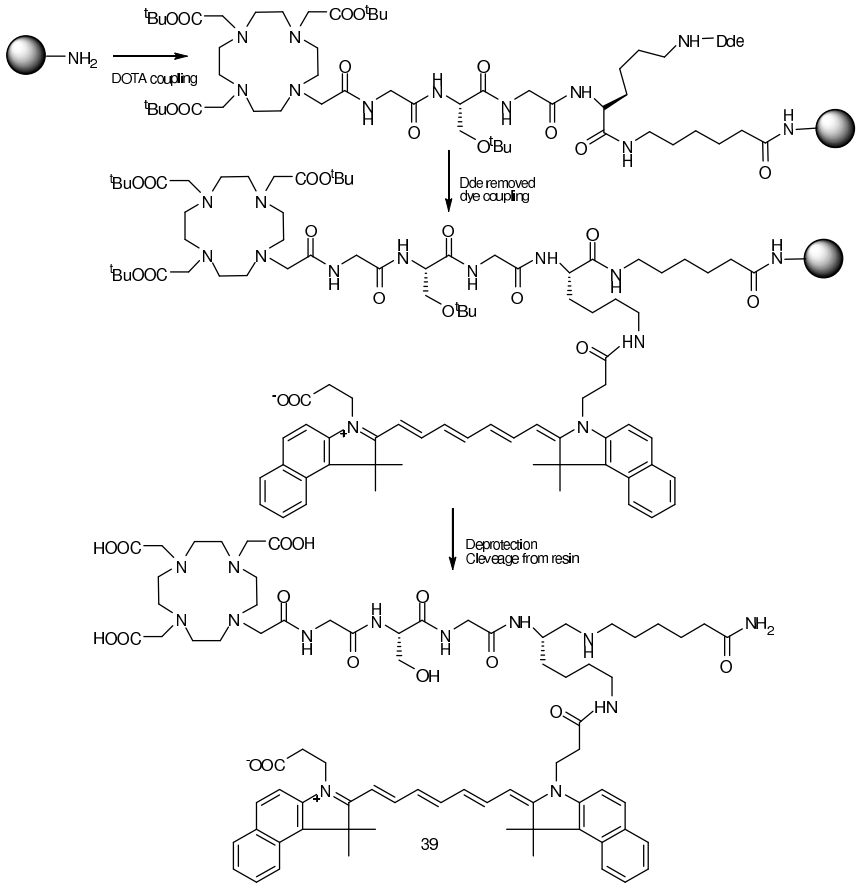

Scheme 35. Solid phase synthesis of 38.

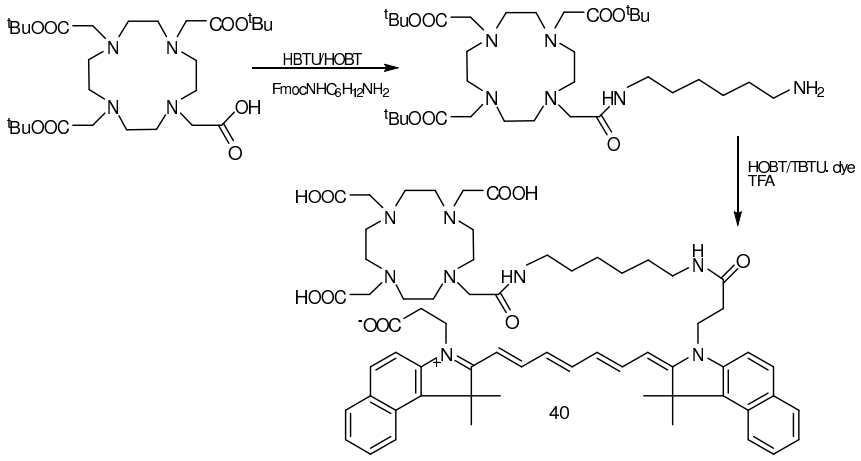

Scheme 36. Synthesis of DOTA derivatives by Solution Method.

Acknowledgement

The authors thank the Polish Ministry of Science and Higher Education for financial support grant No. R0501601 in years 2006-2008.

References:

1. Caravan P., Ellison J. J., McMurry T. J., Lauffer R. B., *Chem. Rev.*, 99, 2293 (1999);
2. Kumr K., and Tweedle M. F., *Pure Apply*., 65, 515 (1993);
3. Aime S., Cabella C., Colombatto S., Geninatti Crich S., Gianolio E., and Maggioni F., *J. Magn. Reson. Imaging*., 16, 394 (2002);
4. Dischino D. D., Delaney E. J., Emswiler J. E., Gaughan G. T., Prasad J. S., Srivastava S. K., Tweedle M. F., *Inorg. Chem.*, 30, 1265 (1991);
5. Denat F., Brandes S., Guilard R., *Synlett*, 5, 561 (2000);
6. Boldrini V., Giovenzana G. B., Pagliarin R., Palmisano G., Sisti M., *Tetrahedron Lett.*, 41, 6527 (2000);

7. Yaouanc J. J., Le Gall N., Clement J. C., Handel H., Des Abbayes H., *J. Chem. Soc. Chem. Commun*., 206 (1991);
8. Filali A., Yaouanc J. J., Handel H., *Angew. Chem. Int. Ed. Engl*., 30, 560 (1991);
9. Bernard H., Yaouanc J. J., Clement J. C., Des Abbayes H., Handel H., *Tetrahedron Lett*., 32, 639 (1991);
10. Roignant A., gardinier I., Bernard H., Yaouanc J. J., Handel H., *J. Chem. Soc. Chem. Commun*., 1200 (1995);
11. Li Z., Undheim K., *Acta Chim. Scand*., 52, 1247 (1998);
12. De Leon- Rodriguez L.M., Kovacs Z., Esqueda- Oliva A.C. and Olvera A. D. M., *Tetrahedron Letters*., 47, 6937 (2006);
13. Izait R. M., Pawlak, K. and Bradshaw *J., Chem. Rev*., 91, 1721 (1991);
14. Kovacs Z. and Sherry A. D., *J. Che. Soc., Chem. Commun*., 185 (1995);
15. Yoo J., Reichert D. E., Welch M. J., *Chem. Commun*., 766 (2003);
16. Brandes S., Gros C., Denat F., Pullumbi P. and Guilard R., *Bulletin de la Societe Chimique de France*., 133, 65 (1996);
17. Li C. and Wong W. T., *J. Org. Chem.,* 68, 2956 (2003);
18. Kruper W. J., Rudolf P. R. and Langhoff C. A., *J. Org. Chem*., 58, 3869 (1993);
19. Hill J. P., Ansin C. E. and Powell A. K., *Tetrahedron Letters*., 43, 7301 (2002);
20. Lauffer R. B., *Chem. Rev*.,1, 752 (1978);
21. Baker W. C., Choi M J., Hill D. C., Thomson J. L. and Petillo P. A., *J. Org. Chem*., 64, 2683 (1999);
22. Lowe M. P., Parker D., Reany O., Aime S., Botta M., Castellano G., Gianolio E., and Pagliarin R., *J. Am. Chem. Soc., 123,* 7601 (2001);
23. Woods M., Kieler G. E., Bott S., Castillo-Muzquiz A., Eshelbrenner C., Michaudet L., Mcmillan K., Mudiguanda S. D. K., Ogrin D., Tirsco G., Zang S., Zhao P. and Sherry D., *J. Am. Chem. Soc., 126,* 9248 (2004);
24. Aime S., Botta M., Cravotta G., Frullano L., Giovenzana G., Crich S., Palmisano G., Sisti M., *Helv. Chim. Acta*., 88, 588 (2005);

25. Aoki S., Kawatani H., Goto T., Kiura E. and Shiro M., *J. Am. Chem. Soc.*, 123, 1123 (2001);
26. Sessler J. L., Mody T. D. and Hemmi G. W., Lynch V., *Inorg. Chem.*, *32*, 3175 (1993);
27. Koike T., Watanabe T., Aoki S., Kimura E., Shiro M., *J. Am. Chem. Soc.*, 118, 12696 (1996);
28. Xue G., Bradshow J. S., Song H., Bronson R. T., Savage P. B., Krakowiak K. E., Izatt R. M., Prodi L., Montalti M., Zaccheroni N., *Tetrahedron*, 57, 87 (2001);
29. Quici S., Marzanni G., Cavazzini M., Lucio Anelli P., Botta M., Gianolio E., Accorsi G., Armaroli N.and Barigelletti F., *Inorg. Chem.*, 41, 2777 (2002);
30. Reichert D. E., Lewis J. S. and Anderson C. J., *Coord. Chem. Re*V., 3,184 (1999);
31. Paris J., Gameiro C., Humblet V., Mohapatra P. K., Jacques V. and Desreux J. F., *Inorg. Chem.*, 45, 5092 (2006);
32. Maffeo D. and Williams J. A. G., *Inorganica Chimica Acta.*, 355, 127 (2003);
33. Shiraishi Y., Kohno Y., and Hirai T., *Ind. Eng. Chem. Res.*, 44, 847 (2005);
34. König B., Pelka M., Zieg H., Ritter T., Bouas-Laurent H. and Bonneau R., and Desvergne J. P., *J. Am. Chem. Soc.*, 121, 1681 (1999);
35. Anelli P.L., Lattuada L., Gabellini M., and Recanati P., *Bioconjugate Chem.*, 12, 1081 (2001);
36. Burai L., Ren J., Kovacs Z., Bruücher E. and Sherry A. D., *Inorg. Chem.*, 37, 69 (1998);
37. Lebduskova P., Hermann P., Helm L., Toth E., Kotek J., Binnemans K., Rudovsky J., Lukes I., Merbach A., *Dalton Trans.*, 493 (2007);
38. Griffin J. M. M., Skwierawska A. M., Manning H. C., Marx J. N., Bornhop D. J., *Tetrahedron Lett.*, 42, 3823 (2001);
39. Aime S., Botta M., Fasano M., and Terreno E., *Chem. Soc. Re*v., 27, 19 (1998*)*;
40. Li C., Li Y. X., Law G. L., Man K., Wong W. T. and Lei H., *Bioconjugate Chem.,* 17, 571 (2006);
41. Hartwig J. F., *Acc. Chem. Res.,* 31, 852 (1998);

42. Stastny V., Lhoták P., Stibor I. and König B., *Tetrahedron*., 62, 5748 (2006);
43. Trokowski R., Zhang S. and Sherry A. D., Bioconjugate Chem., 15, 1431 (2004);
44. Akkaya E. U., Czarnik A. W., *J. Am. Chem. Soc*., 110, 8553 (1988);
45. Edwards W. B., Reichert D. E., d'Avignon D. A., Welch M. J., *Chem. Commun*., 1312 (2001);
46. Carrera C., Diglio G., Baroni S., Burgio D., Consol S., Feldi F., Longo D., Mortillaro A., Aime S., *Dalton Trans*., 4980 (2007);
47. Heppeler A., Froidevaux S., Mäcke H. R., Jermann E., Béhé M., Powell P. and Hennig M., *Chem. Eur. J*., 7, 1974 (1999);
48. Peterson J. J., Pak R.H. and Meares C. F., *Bioconjugate Chem.*, 10, 316 (1999);
49. Yoo B. and Pagel M. D., *Bioconjugate Chem*., 18, 903 (2007);
50. Jaakkola L., Ylikoski A. and Hovinen J., *Bioconjugate Chem*., 17, 1105 (2006);
51. Zhang Z., Liang K., Bloch S., Berezin M. and Achilefu S., *Bioconjugate Chem*., 16, 1232 (2005);
52. Gasperov V., Lindoy L. F., Parkin A., Turner P., *J. of Mol. Struct*., 839, 132 (2007);
53. Davelay S., Tripier R., Bernier N., Le Baccon M., Patinec V., Serratrice G., Handel H., *Dalton Trans*., 1038 (2007);
54. Lacerda S., Campello M. P., Santos I. C., Santos I., Delgado R., *Polyhedron*, 26, 3763 (2007).

Chapter 2

Synthesis of boronic acids – molecular receptors for sugars

Andrzej Sporzyński, Anna Żubrowska and Agnieszka Adamczyk-Woźniak
Faculty of Chemistry, Warsaw University of Technology, Noakowskiego 3, 00-664 Warsaw, Poland

Introduction

Arylboronic acids are systems that attract an increasing scientific interest due to their new applications in organic synthesis, catalysis, supramolecular chemistry, biology and medicine [1]. This interest is essentially stimulated by their extensive use in organic chemistry as chemical building blocks and/or intermediates. Their wide application in biochemistry and medicinal chemistry is worth mentioning, and more recently they've become relevant to the field of material science [2]. In organic synthesis they are predominantly applied for the Suzuki cross-coupling reaction [3]. Because of its versatility, Suzuki coupling is now the best way to obtain aryl-aryl bonds and is extended to alkylboronic acids. Another important application is Petasis synthesis of a-aminoacids [4]. These and many others have been recently reviewed by Cuthbertson [5]. From the point of view of medicinal chemistry, the phenylboronic acid derivatives are used in anticancer therapy as boron neutron capture therapy (BNCT) [6] or chemotheraupeutic agents [7], but also they are used as antibiotics [8], enzyme inhibitors [9] or for treatment of tumors [10]. Their unique feature of forming reversible covalent complexes with sugars [11] has been applied in the construction of new saccharide sensors [12], particularly focused on the measure of the blood glucose level of diabetes patients. Following work on molecular recognition [2], boronic acids have also recently been employed as promising building blocks in crystal engineering in order to achieve predictably organized crystal materials [13].

Boronic acids as sugar receptors

The detection of biologically important sugars (D-glucose, D-fructose, D-galactose and others) is very important in medicine and industry. Especially important is glucose determination due to the relation of its level in the body with various diseases. The possibility of a fast, non-invasive determination of glucose levels allows, in addition to its diagnostic importance, to avoid the risk of complications caused by its improper level. Its industrial application is related mainly to the monitoring of fermentation processes and to the determination of enantiomeric purity of synthetic drugs.

Currently used enzymatic methods allow selective determination of only selected sugars and are not without limits. By contrast, chemical receptors create a possibility of designing a sensor for each sugar, including enantiomers. Boronic acids $RB(OH)_2$ are a very important group of sugar receptors due to the strong covalent binding of sugar molecules, stability and low toxicity.

The action of boronic acids as sugar receptors is based on their ability of fast and reversible ester formation with 1,2- and 1,3-diols. This reaction was not described until 1954 [11]. In 1959 Lorand and Edwards reported the equilibrium constant values of ester formation by phenylboronic acid with various sugars [14]. They stated that cyclic cis-diols, i.e. compounds containing a system of hydroxyl group present in sugars, form more stable cyclic ester than chain- and trans-diols. Due to the possibility of formation of boronate anion in basic media, equilibrium is more complex (Scheme 1) [15].

To standardize quantitative determination of interaction of boronic acids with sugars, Springsteen and Wang [16] introduced the term of overall binding constant in the system receptor – boronic acid (K_{eq} - Scheme 2).

Equilibrium constant values depend on the structure of a sugar, and the differences in its values are the basis of selective sugar determination.

Molecular sugar receptor contains a functional group able to bind sugar molecule (it is the role of $B(OH)_2$ group of boronic acid) and the fragment which changes physical property as the result of sugar binding – "reporter", e.g. fluorophore, chromophore, redox system. The proper structure of the reporter molecule: the

presence of one or several $B(OH)_2$ groups, their space arrangement in relation with other functional groups allows to bind selectively one type of sugar and to construct chemical sensors sensitive to the particular sugar.

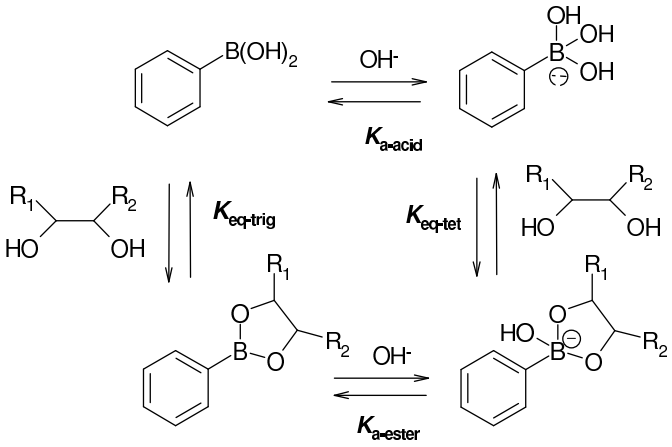

Scheme 1. Equilibrium in the system boronic acid – diol.

.

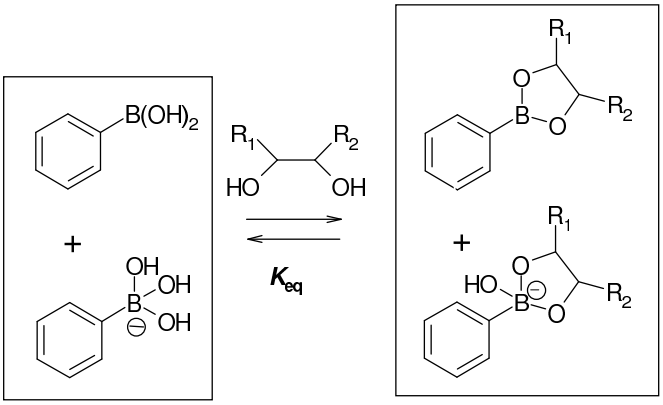

Scheme 2. Overall equilibrium in the system boronic acid – diol.

Due to a great interest in the application of boronic acids as sugar receptors there is a large number of papers covering this area. Recently some elaborate review papers have been devoted to the whole subject or its particular aspects. The newest monograph [12] on boronic acids in sugar recognition discusses the mechanism of receptor activity, reviews receptor types from the point of view of the method of detection and correlations of receptor activity with the structure of sugar molecule, and also decribes the problems of practical construction of sensors, e.g. with the use of polymer matrices. Certain chapters in earlier monographs are similar in character [17-19]. Elaborate review papers deal with the most important fluorecent receptors [15,20,21], molecular imprinting systems [22], biosensors applied *in vivo* [23] and holographic receptors [24].

Present work reviews the synthetic methods described in the papers where boronic acids are applied as molecular receptors for sugars. The first part (Tab. 2) deals with monoboronic acids, the second one (Tab. 3) – with diboronic acids. The construction of special systems, such as polymer matrices with built-in boronic acids, macromoleculs as dendrimers, phase-transition receptors, is not discussed. In Table 1, typical synthetic methods of particular (from the point of view of the structure) boronic acids are shown. For each type of a structure, a method of synthesis (position of Table 1 or scheme for less common methods), a method of detection and sugars for which the receptor was applied are shown.

Table 1.Most common syntheses of sugar receptors

I 1	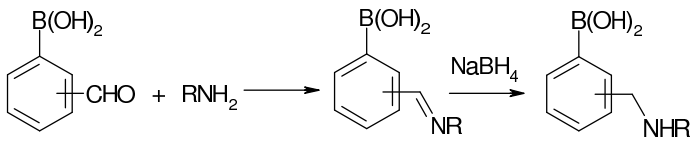

I 2	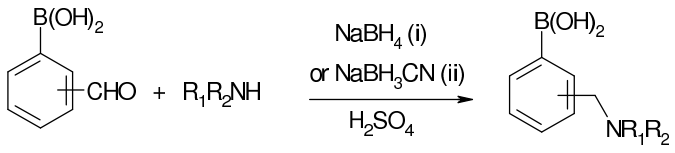
II 1	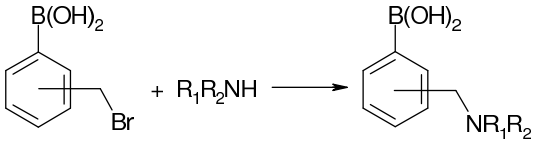
II 2	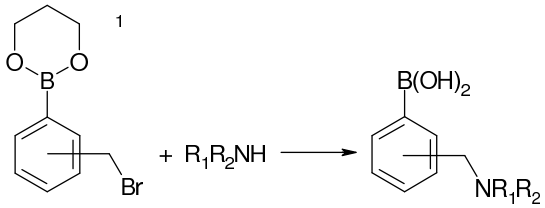
II 3	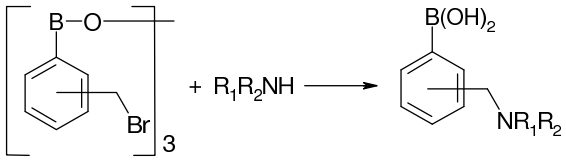
III	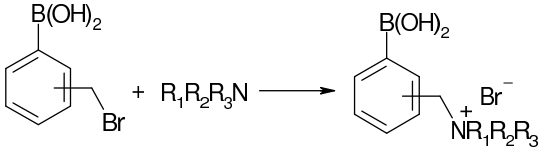
IV	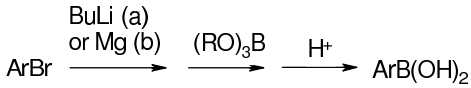

[1] or other cyclic ester (e.g. with pinacol)

Table 2. Syntheses of monoboronic acids

Entry	Structure	Detec-tion method[1]	Synthesis	Detected sugars	Ref.
1	***2***	***3***	***4***	***5***	***6***
	A: (Aminomethyl)phenylboronic acids **A1** 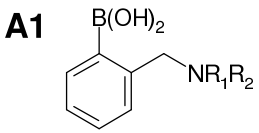 **A2** 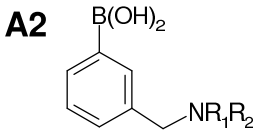 **A3** 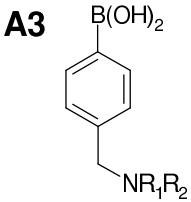				
1	a) A1: R_1=Ph, R_2=H b) A1, A2, A3: R_1=Ph, R_2=H	FLU	I 1	Glc, Fru, Gal, Man	a) 25 b) 26
2	A1: R_1=, R_2=H; R_1=CH_2Ph, R_2=H	POT	I 1	Glc, Fru, mannitol, sorbitol	27
3	A1: R_1= CH_2-9-anthryl, R_2=H	FLU	II 1	Glc, Fru, Gal, sorbitol	28
4	A1: R_1, R_2=Me; R_1=CH_2-9-anthryl, R_2=Me	NMR	I 1	Glc, Fru	29
5	A1: R_1=Me, R_2=CH_2-9-anthryl	FLU	a, b) II 1 c) II 3	a) Glc, Fru, Gal, D-allose b) Glc c) Glc, Fru	a) 30 b) 31 c) 32
6	A1: R_1=Me, R_2=CH_2-3-pyrenyl	FLU	a) II 1 b) II 2	a) Glc, Fru b) Glc, Fru, Gal, Man	a) 33 b) 84

1	*2*	*3*	*4*	*5*	*6*
7	A1: R_1=Me, R_2= CH_2-9-fluorenyl or 4-biphenyl	FLU	II 3	Glc, D-melibiose, D-maltose, methyl-α-glucopyranoside	34
8	A1: R_1=Me, R_2=CH_2-naphthyl, CH_2-2-naphthyl, CH_2-9-anthryl, CH_2-9-phenanthryl or CH_2-3-pyrenyl	FLU	II 2	Glc, Fru, Gal, Man	35
9	A1: R_1=p-CNC_6H_4 R_2=Me	FLU	I 2 (i)	Glc, Fru, Gal, Man	36
10	A1: R_1=Ph, R_2=H R_1=2-fluorenyl, R_2=H R_1=CH_2-9-anthryl, R_2=H or Me R_1=CH_2-2-pyrenyl, R_2=H or Me A2: R_1=Ph, R_2=H R_1=2-fluorenyl, R_2=H A3: R_1=Ph, R_2=H R_1=2-fluorenyl, R_2=H	FLU	I 2(ii)	Dihydrouridine	37
11	A1: R_1=CH_2Ph, R_2=CH_2-9-anthryl	FLU	I 2 (i)	Glc, Fru, Gal, Man, inositol	113
12	A1: R_1=Me, R_2=CH_2-ferrocenyl	EL	II	Glc, Fru, Gal, Man	106
13	A1: R_1=CH(Me)Ph, R_2=CH_2-9-anthryl (R-(-) and S-(+))	FLU	II 2 (a, b) I 1 I	a)[2] b)[3] c)[4]	a) 38 b) 39 c) 40
14	R_1=Me, R_2= 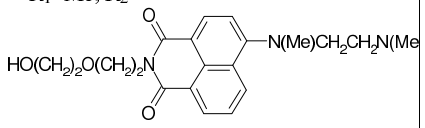	FLU	II 1	Glc, Fru, Gal	41

1	*2*	*3*	*4*	*5*	*6*
15	A1: R_1=H, R_2= 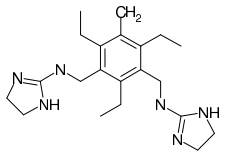	FLU (CB)	I 2 (i)	Glc, Fru	42
16	A1: R_1=H, R_2= 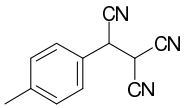	COL	I 1, then 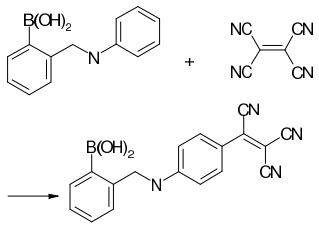	Glc, Fru, Gal	43
17	A1: R_1=H, R_2= 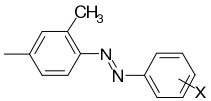 (X=p-NO_2, p-SO_3H, p-CO_2H, p-OMe, or m-CO_2H) R_1=Me, R_2= 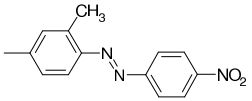	COL	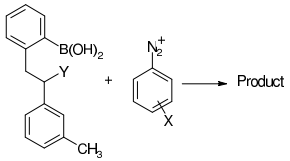 (Y: H or Me)	Glc, Fru	44

1	*2*	*3*	*4*	*5*	*6*
18	A1: R_1=Me, R_2= 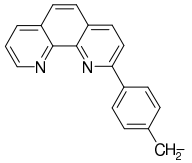	FLU	II 2	a) Glc, Fru, Gal, acids: D-glucoronic, D-galacturonic, sialic b) Fru, Gal, D-galacturonic acid	a) 119 b) 120
19	R_1=Ph, R_2= 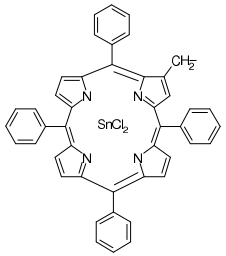	FLU	II 2	1,2,5,6-O-bis (isopropylidene)-D-mannitol	118
20	A1: R_1=Me, R_2= 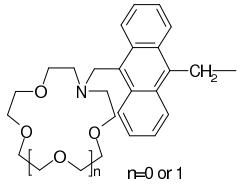	FLU	II 3	D-glucosamine	45

1	*2*	*3*	*4*	*5*	*6*
21	A1: R_1=Me, R_2= 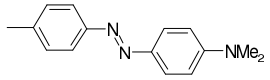	COL	II 1	Glc, Fru, D-ribose	46
22	A1: R_1=H, R_2= 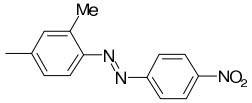	COL	I 1, then + p-$O_2NC_6H_4N_2^+$	Glc	47
23	A1: R_1=Me, R_2= 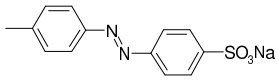	COL	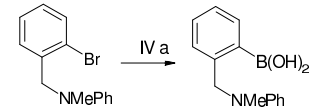 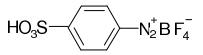 Product	Glc, Fru	48

B: (Aminomethyl)phenylboronic acids quaternary ammonium salts (*Br^-)

B1 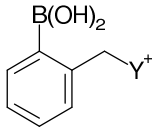

B2 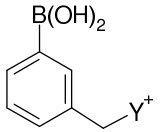

B3 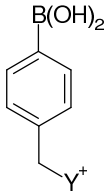

1	*2*	*3*	*4*	*5*	*6*
24	B1, B2, B3: Y^+= 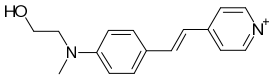	FLU	III	Glc, Fru, Gal	49
25	B1, B2, B3: Y^+= 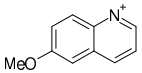	FLU	III	Glc, Fru	50
26	B1, B2, B3: Y^+= 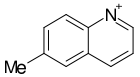	FLU	III	Glc, Fru	51
27	B1: Y^+= 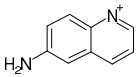	FLU	III	Glc, Fru	52
28	B1: Y^+= 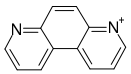	COL, FLU (CB)	III	Glc, Fru, Gal	53
C: Various boronic acids					
29	$ArB(OH)_2$ Ar: 1- or 2-naphthyl, 2-, 3- or 4-biphenyl, 3-pyrenyl	FLU	IV a	Fru	114
30	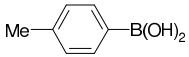	NMR	IV b	Glc	54

1	*2*	*3*	*4*	*5*	*6*
31	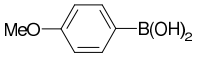	CD	IV a	disaccharides (no CD activity)	55
32	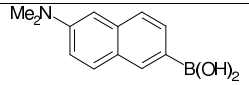	FLU	IV a	Glc, Fru, Gal	117
33	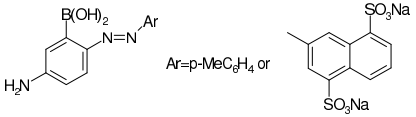	COL	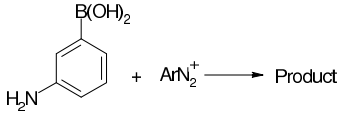	Glc, Fru	56
34	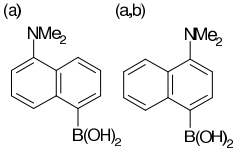	FLU	IV a	Glc, Fru, Gal, sorbitol, tagatose	a) 57 b) 58
35	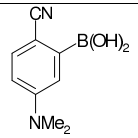	FLU	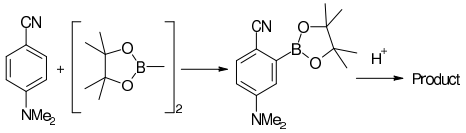	Glc, Fru, Gal, Man	59

1	*2*	*3*	*4*	*5*	*6*
36	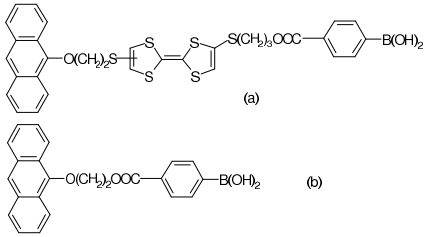	FLU	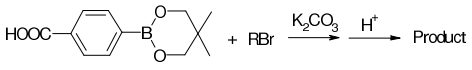	a) Glc, Fru, Gal,Man b) Fru	a,b) 60 b) 61
37	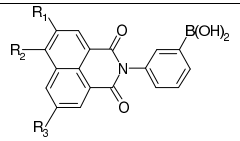 a) R_1=R_2=R_3=H b) R_1=R_2=H, R_3=NO_2 c) R_1=R_2=R_3=H; R_1=R_2=H, R_3=H; R_1=R_2=H, R_3=NH_2; R_1=R_2=H, R_3=CH_3CONH_2; R_1=H, R_2=OCH_3, R_3=H; R_1=SO_3K, R_2=NH_2, R_3=SO_3K	FLU	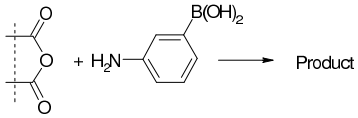 c) Compounds with nitro and acylamino substituent were prepared by reduction and acetylation of amino compounds, resp.	Glc, Fru, Gal	a) 122 b) 123 c) 62

1	*2*	*3*	*4*	*5*	*6*
38	(a) (b) 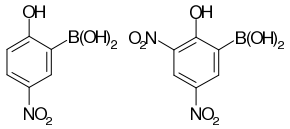	COL	(a) 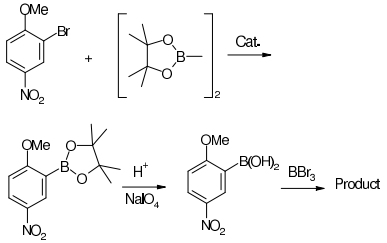 (b) 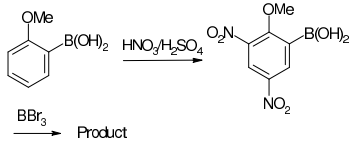	Glc, Fru, Gal	63
39	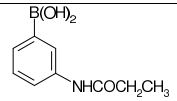	NMR	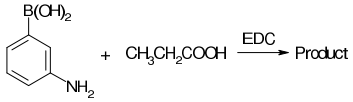	Glc, Gal, Man, Sialic acid	64
40	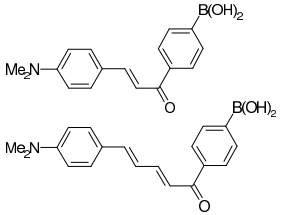	FLU	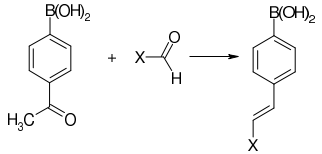	Glc, Fru, Gal	65

1	*2*	*3*	*4*	*5*	*6*
41	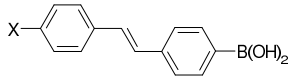 a) X=NMe_2 b) X=H, OMe, NC, NMe_2	FLU	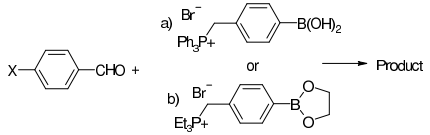	a) Fru b) Glc, Fru	a) 115 b) 66
42	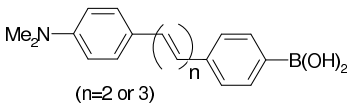 (n=2 or 3)	FLU	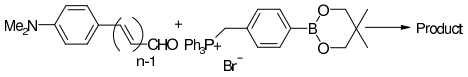	Glc, Fru	116
43	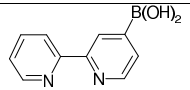	CD	IV a	various sugars (no CD activity)	67
44	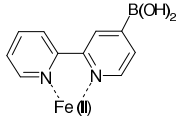	EL	IV a (synthesis of the acid)	Glc, Fru, Gal, Man, Xyl	68
45	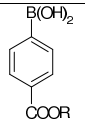 R=Me or $(CH_2)_4$-3-pyrenyl (complexed by β-cyclodextrin)		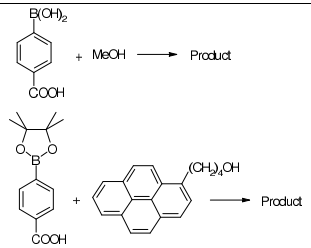	Fru	69
46	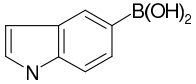	FLU	IV a	Fru, maltose, maltotriose, maltotetraose, maltopentaose	70

1	*2*	*3*	*4*	*5*	*6*
47	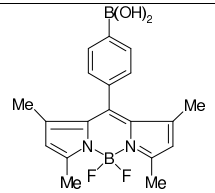	FLU	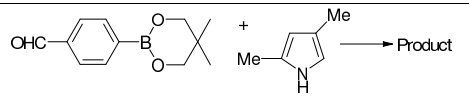	Glc, Fru,Gal	71
48	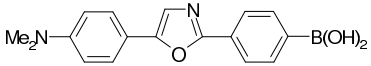	FLU	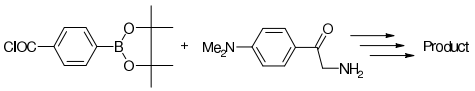	Glc, Fru, Gal	72
49	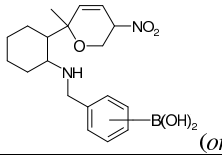 (*ortho*- and *para*)	COL	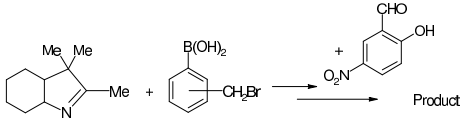	1-O-octyl-β-D-glucopyranoside	73
50	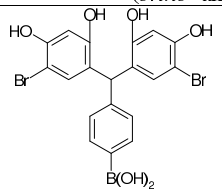	COL, FLU	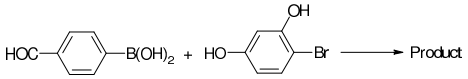	Glc, Fru, Gal	74
51	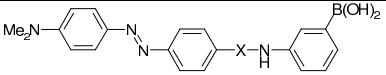 (X=SO_2 or CO)	COL	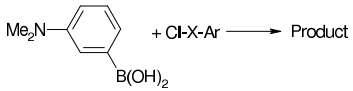	Glc, Fru, Man, Ara	75

1	*2*	*3*	*4*	*5*	*6*
52	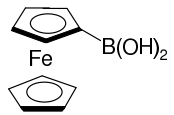	COL, EL	IV a (I step: metalation of ferrocene)	Glc, Fru, Sorbitol	76
53	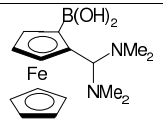 (+) and (-)	EL	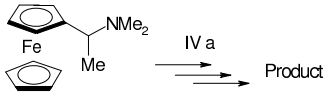	Glc, Fru, D-mannitol, D-sorbitol, L-sorbitol, L-iditol pentaerithritol	77
54	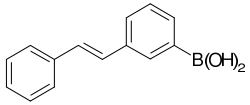	FLU, CD	IV a	Various disaccharides (no FLU or CD activity)	78
55	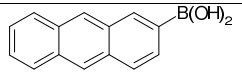	FLU	IV a	Glc, Fru	79

[1] Abbreviations: FLU: fluorescent
COL: colorimetric
CB: competition binding
EL: electrochemical
CD: circular dichroism
CB: competition binding

[2] Sugars: Glc, Fru, Xyl, Ara, D-mannitol, D-sorbitol, dulcitol, D-arabitol, xylitol, adonitol, L-threitol

[3] Sugars: Glc, D-sorbitol, acids: D-glucaric, D-gluconic, D-glucoronic, D-galacturonic, D-(-)-tartaric, L-(+)-tartaric

[4] Sugars: Glc, Fru, Gal, Man, Ara, Xyl, adonitol, xylitol, dulcitol, D-mannitol, D-sorbitol, D-arabitol, L-threitol

Table 3. Syntheses of diboronic acids

Entry	Structure	Detection method[1]	Synthesis	Detected sugars	Ref.
1	***2***	***3***	***4***	***5***	***6***
A: (*ortho*-Aminomethyl)phenyldiboronic acids 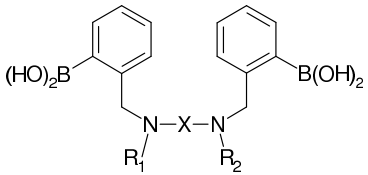					
1	X = 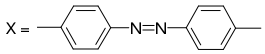 $R_1 = R_2 = Me$	COL	II 2	Fru	46
2	X = 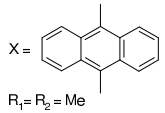 $R_1 = R_2 = Me$	FLU	II 1	a) Glc b) Glc, Fru, Gal, D-allose	a) 31 b) 30
3	X = 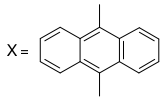 $R_1 = R_2 = CH_2(Me)Ph$ (R-(-) and S-(+))	FLU	I 1	Glc, Fru, Gal, Man, Ara, Xyl, adonitol, xylitol,dulcitol, D-mannitol, D-sorbitol, D-arabitol, L-threitol	40

1	*2*	*3*	*4*	*5*	*6*
4	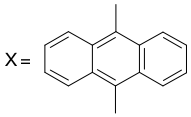 $R_1 = R_2$ = Me or $R_1 = R_2$ = CH_2(Me)Ph (R,R-(-) and (S,S-(+))	FLU	II 2	Glc, D-sorbitol, acids: D-glucaric, D-gluconic, D-glucuronic, D-galacturonic, D and L-tartaric, D-sorbitol	39
5	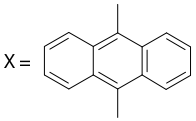 $R_1 = R_2$ = Me	FLU, NMR	II 2	Glc	80
6	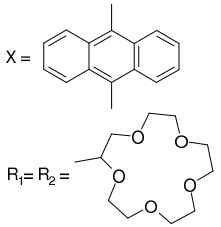	FLU, CD	II 2	Glc (in the presence of metal ions)	81
7	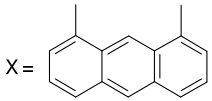 $R_1 = R_2$ = Me	FLU	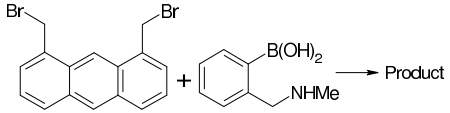	Glc, Fru, Xylitol, D-sorbitol	38
8	X=-$(CH_2)_6$- R_1=CH_2Ph, R_2=CH_2-ferrocenyl	EL	II 2	Glc, Fru, Gal, Man	106

1	*2*	*3*	*4*	*5*	*6*
9	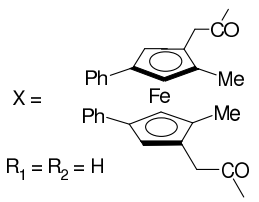	CD	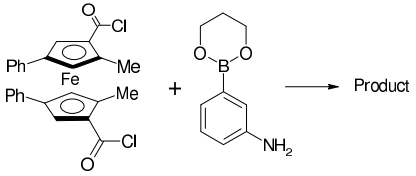	Glc, Gal, Man, Xyl, Ara, allose	82
10	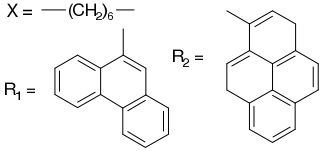	FLU	II 2	Glc, Fru, Gal, Man	83
11	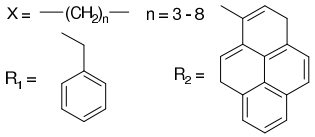	FLU	II 2	Glc, Fru, Gal, Man	84
12	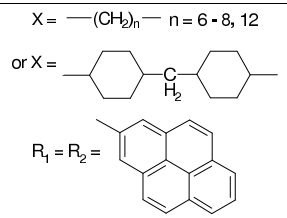	FLU	II 1	Glc	85

1	*2*	*3*	*4*	*5*	*6*
13	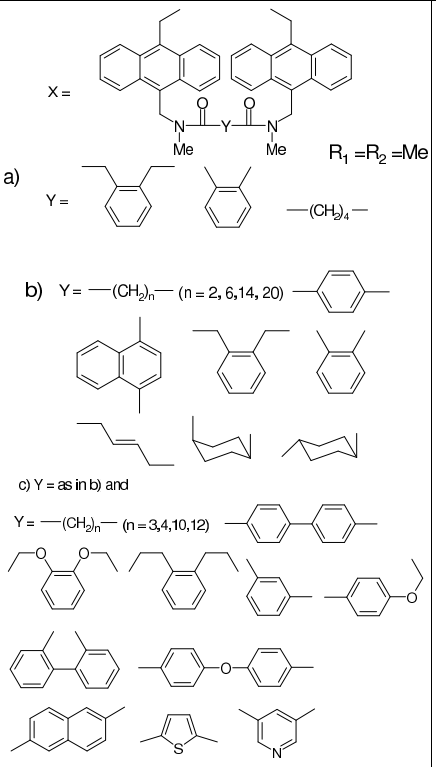	FLU	II 2	a) Glc, Fru, Gal b, c) Sialyl Lewis X	a) 86 b) 87 c) 124

1	*2*	*3*	*4*	*5*	*6*
14	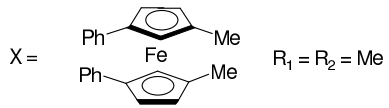	NMR	II 2	Glc	88
15	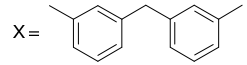	FLU	I 1	Glc, Fru, Gal, Man	89
16	X= -$(CH_2)_6$, R_1=R_2=CH_2-3-pyrenyl	FLU	II 1	Glc, Fru, Gal	33
17	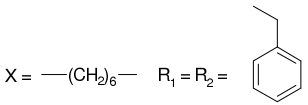	FLU	II 2	Glc, Fru, Gal, Man	90
18	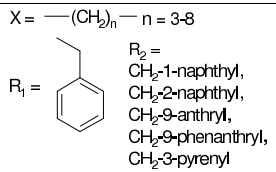	FLU	II 2	Glc, Fru, Gal, Man	35 (n=6) 91
19	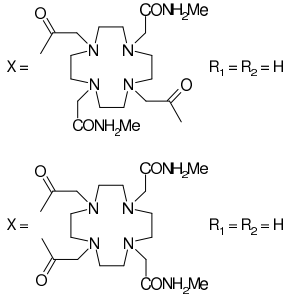	CD, NMR (Eu^{3+} complex)	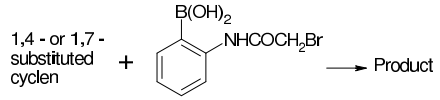	Glc, Fru, Gal, lactose	92

1	*2*	*3*	*4*	*5*	*6*
20	X = 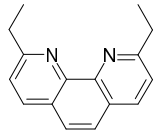 $R_1 = R_2 = Me$	FLU	II 3	Glc	93
21	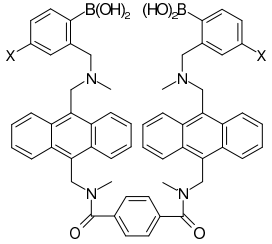 X = CN, NO_2, F	FLU	II 2	Glc, Fru, Gal	94
22	X = 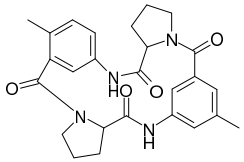 $R_1 = R_2 = Me$ or H	FLU, MS	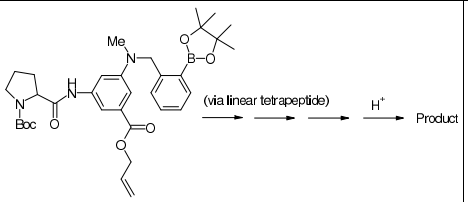	Glc, Fru, Gal, Man, Rib, Xyl, L-glucose, D-allose	95

1	*2*	*3*	*4*	*5*	*6*
B: Various diboronic acids					
23	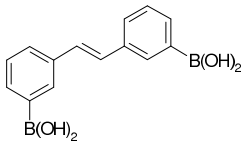	FLU	IV a	Maltotrioze, trehalose, saccharose, maltose, lactose, gentobiose, isomaltose, melibiose	78
24	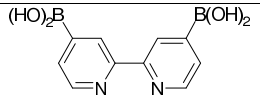	CD	IV a	Glc, Man, Rib, Xyl, D-allose, D-talose, D-cellobiose, D-fucose	67
25	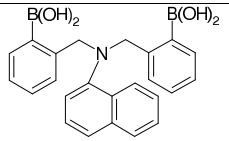	FLU	II 3	Glc, Fru, pentaerythritol, D-threitol	96
26	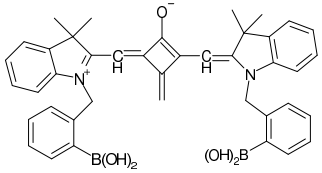	FLU	III, 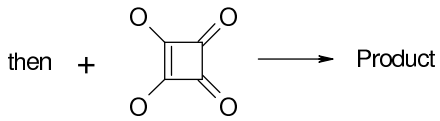	Fru	97

1	*2*	*3*	*4*	*5*	*6*
27	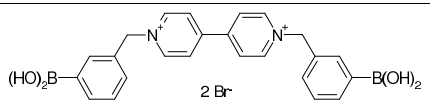	FLU	III	Glc	112
28	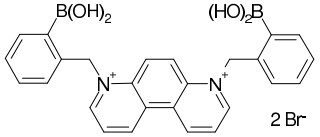	COL, FLU (CB)	III	Glc, Fru, Gal	53
29	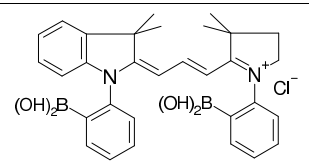	FLU, CD	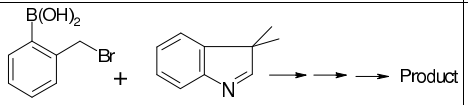	Glc, Fru, Man, Xyl, Ara	98
30	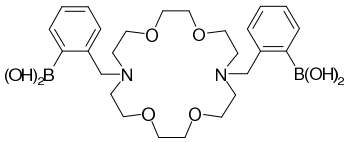	CD	II 3	Glc, allose	99
31	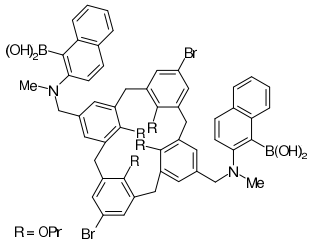	FLU	II 1 (2-bromomethylnaphthalene boronic acid was used)	Glc, Fru	100

1	*2*	*3*	*4*	*5*	*6*
32	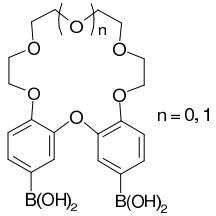	CD	IV a	Glc, Man, D-talose, D-allose	101
33	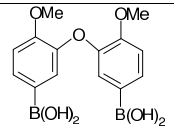	CD	IV a	Glc, Man, D-talose, D-allose	101
34	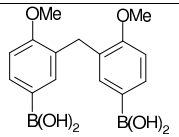	NMR	IV b	Glc	54
		CD	IV a	Glc, Fru, Gal, Man, D-talose, D-maltose, D-cellobiose, D-lactose, D-saccharose	55
35	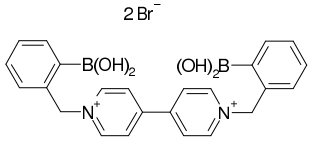	FLU	II 2 (Dimethyl(2-bromomethyl)benzeneboronate was used)	Glc, Fru, Gal	102

1	*2*	*3*	*4*	*5*	*6*
36	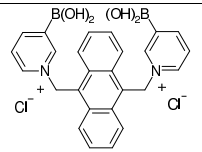	FLU	III (Chloride was used instead of bromide)	Glc, Fru, Gal	103
37	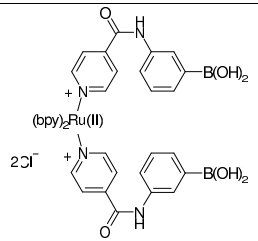	FLU	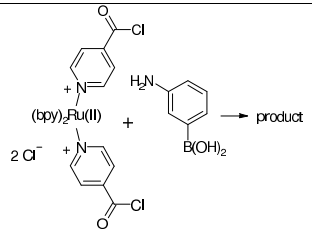	Fru, Man, maltose, xylulose, sorbitol, phosphorylated sugars	104
38	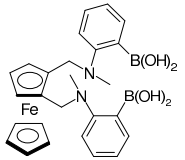	NMR	II 2	Glc	105
39	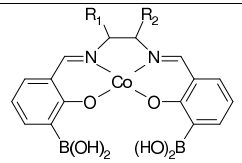 R_1, R_2 = Ph, Ph or $(CH_2)_4$ ((R)- and (S)-)	UV	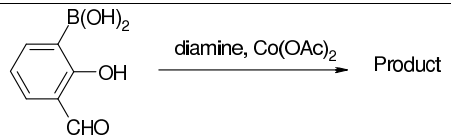	Glc, Fru, Gal, Man, Xyl, D-talose, D-allose	107

1	*2*	*3*	*4*	*5*	*6*
40	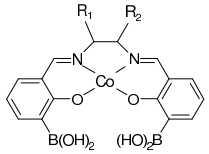 R_1, R_2 = Ph, Ph or $(CH_2)_4$ or *o*-biphenyl ((R)- and (S)-)	CD	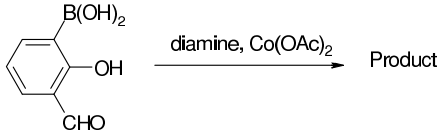	Glc, Fru, Gal, Man, Xyl, D-talose	108
41	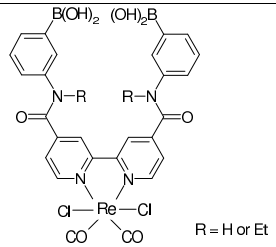 R = H or Et	CD	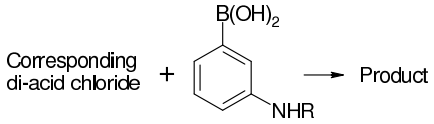	Glc, Fru, Gal, Man, Ara	109
42	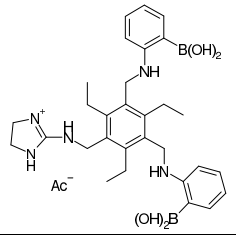	FLU (CB)	I 1	Glc, Fru	42

1	*2*	*3*	*4*	*5*	*6*
43	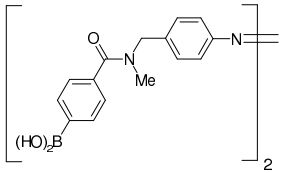	CD	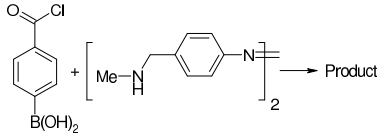	Glc, D-allose	110
44	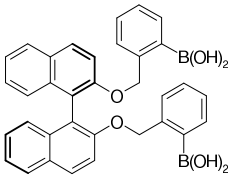	CD	IV a	Glc, Fru, Man, Xyl, Gal, talose, allose	111

[1] Abbreviations: FLU: fluorescent
COL: colorimetric
CB: competition binding
EL: electrochemical
CD: circular dichroism
CB: competition binding

Synthesis of boronic acids used as sugar receptors

The most typical synthetic pathways are shown in Table 1. They can be divided into two groups. The first group of reactions is the functionalization of boronic acid to obtain the desired structure of the organic part. In several cases, before the transformation of the organic part, the boronic group should be protected, mainly in the form of cyclic ester, e.g. in the reaction with pinacol (Scheme 3), and finally deprotected. Regarding the fact that aminomethylarylboronic acids are currently the established standards for the recognition of sugars, the ways of synthesis of these compounds are shown in detail. Starting materials are corresponding formylphenylboronic acids or bromomethylphenylboronic acids. In the first case, secondary aminomethyl compounds can be synthesized by a two step sequence: the formation of a Schiff base and the subsequent reduction with the formation Mannich base (I 1). The isolation of the Schiff base is sometimes difficult due to the formation of by-products: ester formed in the reaction with the solvent and cyclic anhydride (boroxin). Tertiary aminomethylarylboronic acids can be best obtained by reductive amination (I 2) with the use of sodium borohydride or sodium cyanoborohydride. In the second case, the reaction of bromomethyl compound can be realised with boronic acid (II 1), its cyclic ester (II 2) or anhydride (boroxin) (II 3). Finally, quaternary salts are easily obtained in the reaction of bromoderivative with tertiary amine (III). All the above mentioned reactions are also applied in the formation of diboronic acids, for which appropriate diamines are used.

The second group of reactions is the introduction of a boronic unit into an organic molecule. The most common one is a three-step sequence (IVa): the formation of an organolithium compound in the reaction of aryl bromide with butyllithium, the formation of the salt of arylboronic ester in the reaction with trialkyl borate, and hydrolysis. Depending on the functional groups in organic molecules, some alternatives can be applied. Instead of the formation of organolithium compound, the Grignard reagent can be synthesized in the first step (IVb). For the compound with acidic hydrogen atoms, direct metalation is possible. The presence of several reactive functional groups requires their protection, e.g. in the case of phenols or thiols, and deprotection in the last step.

Acknowledgement

The authors thank the Polish Ministry of Science and Higher Education for financial support grant No. R0501601 in years 2006-2008.

Rreferences:

1. Boronic Acids: Preparation and Applications in Organic Synthesis and Medicine, D.G. Hall (ed.), Wiley-VCH, Weinheim, Germany, 2005;
2. K.E. Maly, N. Malek, J.-H. Fournier, P. Rodriguez-Cuamatzi, T. Maris, J.D. Wuest, *Pure Appl. Chem.*, 7 (2006) 1305-1321 ;
3. N. Miyaura, A. Suzuki, *Chem. Rev.,* 95 (1995) 2457-2483 ;
4. N.A. Petasis, I. Akritopolou, *Tetrahedron Lett.* 34 (1993) 583-586 ;
5. E. Cuthbertson, Boronic Acids. Properties and Applications, Alfa Aesar, Heysham, UK, 2006;
6. A.H. Soloway, W. Tjarks, R.A. Barnum, F.G. Rong, R.F. Barth, I.M. Codogni, J.G. Wilson, *Chem. Rev.,* 98 (1998) 1515-1562;
7. S.K. Kumar, E. Hager, C. Pettit, H. Gurulingappa, N.E. Davidson, S.R. Khan, *J. Med. Chem.,* 46 (2003) 2813-2815;
8. A.M. Irving, C.M. Vogels, L.G. Nikolcheva, J.P. Edwards, X.F. He, M.G. Hamilton, M.O. Baerlocher, A. Decken, S.A. Wescott, *New J. Chem.,* 27 (2003) 1419-1924;
9. J. Myung, K.B. Kim, C.M. Crews, *Med. Res. Rev.,* 21 (2001) 245-273.;
10. M.F. Hawthorne, *Angew. Chem., Int. Ed.,* 32 (1993) 950-984;
11. H.G. Kuivila, A.H. Keough, E.J. Soboczenski, *J. Org. Chem*., 19 (1954) 780-783;
12. T.D. James, M.D. Phillips, S. Shinkai, Boronic Acids in Saccharide Recognition, RSC Publishing, Cambridge, UK, 2006;
13. N. SeethaLekshmi, V.R. Pedireddi, *Cryst. Growth Des.,* 7 (2007) 944-949;
14. J. P. Lorand, J. O. Edwards, *J. Org. Chem.*, 24 (1959) 769-774;
15. H. Fang, G. Kaur, B. Wang, *J. Fluorescence,* 14 (2004) 481-489;
16. G. Springsteen, B. Wang, *Tetrahedron*, 58 (2002) 5291-5300;

17. [Functional Synthetic Receptors, T. Schrader, A.D. Hamilton (eds), Wiley-VCH, Weinheim, Germany, 2005, Chapter 2;
18. T.D. James, S. Shinkai, *Top. Curr. Chem.,* 218 (2002) 159-199;
19. Ref. [1], Chapter 12;
20. J.F. Callan, A.P. de Silva, D.C. Magri, *Tetrahedron,* 61 (2005) 8551-8588 ;
21. J.C. Pickup, F. Hussain, N.D. Evans, O.J. Rolinski, D.J.S. Birch, *Biosens. Bioelectronics,* 20 (2005) 2555-2565 ;
22. S. Shinkai, M. Takeuchi, *Biosens. Bioelectronics,* 19 (2004) 1250-1259 ;
23. E.A. Moschou, B.V. Sharma, S.K. Deo, S. Daunert, *J. Fluorescence,* 14 (2004) 535-547 ;
24. S. Kabilan, A.J. Marshall, F.K. Sartin, M.-C. Lee, A. Hussain, X. Yang, J. Blyth, N. Karangu, K. James, J. Zeng, D. Smith, A. Domschke, C.R. Lowe, *Biosens. Bioelectronics,* 20 (2005) 1602-1610 ;
25. A. Arimori, L.I. Bosch, C.J. Ward, T.D. James, *Tetrahedron Lett.*, 42 (2001) 4553-4555.
26. L.I. Bosch, M.F. Mahon, T.D. James, *Tetrahedron Lett*., 45 (2004) 2859-2862 ;
27. L.I. Bosch, T.M. Fyles, T.D. James, *Tetrahedron,* 60 (2004) 11175-11190 ;
28. W. Ni, G. Kaur, G. Springsteen, B. Wang, S. Franzen, *Bioorg. Chem.*, 32 (2004) 571-581;
29. M. Dowlut, D.G. Hall, *J. Am. Chem. Soc*., 128 (2006) 4226-4227;
30. T.D. James, K.R.A.S. Sandanayake, R. Iguchi, S. Shinkai, *J. Am. Chem. Soc*., 117 (1995) 8982-8987;
31. N. DiCesare, J.R. Lakowicz, *Analytical Biochem*., 294 (2001) 154-160;
32. T.D. James, K.R.A.S. Sandanayake, S. Shinkai, *Chem. Commun*., (1994) 477-478;
33. K.R.A.S Sandanayake, T.D. James, S. Shinkai, *Chem. Lett.,* 24 (1995) 503-504;
34. C.R. Cooper, T.D. James, *Chem. Lett.,* 27 (1998) 883-884;
35. S. Arimori, G.A. Consiglio, M.D Phillips, T.D. James, *Tetrahedron Lett.*, 44 (2003) 4789-4792;

36. W. Tan, D. Zhang, D. Zhu, *Bioorg. Med. Chem. Lett.*, 17 (2007) 2629-2633 ;
37. D. Luvino, M. Smietana, J.-J. Vasseur, *Tetrahedron Lett.*, 47 (2006) 9253-9256 ;
38. K.M.K. Swamy, Y.J. Jang, M.S. Park, H.S. Koh, S.K. Lee, Y.J. Yoon, J. Yoon, *Tetrahedron Lett.,* 46 (2005) 3453-3456 ;
39. J. Zhao, M.G. Davidson, M.F. Mahon, G.Kociok-Kohn, T.D. James, *J. Am. Chem. Soc*., 126 (2004) 16179-16186;
40. J. Zhao, T.D. James, *J. Mater .Chem*., 15 (2005) 2896-2901;
41. S. Trupp, A. Schweitzer, G.J. Mohr, *Org. Biomolec. Chem*., 4 (2006) 2965-2968;
42. S.L. Wiskur, J.J. Lavigne, A. Metzger, S.L. Tobey, V. Lynch, E.V. Anslyn, *Chem. Eur. J. ,* 10 (2004) 3792-3804;
43. C.J. Ward, P. Patel, T.D. James, *Org. Lett*., 4 (2002) 477-479;
44. C.J. Ward, P. Patel, T.D. James, *J. Chem. Soc., Perkin Trans. 1,* (2002) 462-470;
45. C.R. Cooper, T.D. James, *J. Chem. Soc. Perkin Trans. 1,* (2000) 963-969;
46. K. Koumoto, S. Shinkai, *Chem. Lett*., 29 (2000) 856-857;
47. C.J. Ward, P. Patel, P.R. Ashton, T.D. James, *Chem. Commun*., (2000) 229-230;
48. K.R.A.S. Sandanayake, S. Shinkai, *J. Chem. Soc., Chem. Commun*., (1994) 1083-1084;
49. S. Trupp, A. Schweitzer, G.J. Mohr, *Microchim. Acta,* 153 (2006) 127-131;
50. R. Badugu, J.R. Lakowicz, C.D. Geddes, *Bioorg. Med. Chem*., 13 (2005) 113-119;
51. R. Badugu, J.R. Lakowicz, C.D. Geddes, *Talanta*, 65 (2005) 762-768;
52. R. Badugu, J.R. Lakowicz, C.D. Geddes, *Dyes Pigm*., 61 (2004) 227-234;
53. J.T. Suri, D.B. Cordes, F.E. Cappuccio, R.A. Wessling, B. Singaram, *Langmuir,* 19 (2003) 5145-5152;
54. J.C. Norrild, H. Eggert, *J. Am. Chem. Soc*., 117 (1995) 1479-1484;
55. Y. Shiomi, M. Saisho, K. Tsukagoshi, S. Shinkai, *J. Chem. Soc., Perkin Trans 1*, (1993) 2111-2117;

56. Y. Egawa, R. Gotoh, S.Niina, J. Anzai, *Bioorg. Med. Chem.*, 17 (2007) 3789-3792;
57. X. Gao, Y. Zhang, B. Wang, *New J. Chem.*, 29 (2005) 579-586;
58. X. Gao, Y. Zhang, B. Wang, *Org. Lett.*, 5 (2003) 4615-4618;
59. W. Tan, D. Zhang, Z. Wang, C. Liu, D. Zhu, *J. Mater. Chem.*, 17 (2007) 1964-1968;
60. Z. Wang, D. Zhang, D. Zhu, J. Org. Chem., 70 (2005) 5729-5732;
61. Y. Yu, D. Zhang, W. Tan, Z. Wang, D. Zhu, *Bioorg. Med. Chem.*, 17 (2007) 94-96;
62. H. Cao, T. McGill, M.D. Heagy, *J. Org. Chem.*, 69 (2004) 2959-2966;
63. W. Ni, H. Fang, G. Springsteen, B. Wang, *J. Org. Chem.*, 69 (2004) 1999-2007;
64. H. Otsuka, E. Uchimura, H. Koshino, T. Okano, K. Kataoka, *J. Am. Chem. Soc.*, 125 (2003) 3493-3502;
65. N. DiCesare, J.R. Lakowicz, *Tetrahedron Lett.*, 43 (2002) 2615-2618;
66. N. DiCesare, J.R. Lakowicz, *J. Phys. Chem. A,* 105 (2001) 6834-6840;
67. T. Mizuno, M. Takeuchi, I. Hamachi, K. Nakashima, S. Shinkai, *J. Chem. Soc., Perkin Trans. 2,* (1998) 2281-2288;
68. M. Nicolas, B. Fabrie, J. Simonet, *Electrochim. Acta,* 46 (2001) 1179-1190;
69. A.-J. Tong, A. Yamauchi, T. Hayashita, Z.Y. Zhang, B.D. Smith, N. Teramae, *Anal. Chem.,* 73 (2001) 1530-1536;
70. Y. Nagai, K. Kobayashi, H. Toi, Y. Aoyama, *Bull. Chem. Soc. Jpn.,* 66 (1993) 2965-2971;
71. N. DiCesare, J.R. Lakowicz, *Tetrahedron Lett.*, 42 (2001) 9105-9108;
72. N. DiCesare, J.R. Lakowicz, *Chem. Commun.*, (2001) 2022-2023;
73. H. Shinmori, M. Takeuchi, S. Shinkai, *J. Chem. Soc., Perkin Trans 1*, (1996) 1-3;
74. P.T. Lewis, C.J. Davis, L.A. Cabell, M. He, M.W. Read, M.E. McCarroll, R.M. Strongin, *Org. Lett.,* 2 (2000) 589-592;
75. T. Nagasaki, H. Shinmori, S. Shinkai, *Tetrahedron Lett.,* 9 (1994) 2201-2204;
76. A.N.J. Moore, D.D.M. Wayner, *Can. J. Chem.*, 77 (1999) 681-686;

77. A. Ori, S. Shinkai, *J. Chem. Soc., Chem. Commun*., (1995) 1771-1772;
78. K.R.A.S. Sandanayake, K. Nakashima, S. Shinkai, *J. Chem. Soc., Chem. Commun*., (1994) 1621-1622;
79. J. Yoon, A.W. Czarnik, *J. Am. Chem. Soc*., 114 (1992) 5874-5875;
80. M. Bielecki, H. Eggert, J.C. Norrild, *J. Chem. Soc., Perkin Trans 1*, (1999) 449-455.
81. T.D. James, S. Shinkai, *J. Chem. Soc., Chem. Commun*., (1995) 1483-1485;
82. M. Takeuchi, T. Mizuno, S. Shinkai, S. Shirakami, T. Itoh, *Tetrahedron Asymmetry,* 11 (2000) 3311-3322;
83. S. Arimori, M.L. Bell, C.S. Oh, T.D. James, *Org. Lett.*, 4 (2002) 4249-4251;
84. S. Arimori, M.L. Bell, C.S. Oh, K.A. Frimat, T.D. James, *J. Chem. Soc., Perkin Trans.1*, (2002) 803-808;
85. B. Appleton, T.D. Gobson, *Sens. Actuators B*, 65 (2000) 302-304;
86. V.V. Karnati, X. Gao, S. Gao, W. Yang, W. Ni, S. Sankar, B. Wang, *Bioorg. Med. Chem. Lett*., 12 (2002) 3373-3377;
87. W. Yang, S. Gao, X. Gao, V.V.R. Karnati, W. Ni, B. Wang, W.B. Hooks, J. Carson, B. Weston, *Bioorg. Med. Chem. Lett.,* 12 (2002) 2175-2177;
88. S. Patterson, B.D. Smith, R.E. Taylor, *Tetrahedron Lett.,* 39 (1998) 3111-3114;
89. S. Arimori, L.I. Bosch, C.J. Ward, T.D. James, *Tetrahedron Lett*., 43 (2002) 911-913;
90. S. Arimori, C.J. Ward, T.D. James, *Tetrahedron Lett*., 43 (2002) 303-305;
91. M.D. Phillips, T.D. James, *J. Fluorescence*, 14 (2004) 549-559;
92. R. Trokowski, S. Zhang, A.D. Sherry, *Bioconjugate Chem*., 15 (2004) 1431-1440;
93. P. Linnane, T.D. James, S. Imazu, S. Shinaki, *Tetrahedron Lett.*, 36 (1995) 8833-8834;
94. G. Kaur, H. Fang, X. Gao, H. Li, B. Wang, *Tetrahedron,* 62 (2006) 2583-2589;
95. G. Heinrichs, M. Schellentrager, S. Kubik, *Eur. J. Org. Chem*., (2006) 4177-4186;

96. T.D. James. H. Shinmori, S. Shinkai, *Chem. Commun*., (1997) 71-72;
97. B. Kukrer, E.U. Akkaya, *Tetrahedron Lett*., 40 (1999) 9125-9128;
98. M. Takeuchi, T. Mizuno, H. Shinmori, M. Nakashima, S. Shinkai, *Tetrahedron*, 52 (1996) 1195-1204;
99. K. Nakashima, R. Iguchi, S. Shinkai, *Ind. Eng. Chem. Res*., 39 (2000) 3479-3483;
100. P. Linnane, T.D. James, S. Shinkai, *J. Chem. Soc., Chem. Commun*., (1995) 1997-1998;
101. G. Deng, T.D. James, S. Shinkai, *J. Am. Chem. Soc*., 116 (1994) 4567-4572;
102. J.N. Camara, J.T. Suri, F.E. Cappuccio, R.A. Wessling, B. Singaram, *Tetrahedron Lett*., 43 (2002) 1139-1141;
103. H. Eggert, J. Frederiksen, C. Morin, J.C. Norrild, *J. Org. Chem*., 64 (1999) 3846-3852;
104. M.J. Deetz, B.D. Smith, *Tetrahedron Lett*., 39 (1998) 6841-6844;
105. J. C. Norrild, I. Søtofte, *J. Chem. Soc., Perkin Trans. 2,* (2002) 303-311;
106. S. Arimori, S. Ushiroda, L.M. Peter, A.T.A. Jenkins, T.D. James, *Chem. Commun*., (2002) 2368-2369;
107. T. Mizuno, M. Takeuchi, S. Shinkai, *Tetrahedron*, 55 (1999) 9455-9468;
108. T. Mizuno, M. Yamamoto, M. Takeuchi, S. Shinkai, *Tetrahedron*, 56 (2000) 6193-6198;
109. T. Mizuno, T. Fukumatsu, M. Takeuchi, S. Shinkai, *J. Chem. Soc., Perkin Trans 1*, (2000) 407-413;
110. H. Shinmori, M. Takeuchi, S. Shinkai, *J. Chem. Soc., Perkin Trans 1*, (1998) 847-852;
111. M. Takeuchi, S. Yoda, T. Imada, S. Shinkai, *Tetrahedron*, 53 (1997) 8335-8348;
112. F.E. Cappuccio, J.T. Suri, D.B. Cordes, R.A. Wessling, B. Singaram, *J. Fluorescence,* 14 (2004) 521-533;
113. C.W. Gray, L.L. Johnson, B.T. Walker, M.C.Sleevi, A.S. Cambell, R. Plourde, T.A. Houston, *Bioorg. Med. Chem*., 15 (2005) 5416-5418;

114. H. Suenaga, M. Mikami, K.R.A.S. Sandanayake, S. Shinkai, *Tetrahedron Lett*., 36 (1995) 4825-4828;
115. H. Shinmori, M. Takeuchi, S. Shinkai, *Tetrahedron*, 51 (1995) 1893-1902;
116. N. DiCesare, J.R. Lakowicz, *J. Photochem. Photobiol. A*, 143 (2001) 39-47;
117. X. Gao, Y. Zhang, B. Wang, *Tetrahedron*, 61 (2005) 9111-9117;
118. H. Kijima, M. Takeuchi, A. Robertson, S. Shinkai, C. Cooper, T.D. James, *Chem. Commun*., (1999) 2011-2012;
119. M. Takeuchi, M. Yamamoto, S. Shinkai, *Chem Commun*., (1997) 1731-1732;
120. M. Yamamoto, M. Takechi, S. Shinkai, *Tetrahedron*, 54 (1998) 3125-3140;
121. W. Yang, J. Yan, H. Fang, B. Wang, *Chem. Commun*., (2003) 792-793;
122. D.P. Adhikiri, M. D. Heagy, *Tetrahedron Lett.*, 40 (1999) 7893-7896;
123. H. Cao, D.I. Diaz, N. DiCesare, J.R. Lakowicz, M.D. Heagy, *Org. Lett.*, 4 (2002) 1503-1505;
124. W. Yang, H. Fan, X. Gao, S. Gao, V.V.R. Karnati, W. Ni, W.B. Hooks, J. Carson, B. Weston, B. Wang, *Chem. Biol*., 11 (2004) 439-448.

Chapter 3

Enzymatic determination of sugars

Alicja Filipowicz-Szymańska, Zbigniew Brzózka
Warsaw University of Technology, Department of Analytical Chemistry,
Noakowskiego 3, 00-664 Warsaw, Poland

Introduction

Nowadays enzymatic methods of sugar determination have great applications in many branches of industry. They are mainly used in pharmaceutical and food industries. These methods are employed in laboratories for the control of the production processes (for instance governmental food inspection) and in pharmaceutical analysis. Sugar detection is necessary for people suffering on diseases that are connected to disorders with sugar metabolism (e.g. diabetics). On the other hand, in food chemistry the determination of sugars in dairy products is of the utmost importance, as there is a strong social demand to know the content of sugars in the products.

Due to the fact, that enzymatic reactions are very specific, they allow to analyze complex samples without previous use of preparation techniques. For example, the nonenzymatic assays often indicate the presence of all reducing sugars, while enzymatic assays are usually sensitive to only one of them, e.g. D-glucose. Enzymes exhibit all the major types of selectivity[1]: chemoselectivity, regioselectivity and diastereoselectivity, enantioselectivity. Another advantages of enzyme catalysis is the fact that enzymes are environmental friendly and that they catalyze broad spectrum of reactions.

In this review significant examples of the enzyme applications in sugar analysis will be presented.

1. Enzymatic detection of glucose

Diabetes mellitus is a metabolic disorder which is chronic and it is almost impossible to be cured completely. The instability of glucose level in blood results from problems with a secretion of insulin by pancreas. This illness is very dangerous because, if untreated, it leads to a lot of complications such as blindness, coma and even death. Nowadays, a lot of people suffer from this illness and the numbers are increasing. At least 171 million people worldwide have diabetics (WHO, 2000). Thus, it is very important to search for a new technology in order to improve treatment. Although there is no cure for diabetes, a strict control of glucose level in blood is needed, in order to reduce of the risk of long-term complications.

Most of commercially available devices for home glucose monitoring use enzymes in this process. The enzymes that are used most frequently in biosensors to detect the level of glucose are glucose oxidase and glucose dehydrogenase. Glucose oxidase is an enzyme that catalyses the glucose oxidation, resulting in the production of gluconolactone and hydrogen peroxide (**Fig. 1**). In this process, cofactor FAD as electron donor is needed.

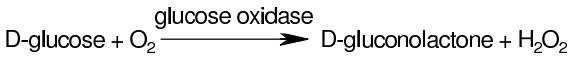

Fig. 1. Biotransformation of glucose at the presence of glucose oxidase

For commercial application in diabetes treatment this enzyme is extracted from *Aspargillus* niger and it is often conjucted with small electrodes.

The second enzyme which is also commonly used in the biosensors construction is glucose dehydrogenase. This enzyme needs cofactor NAD^+ and the biotransformation of glucose by glucose dehydrogenase leads to gluconolactone and NADH (**Fig. 2**).

Fig. 2. Biotransformation of glucose at the presence of glucose dehydogenase.

An enzyme hexokinase can be also used as a part of glucose biosensors. This enzyme catalyses the transfer of γ-phosphoryl group of ATP (adenozine triphosphate) to the hydroxyl group of six-carbon position of glucose (**Fig. 3**).

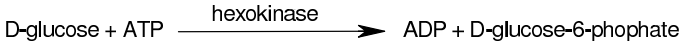

Fig. 3. Biotransformation of glucose at the presence of hexokinase.

Metal cations are necessary for the activity of this enzyme: Mg^{2+} or Mn^{2+}. During the reaction the structure of hexokinase is changing. When glucose is binding by the active side of the enzyme it leads to great conformational change of the enzyme structure. The effects of binding of glucose to the hexokinase compound can be monitored.

In the next chapters some applications of previously mentioned enzymes, and also other enzymes that allow for sugar determination, will be presented.

1.1. Amperometric determination

An amperometric analyses of products of the glucose biotransformations are the most common. This attitude is often based on the fact, that enzymatic oxidation of glucose produces hydrogen peroxide, which is then oxidized on electrode surface. The resulting current is related to glucose concentration. Most of commercially available devices used electrochemistry as a method of detection. In this chapter some solutions will be presented.

The previously mentioned specificity of enzymes allows for simultaneous measuring of the level of different compounds. It is worth to present a technique of a capillary electrophoretic (CE)[2,3] microchip devices with the post-column enzymatic reaction of glucose and lactate.[4] In the first step the glucose and lactate (bioanalytes from blood sample) were separated by capillary electrophoresis and after that the metabolites were mixed with glucose oxidase and lactate oxidase. The hydrogen

peroxide which was liberated during this reaction was amperometricaly detected. Such a microchip can be adopted both in clinical and in biotechnological research.

Capillary electrophoresis was also used in another method of enzymatic glucose determination as a way of substrate transporting to the surface of biosensor.[5] The sensor was a platinum electrode which was modified by chitosan (**Fig. 4**), and (+-)-1-ferrocenylethylamine.

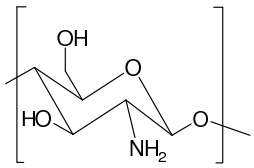

Fig. 4. Structure of chitosan.

The idea was to immobilize glucose oxidase and (+-)-1-ferrocenylethylamine by cross-linking with glutaraldehyde on chitosan membrane. The mediator (+-)-1-ferrocenylethylamine was used in order to transfer electron from the active center of enzyme to the electrode. The biosensor, constructed in this way, was coupled with capillary electrophoresis. Such a system was used for successful determination of glucose in human serum samples. Moreover, this structure consumes less volume of sample, because the CE was applied as a transporting module. The current response was linear to glucose concentration in the range of 0.0025 to 2.5 mM.

Application of a microchip in enzymatic glucose measurement was also presented. An idea of a micro silicon sensor as a device for the continuous monitoring of glucose was described.[6] This sensor employed glucose oxidase as a catalyst for the biotransformation of D-glucose. Hydrogen peroxide, produced in this reaction, is detect by amperometric method. The sensor was constructed of a polymeric flow cell with integrated electrodes. The cell consisted of porous silicon membrane and the cavity where glucose oxidase was immobilized by agarose gel and crosslinked with glutaraldehyde. This method of glucose monitoring allowed for measuring of the glucose concentration in the range 0,05 – 20 mM. This sensor was found to be useful in clinical study.

Immobilized glucose oxidase was also used in a biosensor constructed of graphite electrode modified by carbon nanotube film.[7] The enzyme was immobilized by sol-gel method (**Fig. 5**) which is simple and enzyme is stabile.

1. Step – hydrolysis

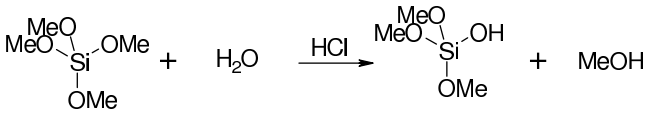

2. Step – condensation

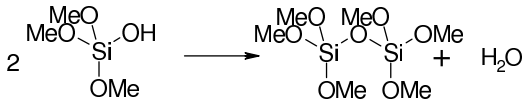

Fig. 5. The sol-gel process.

The sol-gel method of enzyme immobilization finds a lot of interest nowadays.[8] The procedure is simple and everything but time consuming. In the first step a silane derivative is hydrolyzed in acidic environment. The second step is the condensation of the siloxane. An enzyme is closed in this structure.

Hydrogen peroxide, liberated during the enzymatic reaction with glucose, was detected amperometically. Furthermore, the modification of electrode by carbon nanotube allowed for more sensitive determination of glucose. The linear response range of sensor was between 0,2-20 mM of glucose. It was proved that this sensor can be used clinically because the content of glucose in human serum samples was also evaluated.

1.2. Fluorescence determination

Recently, glucose enzymatic sensors, based on fluorescence measurement, are studied, because of many advantages of fluorimetry.[9] In this chapter selected examples of the enzyme applications for the determination of glucose, using fluorescence measurements, will be presented.

Z. Rosenzweig and R. Kopelman described an enzymatic fluorescence sensors for glucose determination.[10] They used glucose oxidase as an enzyme, as it is known to

catalyze the reaction of glucose oxidation with the hydrogen peroxide formation and oxygen consumption. In this research, tris(1,10-phenanthroline)ruthenium chloride, the oxygen indicator, was used as a transducer and the fluorescence of the ruthenium complex was quenched by the oxygen. Both enzyme and indicator were immobilized on an acrylamide polymer, which was covalently connected to sillanized optical fiber. The biosensor detects the concentration of glucose in a range of 1-10 mM and it has a shorter response time in comparison to similar, but larger, biosensors. Described biosensor is 100 times smaller than traditional ones.

Enzymatic determination of glucose can be also performed in PDMS (poli(dimethylsiloxane)) microchip.[11] In such a "Lab-on-a-chip" [12-16] device the two-step enzymatic reactions were carried out. Both enzymes were immobilized through streptavidin/avidin, biotin and phosphotidylcholine bi layer-coated PDMS walls. In the first step, glucose oxidase transforms D-glucose to the D-gluconolactone and hydrogen peroxide is liberated (**Fig. 6**).

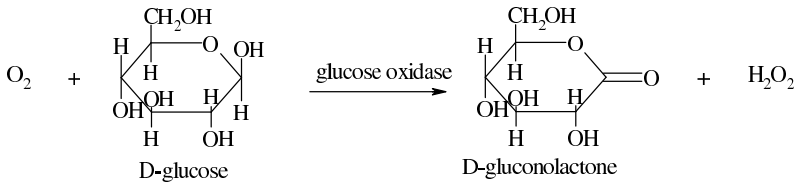

Fig. 6. Biotransformation of glucose by glucose oxidase.

Formed hydrogen peroxide was detected in the second step by conversion of Amplex red (which has little fluorescence) to the high fluorescent molecule resorufin (**Fig. 7**).

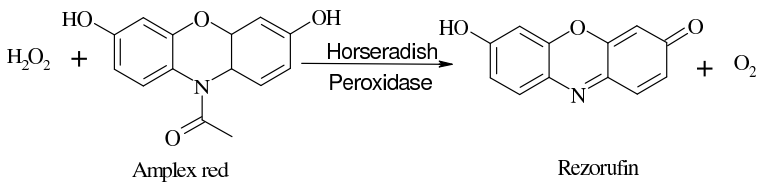

Fig. 7. Biotransformation of Amplex red by horseradish peroxidase.

This reaction was catalyzed by horseradish peroxidase. The fluorescence signal of the product-resorufin was monitored by the fluorescence microscopy.

The enzymatic fluorescence biosensors can be constructed also with hexokinase. Hexokinase conformational changes, induced by glucose, are detected. H. Maity et al. used bis(1-anilino-8-naphthalenesulfonate) (bis-ANS) (**Fig. 8**) as a reporter of changes in the enzyme conformation.[17]

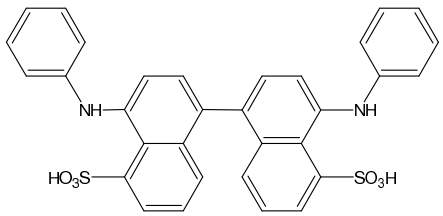

Fig. 8. The structure of bis(1-anilino-8-naphthalenesulfonate) (bis-ANS).

Bis-ANS binds to different sides of protein, depending on the peptide conformation. Two binding modes can be distinguished by spectrofluorimetry measurements. When bis-ANS binds to enzyme, the slow increase in fluorescence intensity is observed, but in the presence of glucose this changes are significantly slower, which allows for the detection of the bioanalyte.

It is known, however, that the hexokinase loses its activity very quickly at room temperature. The enzymes such as human hexokinase or yeast hexokinase are very unstable, so assays that employ them are difficult to perform. Because of long-term stability it is better to use hexokinase from thermophilic microorganisms. S. D'Auria[18] at al. used glukokinase from *Bacillus stearothermophilus* and they compared its activity and intrinsic fluorescence with the activity of yeast hexokinase. The yeast hexokinase loses its activity in several days and decrease of fluorescence intensity is observed. On the contrary, an activity of the hexokinase from thermophilic bacterium

remaines constant over two weeks. In this work a sensing mechanism of resonance energy transfer (RET) was used. Competitive assay for glucose was described where the intrinsic tryptophan emission of unmodified enzyme was used as a donor of electrons. On the other hand *o*-Nitrophenyl-*β*-D-glucopiranoside (ONPG) (**Fig. 9**) was employed as an acceptor.

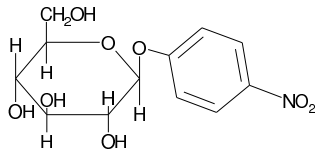

Fig. 9. Structure of o-Nitrophenyl-β-D-glucopiranoside (ONPG).

The addition of ONPG causes the decrease of fluorescence intensity of enzyme. Further addition of glucose results in recovery of fluorescence intensity. So glucokinase from *Bacillus stearothermophilus* can be used as a sensor for glucose.
The enzyme itself can be also modified by some fluorimetric agent. J.F. Sierra at al[19] used glucose oxidase that was covalently attached to fluorescein-5(6)-carboxamido-caproic acid ester. One of a drawbacks of optical methods is the fact, that experiments should be carried out in spectral area where small amount of organic compounds have a maximum of absorption and emission. Otherwise the real samples require pretreatment. The above mentioned fluorophore has a fluorescence in less problematic area of spectrum ($\lambda_{excitation}$ = 489 nm, $\lambda_{emission}$ = 520 nm) and the fluorescence intensity of functionalized enzyme changed by the addition of glucose during the enzymatic reaction. The detection limit of this method was 85 mg/l. Moreover, this techque was applied to the determination of glucose in human serum samples and it gave similar results to those obtained by commercial clinical analyzer.

1.3. Non- invasive glucose measurement

Available methods of glucose determination have a great influence on the increase of diabetes care. However most of commercially available devices for glucose

monitoring have also disadvantages as a discomfort of blood collection and the fact that the glucose level is not measured during sleep or during absorbing activities (e.g. car driving). As a result, hypo- or hyperglycemia threat can pass unnoticed. The most important goal is to avoid traditional blood sampling and to monitor the glucose level constantly in non-invasive[20,21] way in vivo. An interesting example of enzymatic glucose monitoring is a non-invasive method known as a GlucoWatch®. This is the electronic device, being worn like a watch, which measures the level of glucose without injuring the skin. The procedure of determination of glucose is an extraction of glucose through skin by reverse iontophoresis.[22] The glucose is biotransformed by glucose oxidase immobilized in gel matrix and liberated hydrogen peroxide is detected by amperometric biosensor. The measurement is taken every 10 min so disorders in glucose level can be detected. On the other hand this device has also some disadvantages. Although the correlation between traditional blood testing and GlucoWatch® is rather good, sometimes the results of glucose level measurement by this method are different from traditional ones. It can be caused by some environmental changes on the surface of the skin. Some skin irritation occurs as a result of drastic conditions such as sweating or cold temperature.

Another attitude to dealing with the problem of the continuous determination of glucose is a needle type enzymatic electrode.[23] This technique employs glucose oxidase as the catalyst of biotransfomation of glucose to gluconolactone and hydrogen peroxide, that is amperometically detected. The sensor is implemented into the subtucaneous tissue so the detected glucose level is very similar to that obtained from the blood. However some problems with unpredictable drift and impaired response in vivo arose. As a result, the device must be several times a day calibrated against traditional glucose determination associated with blood sampling.

There are already some non-invasive enzymatic methods of glucose determination, there is however still a great field for improvement. [24]

2. Enzymatic detection of other sugars

Enzymes can be also very useful in the determination of sugars in food samples. Usually food samples are complicated matrixes which contain a lot of interfering

compounds, so traditional analytical methods require an extraction step. On the contrary, techniques which use high specificity of enzymatic reactions are much more resistant to the disturbing agents.

M. Luzzana et al. presented an application of kinase (**Fig. 10**) in determination of sugars (glucose, fructose, glycerol, gluconic acid) in milk and wine.

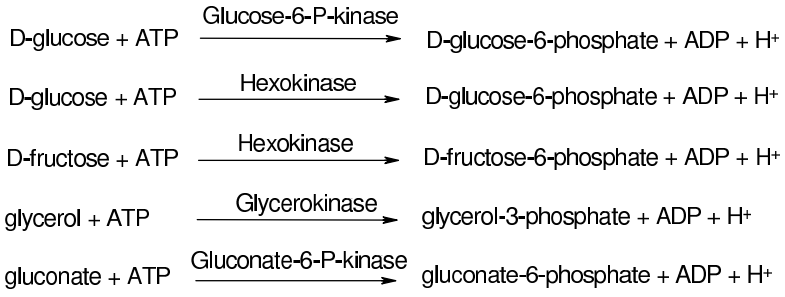

Fig. 10. Enzymatic biotransformation of sugars.[25]

In this research ATP (adenozine triphosphate) is coupled with previously mentioned sugars in the presence of kinases. This biotransformation produces an acidification of reaction solution and as a result the pH changes can be detected and quantify. This method allows to determine a wide concentration range of sugars (1-1500 mmol/L).

S. Campuzano at all presented another attitude towards simultaneous determination of sugars.[26] According to this work the bienzyme biosensor was established, that allows for the determination of glucose and fructose synchronously. On a gold electrode surface 3-mercaptopropionic acid (MPA) self-assembled monolayer was created. Than MPA was coupled to glutaraldehyde. In the last step glucose oxidase, fructose dehydrogenase and mediator tetrathiafulvalene (TTF) were immobilized to the aldehyde group of glutaraldehyde. The constructed biosensor was used for simultaneous determination of fructose and glucose in honey, cola softdrink, apple juice and the results were comparable with those obtained using other reference methods.

Enzymatic reactions are also used to determine the level of disaccharides. P. Thavarungkul et al. presented the method that employs enzymatic reaction in determination of sucrose in sugar cane juice.[27] Sucrose is produced from sugar cane and sugar beets. Extracted sucrose is very useful in food industry since it is often used as a sweetener and nutrient in fermentation process. So from the commercial point of view the content of sucrose in sugar cane should be determined. In literature biotransformation using an enzyme invertase is mentioned. In this research enzyme was immobilized by cocrosslinking on the membrane of the sensing thermistor. The enzyme transforms the sucrose to glucose and fructose and the heat that was generated is measured by the thermistor. This method used the batch injection analysis (BIA) which is described by J. Wang and Z.Taha.[28] As the enzyme was immobilized small its amount were used what is an advantage because enzymes usually are very expensive. Morover, the constructed system responses fast and no interferences caused by others compounds are observed.

Another approach to the application of enzymes in sucrose determination is the analysis of sucrose in coffee beans.[29] The amount of sucrose in coffee beans differs among the species and sources of coffee. The authors presented a method which is easy to handle and cheaper than previous procedures. Invertase was used to hydrolyze sucrose to the glucose and fructose (**Fig. 11**). Than glucose was transformed to D-gluconolactone and hydrogen peroxide by another glucose oxidase. In the last step hydrogen peroxide was involved in the reaction with 4-aminoantipyrine and phenol-4-sulfonic acid sodium salt in the presence of peroxidase. The final product was pink dye with absorption maximum at 505 nm.

Not only enzymes themselves are used for sugar determination but also the whole cells with many enzymes inside. Such biosensors have less selectivity but the application of whole cells instead of one particular extracted enzyme can be very useful because of higher stability of this catalysts. This idea was used in the construction of biosensor for amperometric xylose (**Fig. 12**) detection.[30]

The Gluconobacter oxydans (whole cells) where immobilized noncovalently on chromatographic paper and attached to the surface of a Clark's electrode. The

detection range of the biosensor was 0.5 – 20 mM and was successfully compared with enzymatic electrodes.

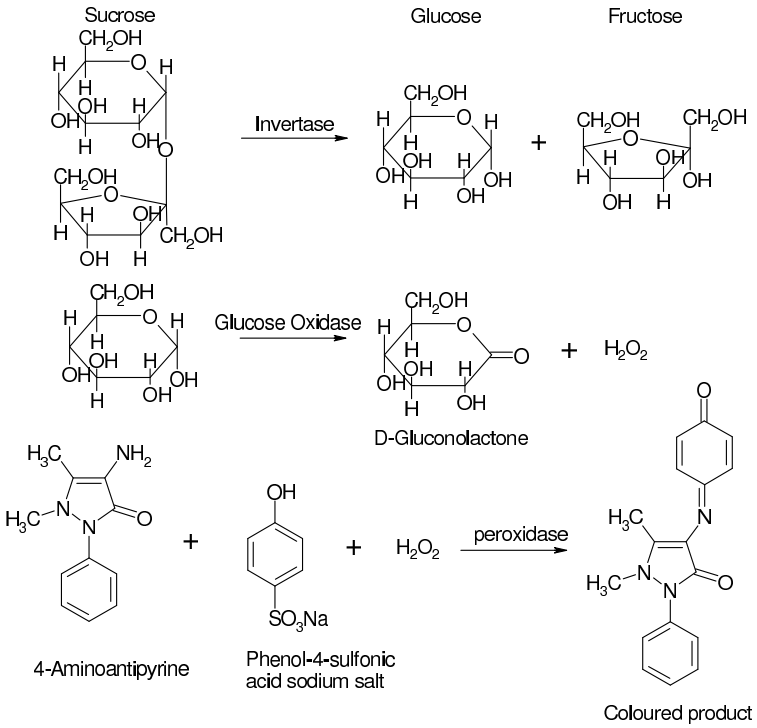

Fig. 11. Biotransformation of sucrose.

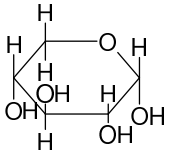

Fig. 12. Structure of xylose

Concluding remarks

Much afford was made to establish new systems for the analysis of the sugar content, especially in blood samples and in food samples, using enzymatic assays.

Enzymatic methods of glucose determination are widely used in commercial applications, because of great importance of glucose level determination especially in diabetes. Enzymatic methods of glucose monitoring contribute to better control of diabetes and improve live of people suffering from this disease. Moreover, they are still developed to increase the comfort of patients and monitor the glucose level constantly in least invasive way. So this is the field for microtechnology to improve the methods of sugars determination especially in vivo.

Acknowledgement

The authors thank the Polish Ministry of Science and Higher Education for financial support grant No. R0501601 in years 2006-2008.

References:

1. K. Faber, Biotransformation in Organic Chemistry, Springer 1997;
2. J. Kraly, Md. A. Fazal, R. M. Schoenherr, R. Bonn, M. M. Harwood, E. Turner, M. Jones, N. J. Dovichi, Bioanalytical Applications of Capillary Electrophoresis, *Analytial Chemistry*, 2006, *78*, 4097-4110;
3. P. Camilleri, Capillary Electrophoresis, Theory and Practice, 1998, CRC Press LLC;
4. J. Wang, M.P. Chatrathi, G.E. Collins, Simultaneous microchip enzymatic measurements of blood lactate and glucose, *Analytica Chimica Acta*, 2007, *585*, 11-16;
5. G. Chen, Y. Wang, P. Yang, Amperometric biosensor coupled to capillary electrophoresis for glucose determination, *Microchimica Acta*, 2005, *150*, 239-245;
6. G. Piechotta, J. Albers, R. Hintsche, Novel micromachined silicon sensor for continuous glucose monitoring, *Biosensors and Bioelectronics*, 2005, *21*, 802-808;
7. A. Salimi, R.G. Compton, R. Hallaj, Glucose biosensor prepared by glucose oxidase encapsulated sol-gel and carbon-nanotube-modified basal plane pyrolytic graphite electrode, *Analytical Biochemistry*, 2004, *333*, 49-56;

8. R. Gupta, N.K. Chaudhury, Etrapment of biomolecules in sol-gel matrix for applications in biosensors: Problems and future prospects, *Biosensors and Bioelectronics*, 2007, *22*, 2387-2399;
9. J.R. Lakowicz, Principles of Fluorescence Spectroscopy, Kluwer Academic/ Plenum Publishers;
10. Z. Rosenzweig, R. Kopelman, Analytical Properties and Sensor Size Effects of Micrometer-Sized Optical Fiber Glucose Biosensor, *Analytical Chemistry*, 1996, *68*, 1408-1413;
11. H. Mao, T. Yang, P.S. Cremer, Design and Characterization of Immobilized Enzymes in Microfluidic Systems, *Analytical Chemystry*, 2002, *74*, 379-385;
12. P. S. Dittrich, K. Tachikawa, A. Manz, „Micro Total Analysis Systems. Latest Advancements and Trends", Anal. Chem., (2006), 78, 3887-3908;
13. A. Manz, N. Gaber, H. Widmer, Miniaturized total chemical analysis systems: a novel concept for chemical sensing, *Sens. Actuators B*, 1990, *1*, 244-248;
14. Y. Liu, C.D. Garcia, Ch.S. Henry, Recent progress in the development of μTAS for clinical analysis, *Analyst*, 2003, *128*, 1002-1008;
15. M. Tokeshi, Y. Kikutani, A. Hibara, K. Sato, H. Hisamoto, T. Kitamori, Chemical processing on microchips for analysis, synthesis, and bioassay, *Electrophoresis*, 2003, *24*, 3583-3594;
16. R. Ehrnstrom, Miniaturization and integration: challenges and breakthroughs in microfluidics, *Lab Chip*, 2002, *2*, 26N-30N;
17. H. Maity, S.R. Kasturi, Interaction of bis(1-anilino-8-naphthalenesulfonate) with yeast hexokinase: a steady-state fluorescence study, *Journal of Photochemistry and Photobiology B*, 1998, *47*, 190-196;
18. S. D'Auria, N. DiCesare, M. Staiano, Z. Gryczynski, M. Rossi, J.R. Lakowicz, A novel fluorescence competitive assay for glucose determinations by using a thermostable glucokinase from the thermophilic microorganism *Bacillus Stearothermophilus*, *Analytical Biochemistry*, 2002, *303*, 138–144;
19. J.F. Sierra, J. Galban, S. De Marcos, J.R. Castillo, Direct determination of glucose in serum by fluorimetry using a labeled enzyme, *Analytica Chimica Acta*, 2000, *414*, 33–41;

20. J.D. Newman, A.P.F. Turner, Home blood glucose biosensors: a commercial perspective, *Biosensors and Bioelectronics*, 2005, *20*, 2435-2453;
21. A. Tura, A. Maran, G. Pacini, Non-invasive glucose monitoring: Assesment of technologies and devices according to quantitative criteria, Diabetes Research and Clinical Practise, 2007, *77*, 16-40;
22. M.J. Tierney, J.A. Tamada, R.O. Potts, L. Jovanovic, S. Garg, Clinical evaluation of the GlucoWatch® biographer: a continual, non-invasive glucose monitor for patients with diabetes, *Biosensors and Bioelectronics*, 2001, *16*, 621-629;
23. J.J. Mastrototaro, The MiniMed Continuous Glucose Monitoring System, *Diab. Technol. Ther*, 2000, 2 (Suppl. 1), 13–18;
24. J.C. Pickup, F. Hussain, N.D. Evans, N. Sachedina, In vivo glucose monitoring: the clinical reality and the promise, *Biosensors and Bioelectronics*, 2005, *20*, 1897–1902;
25. M. Luzzana, D. Agnellini, P. Cremonesi, G. Caramenti, Enzymatic reactions for the determination of sugars in food samples using the differential pH technique, *Analyst*, 2001, *126*, 2149-2152;
26. S. Campuzano, Ó.A. Loaiza, M. Pedrero, F.J.M. Villena, J.M. Pingarrón, An integrated bienzyme glucose oxidase-fructose dehydrogenase-tetrathiafulvalene-3-mercaptopropionic acid-gold electrode for the simultaneous determination of glucose and fructose, *Bioelectrochemistry*, 2004, *63*, 199-206;
27. P. Thavarungkul, P. Suppapitnarm, P. Kanatharana, B. Mattiasson, Batch injection analysis for the determination of sucrose in sugar cane juice immobilized invertase and thermometric detection, *Biosensors & Bioelectronics*, 1999, *14*, 19-25;
28. J. Wang, Z.Taha, Batch injection analysis, *Analytical Chemistry*, 1991, *63*, 1053-1056;
29. A. Álcázar, J.M. Jurado, M.J. Martin, F. Pablos, A.G. González, Enzymatic-spectrophotometric determination of sucrose in coffee beans, *Talanta*, 2005, *67*, 760-766;

30. A.N. Reshetilov, P.V. Iliasov, M.V. Donova, D.V. Dovbnya, A.M. Boronin, T.D. Leathers, R.V. Greene, Evaluation of Gluconobacter oxydans whole cell biosensor for amperometric detection of xylose, *Biosensors & Bioelectronics*, 1997, *12*, 241-247.

Chapter 4

Chirality of Resorcinarenes

Alicja Wzorek and Waldemar Iwanek

Institute of Chemistry, Pedagogical University, Chęcińska 5, 25020 Kielce, Poland

1. Introduction.

Resorcinarenes **1** belong to the macrocycles compounds called calixarenes [1-4] which are forming in reaction of resorcinol or resorcinol derivatives with an aliphatic or aromatic aldehyde [5]. Synthesis methods of resorcinarenes, potential possibilities for using these compounds as synthetic receptors as well as selected examples of theirs applications in HPLC and GC chromatography were described suitably in the first part and in the second part of the monograph concerning the synthetic molecular receptors [6-7]. The molecular structures as well as cavity character of these compounds are shown in Figure 1.

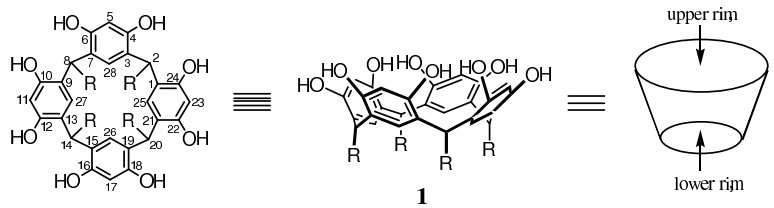

1

Figure 1.

The presence of so many active sites makes this compound convenient platform for synthesis of the new types of resorcinarenes. Their relatively simple chemical modifications can provide a great number of derivatives having the predeterminate

stereochemical proprieties. Structure of this molecule creates many possibilities for the synthesis of new chiral derivatives by modifications of this structure which lead to the structurally chiral derivatives. The hydroxyl groups and "*ortho*" position are the most frequently employed for this purpose. Besides, introduction of the chiral auxiliaries through the mentioned modifications creates the next possibilities for the synthesis of chiral derivatives.

The resorcinarenes, along with their wealth of non-covalent interactions, including hydrogen bonds, hydrophobic interactions, charge-transfer interactions, arene-π-cationic interactions, ion-dipole interactions, and so on, can be excellent models of chiral receptors in biological processes mimicry.

Search for the new effective supramolecular systems exhibiting selective differentiation play and will play more and more roles in the nearest future caused by increasing demands on enantiomeric pure pharmaceutical compounds, pesticides as well as foodstuff. Finally, these compounds can be used for synthesis of receptors interacting selectively with tumour markers.

Easy and various modifications of these class compounds allow us to assume, that we will observe further development of their synthesis methods (including chiral derivatives) as well as these compounds will found many others applications.

In this review we try to systematize information about possible types of chiral resorcinarenes as well as present examples of synthesis methods of these compounds.

2. The general synthesis method of chiral resorcinarenes.

Chirality is the property, which is not limited to the simple molecules. Any given chemical object (eg., the macrocyclic compound) can be optically active, provided it is not identical with its mirror image. In addition, it can also possess the elements of symmetry belonging to the point groups: C_n ($n \geq 1$), D_n ($n > 1$), T, O, or I. However, it cannot possess the plane of symmetry, the centre of symmetry nor the alternating axis [8]. From several possible conformation of resorcinarene, the crown conformer is the most attractive for functionalisation due to the possibilities of forming various chiral derivatives having cavity which is capable of enclosing small molecule of guests.

The chiral resorcinarene derivatives can be obtained by two methods.

1. The first one consists in synthesis or transformation of resorcinarenes in such derivatives which have no stereogenic centre, and their optical activity is a consequence of their spatial structure associated with C_1 symmetry („inherently chiral"), C_2 or C_4 symmetry;
2. The second synthesis method of the chiral resorcinarene derivatives consists in use to synthesis a) suitable chiral derivatives of resorcinol; b) introduction the groups having stereogenic centers into the resorcinarene; c) using suitably selected the chiral aldehydes to the synthesis.

Both general approaches into synthesis of chiral derivatives of the resorcinarene are illustrated in Figure 2:

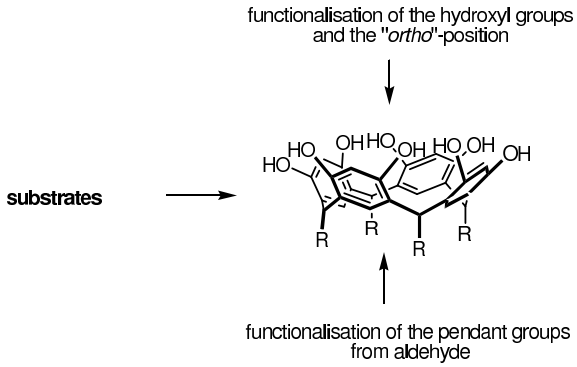

Figure 2.

Introduction of the chiral auxiliary into upper rim of the resorcinarene platform is the most interesting due to the presence of suitable active sites as well as with point of view to increasing of the macrocycles cavity.

These functionalisation can proceed by modification of definite number of hydroxyl groups or "*ortho*" position in resorcinarene. The appropriate choice of reagents and reaction conditions enables the asymmetric synthesis, which leads to the chiral resorcinarene derivatives.

3. **Stereochemical nomenclature of axial symmetric compounds.**

With regard to various possible modifications of hydroxyl groups leading to structural chiral compounds as well as creating the cyclic compounds with part of hydroxyl groups and „*orto*"-position, stereochemical designation of synthesised compounds was not equal. As a consequence of different viewing of the macromolecule- from position inside or outside the cavity, authors described in many various ways direction of closing new cyclic ring or axial chirality of the compounds received by modifications of hydroxyl groups. In 2006 year Heaney and co-workers [9,10] proposed standardization of stereochemical designation for the resorcinarene derivatives. The most important rules of stereochemical designation for the resorcinarene derivatives are explained using an example of representation of resorcinarene with four modified hydroxyl groups, only one in each resorcinol unit, what makes this compound structural chiral with the C_4 symmetry, given in Figure 3.

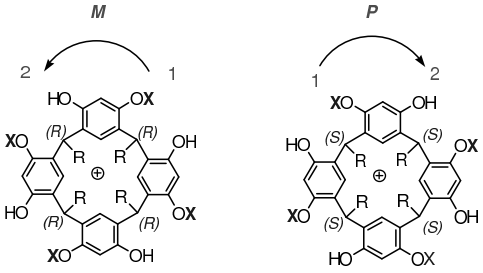

Figure 3. Stereochemical nomenclature of the C_4 symmetric compounds.

As shown in Figure 3, in the stereochemical designation of the C_4 symmetric resorcinarenes we define in following sequence: 1) the priority of the substituents groups of upper rim around an axis of symmetry viewed from a position above the cavity (axial chirality)- *M* or *P*; 2) the configuration of stereocenters in chiral auxiliary; 3) the configuration of the carbon atoms in bridge connecting resorcinol units in lower rim. The *P* and *M* notation is used to define the axis of chirality of C_n symmetric resorcinarenes. A clockwise priority of the sequence of groups that are

attached to the phenolic groups is defined to have *P* axial chirality. In the opposite case- when the priority of substituents is counter-clockwise, we use notation *M*.

In the case of derivatives, in which the forming ring can be oriented outside or inside the resorcinarene cavity, we add to the general accepted rules of the stereochemical nomenclature the prefixes "*out* "- outside or "*in* "- inside cavity. Besides, if the new stereocenters are generated during the course of reaction, we enclose theirs configuration as the next positions in the stereochemical designation for this type of macrocycles.

In the next part of review we will use the rules of stereochemical nomenclature of C_4 symmetric compounds described above.

4. Functionalisation of hydroxyl groups in the resorcinarene.

The resorcinarenes belong to the macrocycles compounds which are characterised by great reactivity. One of the reasons of the reactivity is the presence of the hydroxyl groups in resorcinarene structure, which used for reaction with suitably selected reagents to give the new various derivatives having the new physico-chemical properties. The hydroxyl groups play also a crucial role in stabilisation of the crown conformation. Modification of the hydroxyl groups can be done by transformation correspondently: all eight hydroxyl groups (A); four (B,C) or only one of hydroxyl group (D).

In the case of modification of four hydroxyl groups, there are possible two types of approach:

1) modification of the hydroxyl groups on the resorcinarene platform, what leads to the suitably transformed -OH groups from the opposite resorcinol units in resorcinarenes (B);
2) the choice of appropriate mono-substituted resolcinol derivatives for cyclisation reaction with an aldehyde, which leads to resorcinarene derivative with only one modified hydroxyl group in each resorcinol unit (C). General possibilities for modification of hydroxyl groups are shown in Figure 4.

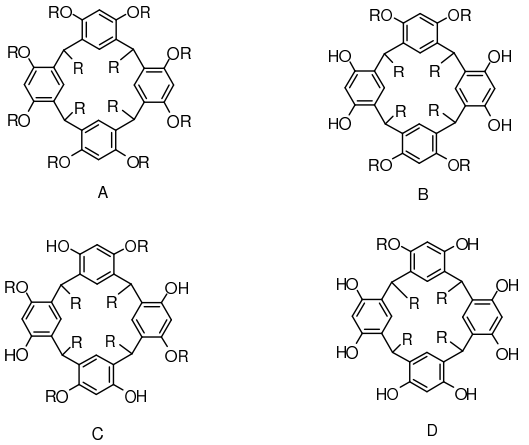

Figure 4.

4.1. Functionalisation of one hydroxyl group in the resorcinarene.

Modification of one resorcinol unit in the achiral forms of the resorcinarene **1** makes them chiral and having the C_1 symmetry (Figure 5) [11], called often the „inherently chiral". The optical activity of these compounds is not a result of the presence of groups having stereogenic centres; it results from their spatial structure. The molecule as a whole has no plane of symmetry, any inversion centre or the alternating axis of symmetry.

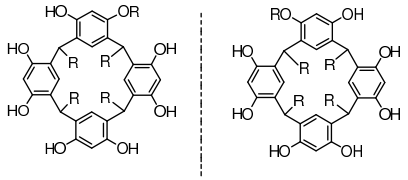

Figure 5.

Many examples of functionalisation of only one out of eight possible OH groups are known in the literature. The reaction of resorcinarene **1** with 4-methylbenzyl chloride in the presence of potassium butoxide as a base in anhydrous DMF under an inert gas atmosphere leads to the racemic mixture of the monobenzyl derivative **2.** Treating the obtained monobenzyl derivative of resorcinarene **2** with acetic anhydride

in the presence of pyridine leads to the heptaacetate, which debenzylated by action of trimethylsilyl bromide yields the monohydroxyheptaacetate **3** (Scheme 1) [12].

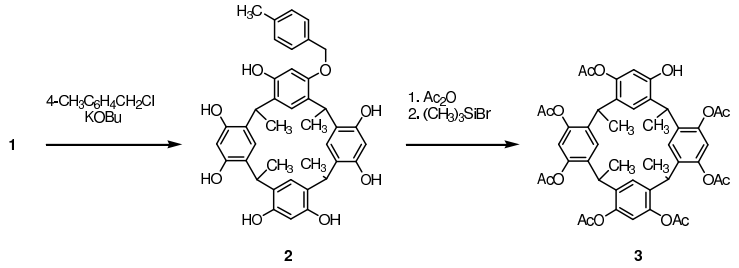

Scheme 1.

Each step of the presented synthesis affords the products in the form of a racemate. The authors did not deal with resolution of these racemates.

Monofunctionalisation of the crown conformer of resorcinarene **1** having was carried out using the optically active (S)-(+)-camphorosulphonyl chloride and gave a mixture of two diastereoisomers **4a** and **4b**, which was separated by HPLC [13]. The separated diastereoisomers **4a** and **4b** were reacted with diazomethane, what resulted in substituted hepta-O-methyl derivatives **5a** and **5b**. The enantiomerically pure „inherently chiral" resorcinarenes **6a** and **6b** were synthesised by subjecting the hepta-O-methyl resorcinarene derivatives **5a** and **5b** to an alkaline hydrolysis (Scheme 3).

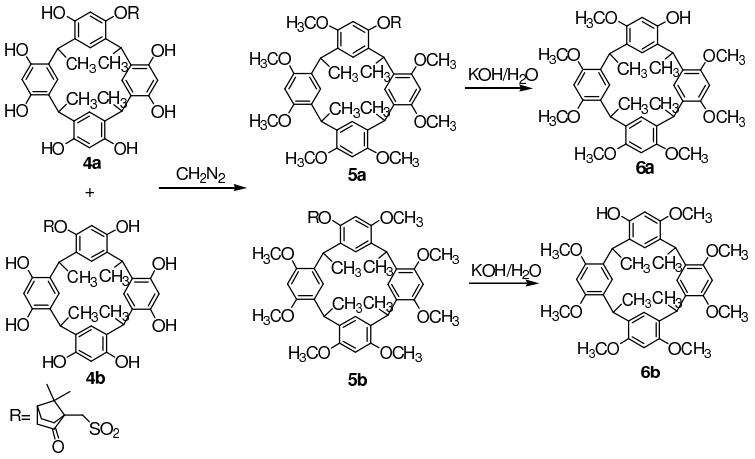

Scheme 2.

4.2. Functionalisation of four hydroxyl groups in the resorcinarene.

The possibilities for functionalisation of four hydroxyl groups were shown in Figure 4.

The first method consists in functionalisation of OH groups of the starting resorcinarene **1**, what leads to the resorcinarene derivatives having the C_{2v} symmetry, where the hydroxyl groups belonging to two opposite resorcinol units are modified. The tetraphospho-O-resorcinarenes **7** as well as the tetrasulpho-O-resorcinarenes **8** (Figure 6) have been synthesised in this way [14-15].

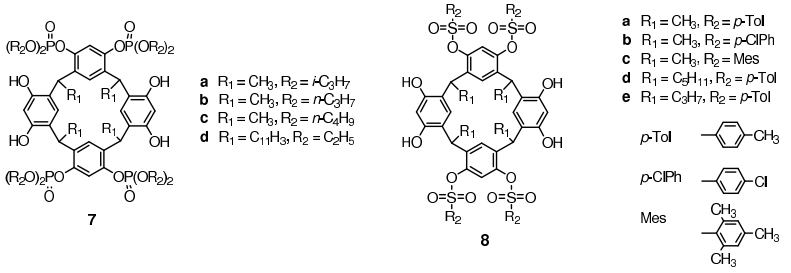

Figure 6.

The resulting tetra-O-substituted derivatives of resorcinarenes having the C_{2v} symmetry are optically inactive. They can however be transformed into chiral compounds by introducing the groups containing stereogenic centres.

The second method of synthesis of the tetra-O-substituted resorcinarenes consists in treating the mono-substituted resorcinol derivatives with aldehydes. The products having the C_4 symmetry are obtained in the form of racemic mixtures (Scheme 3). These compounds are characterised by only one modified hydroxyl group in each resorcinol unit. Such a condensation is catalysed by Lewis acids [16-18].

The method for resolution of the racemic mixtures of tetra-O-methylresorcinarenes **9**, which were synthesised in high yield by cyclisation of monomethylresorcinol with aliphatic aldehydes, was presented by Mattay [17]. Monofunctionalisation of one OH group of the components of the racemate **9** using S-(+)-camphorsulphonyl chloride leads to the mixture of two diastereoisomers **10a, 10b**

separable by HPLC. The alkaline hydrolysis of the diastereoisomers **10a** and **10b** affords the enantiomerically „inherently chiral" tetra-O-substituted resorcinarenes **(+)-9** and **(-)-9** in the yield of 72% and 70%, respectively (Scheme 4).

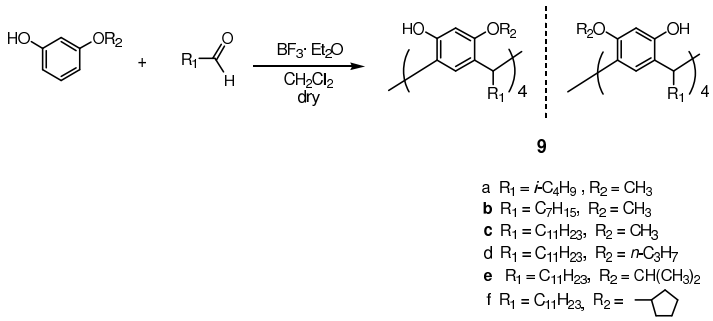

Scheme 3.

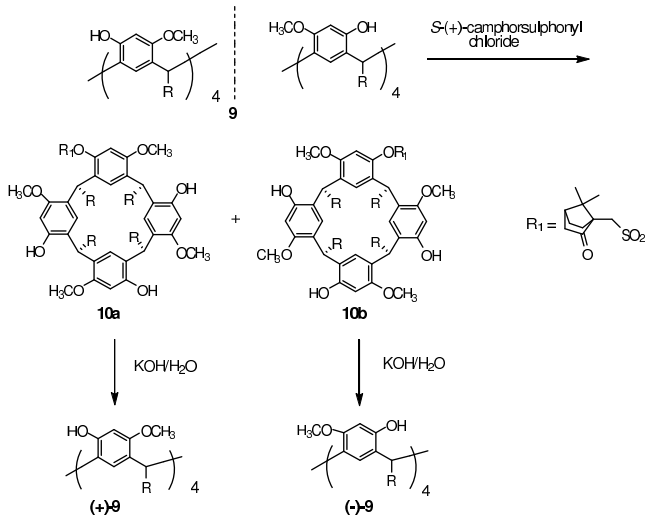

Scheme 4.

In the case, when the condensation reaction employs the chiral 3-[(*2S*)-2-methylbutoxy]phenol **11**, one step yields the mixture of two diastereoisomeric tetra-O-

(2-methylbutyl)resorcinarenes **12a** and **12b**, which can be easily separated by HPLC (Scheme 5) [17].

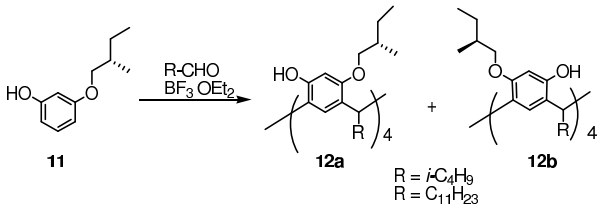

Scheme 5.

The optically active substrate alkoxyphenol **11** was prepared from resorcinol and (2S)-(-)-2-methylbutyl ether [18].

4.3. Functionalisation of eight hydroxyl groups in the resorcinarene.

With regard to the presence of eight hydroxyl groups in resorcinarene structure, there are several possible routes of their transformation, what is shown in Figure 7.

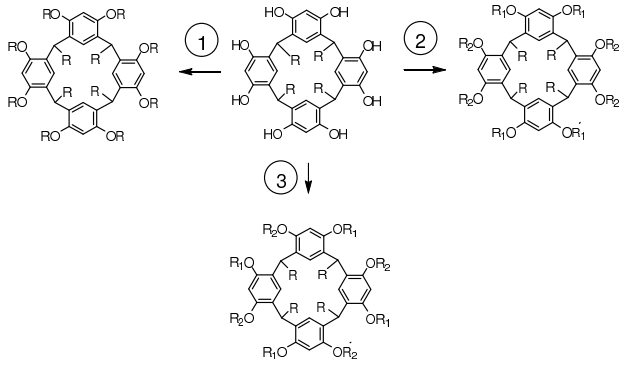

Figure 7.

1. The first method of functionalisation consists in transformation of hydroxyl groups by direct introduction of chiral auxiliary or indirectly by initial transformation of hydroxyl groups into, for example, ester derivatives and subsequent modification of this groups using chiral auxiliaries.

2. The second method consists in initial transformation of four hydroxyl groups of the resorcinarene platform, and further modification of four residual in opposite resorcinol units. This functionalisation can proceed also (similary to 1) directly or indirectly using chiral auxiliaries. Chiral derivatives of resorcinarene can be received through introduction of suitable stereocentres into four or eight modified hydroxyl groups.

3. The third method consists in synthesis of the structurally chiral resorcinarenes having the C_4 symmetry from suitable substrates (see Figure 4, product c). Subsequent separation of received racemic mixture provides the enantiomers with one free hydroxyl group in each resolcinol units. Further modification of these residual hydroxyl groups can be chiral or achiral. Chiral modification leads to diastereoisomers while achiral modification leads to chiral derivatives of resorcinarenes having the C_4 axial symmetry. This type of chirality is often called as a cyclochirality.

Examples of the synthesis of the resorcinarene derivatives having functionalised all hydroxyl groups are also known in the literature [19-25].

Iwanek prepared octaester **13** in 85% yield from resorcinarene **1** and ethyl bromoacetate. Octaester **13** was then melted with chiral amines: (*R*)(+)-phenylethylamine, (S)(-)-phenylethylamine, (S)(+)-cyclohexylethylamine, (*R*)(-)-cyclohexylethylamine, or chiral amino alcohols: (S)(+)-2-amino-1-butanol, (*R*)(-)-2-amino-1-butanol, (+)-norephedrine, (-)-norephedrine, to give the corresponding enantiomers of tetraoctaamidoresorcinarenes **14** and **15** (Scheme 6) [26].

The octamide derivatives of resorcinarene **15a** synthesised from (R)-2-amine-1-butanol were employed for chiral discrimination of amino acid sodium and potassium salts. The stationary phase was prepared by impregnation process of chiral resorcinarene **15a** with polymeric carriers (for example- silica gel). The experiments results show that the L-enantiomers of phenylglycine sodium salts and tryptophan sodium salts were discriminated from D-enantiomers. In addition, the mixture of sodium and potassium salts of the following pairs of chiral pure amino acid: phenylalanine–tryptophan, phenylglycine–tryptophan were separated by column chromatography [27].

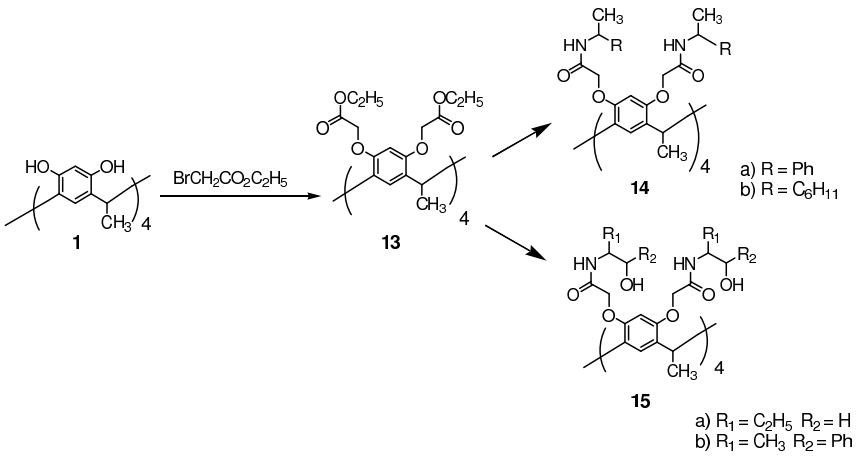

Scheme 6.

Chiral octamide-derivatives of resorcinarenes **16** with long chain having chiral urea termini onto each hydroxyl groups are known in literature (Figure 8).\

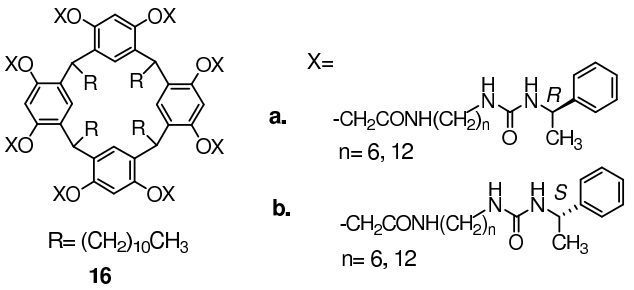

Figure 8.

The presence of the eight amide groups in upper rim creates the possibility of formation intramolecular cyclic hydrogen bonds along the wide of the resorcinarene **16** in non-polar solvents (chloroform). The hydrogen bonds can be oriented in two directions- clockwise or counter-clockwise, what results in creation of two cycloenantiomers (Figure 9). The direction of closing of the hydrogen bonds is controlled by the neighboring chiral termini.

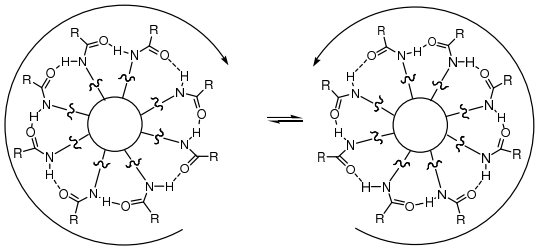

Figure 9.

The formation of asymmetric cyclic hydrogen bonds is responsible for appearing the unique CD spectra in chloroform, in which the information on the chirality of the termini is transferred to the absorption wavelength of the macrocycle (chirality transmission). These characteristic CD spectra for the urea-functionalized macrocycles disappeared upon complexation with anions such as chloride and bromide. The CD spectra also disappeared in solution chloroform- methanol $CHCl_3$/ CH_3OH (3:97 v/v). Methanol breaks intramolecular hydrogen bonds [28].

An example of the synthesis of chiral octa-N-bromo-L-valine-tert-butylamide derivative of resorcinarene **18** is also known in the literature**.** The starting resorcinarene **17** was prepared by condensation of resorcinol and 10-undecenal. The subsequent reaction with N-bromo-L-valine-tert-butylamide led to the chiral product **22** (40% yield), in which all hydroxyl groups have been functionalised. The presence of double bond at the lower rim of **18** enabled hydrosililation in the presence of platinum catalyst. This gave the polysiloxane chiral calixarene **19.** This compound appeared to be an effective chiral stationary phase (named Chirasil-Calixval) and was used for successful separation of substituted amino acids. (Scheme 7) [29].

In search for the universal chiral stationary phase in enantioselectivity gas chromatography capable of separating racemic mixture of polar as well as of non-polar compounds, the new stationary phase were prepared by catalytic hydrosililation of equimolar mixture of octakis-*O*-[(L-val-*tert*-butylamide)-*N*-acetyl]-C-decenyl-resorcinarene **18** and monokis-*O*-octenyl-permethyl-β-cyclodextrin **20**. This mixed nowel stationary phase named Chirasil-Calixval-Dex, retains the individual

enantioselectivites of the single components (Chirasil-Calixval and Chirasil-Dex) and is capable of separation the enantiomers of polar amino acid and of apolar enantiomers such as unfuncionalised hydrocarbons - as a results of the presence cyclodextrin selector [30, 31].

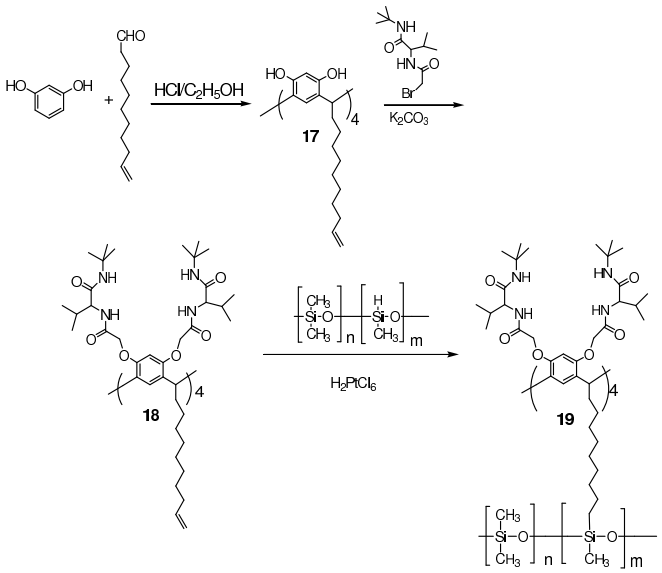

Scheme 7.

Chiral stationary phase in HPLC named RES-Phe **21** were synthesised from resorcinarene derivative containing eight L-phenylalanine ethyl esters units onto each hydroxyl groups (Figure 10). This stationary phase can be used in normal-phase as well as in reversed-phase and were appropiate to separation a variety of racemate of pharmaceutical compounds. For example, the enantiomers of analgetic ketoprofen were separated with hexane/ 2-propanol 9:1 (v/v) and addition of 0.1% triethylamine [32].

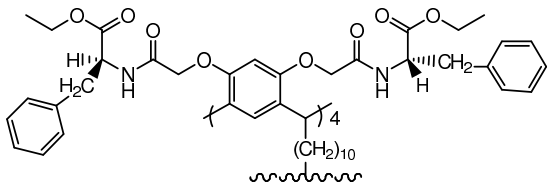

21

Figure 10.

Eight hydroxyl groups can be also substituted by the groups derived from saccharides: galactose, glucose, maltose [33-36]. Such derivatives **22** are prepared by reactions of octaamino resorcinarenes with the appropriate lactone derivatives of sugars.

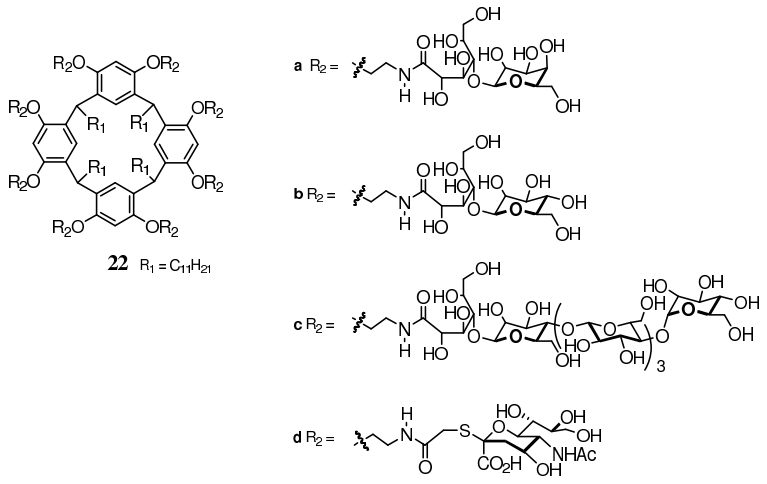

22 $R_1 = C_{11}H_{21}$

Figure 11.

The resorcinarene containing carbohydrate units in theirs structure are interesting objects for investigation, which are employed in potential application of these compounds as artificial glycoviral vector to gene delivery what can open a new strategy of less cytotoxic gene delivery [37].

The next trend in biological investigation is the use of carbohydrate derivatives of resorcinarene for synthesis of new type of proteoglycan mimics which plays important roles in regulation biological cell activities by adhesion process [38].

In search for a therapeutic agent, which could effectively cross-link the neoplastic cells, compound **23** was synthesised (Figure 12). The biological tests demonstrated that the compounds containing many saccharide units in their structure are capable of enclosing the mutant cells and, therefore, inhibiting their further growth as well as metastasis [39].

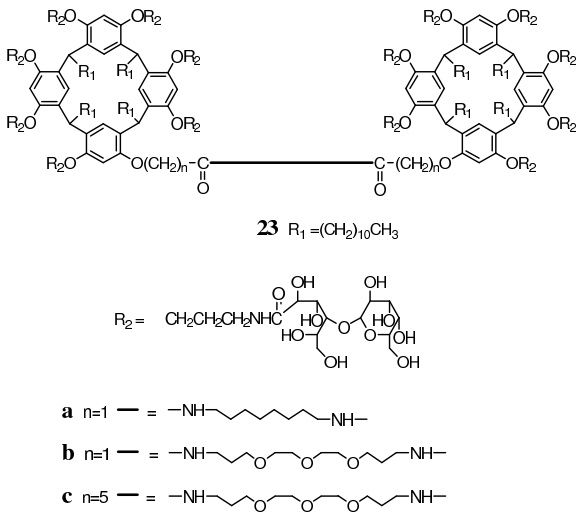

Figure 12.

Alkylation of racemic mixture of tetramethoxyresorcinarene **9** with ethyl 2-bromoacetate results in the formation of a racemic mixture of octa-derivatives **24a** and **24b**. The subsequent aminolysis of this racemic mixture with chiral (-)-phenylethylamine to give two „inherently chiral" diastereoismers: **25a** and **25b,** which can be separate by column chromatography (Scheme 8) [40].

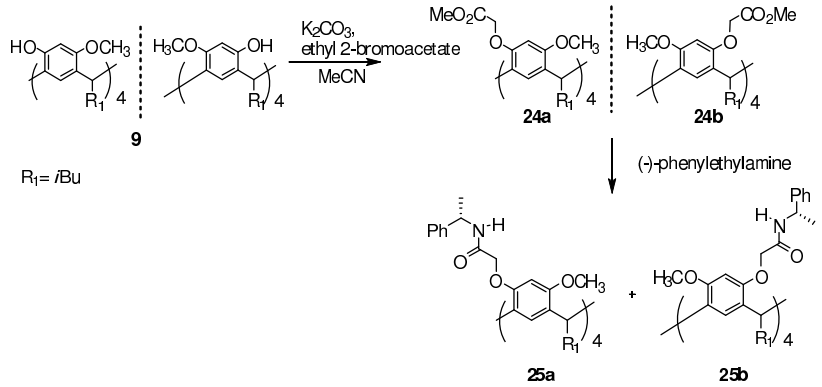

Scheme 8.

The corresponding tetraamid0-derivatives of resorcinarene **25** can be received in one -step reaction from tetraalkoxyresorcinarene **9** or tetraester-resorcinarene **24** and chiral 2-bromo-*N*-[(*R*)-(+)-(α-methylbenzyl)]acetamide by heating the substrates under reflux in acetonitrile for 15 hours. The resulting diastereoisomeric mixture can be easy separate by column chromatography (Scheme 9)[9].

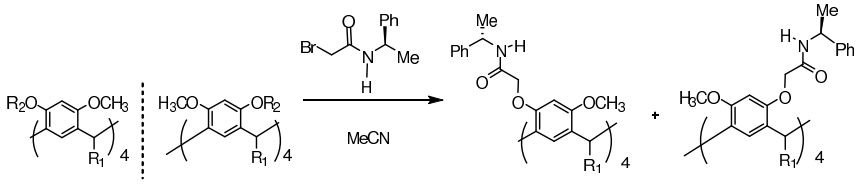

24 R_1= n-C_7H_{15}, R_2= CH_2CO_2Et
9b R_1=nPr, R_2= H
9c R_1= n-C_7H_{15}, R_2= H
9d R_1= n-$C_{11}H_{23}$, R_2= H

a. R_1= nPr
b. R_1= n-C_7H_{15}
c. R_1= n-$C_{11}H_{23}$

Scheme 9.

The reaction of enantiomerically pure tetraalkoxyresorcinarenes **(+)-9** and **(-)-9** (or **12a** and **12b**) with (S)-(-)-2-methylbutyl tosylate (or methyl iodide) affords the enantiomerically pure „inherently chiral" octaalkoxy derivatives **26a** and **26b** (Scheme10) [40].

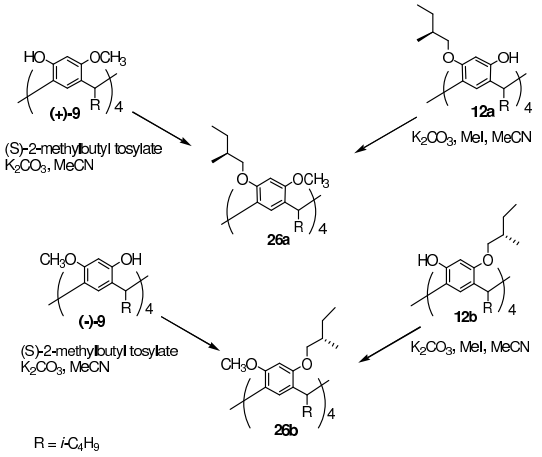

Scheme 10.

The reaction of racemic tetraalkoxyresorcinarene **9** with (S)-(+)-10-camphorosulphonyl chloride can lead to tetra-, tri-, di- or mono-camphorosulphonyl derivatives of tetraalkoxyresorcinarene depending on following components: the bulkiness of alkoxy groups in resorcinarene, the reaction condition used as well as the amount of chloride used [10].

Tetracamphorosulphonate derivatives **27** were synthesised by heating the racemic tetrmethoxyresorcinarene **9** with an excess of (S)-(+)-10-camphorosulphonyl chloride under reflux in pyridine. The resulting mixture of diastereoisomers: *(M,S,R)*- and *(P,S,S)*-27 were separated by column chromatography (Scheme 11).

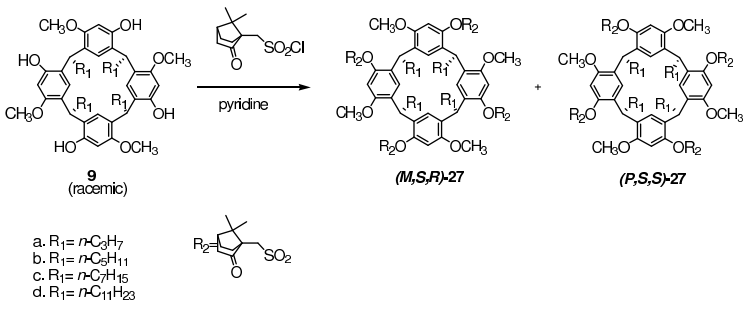

Scheme 11.

In the case of reaction of resorcinarene **9b** with 12 equiv. (S)-(+)-10-camphorosulphonyl chloride heated under reflux for 15 hours in pyridine, the mixture of two diastereoisomeric tetracamphorosulfonates: *(M,S,R)*-27b and *(P,S,S)*-27b together with the two diastereoisomeric tricamphorosulfonates: *(M,S,R)*-28b and *(P,S,S)*-28b were obtained. The tricamphorsulfonates were formed in a 1:4 ratio while the tetracamphorsulfonates were formed in a 4:1 ratio (Scheme 12).

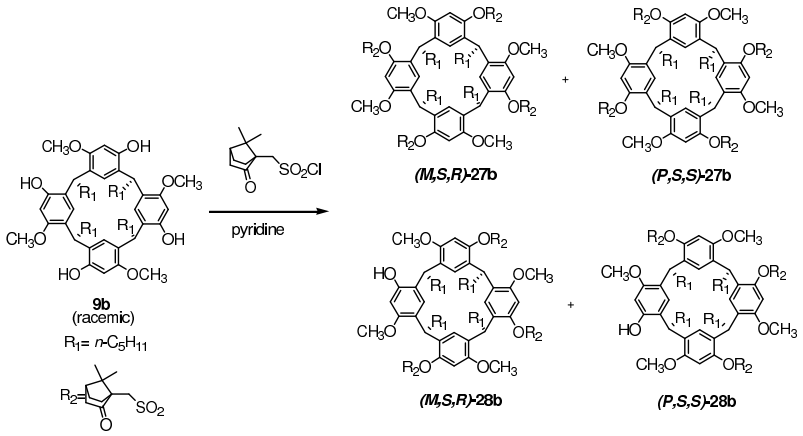

Scheme 12.

The reaction of tetraalkoxyresorcinarenes **9** having bulkier izopropyl groups with (S)-(+)-10-camphorosulphonyl chloride (12 equiv.) carried out in pyridine as a solvent and in the presence of DMAP lead to diastereoisomeric mixture of monocamphorsulphonates **29** (Scheme 13).

In similar reaction of tetraisopropyloxy- or tetracyclopentyloxyresorcinarenes **9** with (S)-(+)-10-camphorosulphonyl chloride, in which the DMAP were omitted, the dicamphorosulphonates **30** were formed.

The camphorosulphonyl derivatives can be also prepared by two-steps method. In the first step, the tetralkoxyresorcinarene undergo deprotonation by the addition of n-butyllitium. In the next step, such obtained tetra-anions react with (S)-(+)-10-

camphorosulphonyl chloride to afford mixture of diastereoisomeric tetracamphorsulfonates or mixture of diastereoisomeric tri-, di- or monocamphorsulfonates depending on the reaction condition used.

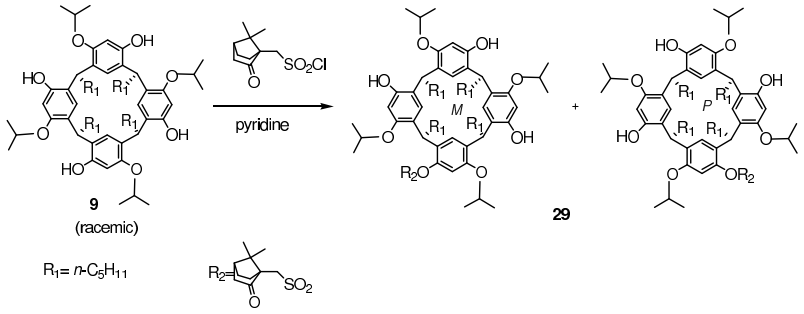

Scheme 13.

The reaction of racemic tetraalkoxyresorcinarenes with chiral (S)-(+)-10-camphorosulphonyl chloride as a chiral auxiliary affords mixture of two diastereoisomeric camphorsulphonates, which can be simply sapareted by column chromatography. The alcaline hydrolysis of the pure diastereoisomeric camphorsulfonates gives the enantiomerically pure tetraalkoxyresorcin[4]arenes. As described, this is a simple method of separation of racemic tetraalkoxyresorcinarenes[10].

The tetramethoxyresorcinarene bis crown ethers **31** were synthesised from tetramethoxyresorcinarene **9** and triethylene or tetraethylene glycol ditosylates (Scheme 14). The complexation properties of the compounds toward alkali metal cations were studied by ^{1}H NMR spectroscopic titration experiments and X-ray crystallography, which indicated that resorcinarene **31b** can accommodate two cations simultaneously inside the crown pockets formed by the crown ether bridges and the resorcinarene skeleton [41].

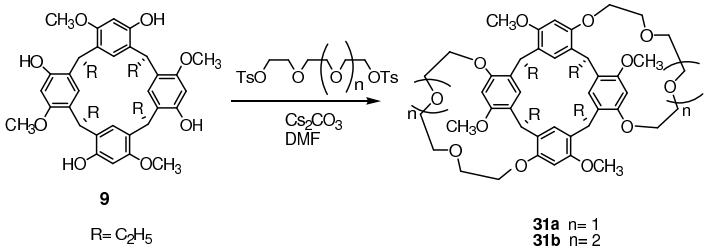

Scheme 14.

4. Functionalisation of the "*ortho*" position in resorcinarenes.

The presence of two electron-donating hydroxyl groups in the aromatic rings of resorcinarene renders the *ortho* position very susceptible to electrophilic substitution. Many electrophilic groups can be easily introduced at this position [42-43]. The *ortho* substituent capable of forming intramolecular hydrogen bonds with the neighbouring hydroxyl groups of the resorcinarene units enables formation of the chiral derivative, which has the C_4 symmetry. This is caused by formation of a cyclic structure which gives racemic mixture of enantiomers classified according to the new conception of nomenclature as: (*P, S*) and (*M, R*) *via* intramolecular hydrogen bonds.

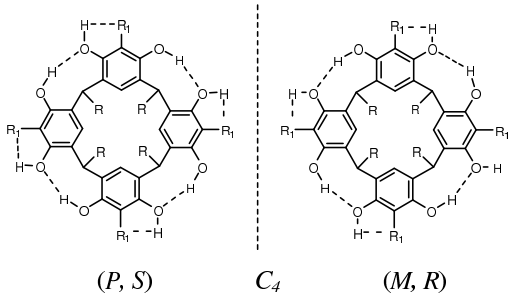

Figure 13.

The creation of the structurally chiral resorcinarene derivatives by introduction of substituents into „*ortho*" position capable of forming intramolecular hydrogen bonds with the neighbouring hydroxyl groups of the resorcinarene units is no limited

to only tetra-substituted resorcinarene but there is also theoretically possible in the mono-(D), di- (B,C)- and tri-substituted (A) resorcinarene, what is shown in Figure 14.

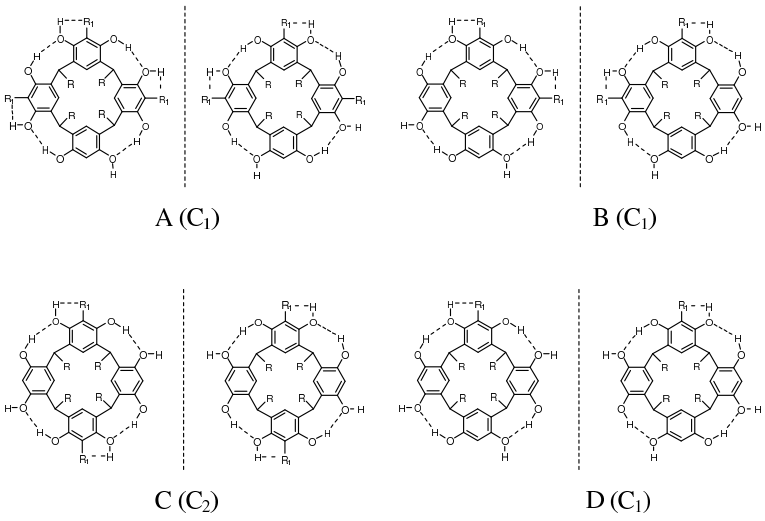

Figure 14.

Independently of synthesis of the structurally chiral resorcinarene derivatives („inherently chiral"), there is also possible functionalisation of „*ortho*"- position by direct or indirect introduction of the chiral auxiliaries. The examples of resorcinarene derivatives with modified „*ortho*" position we present below.

An example of a chiral derivative associated with C_4 symmetry is tetracarboxy-resorcinarene **32**, which was synthesised from 2-carboxyresorcinol and acetaldehyde [44].The carboxyl group of this derivative can participate in two types of intramolecular hydrogen bonds, as shown in Figure 15.

However, the most frequently employed reaction of electrophilic substitution for resorcinarenes is Mannich reaction. Depending on the type and amount of reagents used, various derivatives can be obtained. In the case of the achiral secondary amine, the aminomethyl derivative **33** having the C_4 symmetry is obtained (Figure 16). This conformation exists not only in the crystalline state but also in the solution, as confirmed by ^{1}H NMR spectra. Two doublets of doublets resulting from diastereotopic

protons of the Ar-CH_2-N group and two singlets of protons from phenolic hydroxyl groups are observed [45].

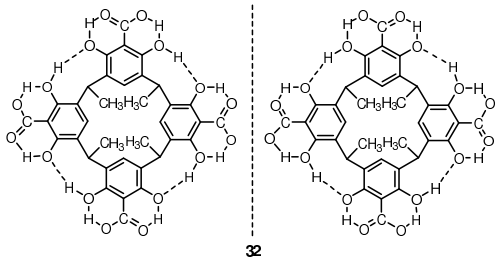

32

Figure 15.

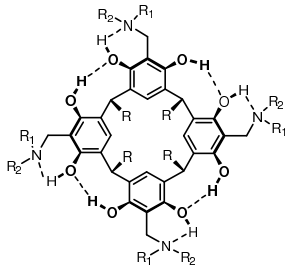

33

Figure 16.

Aminomethylation of resorcinarenes using chiral secondary amines should lead to two diastereoisomers having the C_4 symmetry. Indeed, this was observed for the aminomethylene derivatives **33** as well as the tetraoxazolidine derivatives **34** [46].

There are shown the possible routes for synthesis of the tetraamide derivatives of resorcinarene **37** in Scheme 15. The resulting resorcinarenes **37** exists in two cyclochiral conformation (cycloconformers) stabilized by belts of hydrogen bonds. The cycloisomeization process is characterised by the relatively high racemization barrier which were determined by 2D EXSY measurements. It can be explained that

the transformation of one cycloconformer into the others requires simultaneous rapture of all eight hydrogen bonds.

In the case of the amide substituted resorcinarene with additional stereocenters, two cyclodiastereoisomeric conformations were detected by the experiments. The experimental results were additionally supported by AM1 semi-empirical calculations [47].

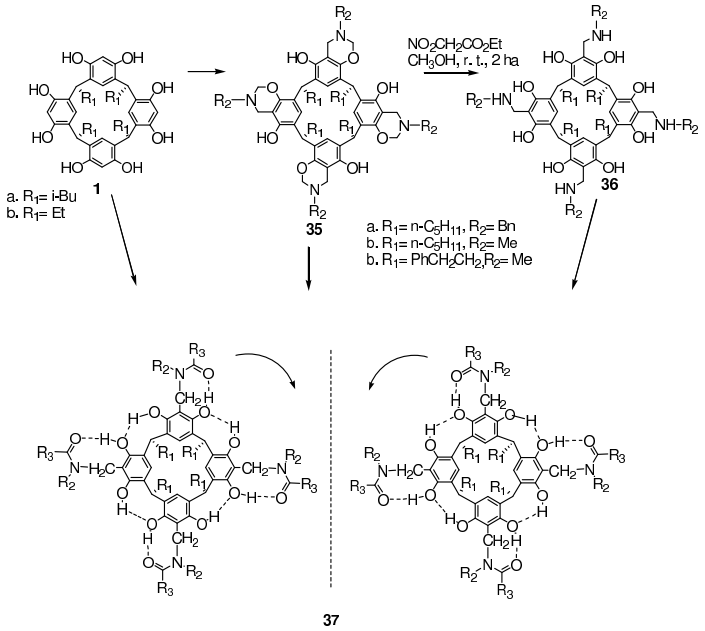

Scheme 15.

The product of Mannich reaction of resorcinarene **1** and *S*-1-(2-naphtyl)ethylamine were use for preparation of the chiral stationary phase **38** in HPLC named RES-Naph (Figure 17).The stationary phase **38** were capable of separation racemic pharmaceutical compounds in normal-phase. The separation of enantiomers of antidepressant mianserin and anaesthetic ketamine as well as 2-(n-propylthio)-3-naphtyl-4(3H)-chinazolinone were observed on this phase with hexane/ 2-propanol as an eluent with addition of 0.1% triethylamine [32].

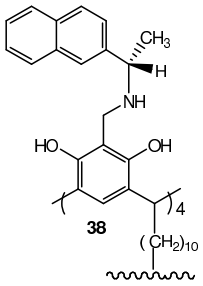

Figure 17.

Chiral 1,3-oxazolidine derivatives **34** are the products of Mannich reaction using chiral primary amino alcohols and formaldehyde, in the presence of catalytic amounts of KOH (Scheme 16)[48].

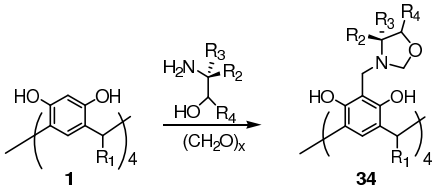

a $R_1 = CH_3$ $R_2 = H$ $R_3 = CH_2CH_3$ $R_4 = H$
b $R_1 = CH_3$ $R_2 = H$ $R_3 = CH_3$ $R_4 = C_6H_5$
c $R_1 = CH_3$ $R_2 = H$ $R_3 = C_6H_5$ $R_4 = H$
d $R_1 = CH_3$ $R_2 = H$ $R_3 = C_6H_5CH_2$ $R_4 = H$
e $R_1 = C_5H_{11}$ $R_2 = H$ $R_3 = CH_3$ $R_4 = H$
f $R_1 = C_5H_{11}$ $R_2 = C_2H_5$ $R_3 = H$ $R_4 = H$
g $R_1 = C_2H_5$ $R_2 = H$ $R_3 = CH(CH_3)_2$ $R_4 = H$
h $R_1 = C_2H_5$ $R_2 = H$ $R_3 = CH_2CH(CH_3)_2$ $R_4 = H$

Scheme 16.

In turn, removal of the formaldehyde molecule from the oxazine derivative of resorcinarene *(M,S,R)*-39 results in formation of the chiral aminomethyl derivative of phenylethylamine **40** (Scheme 17) [49].

The oxazolidine derivatives: **34a** and **34b** as well as benzooxazine derivative *(M,S,R)*-**39** and aminomethyl derivative **40** were use as chiral ligands for investigation of chiral discrimination of the enantiomers of following amines: *S*- and *R*-phenylethylamine, *S*- and *R*-cyclohexylethylamine. In order to determine the influence

of chirality of the resorcinarene derivatives on the interaction with chiral amines, the changes in the UV-VIS absorption spectra of solution of the resorcinarens in different solvents were measured depending on the concentration of amines. On the base of these measurements, the formation of two types of complexes was indicated. The compositions of these complexes were determined by the Benesi-Hildebrandt equation. The authors concluded that there is no hight chiral discrimination in the interaction of chiral amines with chiral resorcinarenes, however the discrimination values were up to 20- 30% compeared to literature data on chiral discrimination by resorcinarenes [50-52].

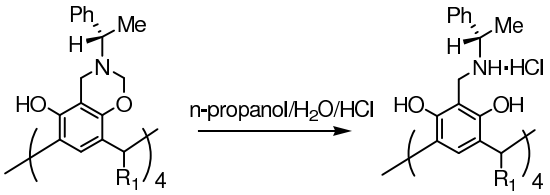

***(M,S,R)*-39** **40**

Scheme 17.

The oxazolidine derivative **34b** synthesised by the Mannich reaction from L-norephedrine were used for preparation of Langmuir monlayer in the water subphase for investigation of chiral recognition of amino acids. It was found that the properties of the Langmuir monolayer with basic ligand containing amino groups as well as the recognition abilities depends on pH of the subphase. The protonation of nitrogen atoms present in the resorcinarene **34b** affected the parameters of the surface pressure and surface potential isotherms. The investigations shown that the enantiomers of valine underwent chiral discrimination on this Langmuir monolayer depending on pH. At pH< 3.66, the D-valine form was recognised, in 4.50- 5.80 pH range no enantiomeric recognition was observed, at pH > 5.80 the L-valine enantiomer was recognized [53].

By subjecting resorcinarene, formaldehyde, and appropriate amino acids to Mannich reaction, the optically active resorcinarene derivatives have been synthesised,

which bear in 2-position the substituents containing stereogenic centres. The reaction with chiral amino acid L-proline leads to the chiral tetra-substituted resorcinarene **41** which is shown in Figure 18 [44, 54, 55].

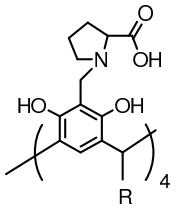

41 a. $CH_2CH(CH_3)_2$
b. $(CH_2)_{10}CH_3$

Figure 18.

The chiral L-proline derivatives of resorcinarene **41b**, with regard to their amphiphilic character: the presence of hydriphilic upper rim and hydrophobic lower rim, form the stabile Langmuir monolayer at the air-water interface (Figure 19).

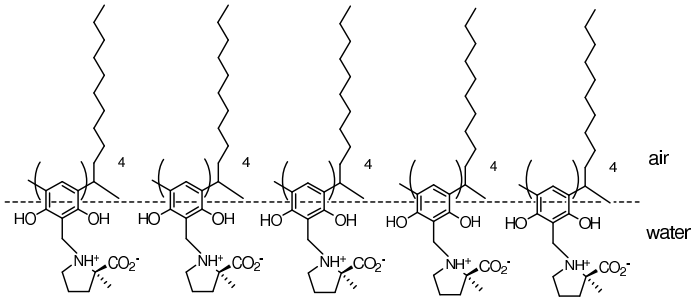

Figure 19.

The experiments demonstrate that this monolayer is slight stabilised by various cations such as: K^+, Cd^{2+}, Co^{2+}, Mg^{2+}, and Ni^{2+}. The monolayer exhibits the selectivity for copper (II) cation, caused by forming supramolecular complex, which has the recognition properties toward phenylalanine, with a greater affinity for D-enantiomer [56].

The chiral stationary phase in HPLC bearing L-prolyl moieties **43** were synthesised by hydrosililation of the chiral resorcinarene **42.** The resorcinarene **42** were received as a product of Mannich reaction of resorcinarene **17** with L-proline (Scheme 18)[57].

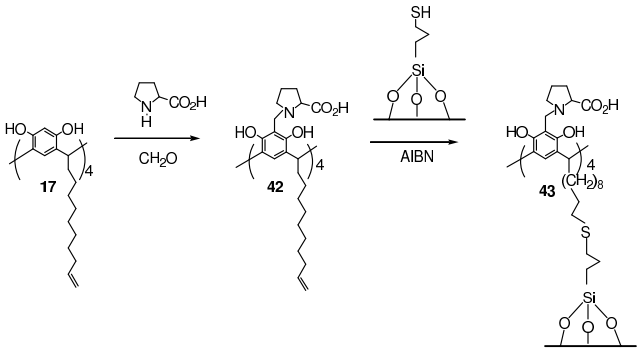

Scheme 18.

5. Mixed functionalisation of resorcinarenes.

Many examples of the resorcinarene derivatives having modified hydroxyl groups as well as „*ortho*" position in theirs structure are known in literature. These compounds will be described in this chapter and they will be ranged to the products which are received by mixed functionalisation.

Although a large number of synthesis such types compounds have been reported in literature we can make some helpful generalizations and introduce following types of experimentally observed resorcinarene derivatives.

1. This type of derivatives gathers the products of reaction which lead to formation of a new heterocyclic ring with a participation of hydroxyl groups and 2-position (Figure 20). These derivatives are stucturally chiral having the C_4 symmetry. If no chiral auxiliary is used, a racemic mixture is obtained. When a chiral reagent is used for formation of a new heterocyclic ring, then a diastereomeric mixture is formed, although the reaction is diastereoselective in many cases.

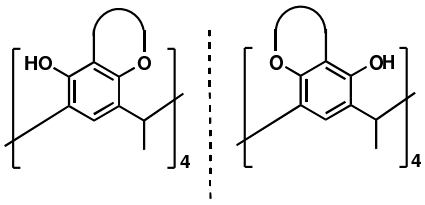

Figure 20.

2. In this type, the resorcinarene derivatives have four modified hydroxyl groups at the opposite resorcinol units and the heterocyclic rings, formed as described above, at the residual resorcinol units. These derivatives are structurally chiral having C_2 symmetry so the reaction leads to racemic mixture. In the case when chiral auxiliary was used for modification of hydroxyl groups or forming the heterocyclic ring, the diastereoismeric mixture is formed.

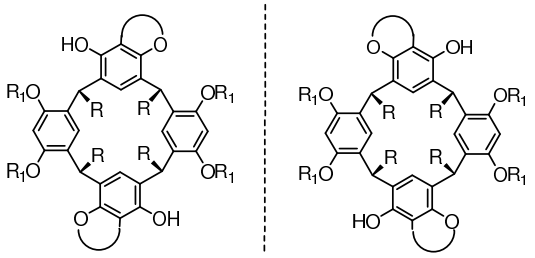

(*M, R*) C_2 (*P, S*)

Figure 21.

3. The next type of compounds with mixed functinalisation gathers together the axially chiral derivatives having four modified hydroxyl groups, only one in each resorcinol units (according to Figure 4, compound c) and substituents at „*ortho*" position (A) or heterocyclic rings formed with a participation of hydroxyl groups and „*ortho*"position (B)- Figure 22.

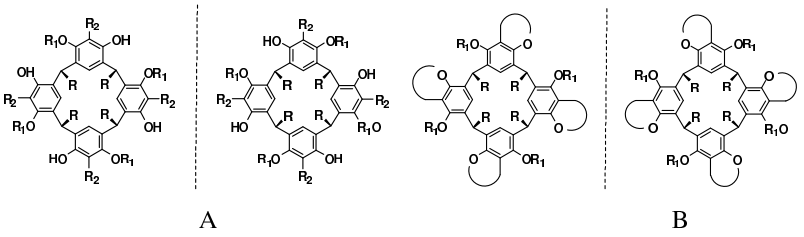

Figure 22.

4. The next type of mixed functionalisation gathers together the resorcinarene derivatives with four modified hydroxyl groups at the opposite resorcinol units (OR_1), and substituents at 2-position at one or two of the residual resorcinol units (R_2) (Figure 23).

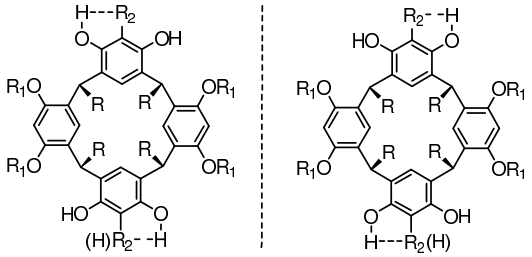

Figure 23.

The examples of chiral resorcinarene derivatives synthesised by mixed functionalisation are present below.

Aminomethylation of resorcinarene **1** with primary amines results in functionalisation of both 2-position and one of hydroxyl groups by formation of benzoxazine ring leading to the racemic mixture of resorcinarenes **35** having the C_4 axial symmetry (Scheme19) [58, 59].

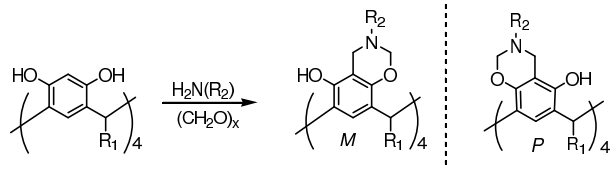

a $R_1 = CH_3$, $R_2 = C_6H_5$
b $R_1 = CH_3$, $R_2 = (CH_2)_nC_6H_5$
c $R_1 = CH_3$, $R_2 = C_6H_{11}$
d $R_1 = C_5H_{11}$, $R_2 = (CH_2)_nC_6H_5$
e $R_1 = C_5H_{11}$, R_2 = cykloheksyl
f $R_1 = C_5H_{11}$, R_2 = adamantyl
g $R_1 = C_5H_{11}$, R_2 = allil
h $R_1 = C_5H_{11}$, R_2 = 2-metoksyetyl
i $R_1 = C_5H_{11}$, R_2 = benzyl
j $R_1 = C_5H_{11}$, R_2 = 3,4-dimetoksybenzyl
k $R_1 = C_5H_{11}$, R_2 = 4-nitrofenyl
l $R_1 = C_{11}H_{23}$, R_2 = 6-hydroksyheksyl
m $R_1 = C_{11}H_{23}$, R_2 = benzyl
n $R_1 = C_{11}H_{23}$, R_2 = adamantyl

Scheme 19.

Mannich reaction of resorcinarene **1** with benzylamine yielded a racemic mixture of tetrabenzoxyresorcinarenes **35i**, which was separated by HPLC using CHIRALPAC AD chiral stationary phase (Scheme 19) [60].

The reaction of resorcinarene **1** and formaldehyde with chiral primary amines: either (*R*)-1-phenylethylamine or (*S*)-1-phenylethylamine, as well as their analogues (*para*-substituted with Br and Me), gave the corresponding diastereoisomer of tetrabenzooxazine **39** having the C_4 symmetry (Scheme 20).

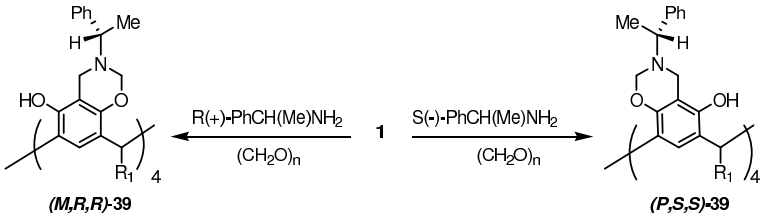

***(M,R,R)*-39** ***(P,S,S)*-39**

Scheme 20.

The reaction with (*R*)-1-aminoindane resulted in tetrabenzooxazine derivatives **44a** as a mixture of diastereoisomers (60:40) (Scheme 25). Similarly, use of (*S*)-1-(1-naphthyl)ethylamine led to a mixture of diastereoisomers **44b** [61].

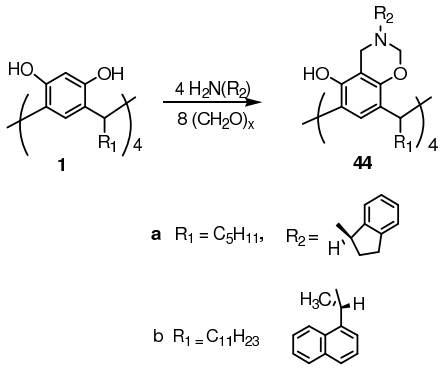

Scheme 21.

For some chiral amines or suitably adjusted reaction conditions, pure diastereoisomers can be obtained because of precipitation of one of the diastereoisomers [62]. Besides, the diastereoisomeric purity can be raised to 98% by opening the oxazine rings of the diastereoisomeric mixture **39** using trimethylchlorosilane, followed by repeated closure using sodium methoxide in methanol (Scheme 22) [63].

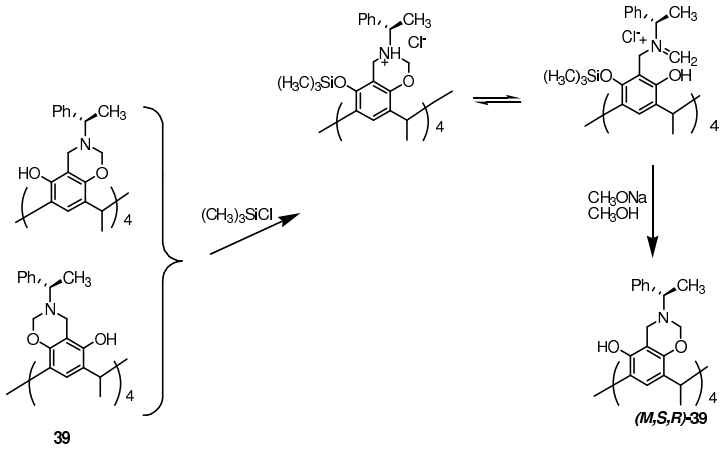

Scheme 22.

The tetraoxazine derivatives of resorcinarenes isomerise readily in acidic solutions: if R is not a chiral substituent, then racemisation occurs; if R has a stereogenic centre, then epimerisation is observed (Scheme 23) [58,60].

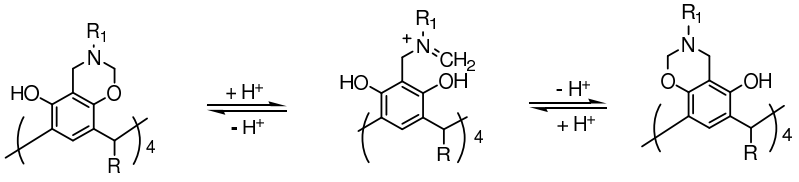

Scheme 23.

Heating the resorcinarene **1** with z N,N-bis(methoxy)-N-(S)- α-methylbenzylamine at 85 °C in toluene as a solvent lead to mixture of two diastereoisomers **39** in a ratio 1:1. Further heating of resulted diastereoisomeric mixture under reflux in ethanol gives chiral oxazine derivatives of resorcinarene ***(M,S,R)*-39** (Scheme 24) [64]

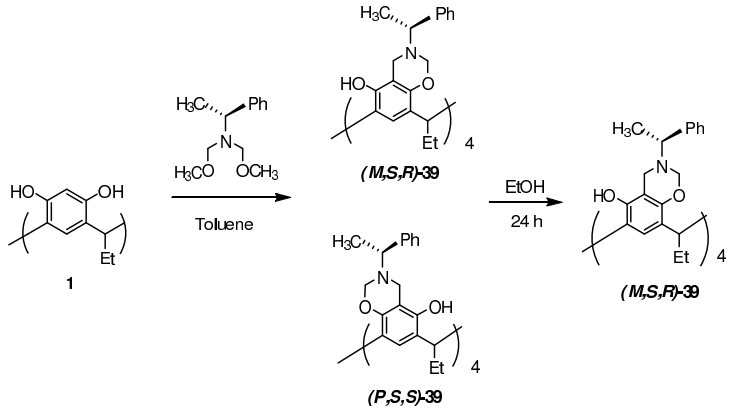

Scheme 24.

Enantiomerically pure derivatives **46** were synthesised from enantiomerically pure tetrabenzooxazine derivatives **45** in high yields (63-94%) by deprotonation of

residual free hydroxyl groups in this compounds by addtition of n-butyllitium at -78°C and subsequent alkylation in the presence of TfOMe or TfOEt (Scheme 25)[9].

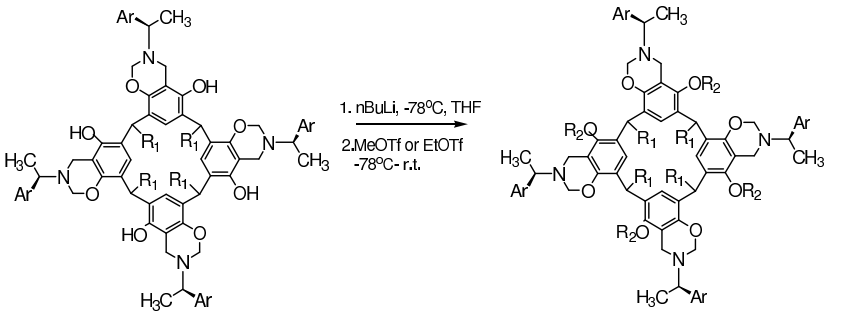

(P,R,S)-45

a. Ar= Ph, R_1= n-$C_{11}H_{23}$
b. Ar= Ph, R_1= $PhCH_2CH_2$
c. Ar= 4-$MeOC_6H_4$, R_1= n-$C_{11}H_{23}$

(P,R,S)-46

a. Ar= Ph, R_1= n-$C_{11}H_{23}$, R_2= CH_3
b. Ar= Ph, R_1= $PhCH_2CH_2$, R_2= CH_3
c. Ar= Ph, R_1= $PhCH_2CH_2$, R_2=Et
d. Ar= 4-$MeOC_6H_4$, R_1= n-$C_{11}H_{23}$, R_2= CH_3

Scheme 25.

Tetramethoxyresorcinarene **9** (racemic) heated with z N,N-bis(methoxymethyl)-N-benzylamine lub N,N-bis(2-metoxyethoxymethyl)-N-methylamine for 96 hours to afford racemic derivatives **47** in 73% yield (Scheme 26).

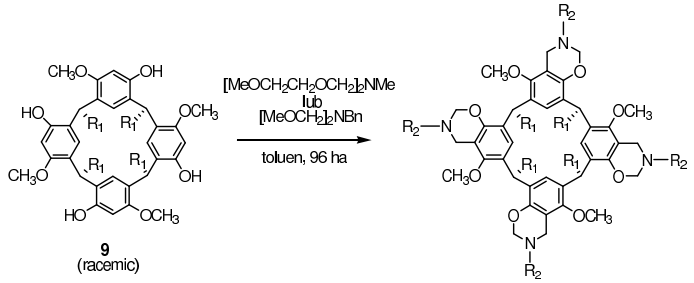

9
(racemic)
a. R_1= n-C_5H_{11},
b. R_1= $PhCH_2CH_2$,

47
(racemic)
a. R_1= n-C_5H_{11}, R_2= Bn
b. R_1= n-C_5H_{11}, R_2= Me
b. R_1= $PhCH_2CH_2$,R_2= Me

Scheme 26.

Reaction of racemic tetraalkoxyresorcinarene **9** and chiral ethers, synthesised from *R*- lub *S*-(α-methylbenzyl)amine, carried out in mixture of xylenes as a solvent under reflux gives after 96 hours diastereoisomeric mixture of **48a** and **48b** in a ratio 1:1 separable by column chromatography (Scheme 27).

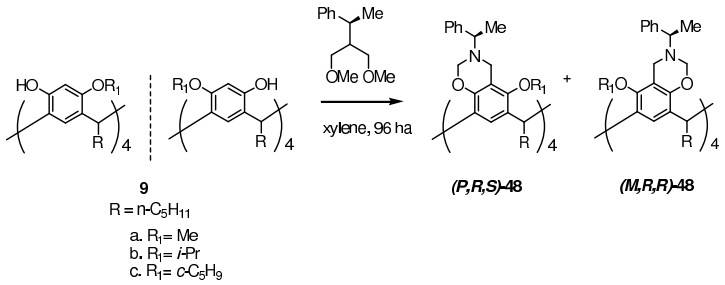

9
R = n-C_5H_{11}
a. R_1= Me
b. R_1= *i*-Pr
c. R_1= *c*-C_5H_9

***(P,R,S)*-48** ***(M,R,R)*-48**

Scheme 27.

The synthesis shown in Scheme 26 and Scheme 27 affords the resorcinarene derivatives: **47** and **48** with good yields, however these synthesis required the long time of heating at high temperatures. This observation promoted Haney's group to investigate the use of microwave-assisted Mannich reaction for synthesis of resorcinarenes derivatives. There are some advantages of the use microwave-assisted reaction in comparison to traditional method in solvent. The cleaner products can be obtained in shortened time in improved yield.

There is shown synthesis of racemic resorcinarene **49** in Scheme 28. The racemic tetramethoxyresorcinarene **9** heated in bis(dimethylamin)-methane in microwave apparatus affords after 10 min and a power of up to 300W a quantitative yield of compound **49.**

Reactions of bis(aminol) ethers with tetraalkoxyresorcinarenes with the use of focused microwave irradiation afford after short time racemic resorcinarene derivatives **50** (Scheme 29) [9].

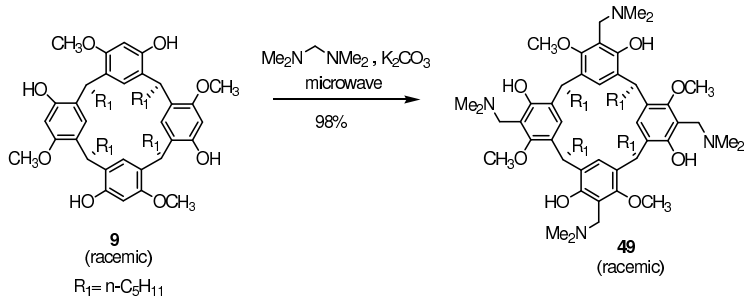

Scheme 28.

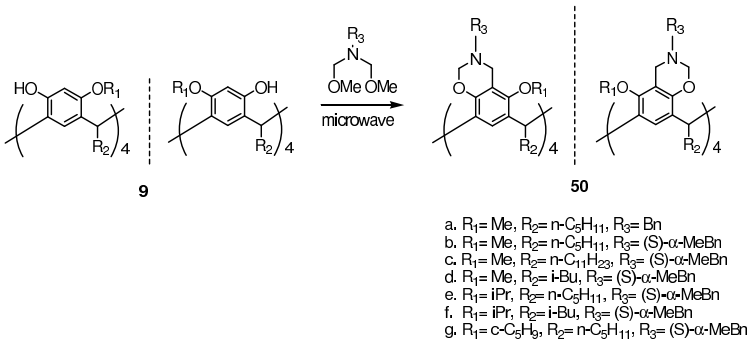

Scheme 29.

As a result of regioselective condensation of tetratosyl resorcinarenes **8a** with formaldehyde and selected primary amines, the corresponding bis-oxazine tetratosyl resorcinarenes **51** were prepared in high yields (above 65%) (Scheme 30) [65].

Theoretically, two regioisomers of bis-oxazine resorcinarenes **51** can be formed: a chiral structure having oxazine rings *trans* to each other, having double axial symmetry as well the *meso* form having oxazine rings *cis* to each other and a plane of symmetry (see Figure 24). The product analysis indicates exclusive formation of chiral *trans*-**51.**

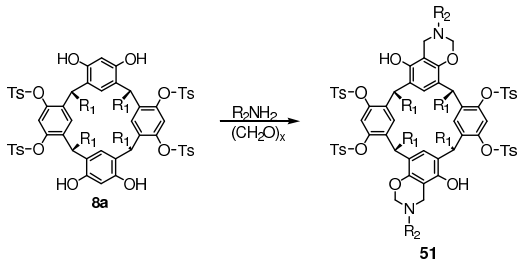

Scheme 30.

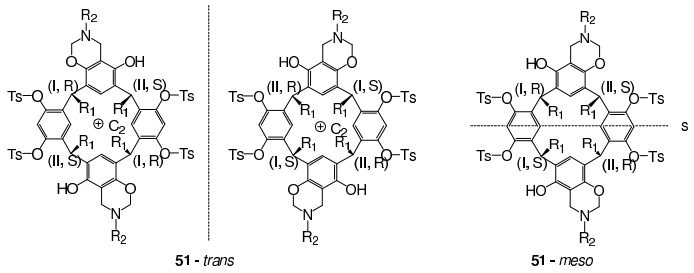

Figure 24.

Condensation of chiral *R*-α-cyclohexylethylamine with tetratosyl derivatives **8a** led to formation of two diastereoisomers having the C_{2v} symmetry in a ratio of 60:40.

Aminomethylation of tetratosyl derivatives of resorcinarenes with diamines having a sufficiently long alkylene chain R can result in formation of novel derivatives of resorcinarenes **52**, where two opposite oxazine units are linked by this alkylene chain (Figure 25).

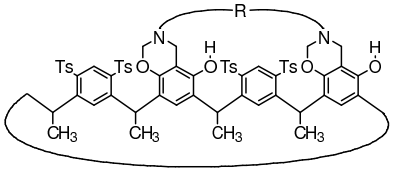

52

a R = -$(CH_2)_2O(CH_2)_2O(CH_2)_2O(CH_2)_2$-
b R = -$(CH_2)_3O(CH_2)_4O(CH_2)_3$-
c R = 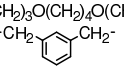

Figure 25.

Aminomethylation of tetratosyl derivatives of resorcinarenes **8a** with diamines having short alkylene chain, such as ethylenediamine, produces only macrobicyclic dioxazines **53** (Figure 26).

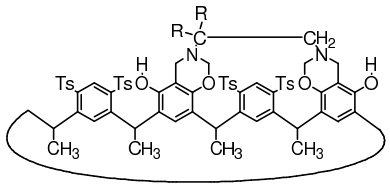

53

a R = H
b R = CH_3

Figure 26.

Tetratosyl derivative of resorcinarene **8a** undergo the Mannich reaction with formaldehyde and N-methylamide derivatives of amino acid: racemic phenylalanine, (S)-phenylalanine, racemic phenylglycine or (S)-phenylglycine in the presence of catalytic amounts of acetic acid to afford cyclochiral mono- (**54A**) or dibenzooxazine (**54B**) derivatives of tetratosyled resorcinarenes depend on types of amide derivatives of amino acid used as well as heating time. In the case of reaction with using racemic or enantiomeric phenylalanine N-methylamides after short heating time, the racemic or enantiomerically pure monobenzooxazine derivatives were obtained in good yields, while after longer heating time the dioxazine derivatives were obtained. The Mannich

reaction with phenylglycine methylamide, despite many different conditions used, affords only monooxazine derivative **54A-b** (Figure 27) [66]. X-ray structure of monobenzooxazine derivatives indicates that these compounds are the boat conformers, which can be classified as *(M,S,R)*- isomers according to the new stereochemical nomenclature proposed by Haney. The amino acid arms is involved in an intramolecular hydrogen bond across the molecule, that is, the carbonyl oxygen atom interacts with the phenolic OH group from the opposite aromatic ring. Additionally, each amino acid fragments adopts such a conformation that the amide hydrogen atom can interact with the free electron pair of the amino groups. X-ray structure of dibenzooxazine derivatives shows that these compounds are the boat conformers having C_2 symmetry with the same priority of substituents in upper rim as well as the same interaction are formed as in the mono-substituted derivatives [66].

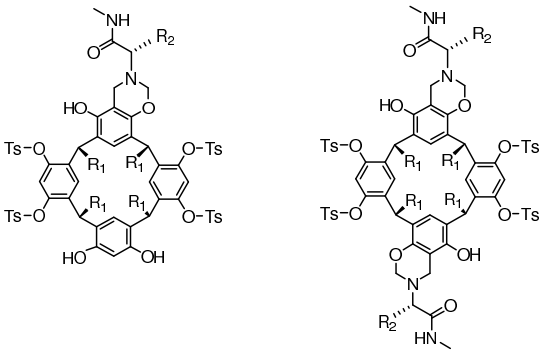

54A
a. R_1= *i*- Bu R_2= CH_2Ph
b. R_1= *i*- Bu R_2= Ph

54B
R_1= *i*- Bu R_2= CH_2Ph

Figure 27.

Acid-catalysed aminomethylation of tetra-O-sulpho-derivatives **8** with L-proline provides the chiral products **55** with C_2 symmetry (Figure 28) [67].

Aminomethylation of tetratosylated resorcinarene **8a** with chiral diamines affords by standard Mannich reaction of chiral bridged products **56** (Scheme 31) [68].

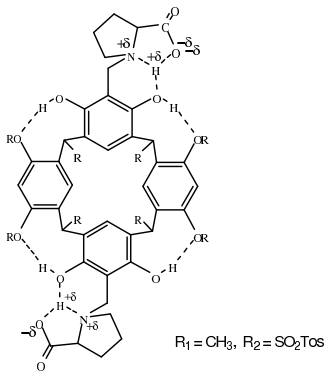

Figure 28.

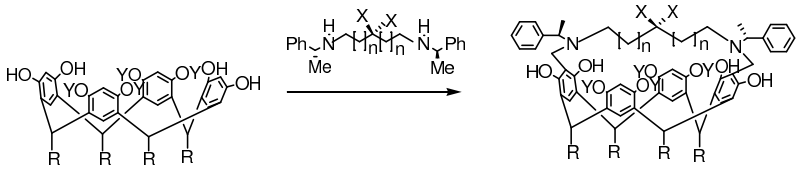

a. n= 1 R= CH_3 Y= OTs X= H
b. n= 1 R= C_5H_{11} Y= OTs X= H
c. n= 1 R= $C_{11}H_{23}$ Y= OTs X= H
d. n= 1 R= CH_3 Y=OTs X= $OCH_2C(CH_3)_2CH_2O$
e. n= 1 R= CH_3 Y= OTs X= OMe
f. n= 1 R= CH_3 Y= OMs X= H
g. n= 1 R= CH_3 Y= OTrips X= H
h. n= 1 R= CH_3 Y= OAc X= H
i. n= 1 R= CH_3 Y= OTol X= H
j. n= 1 R= CH_3 Y= OCbz X= H
k. n= 2 R= CH_3 Y= OTs X= H
l. n= 2 R= CH_3 Y= OTs X= OMe

Scheme 31.

The synthesised bridged derivatives **56** were used as catalysts for asymmetric addition of diethylzinc to benzaldehyde [69]. All of reactions produced 1-phenyl-1-propanol as a product of addition in good yields (>90%) but with enantiomeric excess in the 5- 49% range.

The influence of various steric and electronic factors (lenght of pendant groups in lower rim, lenght of bridge, steric and electronic environments near the cavity by

using several types of protecting groups, chemical character of groups introduced into the bridge) on the enantioselectivity of addition diethylzinc to benzaldehyde were investigated by using the bridged resorcinarene derivatives with different structural modification as catalysts. On the base of all results, the authors proposed mechanistic model for asymmetric addition diethylzinc to benzaldehyde catalysed by bridged resorcinarenes **56** in which, the cavity of resorcinarene played also role [69].

Mannich reaction of tetratosyl resorcinarene **8a** using diizopropylamine in a ratio of 1:1:1 in ethanol yields the mono-2-substituted chiral product **57** (Scheme 32) [70].

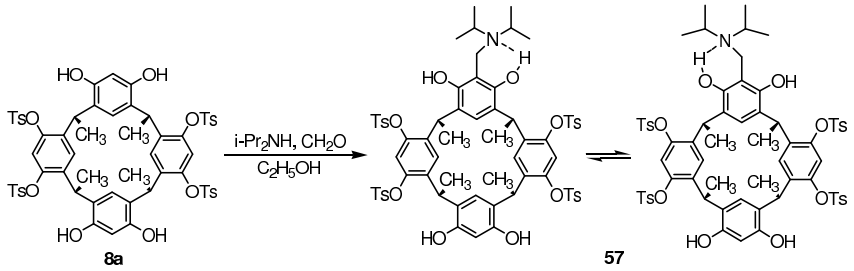

Scheme 32.

Chiral resorcinarene **58** prepared by Mannich reaction with L-prolinol and formaldehyde has an electron lone pair at the nitrogen atom and the free hydroxyl groups, which can be "clipped" together by the reaction with phenylboronic acid. The resulting novel resorcinarenes **59**, containing bora-oxazine-oxazolidine rings in their structure, are obtained in 65% yield (Scheme 20) as a mixture of two diastereoisomers: *out-(M,S,R,S$_N$,R$_B$)*-59 and *in-(P,S,S,S$_N$,R$_B$,)*-59 in ratio 80:20. The thus synthesised resorcinarenes **59** contain two new stereogenic centres: at the boron atom and at the nitrogen atom, what is marked in stereochemical designation of this compounds. In both isomers, the nitrogen atom has the *S* configuration, whereas the boron atom has the *R* configuration [71].

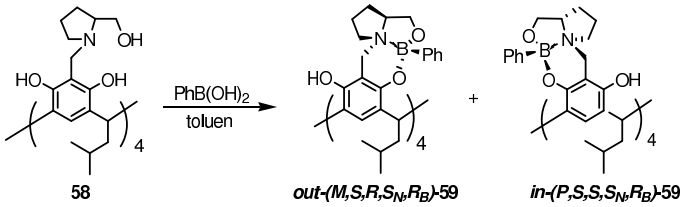

Scheme 33.

There are also known reactions with others chiral amino alcohols.The analogous reaction with (*1S,2R*)-ephedrine as amino alcohol component led to mixture of two diastereoisomers of bora-oxazine-oxazolidine derivatives: the crown conformer *in-(M,S,R,R,S$_N$,S$_B$)*- 61a and the diamond conformer **61b** (Scheme 34) [72].

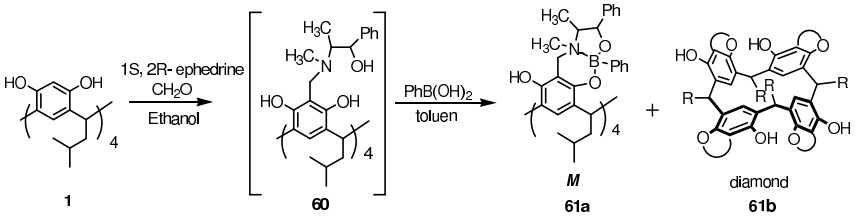

Scheme 34.

However, the reaction with (-)-(1R, 2R)- norpseudoephedrine affords with high diastereoselectivity (>99%) only one from several possible diastereoisomers, classified as *out-(P,R,R,S,R$_N$,R$_B$)*-63. The crystallographic structure of the bora-oxazine-oxazolidine derivative **63** indicates, that this diastereoisomer has priority of substituents around an axis of symmetry type ***P*** and „*out*" orientation of bora-oxazine rings (Scheme 35) [73].

The chiral boron derivatives of resorcinarenes via Mannich reaction from boron-chelates obtained from chiral amino alcohols and triethylborane were synthesised (Scheme 36).

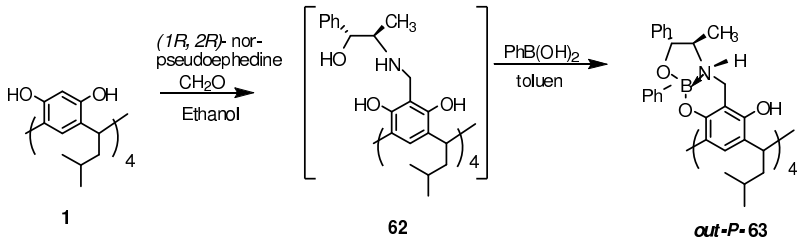

Scheme 35.

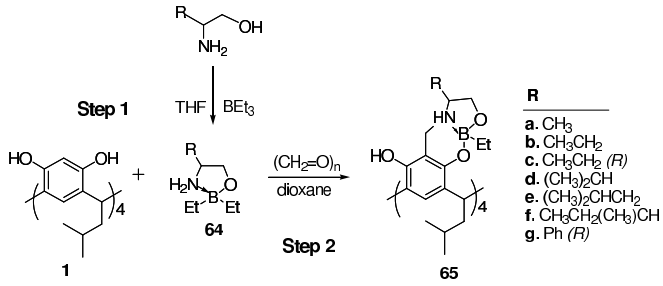

Scheme 36.

Reactions with the S-amino alcohol led to boron derivatives *out-(P,S,S,S$_N$,S$_B$)*-65. In case of reactions with the part R-amino alcohol, *out-(M,R,R,R$_N$,R$_B$)*-65 diastereoisomers were received, but with the same location of ethyl group linked to the boron atom as well as orientation of the bora-oxazine-oxazolidine rings in relation to the resorcinarene cavity [74].

Also the reaction of "clipping" the chiral resorcinarene 41a, (synthesised *via* Mannich reaction using L-proline) with boron compounds leads to the chiral bora-oxazine-oxazolidinone derivatives *out-(M,S,R,S$_N$,S$_B$)*-66 (Scheme 37) [75]. The reported syntheses are characterised by high diastereoselectivity (>98%).

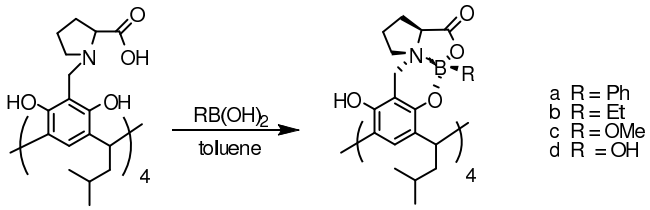

41a **out-** (*M,S,R,S*$_N$*S*$_B$)**- 66**

Scheme 37.

5. Functionalisation of the lower rim of resorcinarenes.

There are know three possible approaches in the functionalisation of lower rim in literature:

1. The most often used and simplest method is using the chiral aldehyde for the condensation reaction;

2. The stereogenic centre at the lower rim of the resorcinarene can be created by modification of the functional groups introduced with the aldehyde;

3. An example of the synthesis of the chiral resorcinarene from the derivative of resorcinol is also known.

The mentioned possible methods of modification of lower rim are described in this chapter. As a consequence of the using of chiral aldehydes for condensation with resorcinol are the resorcinarenes, which have identical pendant groups at the lower rim.

The potential chiral receptors- glycoside resorcinarenes **67**, having the tetraacetylglycoside ring at the lower rim, were synthesised by condensation of resorcinol with glycoside aldehydes **66** in the presence of aluminium chloride as a catalyst (Figure 29). The major product was the *rctt* isomer, whereas the crown conformer (*rccc*) isomer formed in lesser amounts [76].

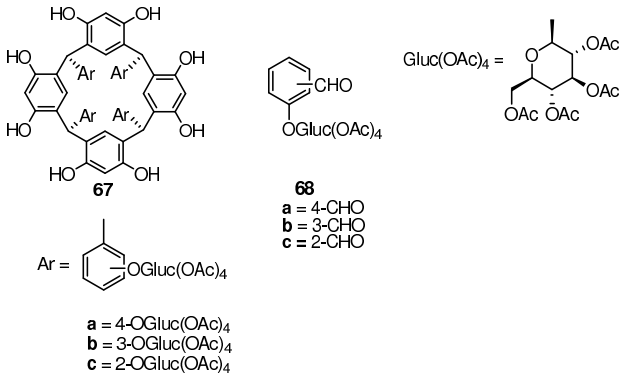

Figure 29.

The macrocyclic resorcinarenes **69** were prepared by „one-pot" reaction of resorcinol with 3,7,12-trimethylcholanal. These products have the C_{4V} symmetry, where the four steroid units occupy axial positions (Figure 30) [77].

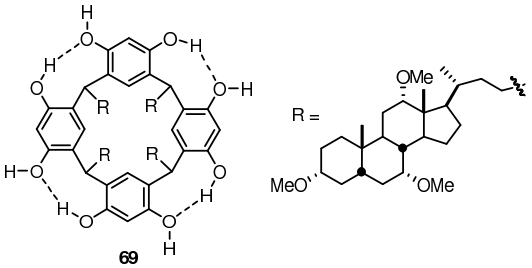

Figure 30.

Condensation of resorcinol with 4-formylphenylboronic acid in the presence of acidic catalyst yields a mixture of two resorcinarenes having the *rccc* and *rctt* configurations, which contain four phenylboronic acid units at carbon bridges. Estrification using (-)-pinanediol affords the chiral boronic esters **70** (Figure 31). The resulting mixture was separated by liquid-solid extraction [78].

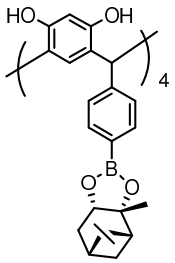

70

Figure 31.

Chiral octamethoxyresorcinarenes **71** (Figure 32) were synthesised from chiral monomers of D- and L-valinamides of (E)-2,4-dimethoxycinnamic acid using catalytic amounts of $BF_3{\cdot}Et_2O$. The prepared mixture of conformers was separated chromatographically [79].

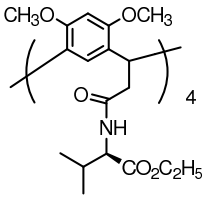

71

Figure 32.

The crown conformer of chiral resorcinarene **71** were employed as receptor for investigation of the molecular recognition of representative amino acids in the gas phase by ESI-FT-ICR mass spectrometry [80, 81]. The synthesis of compound **71** is an example of synthesis resorcinarene derivative having chiral pendant groups, with using chiral derivative of resorcinol.

References:

1. C. D. Gutsche, "*Calixarenes*", Monographs in Supramolecular Chemistry No 1; J. F. Stoddart,Ed.; Royal Society of Chemistry, Cambridge, U. K. (1989);

2. J. Vicens and V. Böhmer, eds. "*Calixarenes*: *A Versatile Class of Macrocyclic Compounds*", Kluwer Academic Publishers (1991);
3. C. D. Gutsche, "*Calixarenes Revisited*", Royal Society of Chemistry (1998);
4. L. Mandolini and R. Ungaro eds., "*Calixarenes in Action*", Imperial College Press (2000);
5. a) P. Timmerman, W. Verboom. D. N. Reinhoudt, Tetrahedron, 52, 2663 (1996); b) M. Vysotsky, Ch. Schmidt, V. Boehmer, in *Advanced in Supramolecular Chemistry*, V. 7, 199 (2000); c) B. Botta, M. Cassani, I. D'Acquarica, D. Misiti, D. Subissati, G. DelleMonache, *Current Organic Chemistry*, 9, 337 (2005); d) M. Urbaniak, W. Iwanek, *Pol. Chem.. Rev*., 58, 203 (2004);
6. M. Urbaniak, W. Iwanek, in *Synthetic Molecular Receptors*, V. 1, eds. G. Schroeder, Betagraf U.H.U, Poznań (2007);
7. K. Wołowiec W. Iwanek, in *Synthetic Molecular Receptors*, V. 2, eds. G. Schroeder, Betagraf U.H.U, Poznań (2007);
8. E. L. Eliel, S. H. Wilen, *Stereochemistry of organic compounds*, J. Willey & son (1994);
9. B.R.Buckley, I.Y.Boxhall, P.C.B.Page, Y.Chan, M.R.J.Elsegood, H.Haney, K.E. Holmes, M.J.MacIldowie, M.McKee, M.J.McGrath, M.Mocerino, A.M.Poulton, E.P. Sampler, B.W.Skelton and A.H.White, *European Journal of Organic Chemistry*, 5117 (2006);
10. B.R.Buckley, P.C.B.Page, H.Haney, M.Klaes, M.J.MacIldowie, M.McKee, J.Mattay, M.Mocerino, E.Moreno, B.W.Skelton and A.H.White, *European Journal of Organic Chemistry*, 5135 (2006);
11. M. Vysotsky, Ch. Schmidt, V. Böhmer, *Chirality in calixarenes and calixarene assemblies, advances in supramolecular chemistry,* 7, 139 (2000);
12. H. Konishi, T. Tamura, H. Ohkubo, K. Kobayashi, O. Morikawa, *Chemistry Letters*, 15, 685 (1996);
13. C. Agena, Ch. Wolff, J. Mattay; Eur. *J. Org. Chem.*, 2977 (2001);
14. a) J. Lipkowski, O. I. Kalchenko, J. Slowikowska, V. I. Kalchenko, O. Lukin, L. N. Markovsky, R. Nowakowsky, *J. Phys. Org. Chem.*, 11, 426 (1998);

b) V. I. Kalchenko, A. N. Shivanyuk, V. V. Pirozhenko, L. N. Markovsky, *Zhurn. Obshch. Khim.*, 64, 1558 (1994); *Chem. Abstr.*, 122, 314625u (1995);

15. O. Lukin, V. Pirozhenko, A. N. Shivanyuk, *Tetrahedron Letters*, 36, No 42, 7725 (1995);
16. M. J. McIldowie, M. Mocerino, B. W. Skelton, A. H. White, *Organic Letters*, 2(24), 3869 (2000);
17. M. Klaes, C. Agena, M. Köhler, M. Inoue, T. Wada, Y. Inoue, J. Mattay; *J. Org. Chem.* 1404 (2003);
18. J. Y. Boxhall, Ph. C. B. Page, M. R. J. Elsegood, Y. Chan, H. Heaney, K. E. Holmes, M. J. McGrath, *Synlett.*, 7, 1002 (2003);
19. S. Kim, J. Sohn, S. Y. Pork, *Bull. Korean Chem. Soc*. 20, 473 (1999);
20. J. Fransen, P. J. Dutton, *Can. J. Chem.*, 73, 2217 (1995);
21. a) M. Inouye, K. Hashimoto, K. Isagawa, *J. Am. Chem. Soc.*, 116, 5517 (1994); b) J. Hayatt, *J. Org. Chem.*, 43, 1808 (1978);
22. W. Iwanek, unpublished results;
23. W. Xu, J. P. Rourke, J. J. Vittal, R. J. Puddephatt, *Inorg. Cham.*, 34, 323 (1995);
24. V. W. Kalchenko, D. Rudkievich, A. Shivaniuk, I. Cymbal, V. Pirozhenko,L. Markovsky, *Zhurnal Obschch. Chim.*, 64, 731 (1994);
25. S. Pellt-Rostaing, J-B. de Vains, R. Lamartine, *Tetrahedron Letters*, **36**, No 32, 5745 (1995);
26. W. Iwanek, *Tetrahedron: Assymetry*, 9, 3171 (1998);
27. S. Seyhan, O. Ozbayrak, N. Demirel, M. Merdivanb, N. Pirinccioglu, *Tetrahedron: Asymmetry*, 16, 3735 (2005);
28. O. Hayashida, J.Ito, S. Matsumoto, I. Hamachi, *Org. Biol. Chem.*, 3, 654, (2005);
29. A. Ruderisch, J. Pfeifer, V. Schurig, *Tetrahedron: Assymetry*, 12, 2025 (2001);
30. A. Ruderisch, J. Pfeiffer, V. Schurig, *Chromatogr. A* 994, 127 (2003);
31. P. A. Levkin, A. Ruderisch, V. Schurig, *Chirality*, 18, 49 (2006);

32. T. Sokolies, A. Opolka, U. Menyes, U. Roth, Th. Jira, *Pharmazie*, 57 (8), 589 (2002);
33. T. Fujimoto, C. Shimizu, O. Hayashida, Y Aoyama, *J. Am. Chem. Soc.,* 119, 6676 (1997);
34. T. Fujimoto, C. Shimizu, O. Hayashida, Y. Aoyama, *J. Am. Chem. Soc*., 120, 601 (1998);
35. O. Hayashida, M. Kato, K. Akagi, Y. Aoyama, *J. Am. Chem. Soc.,* 121, 11597 (1999);
36. K. Fujimoto, O. Hayashida, Y. Aoyama, C.- T Guo, K. I.-P. J. Hidari, Y. Suzuki, *Chemistry Lett*., 1259 (1999);
37. a) Y. Aoyama, T. Kanamori, T. Nakai, T. Sasaki, S. Horiuchi, S Sando, T. Niidome, *J. Am. Chem. Soc.* 125, 3455 (2003); b) Laura Baldini, Alessandro Casnati, Francesco Sansone, R. Ungaro in *Calixarenes in the Nanoworld*, eds. J. Vicens, J. Harrowfield, L. Baklouti, Springer, Dordrecht (2007);
38. N. Tomita, S. Sando, T. Sera, and Y. Aoyama, *Bioorganic & Medicinal Chemistry Letters*, 14, 2087 (2004);
39. F. M. Menger, J. Bian, E. Sizova, D. E. Martinson, V. A. Seredyuk, *Organic Letters*, 78, 261 (2004);
40. M. Klaes, B. Neumann, H-G Stammler, J. Mattay, *Eur. J. Chem*., 864 (2005);
41. K. Salorinne, M. Nissinen, *Organic Letters*, 8, 24 (2006);
42. D. J. Cram, S. Karbach, H. E. Kim, C,B. Knober, E. F. Maverick, J. L. Ericson, R. C. Helgeson, *J. Am. Chem. Soc*., 110, 2229 (1998);
43. O. Manabe, K. Asakura, T. Nishi, S. Shinkai, *Chem. Lett*., 1219 (1990);
44. U. Schneider, H. J. Schneider, *Chem. Ber*., 127, 2455 (1994);
45. D. A. Leigh, P. Linnane, R. G. Pritchard, G. Jakson, *J. Chem. Soc., Chem. Commun.,* 389 (1994);
46. C. Schmidt, T.Straub, D. Falabu, E. F. Paulus, E. Kolehmainen, V. Böhmer, K. Rissanen, W. Voght, *Eur. J. Org. Chem*., 3937 (2000);
47. A. Szumna, *Org. Biomol. Chem.,* 5, 1358 (2007);
48. W. Iwanek, Ch. Wolff, J. Mattay, *Tetrahedron Lett*., 36, 8469 (1995);
49. W. Iwanek, *Polish J. Chem*., 73, 1777 (1998);

50. W. Iwanek, M. Urbaniak, *Polish J. Chem*., 73, 2067 (1999);
51. a) Y.Kikuchi, K. Kabayashi, Y. Aoyama, *J.Am. Soc.,* 114, 1351 (1992); b) K. Kobayashi, Y.Asakawa, Y. Kato, Y.Aoyama, *J.Am. Soc.,*10307 (1992);
52. R. Yanagihara, M.Tominaga, Y. Aoyama, *J.Org. Chem.,*59, 6865 (1994);
53. M. Pietraszkiewicz, P. Prus, R. Bilewicz, *Polish J. Chem.,* 1845 (1999);
54. Y. Matsushita, T. Matsui, *Tetrahedron Lett*. 34, 7433 (1993);
55. R. Yanagihara, A. M. Tominaga, Y. Aoyama, *J. Org. Chem*., 59, 6865 (1994);
56. P. Shahgaldian, U. Pieles, M. Hegner, *Langmuir*, 21, 6503 (2005);
57. A. Ruderisch, *Dissertation; Synthese von Calixaren und Resorcinarenderivaten und deren Anwendung in Chromatographie und Nanotechnologie*, Tübingen (2003);
58. W. Iwanek, J. Mattay, *Liebigs Ann*., 1463 (1995);
59. K. Airola, V. Böhmer, E. F. Paulus, K. Rissanen, Ch. Schmidt, I. Thondorf, W. Vogt, *Tetrahedron*, 53, No. 31, 10709 (1997);
60. O. Trapp, S. Caccamese, Ch. Schmidt, V. Böchmer, V. Schurig, *Tetrahedron Assymetry*,12, 1395 (2001);
61. Ch. Schmidt, E. F. Paulus, V.Böhmer, W. Voght, *New J. Chem*., 25, 374 (2001);
62. R. Arnecke, V.Böhmer, S. Friebe, S. Gebauer, I. Thondorf, W. Voght, *Tetrahedron Lett*., 35, 6221 (1995);
63. W. Iwanek, *Tetrahedron Assymetry*, 9, 4289 (1998);
64. B. R. Buckley, P. C. Bulman Page, H. Heaney, E. P. Sampler, S. Carley, C. Brockeb and M. A. Brimble, *Tetrahedron*, 61, 5876 (2005);
65. A. Shivanyuk, Ch. Schmidt, V. Böhmer, E. F. Paulus, O. Lukin, W. Vogt, *J. Am. Chem. Soc*., 120, 4319 (1998);
66. A. Szumna, M.Górski, O. Lukin, *Tetrahedron Letters* ,46, 7423–7426 (2005);
67. a) O. Lukin, A. Shivanyuk, V. V. Pirozhenko, I. F. Tsymbal, V. I. Kalchenko, *J. Org. Chem*., 63, 9510 (1998); b) W. Iwanek, unpublished results;
68. G. Arnott, R. Hunter, H. Su, *Tetrahedron*, 62, 977 (2006);
69. G.Arnott and R.Hunter, *Tetrahedron*, 62, 992 (2006);
70. M. Luostarinen, A. Shivanyuk, K. Rissanen, *Organic Letters* , 3, 4141 (2001);

71. W. Iwanek, R. Fröhlich, P. Schwab, V. Schurig, *Chem. Commun*., 2516 (2002);
72. W. Iwanek, R. Fröhlich, V. Schurig, *Journal of Inclusion Phenomena and Macrocycic Chemistry*, 49, 75 (2004);
73. W. Iwanek, M. Urbaniak, B. Gawdzik, V. Schurig, *Tetrahedron Assymetry*, 14, 2787 (2003);
74. A. Wzorek, J. Mattay, W. Iwanek, *Tetrahedron Asymm*., 18, 815 (2007);
75. W. Iwanek, M. Urbaniak, B. Gawdzik, V. Schurig, *Tetrahedron Assymetry*, 14, 2787 (2003);
76. A. D. M. Curtis, *Tetrahedron Letters*, 38, No 24, 4295 (1997);
77. N. Yoshimo, A. Satake, Y. Kobuke, *Agnew. Chem*.,113, Nr 2 (2001);
78. P. T. Lewis, C. J. Davis, M. C. Saraiva, W. D. Treleaven, R. M. Strongin, *J. Org. Chem.*, 62, 6110 (1997);
79. B. Botta, G. D. Monache, P. Salvatore, F. Gasparrini, C. Villani, M. Botta, F. Corelli, A. Tafi, E. Gacs-Baitz, A. Santini, C. F. Carvalho, D. Misiti, *J. Org. Chem.,* 62, 932 (1997);
80. B. Botta, M. Botta, A. Filippi, A.Tafi, G. Delle Monache, M. Speranza, *J. Am. Chem. Soc.* 124, 7658 (2002);
81. A. Tafi, B. Botta, M. Botta, G.Delle Monache, A. Filippi, M. Speranza, *Chem. Eur. J.* 10, 4126 (2004).

Chapter 5

Oligonucleotides complexing metal ions

Jan Milecki

Faculty of Chemistry, A. Mickiewicz University, Grunwaldzka 6, 60-780 Poznań, Poland

Nucleic acids due to their ubiquitous presence in all living organisms and key role in the process of life are the object of constant research effort aimed at exploiting their functions for different purposes. Genetic information contained in the nucleic acid sequence can be modified in order to repair mutation errors and cure genetic diseases or can be used to achieve suppressing of gene expression as for example in antisense [1] or siRNA [2] therapeutic approaches. There are also numerous examples of chemical modification of the original nucleic acid molecule intended for enhancing some of its properties or creating new ones.

DNA molecule can be regarded as molecular assembly consisting of repeating units which form scaffold of repeating [3,4] heterocyclic bases held together by a phosphoro-sugar backbone. This scaffold in its native form is rigid enough to maintain defined structure of straight rod-like molecule of several nanometers in length [4] but flexible under the influence of specific agents, mainly proteins, which are capable to induce conformational changes necessary for specific biological functions.

RNA are much more flexible and prone to folding into various unique shapes [4], their tertiary structures depending mainly on the nucleotide sequence and possible base pairing of the nucleotide units which came in close contact. Any modification introduced into stacked base or backbone will affect the initial properties of the oligonucleotide chain. From the other hand the rigid scaffold nature and overall shape of the molecule can be used as a way to precisely place in space the modified units. If

we take into account that oligonucleotides can presently be easily assembled by means of automatic synthesis [5], potential of this approach becomes obvious.

Among different chemical modifications the one based on introducing metal ions into the nucleic acid molecule appears as particularly versatile and fruitful [6].

Native nucleic acids associate with different cations and this association is crucial for achieving proper conformational shape and function [1,4,7]. Introducing additional metal ions will modify properties of oligonucleotide and possibly create new functional capabilities, Such modified oligonucleotides can be used as therapeutic agents [8,9], analytical and diagnostic tools [10], can catalyze chemical reactions in the manner of enzymes [11-15], can be building blocks for different supramolecular structures[16-22] or nanoelectronic devices [23].

Therapy

One of the very promising techniques in therapy of cancerous tumors is the boron neutron capture therapy, where the malignant tumor is saturated with a compound containing boron atom(s) and then the tissue is irradiated with harmless low-energy neutron beam. Nuclear reaction converts stable ^{10}B boron isotope into unstable ^{11}B which splits into lithium and alpha particles. The latter carry almost 95% energy of the nuclear fission and are absorbed very efficiently within the distance of few millimeters, limiting damage of the tissue only to the tumor without any harm to healthy cells.

Crucial element of this promising therapy is to have boron compound which will be non toxic, will be absorbed by organism and will accumulate selectively in the tumor, showing no undesired affinity to healthy tissues. Since desirable saturation of the malignant tissue is in the range of 20-40 μg per g, the boron compound should posses as many boron atoms in its molecule as possible. One of the best candidates for this are clusters of boron and carbon atoms, carboranes [9]. They are relatively non-toxic, have ten atoms of boron per molecule, but are only weakly absorbed by tissues. If the carborane would be conjugated with other molecule of high affinity to the tumor tissue, as for example nucleotide which can be utilized by rapidly growing cancer cells or oligonucleotide of sequence complementary to the fragment of the tumor RNA, the

boron carrier would fulfill its mission and implement boron rich compound into malignant cells.

It is possible to synthesize conjugates of metallacarboranes (complexes of carboranes with metal ion) with different deoxynucleosides and introduce them into oligonucleotides [8], either *via* chemical synthesis or biochemically, after converting them into triphosphates. As metallacarborane contains 20 atoms of boron in the molecule it can be extremely efficient as a source of boron centers.

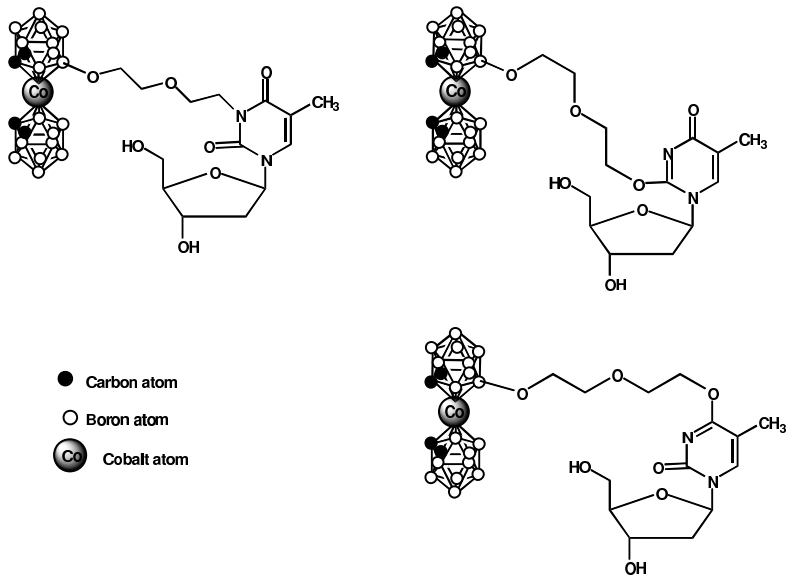

Fig. 1. Metallacarborane conjugates with thymidine

From the other point of view, the preparation of metallacarborane-nucleoside conjugates can be regarded as new efficient way to label DNA with metal ions [9].

Enzymatic activity

The discovery of ribozymes – RNA fragments of catalytic activity [1] was the starting moment of search for oligoribonucleotides capable of catalyzing different

types of reactions *i.e.* mimicking the action of enzymes. Until now numerous RNA sequences are known which are catalyzing reactions of acyl transfer, oligonucleotide chain hydrolysis, red-ox reactions or Diels-Alder cyclization [13]. All of naturally occurring ribozymes require presence of metal ions [24], which cooperate in achieving proper conformation, or serve as Lewis acid centers. Introducing metal ions into artificially constructed NA-zymes creates new or enhances existing catalytic activities. Artificial ribozyme consisting of two oligonucleotides, one of them possessing Cu^{2+} coordinating site at the 3' end and the other with the same ion complexed at the 5' cooperate in hydrolyzing RNA fragment of the sequence complementary to both oligonucleotides [14,15]. The catalytic oligonucleotides associate with the target sequence in the way which places them in the duplex next to each other with the copper ions in close contact enabling cooperation in hydrolysis of the matrix. Although oligomers showed hydrolyzing properties, when acting alone, they worked much less efficiently (18% of hydrolysis for the 3'-Cu^{2+}, and negligible for the 5'-Cu^{2+} oligomer against 92% efficiency for both of them cooperating).

When naturally occurring RNA-enzyme D22 with the Diels-Alderase activity was modified by introducing nucleoside analogue with pyridyl substituent, it gained the ability of complexing copper ions. Catalytic sequence was artificially mutated and by *in vitro* evolution the most active sequences were selected. The so-obtained ribozyme showed considerably higher activity than D22 and was absolutely Cu-dependent. All the obtained 53 different active oligomers were sequenced and their sequences compared. From 100 bases present in the active strand 36 were identified as conservative, probably forming the active site of this ribozyme [13].

New base pairing

Genetic code consists of four bases A,T,G,C, arranged in pairs according to the Watson-Crick pattern (A-T and G-C) [4]. By adding new way of connecting of opposite bases or their mimics with their partners by different way of coordination it would be possible to establish new "letter" of genetic code [25,26]. It can serve the purpose of additionally stabilize the duplex or to diversify the genetic sequences.

If the metal-mediated pairing of bases is to be applicable for construction of artificial pairs, it has to fulfill some requirements. Geometry of the complex (proper interstrand distance, planar arrangement of bases, stacked perpendicularly to the helix axis) has to follow the geometry of natural duplex [27]. If there are differences, they are to be acceptable to the requirements of double-stranded nucleic acid fragment.
Bonding strength of such artificial base pair also has to be in the range of the natural hydrogen-bonded pair. Stronger bonding can affect (rise) the T_m of duplex into which such a base pair was included. This effect can be utilized to additionally stabilize the double stranded molecule or to start the bonding of strands from the chosen point of the oligomer or to induce conformational changes (for example B to Z transition [25]). Several possible base equivalents were tested [25,28]. Some of them have planar geometry, other are bipyramidal.

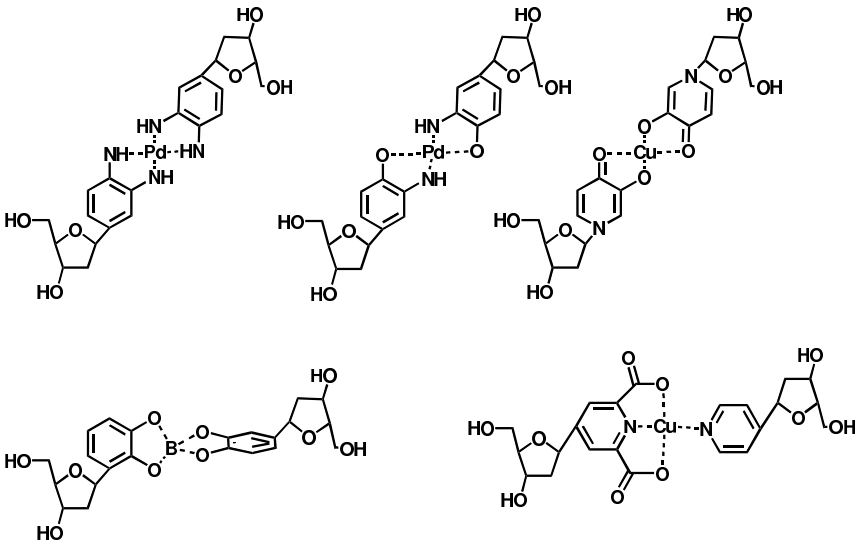

Fig. 2. Different artificial, metal mediated „base pairs"

If softer coordinating center (sulfur atoms) were used, strength of silver-mediated bonding was considerably higher than strength of regular W-C pair [29].

Presence of a metal ion can also induce formation of triplexes [26] or quadruplexes [6] instead of duplexes.

Strong attachment of the metal ion to the complexing center locks it in place within the duplex and gives opportunity to construct stable spatial arrangements of ions [28] of predictable electronic or magnetic properties.

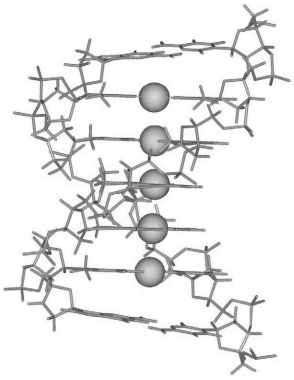

Fig. 3 Five Cu ions in line held together by DNA duplex. Reproduced from [28].

Analytical tool

Detection of metal ions by fluorescence is a well-established analytical method. Changes in the emission spectra of fluorophore are caused by electronic changes accompanying complexation of the ion. Fluorescent ligands supported on deoxyoligonucleotides give the unique opportunity to combine high susceptibility of fluorescence method with DNA ability to specifically recognize different types of molecules. In addition to specificity of interaction with different ions, oligonucleotide enhances water solubility of fluorophores . When two fluorescent ligands were introduced into the opposite strands of 13-mer duplex in three possible arrangements (pairs **aa**, **ab** and **bb**), the duplex became a tool capable to detect and estimate concentration of up to 12 different ions in mixtures [10].

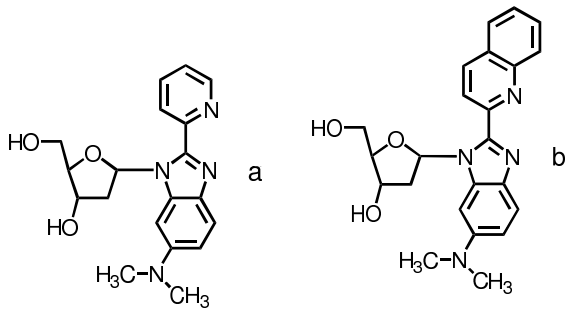

Fig. 4. Two fluorophore analogs of nucleosides.

Changes in fluorescence induced by metal complexation included shifting of emission maximum (red or blue shift) and enhancement or lowering of emission intensity. Combination of these effects was characteristic for each of the 12 ions and allowed their precise detection and quantitation. Even ions, which are hard to estimate in mixture, as Cd^{+2} and Zn^{+2} could be differentiated easily.

Modification of overall charge

Many of the promises of antisense therapy [30] were not possible to be fulfilled due to poor cellular uptake of oligonucleotides. It is caused mainly by the fact that the nucleic acids are polyanionic molecules and are repelled by cellular wall. Different ways were tested order to improve the penetration of the oligomers into cells. One concept is to attach positive ions, thus lowering net negative charge. It can be effected by placing chelating moieties within the oligonucleotide chain [31-33]. The moiety can be inserted into the phosphoro-sugar backbone [31], thus avoiding undesired influence of the ion on base pairing or if placed close to the base it should be flexible to allow for easy conformational changes [34,35].

For the derivative containing dipyridyl, piperazinyl or dithioether chelating centers noble metals ions proved to be effective in forming stable complexes and enhancing duplex stability.

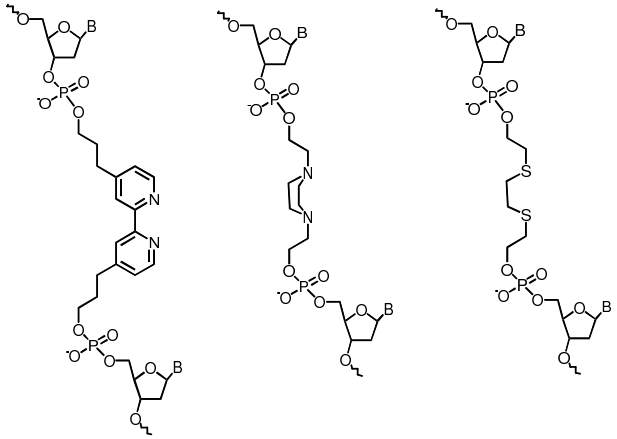

Fig. 5. Metal complexing site in DNA backbone.

Other approach is based on complexing alkali metal ions [34,35], which are always present in cytoplasm, thus alleviating danger of harmful effects caused by the metal ion. The derivatives shown on Fig.6 exhibited good complexing of lithium, sodium and potassium ions [35]. When the podand moiety was placed at the N3 atom of the uracil ring (nucleoside A), two ways of forming of the complexing cavity were detected.

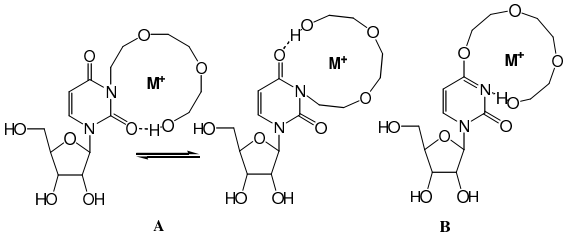

Fig. 6. Alkali metal ions complexing by podand moiety conjugated with uridine.

Construction of supramolecular structures

Ability of nucleic acids to form secondary and tertiary structures in a programmed way and maintaining relatively rigid structure can be employed for

constructing higher-order assemblies containing metal ions placed in well defined positions in space. Such a supramolecular assembly can have linear [17,22], planar [17-19] or three-dimensional [16] shape, depending of the number of oligonucleotides tethered to a metal complexing center. DNA duplex can be used as a backbone for regular spacing of these centers. They can be installed not only inside the double helix, but also on the outer surface of the duplex, especially in the large groove of canonical B structure. For example up to 11 porphyrine moieties were attached next to each other to a DNA oligomer. They formed regularly arranged additional helix of stacked porphyrines [20]. This assembly can serve as light-harvesting device or metal complexing part of the molecule. Stacking interactions of the porphyrines add considerably to the stability of the duplex [20] and keep regular helix structure even after thermal dissociation of two strands.

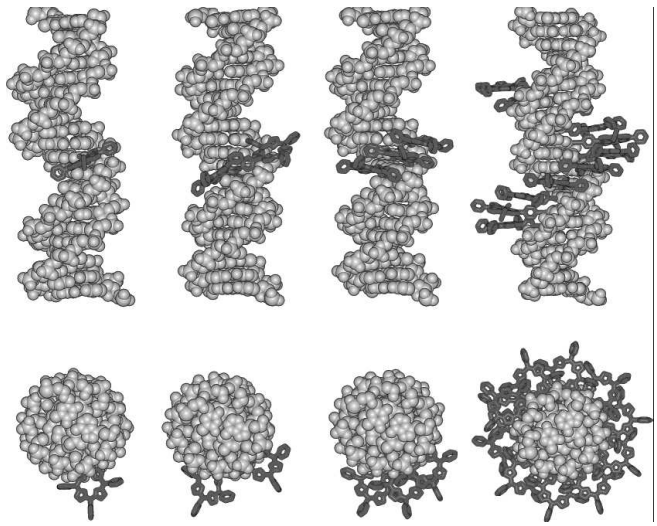

Fig.7. Different number of porphyrines conjugated with oligonucleotide. Note regular arrangement and stacking of added molecules. Reproduced from [20].

Conclusion

Nucleic acids complexing of metals can lead to extremely diversified structures, which can be programmed in advance and assembled easily due to nucleic acids ability to self-organization. Few of chemical fields have such rich perspective for development and respond to the phrase "sky is the limit" and in true further development is limited only by human imagination.

References:

1. T.R. Cech, A.J. Zaug, P.J. Grabowski *Cell* 29, 487-496 (1981);
2. P.A. Sharp *Genes & Develop.* 15, 485-490 (2001);
3. A. Hatano, K. Tanaka, M. Shiiro, M. Shinoya *Tetrahedron* 58, 2965-2972 (2002);
4. „Nucleic Acids in Chemistry and Biology", G.M. Blackburn, M.J. Gait (editors), Oxford University Press Oxford, New York, Tokyo, (1995);
5. C.B. Reese *Tetrahedron* 58, 8893-8920 (2002);
6. R.Di Felice, A. Calzolari, H. Zhang *Nanotechnology* 15, 1256-1263 (2004);
7. W.G. Scott *Curr. Opin. Chem. Biol.* 3, 705-709 (1999);
8. A.B. Olejniczak, J. Plesek, O, Kriz, Z.L. Leśnikowski *Angew. Chem. Int. Ed.* 42, 5740-5743 (2003);
9. A.B. Olejniczak, J. Plesek, O, Kriz, Z.L. Leśnikowski *Chem. Eur. J.* 13, 311-318 (2007);
10. S.J. Kim, E.T. Kool *J. Am. Chem. Soc.* 128, 6164-6171 (2006);
11. T.M. Tarasov, S.L. Tarasov, C. Tu, E. Kellogg, B.E. Eaton *J. Am. Chem. Soc* 121, 3614-3617 (1999);
12. J.K. Bashkin, J. Xie, A.T. Daniher, U.S. Sampath, J.L.-F. Kao *J. Org. Chem.* 61, 2314-2321 (1996);
13. T.M. Tarasov, B.L Holley, D. Nieuwlandt, S.L. Tarasov, C. Tu, E. Kellogg, B.E. Eaton *J. Am. Chem. Soc.* 126, 11843-11851 (2004);
14. H. Inoue, T. Furukawa, T. Tamura, A. Kamada, E. Ohtsuka *Nucleosides, Nucleotides & Nucleic Acids* 20, 833-835 (2001);

15. S. Sakamoto, T. Tamura, T. Furukawa, Y. Komatsu, E. Ohtsuka, M. Kitamura, H. Inoue *Nucleic Acids res.* 31, 1416-1425 (2003);
16. K.M. Stewart, L.W. McLaughlin *J. Am. Chem. Soc.* 126, 2050-2057 (2004);
17. K.V. Gothelf, A. Thomsen, M. Nielsen, E. Clo, R.S. Brown *J. Am. Chem. Soc.* 126, 1044-1046 (2004);
18. J.S. Choi, C.W. Kang, K. Jung, Y.-G. Kim, H. Han *J. Am. Chem. Soc.* 126, 8606-8607 (2004);
19. D. Mitra, N. DiCesare, H.F. Sleiman *Angew. Chem. int. Ed.* 43, 5804-5808 (2004);
20. L.-A. Fendt, I. Bouamaied, S. Thoni, N. Amiot, E. Stulz *J. Am. Chem. Soc.* 129, 15319-15329 (2007);
21. K. Tanaka, M. Tasaka, H. Cao, M. Shionoya *Supramolecular Chemistry* 14, 255-261 (2002);
22. S.M. Waybright, C.P. Singleton, K. Wachter, C.J. Murphy, U.H.F. Bunz *J. Am. Chem. Soc.* 123 1828-18333 (2001);
23. B.M. Frezza, S.L. Cockroft, M.R. Ghadiri *J. Am. Chem. Soc.* 129, 14875-14879 (2007);
24. R.E. Christoffersen, J.J. Marr *J. Med. Chem.* 38, 2023-2037 (1995);
25. S. Atwell, E. Meggers, G. Spraggon, P.G. Schultz *J. Am. Chem. Soc.* 123, 2364-12367 (2001);
26. K. Tanaka, Y. Yamada, M. Shionoya *J. Am. Chem. Soc.* 124,8802-8803 (2002).
27. E.T. Kool *Acc. Chem. Res.* 35, 936-943 (2002);
28. M.Shionoya, K.Tanaka *Curr. Op. Chem. Biol.* 8, 592-597 (2004);
29. N. Zimmermann, E. Meggers, P. G. Schultz *J. Am. Chem. Soc.* 124, 13684-13685 (2002);
30. T.D. Ros, G. Spalluto, M. Prato, T. Saison-Behmoaras, A. Boutorine, B. Cacciari *Curr. Med. Chem.* 12, 71-79 (2005);
31. M.M. Knagge, J.J. Wilker *Chem. Commun.* 3356-3358 (2007);
32. P. Wittung, P.E. Nielsen, O. Burchardt, M. Egholm, B. Norden *Nature* 368, 561-565 (1994);

33. J. Summerton *Biochim, Biophys. Acta* 1489, 141-147 (1999);
34. J. Milecki, G. Schroeder *Polish. J. Chem.* 79, 781-1785 (2005);
35. J. Milecki, G. Schroeder, *Mendeleev Commun.* 17, 2-24 (2007).

Chapter 6

Ionophores as metal cation receptors

Radosław Pankiewicz and Grzegorz Schroeder

Faculty of Chemistry, Adam Mickiewicz University, Grunwaldzka 6, 60-780 Poznań, Poland

Introduction

Ionophores make a wide class of natural and artificial compounds. The main feature of this group is the ability to complex ions and transport them through the natural and artificial membranes. This means that ionophores are host molecules that bind ionic quests and transport them across a membrane, such as a bulk organic phase or phospholipid bilayer. In the latter case, the bilayer may be present in a cell or subcellural organelle [1]. Ionophores can transport and hence regulate the concentrations of the main biological cations such as Li^+, Na^+, K^+, Ca^{2+} [2] and some anions (Cl^-) or neutral molecules (NH_3). Typical ionophore molecule contains hydprohobic and hydrophilic groups, in the process of cation complexation the hydrophilic groups are directed inside and interact with the guest, while the hydrophobic groups are directed outside to the nonpolar phase. Thanks to this features the ionophores can work as cation carriers. The ionophore molecule is soluble in a hydrophobic or membrane phase. The ionophore as a host compound captures the quest ion at the aqueous – hydrophobic phase interface. The complex diffuses across the hydrophobic membrane or barrier phase. At the opposite side of the interface, the ions are released so the guest is in the other aqueous phase. The host molecule then diffuses back to the opposite side of the interface, where the process is repeated until an equilibrium is reached. Many classification systems of the ionophores have been

proposed, but the most appropriate is that dividing this group into two subclasses of cyclic and noncyclic ionophores.

Many ionophores show preferences in forming complexes, e.g. salinomycin forms complexes with K^+ ions four orders of magnitude more stable than with Na^+ cations. These features are useful for molecular recognition and make basis for development of ion receptors and ion-selective electrodes.

Ionophores

Cyclic ionophores

Gramicidin S is a well known natural cyclic antibiotic consisting of two identical pentapeptide sequences, as shown in Fig 1., for gramicidin S extracted from *Bacillus brevis* [3-6].

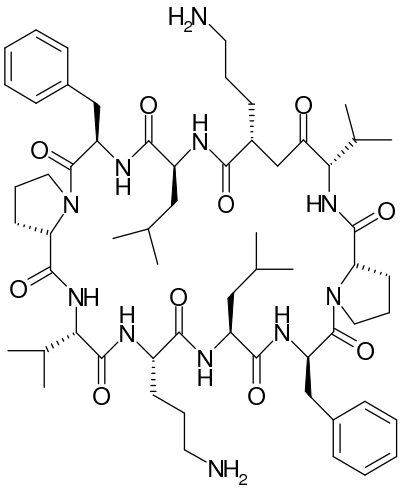

Fig 1. Chemical structure of Gramicidin S

The macrocyclic ring of gramicidin S contains two groups of five aminoacids L-Orn, L-Pro, L-Val, L-Leu and D-Phe. The molecular structure contains two β-sheets built of L-Pro and D-Phe. The polar part is built of L-Orn, the unpolar part is built of side chains of L-Val, L-Leu (Fig.2).

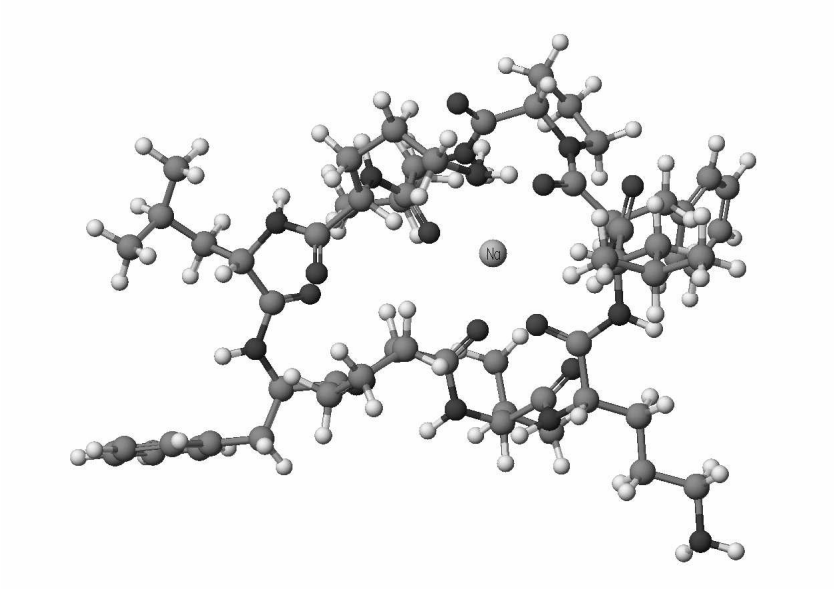

Fig. 2. The calculated structure of the gS-Na$^+$ complex [7]

Another representative of cyclic ionophore is Valinomycin. Its dodecadepsidepeptide contains 12 amino and hydroxyacids (Fig. 3).

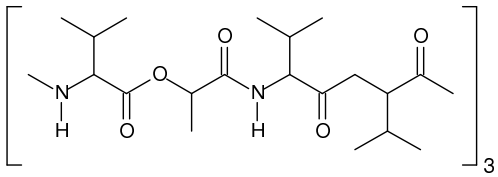

Fig. 3. Chemical structure of valinomycin.

Valinomycin [8-13] is a K^+ - selective carrier molecule isolated from *Streptomyces fulvissimus* [14]. Its flexible macrocyclic ring is too large to complex a K^+ ion, in a two-dimensional fashion. Instead, it wraps about the cation making a "tennis ball seam" conformation. Thanks to the conformational flexibility, the host molecule readily binds and releases the guest. In the complexation process two water molecules

may be included in the K^+ cation coordination sphere. As the carbonyl groups turn inwards to complex the cation, the methyl and isopropyl groups turn outwards to interact with the hydrophobic medium. This makes the complex soluble in hydrophobic membranes enabling trans-membrane transport .

Noncyclic ionophores

The family of noncyclic ionophores includes many compounds which all are carboxylic acids and contain tetrahydropyran and tetrahydrofuran structural units. The most interesting and useful among them are lasalocid, salinomycin, ionomycin, monensin, nigericin, lonomycin (Fig. 4).

All the molecules are acyclic [15] but they can adopt pseudocircular conformations in which the oxygen heteroatoms are focused for cation binding [16]. The pseudocyclic structures are usually stabilized by the hydrogen bond between the molecule's "head" and "tail" (Fig. 5).

The ionophores of this group are deprotonated at physiological pH (7.4), so their complexes with monovalent cations are neutral. Many of them are widely used in stock-farming as veterinary drugs. Lasalocid is one of the most popular ionophorous antibiotic, isolated from *Streptomyces lasaliensis* and it is a good anticoccidial drug for cattle, sheep and chicken. In the cell membrane lasalocid exchanges metal ions against H^+, leading to changes in the pH values and to an increase in osmotic pressure inside the cell, which finally leads to the cell death [17-23].

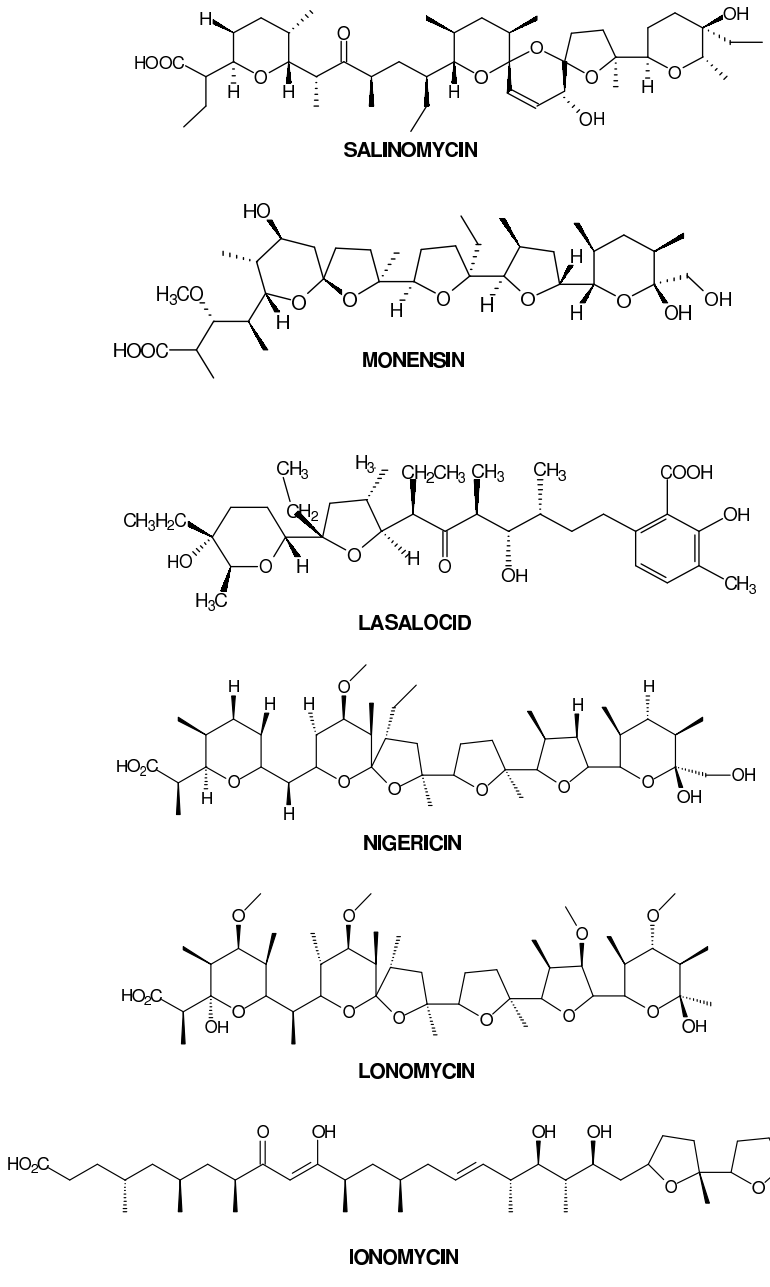

Fig. 4. Structures of noncyclic ionophores.

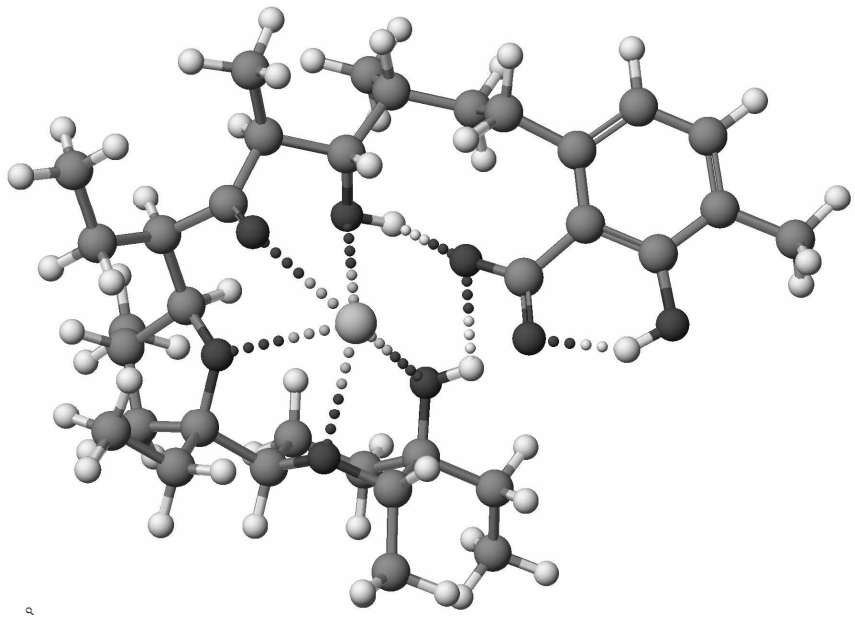

Fig. 5. Calculated structure of lasalocid-Na^+ complex.

Ion-Selective Electrodes

Ion-selective electrodes (ISEs) are one of the major chemical sensors whose activity is based on bio-, gas-, ion- affinity and the affinity to the receptor molecules. A common feature of these chemicals is that molecular recognition takes place chemically, e.g., through bioreceptors and various synthetic supramolecular receptors, immobilized in many cases on solid substrates. The molecular recognition process is followed by appropriate signal transductions, such as electrochemical, optical, and gravimetric methods [24]. The ISE chemistry based on permselective transport analyte ions from aqueous sample solution into ionophore-incorporated organic liquid membranes. In this way we obtain ion-selective charge separation at the aqueous/organic interface, and the change in boundary potentials becomes a measure for the analyte ion activities.

For good charge separation at the interface and consequently reliable measurements, a very important question is the hydrophilicity of the counterion. If counterions are hydrophobic, such as SCN^- or ClO_4^-, the salt extraction (coextraction) takes place. It is called the anion effect [25,26] Fig. 6.

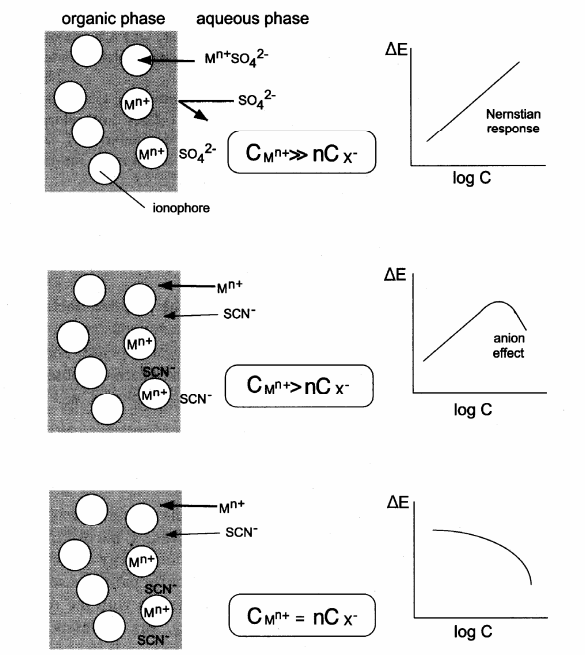

Fig. 6. Partition of metal ions and counterions at the polymer (PVC)-supported ionophore liquid-membrane/aqueous-solution interface; relation with interfacial boundary potentials. $C_M n+$ and C_x- are concentrations of the ionophore-metal-ion complex and its counterions, respectively. These concentrations were measured with FT-IR-ATR to a depth of μm range in the organic phase near the interface. When $C_M n+ > nC_x-$, the observed membrane potential (ΔE) exhibits a Nernstian response that meets Eq. 2. When the value of $C_M n+$ is small but still higher than nC_x-, the anion effect distorted the log C-ΔE relation observed for a non-Nernstian response. When permselectivity was completely lost, i.e., $C_M n+ - C_x-$, ΔE showed no M^{n+} concentration dependence. The presence of the hydrophilic SO_4^{2-} ion and the hydrophobic SCN^- ion was responsible for the difference observed. [25]

Due to the anion effect, the ionophore based ISEs contain not only ionophores but also ion exchangers (ionic sites) (Fig. 7). Thanks to the above, even in the solutions containing lipophilic counteranions it is possible to obtain charge separation at the interface. The ionic sites prevent the counterions from being coextracted into the organic phase and are needed for generation of analyte-ion activity dependent membrane potential changes.

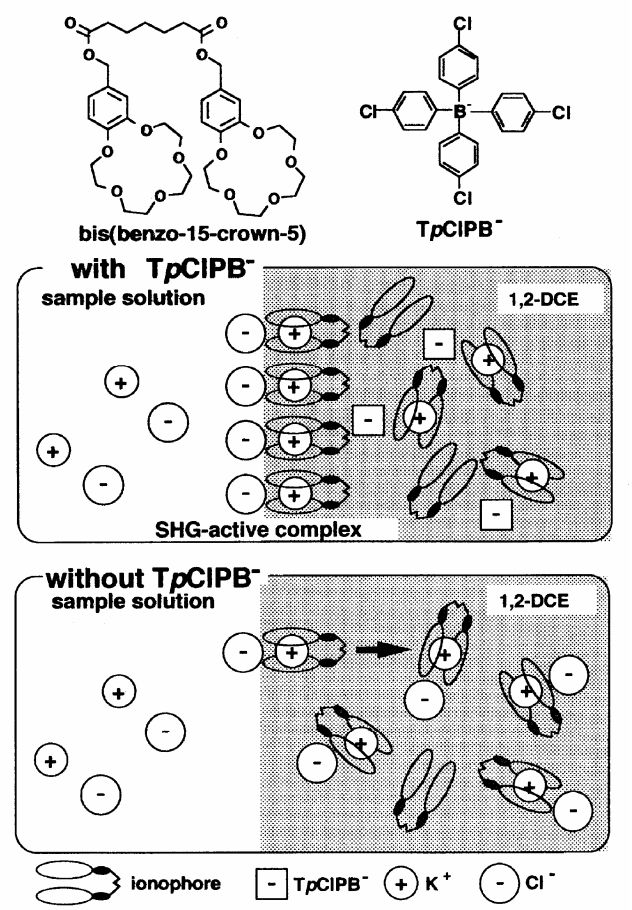

Fig. 7 Surface model showing the orientation of active K^+-ionophore complexes across the aqueous/1,2-dichloroethane (1,2-DCE) interface in the presence of added anionic sites in the membrane phase [27,28].

Acknowledgements

The authors thanks the Polish Ministry of Science and Higher Education for financial support under Grants No. R015 016 01 in the years 2006–2008.

References:

1. R. Ferdani, G.W. Gokel, Encyclopedia of Supramolecular Chemistry 2004, DOI: 10.1081/E-ESMC 120012686, p 760;
2. D.W. Urry, Top. Curr. Chem. 128 (1985) 175;
3. G. Pietrzyn´ski, B. Rzeszotarska, Pol. J. Chem. 69 (1995) 1594;
4. T. Arai, T. Imachi, T. Kato, H.I. Ogawa, T. Fujimoto, N. Nishino, Bull. Chem. Soc. Jpn 69 (1996) 1383;
5. Y.H. Chen, W.F. Siems, H.H. Hill Jr., Anal. Chim. Acta 334 (1996) 75;
6. G.N. Tishchenko, V.I. Adrianov, B.K. Vainstein, M.M. Woolfson, E. Dodson, Acta Crystallogr. D 53 (1997) 151;
7. R. Pankiewicz, A. Gurzkowska, B. Brzezinski, G. Zundel, F. Bartl, J. Mol. Struct. 646 (2003) 67;
8. M. Ohnishi, D.W. Urry, Science 168 (1970) 1091;
9. W.L. Duax, H. Hauptman, C.M. Weeks, D.A. Norton, Science 176 (!972) 911;
10. K. Neupert-Laves, M. Dobler, Helv. Chim. Acta 58 (1975) 432;
11. K.R.K. Easwaran, Met. Ions Biol. Syst. 19 (1985) 109;
12. W.L. Duax, J.F. Griffin, D.A. Langs, G.D. Smith, P. Grochulski, V. Pletnev, V. Ivanov, Biopolymers 40 (1996) 141;
13. M. Dobler, Biochem. Soc. Trans. 1 (1973) 828;
14. H. Brockmann, G. Schmidt-Kastner, Chem. Ber. 88 (1955) 57;
15. N. A. Rodios, M.J.O. Anteunis, Bull. Soc. Chim. Belg. 89 (1980) 537;
16. M.J.O. Anteunis, Bull. Soc. Chim. Belg. 90 (1981) 449;
17. H. Tsukube, Cation – Binding by macrocycles; Marcel–Dekker: New York, 1990; p 497;
18. Y. Pointud, E. Passelaigue, J. Juillard, J. Chem. Soc., Faraday Trans. I 84(5) (1988) 1713;

19. R.V. Antonio, L.P. da Silva, A.E. Vercesi, Biochimica et Biophysica Acta, 1056 (1991) 250;
20. G. Schroeder, B. Łęska, B. Gierczyk, K. Eitner, G. Wojciechowski, B. Różalski, F. Bartl, B. Brzezinski, J. Mol. Struct. 508 (1999) 129;
21. L. Wittenkeller, D. Mota de Freitas, R. Ramasamy, Biochemical and Biophysical Research Communications 184 (1992) 915;
22. X. You, R.F. Schinazi, M.J. Arrowood, J. of Antimicrobial Chemotherapy 41 (1998) 293;
23. N. Safran, D.V.M. Aizenberg, H. Bark, JAVMA 202 (1993) 1274;
24. Y. Umezawa, Encyclopedia of Supramolecular Chemistry 2004, DOI: 10.1081/E-ESMC 120012686, p 747;
25. K. Umezawa, X.M. Lin, S. Nishizawa, M. Sugawara, Y. Umezawa, Anal. Chim. Acta 282 (1993) 247;
26. K. Tonda, S. Yoshiyagawa, M. Kataoka, K. Odashima, Y. Umezawa, Anal. Chem. 69 (1997) 3360;
27. K. Tonda, Y. Umezawa, S. Yoshiyagawa, S. Hashimoto, M. Kawasami, Anal. Chem. 34 (1995) 570;
28. S. Yajima, K. Tonda, P. Buhlmann, Y. Umezawa, Anal. Chem. 69 (1997) 1919.

Chapter 7

Application of podands

Bogusława Łęska and Grzegorz Schroeder

Faculty of Chemistry, Adam Mickiewicz University, Grunwaldzka 6, 60-780 Poznań, Poland

Introduction

The beginning of supramolecular chemistry dates back to the 1960s, when an American chemist, Charles Pedersen realised that the crown can form stable complexes with alkali metals and alkali earth metals (Fig. 1) [1-4]. These compounds, known henceforth as crown ethers, have been found to show unusual properties of dissolving inorganic salts in nonpolar solvents such as benzene, hexane or tetrahydrofurane [5].

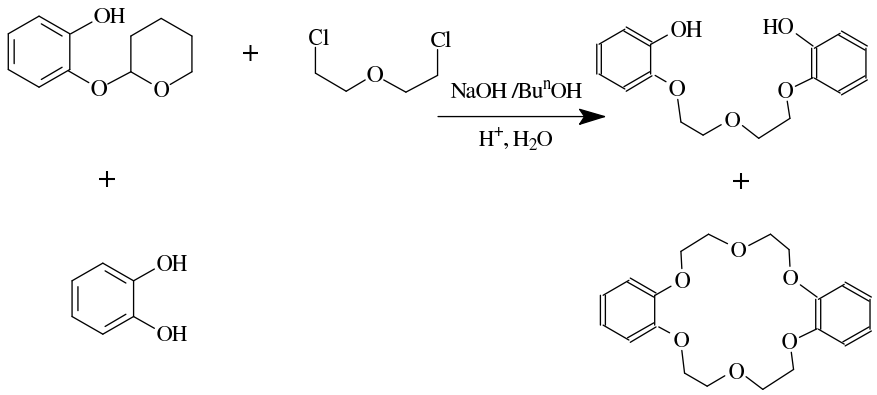

Fig. 1. Synthesis of crown ether by Pedersen.

This discovery has stimulated a rapid development of supramolecular chemistry, in particular the synthesis of new macrocyclic systems capable of selective complexation of small chemical individua such as ions or neutral molecules [6-11]. The recognition of importance and impact of the new field of chemistry was the Nobel Prize awarded to Charles Pedersen, Donald Cram and Jean-Marie Lehn in 1987 for the discovery of the synthetic routes to and binding properties of crown ethers [12-14].

The concept of a macrocyclic ligand or host or a molecular receptor is fundamental in supramolecular chemistry. Molecular receptors comprise the following groups of compounds: podands, crown ethers, cryptands, spherands, lariat ethers, catenanes, calixarenes, cyclodextrins, carcerands, cavitands, cryptophanes and others [15]. The ligands contain electron donor atoms of oxygen, nitrogen, sulphur or trivalent phosphorus and are capable of making complexes with the guests being metal ions, anions or neutral molecules [2, 8, 9, 15]. The host-guest complexes are formed in a selective way on the basis of the molecular recognition following from the complementarity of sizes of the host and guest molecules and other information carried by the architecture of the two molecules [2, 16]. The matching of the host and guest molecules is governed by the law of the double geometric and energetic complementarity of the receptor and the substrate, the so-called lock and key principle [17,18].

One of the major fields of research in supramolecular chemistry has become the design of efficient methods of synthesis of molecular receptors of specific target properties and ability to recognise selectively a certain guest molecule, and the use of the complexes for particular purposes.

Pedersen'discovery caused the huge progress the group of enormous number and structural variety of compounds tracing back to the original crown ethers. This group ranges over the monocyclic coronands, bicryptands, oligocryptands, spherands, cavitands, carcerands and even more structures connecting with ability of complex formation. Taking advantages and disadvantages of described above structures into consideration, such as high ability and stability to complex formation on the one hand, but difficulties and expenditure of synthesis, low kinetics of complexation on the other

hand, it was natural to find less-complicated acyclic systems. In this way the podands were appeared [15].

The term "podands" appeared in the chemical literature comparatively recently—towards the end of the 1970s. It embraces various types of acyclic polyether complex-forming agents. The name comes from the Greek word "podos"—foot. In the podand molecule, there is one or several "feet" formed by polyether chains with various end groups. According to the number of such feet, podands are divided into mono-, di-, tri-, and polypodands. Compounds of this type can be investigated long before the appearance of the term "podands" itself.. The Fig. 2 presents the structural features characteristic of podands, the donor atoms (D) in the open-chain framework. Podands (oligo- and polyethylene glycols and glymes) began to be regarded as open-chain analogues of crown ethers or cryptands (Fig. 2b and c) [15, 19].

Acyclic podands featuring an open-chain framework with alignment of oxygen atoms bridged via ethylene units and having hydroxyl or alkoxy (metoxy) terminal groups) (Fig 3) [15].

Podands make a group of compounds of diverse structures, varying from simple monopodands of polyethylene glycols (PEGs) and their dimethyl esters (Fig. 4A), through the di-, tri- and oligopodand species, to highly branched dendrimers. The compounds can include different electron donor atoms such as oxygen, nitrogen or sulphur (Fig. 4B).

The natural ionophores such as antibiotics or siderophores, are also classified as podands [20-23]. As follows from literature, podand compounds have good complex-forming abilities and form stable complexes with alkali metals and alkaline earth metals [9, 20-23] as well as with the cations of transition metals (Ag, Cd, Hg, Co, Cu or Ni) [24]. Also the complexes of podand ligands with anions [22, 25, 26] and neutral molecules have been reported [22, 25]. Taking into regard their specific complex forming abilities they are of prospective wide use in many areas of chemistry. They have been applied in organic synthesis [20-22, 27-30], chemical analysis (as extraction agents, carriers in transportation through selective membranes) [22, 31, 32], in catalysis of interphase transfer as catalysts [22, 32], in food, cosmetic and pharmaceutical industries [20, 22].

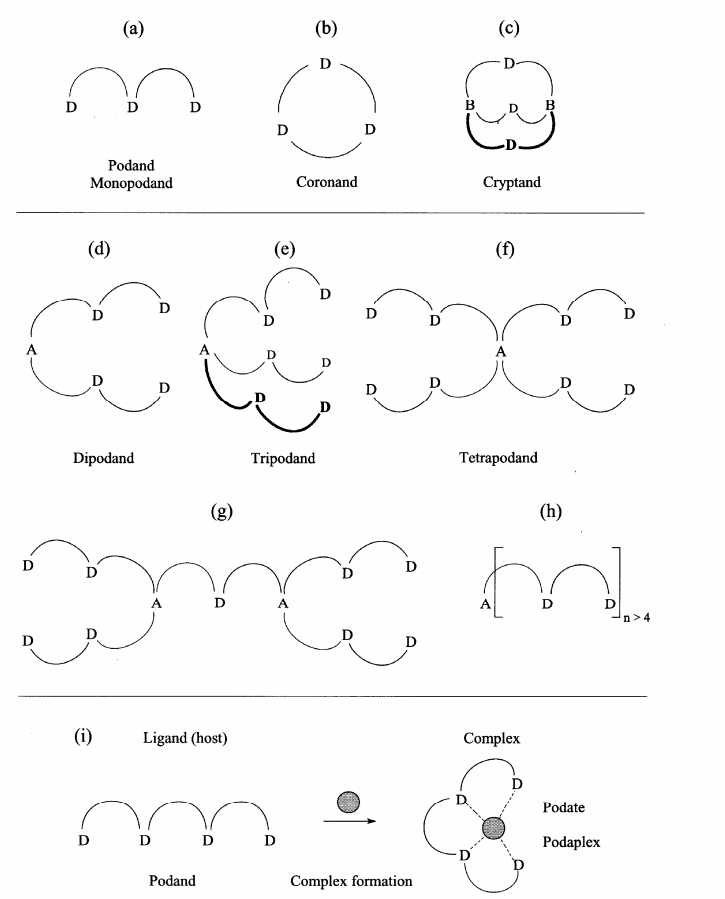

Fig. 2. Definition, specification and nomenclature of podands (a-h) and podands complexes (i) [15].

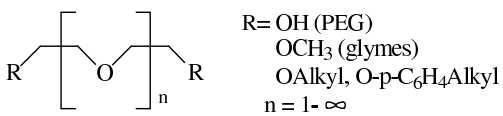

Fig. 3. Exemplary cases of linear podands [15].

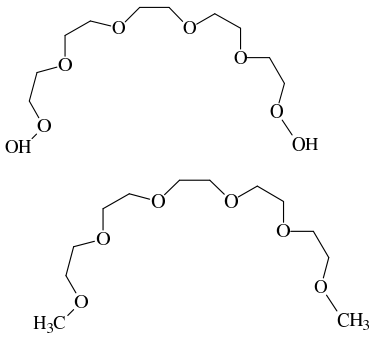

Polyethylene glycol (PEG) Dimethyl ethers of polyethylene glycol (glyme)

A – Monopodands

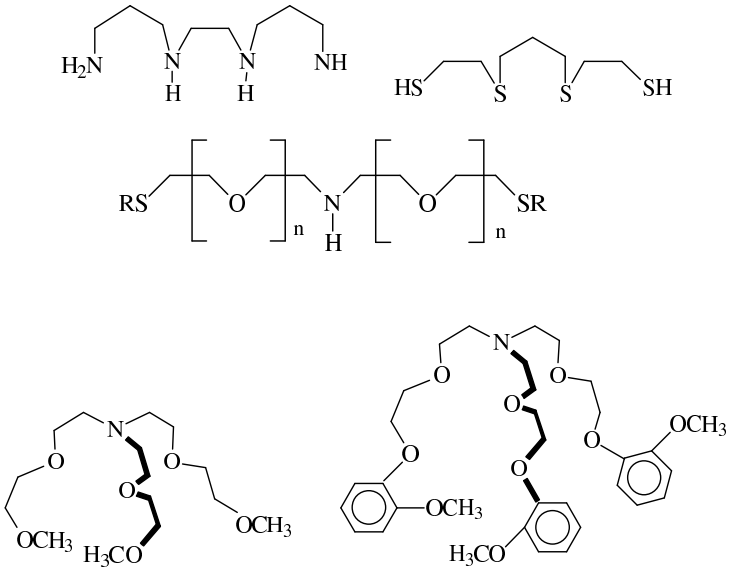

B – Varied structures of podands

Fig. 4. Exemplary cases of podand's structures: A-monopodans, B- varied podand's structures

Complexation of podands

Podands have the similar properties to the crown compounds and are able to form complexes. These complexes are called “podates” or “podaplexes”. But the nature of acyclic structures are contrasted with macrocyclic crown compounds and they are also differences in the behaviors of these two types of compounds. Thus the simplest representatives of monopodands [diethyl ethers of oligo(ethylene glycols — glymes] became well known in the 1950s—1960s as solvents solvating alkali and certain other metal cations. Polyether acyclic antibiotics (nigericin, monensin, etc.), containing tetrahydrofuran and tetrahydropyran rings in the chain, which were discovered and vigorously investigated in the 1950s —1970s, belong to the same type of complex-forming agents [19]. These compounds effect the transport of alkali metals through artificial and biological membranes. In the complex formation reaction, the molecules of acyclic antibiotics twist round a cation and form a pseudoring stabilised by the intramolecular interaction of the end groups. Podands form complexes with alkali metal cations of increasing stability with increasing chain length of the podand. For comparison in Fig 5, the stabilities of the potassium cation complexes of pentaglyme and 18C6 are presented. The enormous binding difference result from “macrocyclic effect” and could be explained by enthalpic and entropic effects, favorable for crown ether [15, 24]. The potassium complex of cryptand 222 is still more stable and it is a consequence of the macrobicyclic or cryptate effects [15].

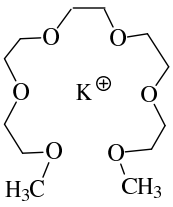

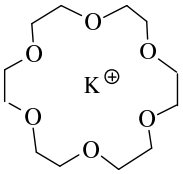

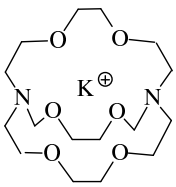

log K_S 1.5 (Na^+) 4.4 (Na^+) 7.9 (Na^+)

2.3 (K^+) 6.1 (K^+) 10.4 (K^+)

Fig. 5 The comparison of complex formation of podand, crown ether 18C6 and cryptand 222, log Ks of the Na+ and K+ complexes demonstrating the macrocyclic and cryptate effects.

The character of donor atoms contained in the podand framework affinity for metal cations has an influence of affinity for metal cations. Podands with all-oxygen atoms in the polyoxaalkyl chains favor the formation of complexes with alkali and alkaline earth metal cations (Fig. 6) [33], while podands with nitrogen and sulfur donor atoms (but also with oxygen donor atoms) into the podand framework are very susceptible to complex the transition metal cations, such as Ag [Fig. 7], Cd, Hg, Co or Ni [15, 24, 34].

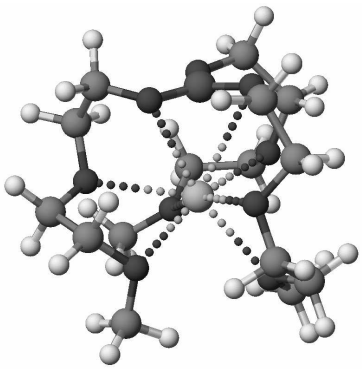

Fig. 6. The structure of the 1:1 complex of B3.3 with sodium(I) cations (PM5).

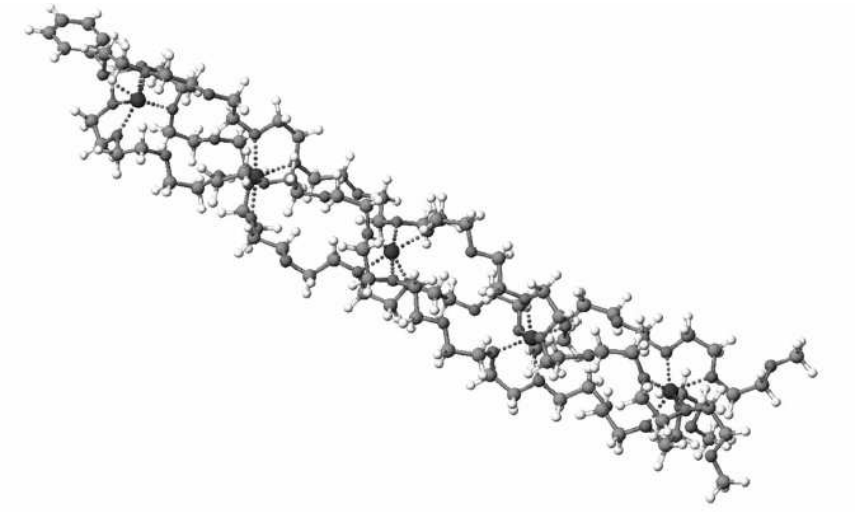

Fig. 7. The structure of the 1:5 complex of PhSi15.3 with silver(I) cations (PM5) [34].

Complexation between podands and anions is rather recent development [15, 25]. Anions often complexed by host range from simple inorganic halide ions to the biologically relevant phosphate or carboxylate ions (Fig. 8).

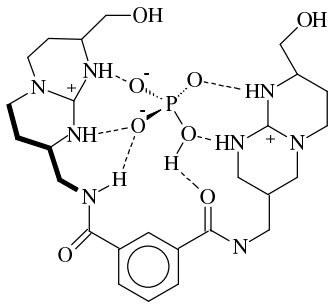

Fig. 8. Complex formation of podand with ion HPO_4^{2-}.

The forming complexes between podands and uncharged molecules are also possible, but they are less strongly explored than between podands and cations (Fig. 9) [35].

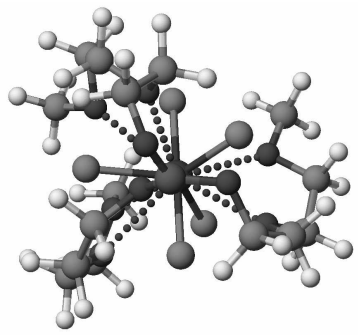

Fig. 9. The structure of the 1:1 complex of B3.3 with $SbCl_5$ (PM5) [35].

The ability of podands to interact with metal cations is used in membrane processes. However, there is no direct relation between the effectiveness of the complex-forming agent and its membranotropic properties. Ligands which are effective complex forming agents for alkali and alkaline earth metal cations are not

always good agents for the transfer of ions through membranes. Ion transport can be achieved subject to the condition that the complex formation process is selective and dynamic. It has been shown that [36] there exists a range of optimum stability constants of complexes for the most effective transport of cations. Above and below this range, the rate of transport falls sharply. For a series of alkali and alkaline earth metal cations, ion transport is slight or is altogether absent if the logarithms of the complex formation constants in methanol are less than 3.5—4.0 units.

Open-chain ligands of the amide type with aromatic or hydrocarbon substituents and with a long chain at the nitrogen atom are selective agents transferring alkali and alkaline earth metal ions through liquid membranes [19] (Fig.10).

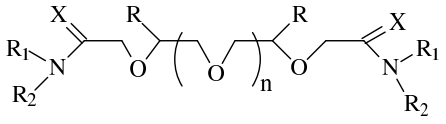

$R=R_2=Alk$, n=0-2, X=O, S $R_1=(CH_2)_mCO_2Alk$ (m=1-11)

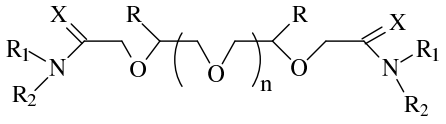

$R=CH_3$, $R_1=C_7H_{15}$, $(CH_2)_5COOC_4H_9$

Fig.10. Podands - selective agents transferring alkali and alkaline earth metal ions through liquid membranes

Podand's complex-forming agents of a new type were created on their basis and found extensive application as solvents. Despite certain advances, this field nevertheless remained of secondary importance compared with the much more thoroughly developed and popular field of macrocyclic complex-forming agents. However, in recent years open-chain analogues of crown-ethers have attracted increasing attention because of their availability, fairly high effectiveness, and the possibility of regulating on a wide scale their complex-forming properties by altering their structure. Their properties as phase transfer catalysts, extractants, and as

components of ionselective electrodes are being investigated. The growing interest in this new class of complex-forming agents is reflected by review articles on this topic. The present review differs from those already published by a much more complete coverage of literature (up to 1988), an attempt at the analysis of the dependence of the complex-forming capacity of podands on their structure, and a discussion of the applied aspects of the problem [19].

Podands as solvents for chemical reactions

At the present time, the number of studies devoted to the practical use of podands is small but these compounds have considerable potential possibilities for applications in chemistry and technology. At [36] podands were applied as solvents for the proton transfer reactions between C-acids such as phenyl(4-nitrophenyl)cyanomethane and dimethyl (4-nitrophenyl)malonate with a strong N-base: 7- methyl-1,5,7-triazabicyclo[4.4.0]dec-5-ene (MTBD), studied by kinetic methods. These usewed podands are characterized by the different lengths of the polyoxaalkyl chains and central atoms: Si and P {Fig. 11].

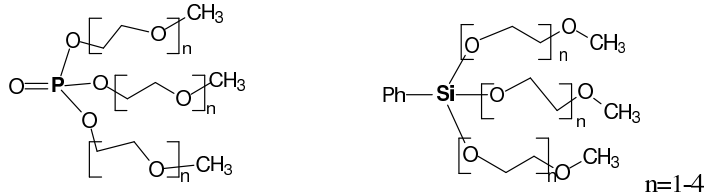

Fig. 11. Structures of podands used as solvents [37]

It is interesting to no that one of the most important factors in the kinetic studies of reactions in solutions is the selection of an appropriate solvent. The solvents have a strong influence on the kinds of reaction, the form of the substrate and the structure of the product and should not be considered only as a macroscopic medium characterized by physical constants such as density, dielectric constant and index of refraction, but also as a medium that consists of individual, mutually interacting solvent molecules. The interaction between species in solvents is on the one hand too big for it to be

treated by the laws of the kinetic theory of gases, but on the other hand, it is too small for it to be treated by the laws of solid state physics [38, 39].

The spectroscopic study of the stability of the ionic product of proton transfer reaction indicates the long lifetime of this product in podand solvents. Furthermore, this lifetime increases with an increasing of length of the polyoxaalkyl chain. Podand solvents in studying the proton transfer reactions very strong determined the kinetic parameters as well as the stabilisation of products. This observation may play a very important role in studies of the transition states of organic reactions in which proton transfer occurs [37].

Podands in Phase Transfer Catalysis

Because of cation complexation and relating to the increased solubility of inorganic salts in low polarity organic solvents and better activity of "naked anion" the podands, similar as crown ethers and cryptands, are used is Phase Transfer Catalysis (PTC), which constitutes a promising method for effecting chemical reactions, both solid-liquid and liquid-liquid systems. Oligo- and polyethylene glycols accelerate the nucleophilic substitution reactions at a carbon atom between anions and water-insoluble neutral organic compounds in two-phase systems. Phase transfer catalysis (PTC) is now a well-established method of organic synthesis applicable to reactions of inorganic and organic anions and other active species with organic compounds. Phase transfer catalysis has been widely used in organic chemistry and is usually, but not always, based on the reactions involving transfer of anion from an aqueous or solid phase into an organic phase, followed by the reaction of the anion with the substrate in the organic phase. The reacting anions are continuously introduced into the non-polar organic phase as ion pairs with complexed cations supplied by the catalyst. Further reactions of these ion pairs proceed in the organic phase[40-43].

Nowadays the term "phase transfer catalysis" refers to several effective techniques attractive for their simplicity, mild conditions required, high reaction rates and rather inexpensive reagents, and belonging to the most versatile preparative methods. The search for new catalysts to be used in PTC asymmetric synthesis and the attempts to understand their mechanistic role are current topics of investigation. The

PTC technique was introduced almost 40 years ago by the three independent research groups of Mąkosza, [40], Braensdtroem and Gustavii [41] and Starks [42]. Since then there has been great interest in organic reactions carried out using PTC catalysts, most often tetra-alkylammonium salts, crown ethers, cryptands, etc. The most important problems in PTC are to find the optimum reaction conditions and the most effective catalysts [43-45].

In recent years, polypodands being open chain ligands with several polyether chains linked to the same binding centre, have attracted increasing interest as anion activators in homogeneous and heterogeneous systems. They represent a valid alternative to the cyclic analogues of crown ethers and cryptands because of their substantially lower cost, relative non-toxicity and high effectiveness. Several important applications of podands are given [15, 20, 23, 46] including their use in phase transfer catalysis. The first application of podands in PTC was reported by Lehmkuhl et al. [47], who studied a variety of nucleophilic substitution of benzyl bromide with different potassium salts.

The use of silicon, phosphorus or boron polypodands, characterized by different length of polyoxaalkyl chains (Fig. 12) as phase-transfer catalysts was the first reported a few years ago [48-53]. Relative to the traditional classical phase transfer catalysts such as crown ethers, cryptands and polyethylene glycols, which have been by far the most studied phase transfer catalysts, polypodands are easy to prepare and much cheaper.

The effectiveness of podands increases with increase in concentration and in the molecular weight of the ligand. The increase in the rates of reactions (for example nucleophilic substitution) in the presence of podands has been explained by the cooperative salvation of alkali metal cations by oxygen atoms leading to the activation of the anions. The influence of the length of the alkyl group (CH_3 or $C_{16}H_{33}$ or Tr) terminating the polyoxaalkyl chain on the complexation properties of the ligands was also observed

The catalytic activity of polypodands (Fig 12) was measured in typical SN2 nucleophilic substitution reactions of *n*-octyl methanesulfonate or 1-bromooctane in organic solvent:solid MY two phase systems and compared with that exhibited by

catalytic amount of ligands (PEG, crown ethers cryptands) under the same conditions (reactions (1a) and (1b)). Chlorobenzene or acetonitrile determined the organic solvent and the solid state (MY) was defined by NaI, NaBr or KI.

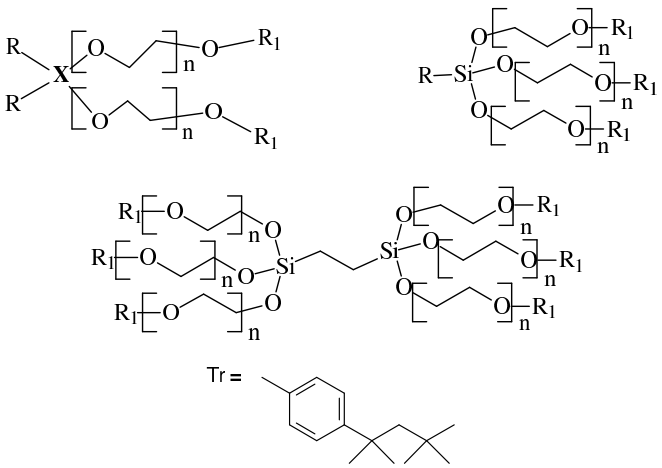

Fig. 12 Podands used as catalysts in some anion promoted reactions.

$$n\text{-}C_8H_{17}X + MY_{solid} \xrightarrow[PhCl\,(AN),\,60^{o}C]{cat.} n\text{-}C_8H_{17}Y + MX_{solid} \quad (1)$$

where X = OSO_2Me, Br; MY = NaI, NaBr, KI

The reduction of benzaldehyde to the corresponding benzylic alcohol with NaBH4 was performed in a chlorobenzene-solid NaBH4 two-phase system by using catalytic amounts (0.1 mol equiv) of polypodands and comparative ligands (reaction (2)) at 25◦C:

$$C_6H_5CHO \xrightarrow[PhCl,\,25^{o}C]{NaBH_4,\ cat.} C_6H_5CH_2OH \quad (2)$$

The *N*-alkylation reaction of potassium phthalimide by 1-bromooctane was carried out at 80°C in an acetonitrile-solid $C_6H_4(CO)_2NK$ two-phase system in the presence of catalytic amounts (0.1 mol/mol substrate) of ligands and with a 1:1 molar ratio potassium phthalimide to alkylbromide (reaction (3)) in acetonitrile as a solvent.

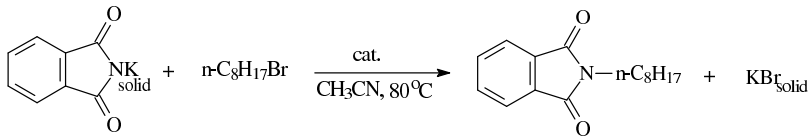

(3)

The *O*-alkylation reaction of phenol by 1-bromooctane (with a 1:1 molar ratio) performed at 110°C in toluene-solid K2CO3 two-phase system in the presence of catalytic amounts (0.1 mol/mol substrate) of ligands

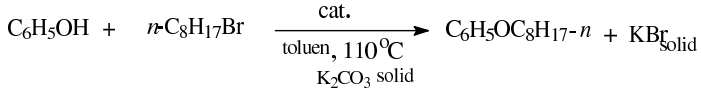

(4)

It has been proved that the class of boron, silicon or phosphorus polypodands, combining easy availability and good stability with excellent complexing properties and high catalytic activity, make a valid alternative to more sophisticated crown ethers as catalysts in solid–liquid phase-transfer reactions, particularly in large scale processes. Podands behave as efficient phase transfer (PT) agents under SL-PTC conditions and they are more stable and insensitive to water, with their catalytic activity being generally superior to those of PEGs, crown ethers.

Another effective application of podands is association with their ability to solubilise salts in solvents of low polarity (chlorobenzene). This makes it possible to carry out a whole series of reactions under homogeneous conditions in non-polar media.

A series of applications of podands are also associated with their membrane activity. Some of them can be used in cation-sensitive membrane electrodes specific to

alkali and alkaline earth metal ions The great variety of structures of the neutral acyclic polydentate ligands makes it possible to vary their selectivity with respect to cations within wide limits. The ability of podands to form complexes with neutral organic molecules can be of pharmacological interest, particularly in the case of urea. But the most important advantage podands is their inherent inexpensiveness. The availability of these compounds makes them promising complex forming agents which can find applications in various branches of chemistry and the national economy. The some practical application of podands is presented in Fig. 13 [15, 19].

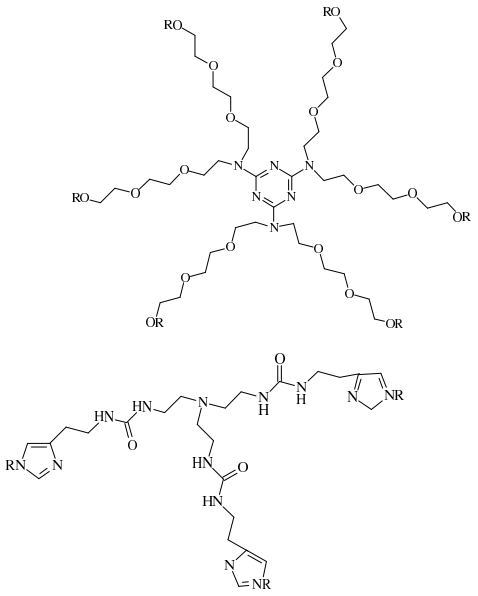

R = n-C_4H_9, n-C_8H_{17}

A – PT-catalyst

R = $(CH_2)_{11}CH_3$

B – enzyme model

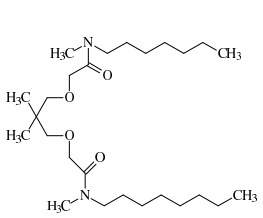

(Li^+)

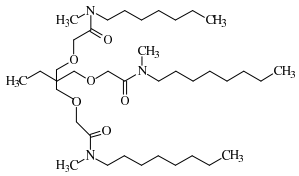

(Na^+, $Na^+ >> K^+$)

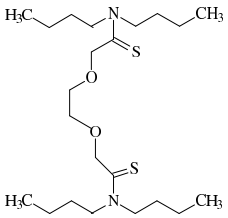

(Cd^{2+})

C-E – selective membrane carries (ions to be determined in parentheses)

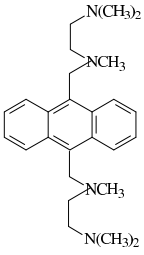

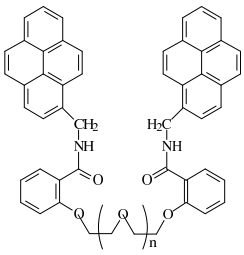

F, G – fluoroionophores

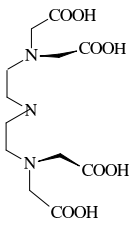

H – imaging agent

Fig. 13. Some practical application of podands [15].

Acknowledgements

The authors thanks the Polish Ministry of Science and Higher Education for financial support under Grants No. R015 016 01 in the years 2006–2008 and No N204 109 31/2553 in the years 2006–2007.

References:

1. J.-M. Lehn, *Angew. Chem. Int. Ed. Eng.*, 29 (1990) 1304-1319.

2. J.W. Steed, D.R. Turner, K.J. Wallace, *Core Concepts in Supramolecular Chemistry and Nanochemistry*, John Wiley&Sons, 2007.

3. C.J. Pedersen, *J. Am. Chem. Soc.*, 89 (1967) 2495 2496.

4. C.J. Pedersen, *J. Am. Chem. Soc.*, 89 (1967) 7017-7036.

5. U. Olsher, M.G. Hankins, Y.D. Kim, R.A. Bartsch, *J. Am. Chem. Soc.*, 115 (1993) 3370-3371.

6. B. Dietrich, J.-M. Lehn, J.-P. Sauvage, *Tetrahedron Lett.*, 34 (1969) 2885-2888.

7. B. Dietrich, J.-M. Lehn, J.-P. Sauvage, *Tetrahedron Lett.*, 34 (1969) 2889-2892.

8. J.L Atwood, J.E.D. Davies, D.D. MacNicol, F. Vögtle, *Comprehensive Molecular Chemistry*, Elsevier Sciece: Oxford, 1996.

9. F. Vögtle, E. Weber, *Host-Guest Complex Chemistry*, Springer Verlag: Berlin, 1985.

10. H.M Colquhoun, J.F. Stoddart, D.J. Williams, *Angew.Chem. Int. Ed. Engl.*, 25 (1986) 487-507.

11. L.F. Lindoy, *The Chemistry of Macrocyclic Ligands Complexes*, Cambridge University Press, Cambridge, 1989.

12. C.J. Pedersen, *Angew.Chem. Int. Ed. Eng.*, 27 (1988) 1021-1027.

13. D.J. Cram, *Angew.Chem. Int. Ed. Eng.*, 27 (1988) 1009-102.

14. J.-M. Lehn, *Angew.Chem. Int. Ed. Eng.*, 27 (1988) 89-112.

15. E. Weber, *Podands,* in *Encyclopedia of Supramolecular Chemistry*, (Ed. J.L Atwood, J.W. Steed), Marcel Dekker, New York, 2004, 1106-1119.

16. A.D. Buckingham, A.C. Legon, S.M. Roberts, *Principles of Molecular Recognition*, Kluwer Academic Publishers, Dordrecht, 1993.

17. E. Fisher, Chem. Ber., 27 (1894) 2985-2993.

18. J.P. Behr, *The Lock and Key Principle*, Wiley, Chichester, 1995.

19. T.E. Kron, E.N. Tsvetkov, Russ. Chem. Rev., 59 (1990) 283-295.

20. G.W. Gokel, O. Murillo, *Podands*, in *Comprehensive Molecular Chemistry* (Eds. J.L Atwood, J.E.D. Davies, D.D. MacNicol, F. Vögtle), Elsevier Sciece: Oxford, 1996, vol.1, 1-33.

21. G.W. Gokel, Crown Ethers and Cryptands, in *Large Ring Molecule* (Ed. J.A. Semlyen), John Wiley, New York, 1996, 263-307.

22. J.W. Steed, J.L. Atwood, *Encyclopedia of Supramolecular Chemistry*, Marcel Dekker, New York, 2004.

23. F. Vögtle, E. Weber, *Angew. Chem. Int. Ed. Eng*., 18 (1979) 753-776.

24. H.-J. Schneider, A. Yatsimirsky, *Principles and Methods in Supramolecular Chemistry*, Wiley, Chichester, 2000.

25. J.W. Steed, J.L. Atwood, *Supramolecular Chemistry*, Wiley, Chichester, 2000.

26. C. Seel, J. De Mendoza, *From Chloride Katapinates to Trinucleotide Complexes: Developments in Molecular Recognition of Anionic Species*, in *Comprehensive Molecular Chemistry* (Eds. J.L. Atwood, J.E.D. Davies, D.D. MacNicol, F. Vögtle), Elsevier Sciece: Oxford, 1996, vol.2, 519-552.

27. C. Piguet, G. Bernardinelli, G. Hopfgartner, *Chem. Rev.*, 97 (1997) 2005-2062.

28. G.R. Newkome, C.N. Moorefield, F. Vögtle, *Dendrimers and Dendrons*, Wiley-VCH, Weinheim, 2001.

29. S.M. Grayson, J.M. J. Fréchet, *Chem. Rev.*, 101 (2001) 3819-3867.

30. J.-P. Sauvage, C. Dietrich-Buchecker, *Molecular Catenanes, Rotaxanes and Knots*, Wiley-VCH, Weinheim, 1999.

31. E. Blasius, K.-P. Janzen, *Analytical Applications of Crown Compounds and Cryptands,* in *Host-Guest Complex Chemistry I* (Ed. F. Vögtle), Springer-Verlag, Berlin, 1981, vol.98, 163-189.

32. B.A. Moyer, *Complexation and Transport*, in *Comprehensive Molecular Chemistry* (Ed. J.L Atwood, J.E.D. Davies, D.D. MacNicol, F. Vögtle), Elsevier Sciece: Oxford, 1996, vol.1, 377-416.

33. B. Łęska, R. Pankiewicz, O. Nevecheriya, V. I. Rybachenko, G. Schroeder, B. Brzezinski, *J. Mol. Struct.*, 840 (2007) 1-5.

34. J. Kira. B. Łęska, G. Schroeder, P. Przybylski, B. Brzezinski, *J. Mol. Struct.*, 738 (2005) 227-231.

35. B. Gierczyk, G. Schroeder, G. Wojciechowski, B. Łęska, V.I. Rybachenko, B. Brzezinski, *J. Mol. Struct.*, 516 (2000) 153-156.

36. J D Lamb, J J Christensen, J L Oscarson, J. Am. Chem. Soc, 102 (1980) 6820-6825.

37. B. Gierczyk, B. Łęska, B. Brzezinski,G. Schroeder, *Supramol. Chem.*, 14 (2002) 497-502.

38. K.A. Connors, *Chemical Kinetics The Study of Reaction Rates in Solution,* VCH, New York, 1999.

39. J.I. Steinfeld, J.S. Francisco, W.L. Hase, *Chemical Kinetisc and Dynamics*, Prentice Hall, New Jersey, 1999.

40. M. Mąkosza, *Tetrahedron Lett*., (1966) 4621-4627.

41. A. Braensdtroem, K. Gustavii, *Acta Chem. Scand.*, 23 (1969) 1215.

42. C.M. Starks, *J. Am. Chem. Soc*., 93 (1971) 195.

43. E.V. Dehmlow, S.S. Dehmlow, *Phase Transfer Catalysis*, 3rd ed. Verlag Chemie, Weinheim 1993.

44. F. Montanari, S. Quici, S. Banfi, *Phase Transfer Catalysis* in *Comprehensive Molecular Chemistry* (Eds. J.L Atwood, J.E.D. Davies, D.D. MacNicol, F. Vögtle), Elsevier Sciece: Oxford, 1996, vol.10, 389-416.

45. S. Quici, A. Manfredi, G. Pozzi, *Phase-Transfer Catalysis in Environmentally Benign Reaction Media* in *Encyclopedia ofSupramolecular Chemistry* (Eds.

J.L. Atwood, J.W. Steed vol. 2, Marce l Dekker, Inc., New York, USA, 2004, 1042-1052.

46. D. Landini, A. Maia, M. Penso, *Anion Activation* in *Comprehensive Molecular Chemistry* (Eds. J.L Atwood, J.E.D. Davies, D.D. MacNicol, F. Vögtle), Elsevier Sciece: Oxford, 1996, vol.1, 417-464.

47. H. Lehmkuhl, R. Farroch, K. Hauschild, *Synthesis,* 3 (1977) 184-201.

48. B. Łęska, R. Pankiewicz, G. Schroeder, A. Maia, *Tetrahedron Lett*., 47 (2006) 5673-5676.

49. B. Łęska, R. Pankiewicz, G. Schroeder, A. Maia, *J. Mol. Catal. A: Chemical*, 269 (2007) 141-148.

50. A. Maia, D. Landini, B. Łęska, G. Schroeder, *Tetrahedron Lett*., 44 (2003) 4149-4151.

51. A. Maia, D. Landini, B. Łęska, G. Schroeder, *Tetrahedron*, 60 (2004) 10111-10115.

52. A. Maia, D. Landini, C. Betti, B. Łęska, G. Schroeder, *New J. Chem*., 29 (2005) 1195-1198.

Chapter 8

Advances in Li-ion battery materials with the application of silanes and other organosilicon compounds - overview of possible strategies

Mariusz Walkowiak

Institute of Non-Ferrous Metals, branch in Poznan, Central Laboratory of Batteries and Cells, Forteczna 12, 61-362 Poznań, Poland

1. Introduction

1.1. Basic principles of Li-ion batteries

High energy rechargeable batteries based on lithium (lithium-ion batteries) have achieved an incredible success over the last fifteen years. Practically all types of portable electronic devices available on the market, including cellular phones, laptop computers, palmtops, GPS navigation sets, etc. are today powered by small Li-ion batteries. This type of batteries is also believed to be the most prospective energy source for a variety of demanding future applications, such as electric vehicles, medical equipment and various devices for space exploration. In spite of this remarkable progress that has been made, however, basic chemistry involved in the Li-ion battery technologies has not changed significantly over these years. Graphite remains the material of choice as far as anode active materials are considered. Lithiated oxides of manganese, cobalt or nickel are still commonly used as active cathode materials. Finally, liquid electrolytes based on the mixtures of organic carbonates as solvents can still most commonly be found in commercial batteries [1]. Basic processes occurring in Li-ion batteries during their operation involve reversible lithium cation insertion and shuttling between two insertion-type electrodes (Fig 1).

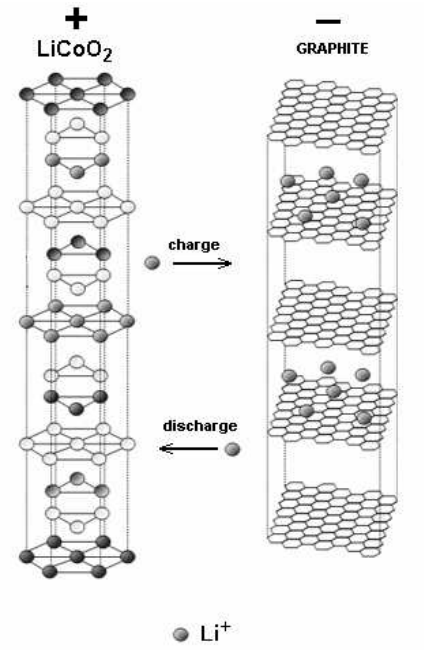

Fig. 1. Scheme of Li-ion cell

Upon discharging the cations are deintercalated from between the graphene sheets of the graphitic active material to the near-electrode area of the electrolyte. During this process the so-called lithium-graphite intercalation compound (Li-GIC) changes to pure graphite. The process is reflected by the following schematic equation:

$$\text{Li-GIC} \rightarrow \text{graphite} + Li^+ + e^-$$

De-intercalated cations migrate in the electric field towards cathode, where they undergo the process of insertion into the free sites of suitable transition metal oxide lattice, according to the equation:

$$Li^+ + e^- + \text{oxide} \rightarrow \text{Li-oxide}$$

Both the reaction on anode and cathode side are topotactic, which means that the basic framework/matrix for Li cations (the carbon lattice in case of anode and oxygen lattice in case of cathode) remains, in principle, unchanged. Based on this elegant concept, the present-day commercial batteries are capable of being discharged and recharged more then one thousand times without significant loss of capacity.

1.2. Limitations of the existing technologies

The advantages of Li-ion batteries based on the design scheme described above can be summarized as high working voltage (3.6-3.8 V, depending mainly on the type of cathode active material), relatively high energy density as compared to other battery technologies and long cycle life. Early disadvantages, such as high manufacturing cost or poor high power capability have been removed to a certain extent. Safety remains still the most serious problem, hindering the wide-spread utilization of large-scale cells, however this issue is not so important in the case of small batteries designed for fuelling portable electronics, especially if appropriate safety features (including protecting electronic circuits) are applied. Another inherent limitation of traditional Li-ion cells is the inability to work in extremely low temperatures (below ca. -20 °C). This limitation is connected to the fact that ethylene carbonate (EC) is commonly applied as electrolyte co-solvent. Application of EC is inevitable since this compound enables formation of appropriate passive layer on graphite anode, which is essential for effective function of the whole Li-ion cell. Unfortunately, EC is characterized by a high melting point (in fact, EC is solid in room temperatures), thus limiting the low-temperature viscosity and conductivity of traditional electrolytes.

In spite of the mentioned drawbacks, incredible efforts made in research institutes and in battery companies have made it possible to achieve an outstanding progress. This progress, however, is based on incremental improvements of the core concept rather that on any major breakthroughs. Nevertheless, it is widely recognized among battery researchers and engineers that the existing Li-ion battery technologies quickly approach limits beyond which they will no longer be able to keep pace with more and more demanding applications. New electronic devices are more power consuming then ever. For example, new cellular phone features, such as bigger

displays, modems, cameras, applications for watching TV, video calls, browsing the internet, etc., are about to increase very markedly the demand for energy, whereas the expected increase in the batteries energy density (at the existing core technologies) is expected to rise only by 8% per year in the next 5 years (most of this improvement will be used to reduce physical size of batteries). This "energy gap" will put pressure on manufacturers to look for more efficient energy sources for cellular phones and other portable devices [2].

Great efforts are being done in the research laboratories worldwide, aiming at developing new battery materials. Further in this chapter, some of the possible routes of improvements of the existing electrode and electrolyte active materials will be briefly outlined, based on the application of organosilicon compounds, either applied directly or as precursors.

2. Prospects for silanes as components of Li-ion battery electrolytes

2.1. Silanes as electrolyte solvents

Liquid silanes with polyether units may be considered as possible electrolyte solvents for Li-ion batteries. Free electron pairs on ether oxygen atoms will co-ordinate Li^+ cations, thus enabling dissolution of lithium salts. Silanes with polyether units are often designated as silicon podands (Si-podands) and have recently attracted considerable attention as potential solvents for certain organic syntheses and phase transfer catalysis [3-7]. Lithium cation easily enters in host-guest interactions with Si-podands (especially tripodands) playing role of cation acceptor. Formation of complexes between Li^+ and such Si-tripodands as ethyl tris-2-methoxyethoxy silane and vinyl tris-2-methoxyethoxy silane has been found to be thermodynamically and sterically favorable (heats of formation: -115.55 and -330.86 kJ/mol, respectively [3]).

Not every Si-podand can automatically become viable electrolyte solvent, despite of being excellent solvent for Li salts. Sufficiently low viscosity (and, consequently, sufficiently high room temperature conductivity, preferably higher then 10^{-3} S/cm) is required, as well as appropriate film forming properties in relation to graphite anode. The two conditions impose stringent restriction as for the selection of possible electrolyte solvent. Nevertheless, Amine *et al.* [8] have demonstrated that

certain podand-type silanes can be used as single electrolyte solvents for Li-ion cells. Molecular structures examined by them are given below:

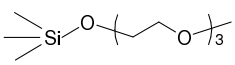

1

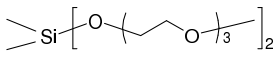

2

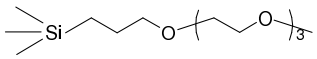

3

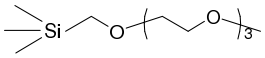

4

It has been found that electrolytes based on the above solvents and lithium bis(oxalato)borate (LiBOB) salt are electrochemically stable up to 4.4 V and exhibit high conductivities, exceeding 10^{-3} S/cm at room temperature. Performance of full Li-ion cells with graphitic anodes and transition matal oxide as cathodes has also been demonstrated. The results are encouraging for further consideration of podand-type silanes as single solvents. It should be kept in mind, however, that proper graphite passivation is only possible with the application of specially selected lithium salts.

2.2. Silanes as functional co-solvents/additives

Electrolyte additives are compounds or substances added in relatively small amounts (typically 1-10 w/w) to the main solution in order to enhance certain key physico-chemical parameters (viscosity, conductivity, etc.) or to fulfill certain specific function (for example to assist the formation of passive layer) Additives play sometimes crucial role in the design of successful electrolyte composition. Excellent review of electrolyte additives found in Li-ion cells has recently been given by Zhang [9].

Podand type silanes can be regarded as attractive candidates for electrolyte additives. This is due to a relative ease of functionalization and because of the fact that these compounds have themselves the ability of dissoluting lithium salts, thus can be added to the main solution in fairly large quantities without significant loss in

conductivity. Apart from that, many silanes are relatively cheap and easy to synthesize. Schroeder *et al.* [10-11] reported recently the application of ethyl tris-2-methoxyethoxy silane and vinyl tris-2-methoxyethoxy silane as additives for Li-ion battery electrolytes containing propylene carbonate (PC) as the main solvent and graphitic anodes.

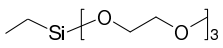

5

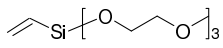

6

This particular type of additives can be classified as passive layer formation enhancers. It is widely known that graphite anodes are inherently incompatible with PC-based electrolytes, due to the detrimental phenomenon of solvent co-intercalation and subsequent graphite exfoliation. It was found that addition of Si-tripodands with vinyl and ethyl functional groups suppresses these undesirable processes, enabling effective cell functioning. The authors claim that a new mechanism of electrode passivation may occur in the systems containing Si-tripodands, involving condensation of tripodand centers to form a kind of network. Formation of such a network, being a barrier for PC molecule penetration, would be a specific feature of Si-tripodands.

2.3. Polymer electrolyte architectures comprising silane structural units

Polymer electrolytes based on polyether units grafted to a siloxane backbone have been reported by Khan *et al.* [12] as early as in 1988. Later on a similar approach was presented by Oh *et al.* [13] and Rossi *et al.* [14]. Ether oxygen atoms ensure complexation of lithium cation in a manner similar to that known for poly(ethylene oxide) (PEO) based electrolytes. Interesting variant of this general concept has very recently been proposed by Walkowiak *et al.* [15]. Silicon tripodand centers have been attached to the polysiloxane main chain in the hydrosilylation reaction between the double bond of vinyl tris-2-methoxyethoxy silane and Si-H bond of suitable polysiloxane reagent. The resulting polymer structure is given below:

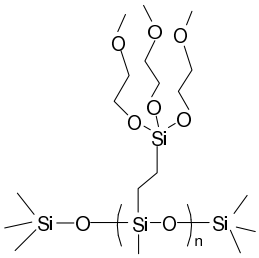

7

An interesting feature of this polymer architecture is that short polyether units can self-assemble in the presence of Li^+ exactly as in the case of "free" Si-tripodand molecules. In such a way a highly ordered arrangement of lithium co-ordination sites along the polysiloxane chain is obtained, creating pathways of high ionic mobility. It is supposed that Li cations will hope between the neighboring Si-tripodand "cages" rather then be subjected to random movements assisted by thermal motions of polymer segments (Fig. 2).

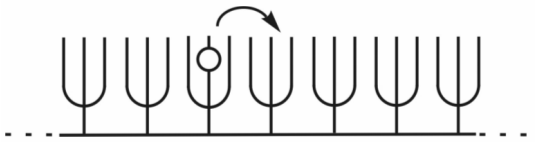

Fig. 2. Model representation of "inter-cage hopping" of lithium cation within the polymer host

Indeed, room temperature conductivities recorded for electrolyte membranes prepared from such polymer are exceptionally high, even exceeding 10^{-3} S/cm, which is probably one of the best results ever reported for non-plasticized lithium conducting polymer electrolytes. It seems that the idea of grafting the main polysiloxane chain with Si-tripodand centers to produce polymer electrolytes has a significant potential and deserves further consideration. Fig. 3 shows exemplary structures based on the this general scheme. Elongating the main chain should result in more robust membranes, whereas the two other options shown on the picture are expected to give higher charge carrier concentrations.

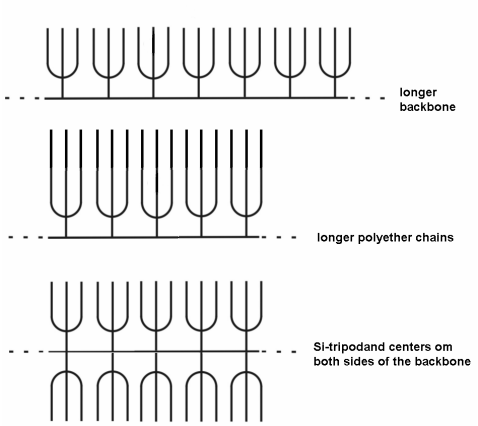

Fig. 3. Possible variants of the concept of polymer with tripodand centers

2.4. Silanized nanoparticles for composite polymer electrolytes

Functionalized nanoparticles attract more and more attention in many areas of science and technology. As far as Li-ion battery materials are considered, functionalized ceramic nano and sub-microparticles (mainly silica) evoke some interests among researchers as potential fillers for polymer electrolytes. Both dry (non-plasticized) and gel polymer electrolytes are widely regarded as potential candidates to replace traditional liquid carbonate-based electrolyte solutions. Polyethylene oxide (PEO) has been the most typical and thoroughly studied polymeric host and solvent for lithium cations. As early as in 1973 Armand discovered that solid PEO-lithium salt complexes exhibit appreciable conductivities, of the order of 10^{-7} S/cm [16]. Since then, great amount of work has been devoted to elevating the room temperature conductivities to a practically acceptable level. One of the possible approaches is to disperse ultra-fine ceramic powders in the polymer-salt complex. Composite polymer-ceramic electrolytes obtained this way show markedly enhanced cation transport properties, as well as improved electrochemical and mechanical stability (see review works [17-21]). One of the latest trends in composite polymer-ceramic electrolytes for Li-ion cells is the application of surface functionalized ceramics. Silica particles have

been modified and studied using various silane coupling agents, according to the general scheme:

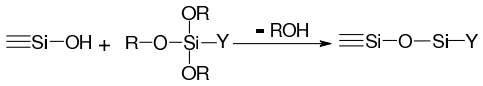

A number of researchers have reported that addition of silica particles modified via the above scheme resulted in significant enhancements. Liu *et al.* [22] applied silica filler functionalized with polyether segments through the following silane coupling agent (for n = 6-9) as filler in PEO-$LiBF_4$ system:

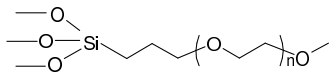

Compared with unmodified silica as ceramic filler, improved Li/polymer interfacial stability was observed, as well as enhanced mechanical stability and ionic conductivity.

Walkowiak *et al.* [23-24] studied gel-type systems consisting of poly(vinylidene fluoride-co-hexafluoropropylene) (PVdF/HFP) as polymeric matrix, suitable liquid electrolyte and a broad range of silica fillers functionalized with such modifying agents as N-2-(aminoethyl)-3-amino propyltrimethoxysilane, 3-glycidoxypropyltrimetoxysilane, 3-mercaptopropyltrimetoxysilane, n-octyltriethoxysilane, 3-(chloropropyl)trimethoxysilane, 3-methacryloxypropyltrimetoxysilane and vinyltrimethoxysilane. It was found that conductivity of such hybrid organic/inorganic electrolyte membranes may rise by ca. 1.5 orders of magnitude in result of the application of a silanized silicas.

It is believed that the role of surface functionality is based on the creation of space charge layer on the ceramic boundaries (Fig. 4), having favorable cation transport properties. Fast conduction pathways formed this way contribute to the overall enhancement of the membrane's specific conductivity. Enhancement of the

electrode/electrolyte interface stability, often observed after addition of functionalized fillers, is widely attributed to scavenging of trace impurities on the filler surfaces.

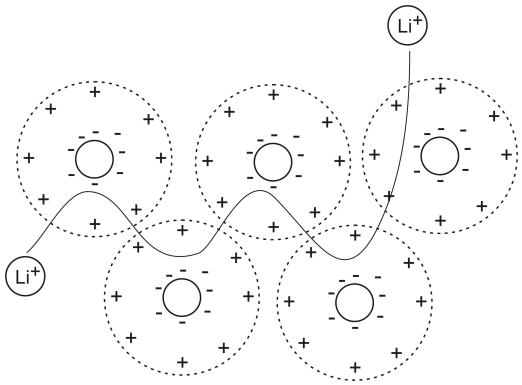

Fig. 4 Fast conduction pathway for lithium cations in the presence of functionalized ceramic filler

2.5. Siloxane polymers and networks as hosts for lithium cations

Polysiloxanes has been proved to be potentially useful as components of liquid and polymer electrolytes. Siloxane units are combined with polyether units (having the ability of co-ordinating lithium cations) in various copolymeric arrangements, in which siloxane component plays role of a backbone. Polysiloxanes have relatively low glass transition temparatures, which is caused by a low bond rotation energies associated with Si-O-Si units.

One example of such structure has already been described in Section 2.3. Rossi *at al*. [25] have recently reported a family of oligomeric structures analogous to the one shown below:

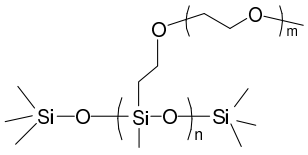

8

Depending on the parameters n (1-2), m (2-7) and the number of carbon atoms in the spacer between the polyether chain and the siloxane backbone (0-3), conductivities ranging from 1.87 mS/cm up to 5.75 mS/cm have been measured at 25 °C. LiBOB or LiTFSI (lithium bis(trifluoromethanesulfonyl) have been uses as lithium salts. Based on a similar concept, various copolymers with comb, double comb, cyclic and cross-linked structures have been reported during the past several years [26-38].

3. Advanced anode materials based on silanes

3.2. Silane-modified carbon anodes

It is well known that silicon-based anode materials may exhibit much larger specific capacities than graphite, today widely regarded as bench-mark anode material for Li-ion batteries. Silicon can react with lithium to form alloys with high Li/Si ratio, such as $Li_{22}Si_5$. Unfortunately, one disadvantage of such materials is very poor cycleability, affected by a large volume changes occurring during lithium insertion and de-insertion into the silicon crystal lattice. Excessive material degradation which accompanies these changes excludes any practical application of silicon-based materials for now. Nevertheless, great potential benefits still incline many research groups to look for new strategies of applying this kind of materials, and combining silicon with carbon in one composite material seems to be the most popular approach.

Silanes may serve as precursors either for silicon or silicon/carbon composite anodes for Li-ion cells. By pyrolysis of pitch-polysilane blends various composite anode materials have been obtained. Reversible capacities of lithium insertion approaching 600 mAh/g and relatively small irreversible capacities in the first cycle were observed for some of these materials. The materials consisted of nano-dispersed Si-O-C or Si-O-S-C domains [39-42]. In a more recent work *Ng et al.* [43] investigated composite materials obtained by encapsulation of graphite/silicon mixtures in a network produced by sol-gel transformation of alkoxysilanes. Specific capacity close to 500 mAh/g was recorded for this type of material. Silicon-carbon core-shell material has recently been proposed by Jung *et al.* [44]. The authors first silylated Si nanoparticles using hexamethyldisilazane and chlorotrimethylsilane as reagents, following by heat-treatment of the resulting Si-resorcinol-formaldehyde composite at

1000 °C in argon atmosphere. Improved performance in terms of reversible lithium insertion was observed for this type of composite anode material. Different approach has been proposed by Xie et al. [45]. Crystalline silicon has been deposited onto the surface of mesocarbon microbeads (MCMB) particles by chemical vapor deposition (CVD) using silane as the precursor gas. It was found that Si-coated graphitic material exhibited increased reversible capacity as compared to pristine MCMB, with reasonable cycleability.

3.3. Silicon-based anodes from silane precursors

As has already been pointed out, pure silicon is unlikely to become material of choice for Li-ion battery engineers due to large volume changes connected to lithium insertion. In one of interesting attempts to overcome this drawback amorphous thin film of silicon has been deposited onto a porous nickel substrate using silane as precursor [46].

4. Summary

The aim of this concise review was to briefly outline some of the possible routes for the application of organosilicon compounds, mainly silanes, in various aspects of Li-ion battery technologies. The existing relevant scientific literature is still relatively scarce as compared to total number of works devoted to Li-ion battery materials, however there seems to be a rising trend in this area of research.

Electrolytes, both liquid and solid, seem to make by far the most promising group of direct applications for silanes and siloxanes and there is a considerable amount of scientific data covering this area. Some of the obvious possible applications of silanes still wait for systematic studies. One example are plasticizers for gel-type polymer electrolytes. As far as anode materials are considered, silanes may become promising precursor compounds for the preparation of innovative anodes based on elemental silicon, mostly as composites with carbon.

References:

1. "Modern Batteries", C. A. Vincent, B. Scrosati, John Wiley & Sons, Inc., New York, 1997;
2. S. Robinson, *Cellphone Energy Gap: Myth or Reality?*, Proceedings of *Lithium Mobile Power 2007* Conference, San Diego, October 29-30, 2007;
3. B. Łęska, P. Przybylski, J. Wyrwał, B. Brzeziński, G. Schroeder, V. Rybachenko, J. Mol. Struct. 741 (2005) 11;
4. B. Gierczyk, I. Kałużna, B. Brzeziński, G. Schroeder, Supramol. Chem. 14 (2002) 497;
5. B. Łęska, I. Kałużna, B. Gierczyk, G. Schroeder, P. Przybylski, B. Brzeziński, J. Mol. Struct. 643 (2002) 9;
6. A. Maia, D. Landini, B. Łęska, G. Schroeder, Tetrahedron Lett. 44 (2003) 4149;
7. A. Maia, D. Landini, B. Łęska, G. Schroeder, Tetrahedron Lett. 60 (2004) 10111;
8. K. Amine, Q. Wang, D.R. Vissers, Z. Zhang, V.A.A. Rossi, R. West, Electrochem. Commun. 8(3) (2006) 429;
9. S.S. Zhang, J. Power Sources, 162 (2006) 1379;
10. G. Schroeder, B. Gierczyk, D. Waszak. M. Kopczyk, M. Walkowiak, Electrochem. Commun. 8 (2006) 523;
11. G. Schroeder, B. Gierczyk, D. Waszak, M. Walkowiak, Electrochem. Commun. 8 (2006) 1583;
12. I. M. Khan, Y. Yuan, D. Fish, E. Wu, J. Smid, Macromolecules, 21 (1988) 2684;
13. B. Oh, D. Vissers, Z. Zhang, R. West, H. Tsukamoto, K. Amine, J. Power Sources, 119-121 (2003) 442;
14. N.N.A. Rossi, Z. Zhang, Y. Schneider, K. Morcom, L.J. Lyons, Q. Wang, K. Amine, R. West, Chem. Mater., 18 (2006) 1289;
15. M. Walkowiak, G. Schroeder, B. Gierczyk, D. Waszak, M. Osińska, Electrochem. Commun. 9 (2007) 1558;

16. M.B. Armand, 1973, in "Fast Ion Transport in Solids", W. Van Gool. (Ed.), Elsevier, North Holland;
17. B. Kumar, L.G. Scanlon, J. Power Sources 52 (1994) 261;
18. E. Quartarone, P. Mustarelli,A. Magistris, Solid State Ionics 110 (1998) 1;
19. J. Zhou,P.S. Fedkiw, Solid State Ionics 166 (2004) 275;
20. A.M. Stephan, K.S. Nahm, Polymer 47 (2006) 5952;
21. M. Walkowiak, *New concepts in composite polymer-ceramic electrolytes for Li-ion batteries*, Chap. 15 in *Advanced Materials and Methods for Lithium-ion batteries*, Ed. by Sheng Shui Zhang, Research Signpost, India, 2008;
22. Y. Liu, J.Y. Lee, L. Hong, J. Power Sources, 109 (2002) 507;
23. M. Walkowiak, A. Zalewska, T. Jesionowski, D. Waszak, B. Czajka, J. Power Sources, 159 (2006) 449;
24. M. Walkowiak, A. Zalewska, T. Jesionowski, M. Pokora, J. Power Sources, 173 (2007) 721;
25. N.A.A. Rossi, Z. Zhang, Y. Schneider, K. Morcom, L.J. Lyons, Q. Wang, K. Amine, R. West, Chem. Mater. 18 (2006) 1289;
26. I.M. Khan, Y. Yuan, D. Fish, E. Wu, J. Smid, Macromolecules 21 (1988) 2648;
27. G.B. Zhou, I.M. Khan, J. Smid, Macromolecules 26 (1993) 2202;
28. R. Spindler, D.F. Shriver, Macromolecules 21 (1988) 648;
29. R. Spindler, D.F. Shriver, J. Am. Chem. Soc. 110 (1988) 3036;
30. D.P. Siska, D.F. Shriver, Chem. Mater 13 (2001) 4698;
31. E. Morales, J.L. Acosta, Electrochim. Acta 45 (1999) 1049;
32. R. Hooper, L.J. Lyons, M.K. Mapes, D. Schumecher, D. Moline, R. West, Macromolecules 34 (2001) 931;
33. Z.C. Zhang, D. Scherlock, R. West, L. Lyons, K. Amine, R. West, Macromolecules 36 (2003) 917;
34. Z.C. Zhang, J.J. Jin, F. Bautista, L.J. Lyons, N. Shariatzadeh, D. Sherlock, K. Amine, R. West, Solid State Ionics 170 (2004) 233;
35. J. Lee, Y. Kang, D.H. Suh, C. Lee, Electrochim. Acta 50 (2004) 351;
36. K. Noda, T. Yasuda, Y. Nishi, Electrochim. Acta 50 (2004) 343;

37. Y. Kang, J. Lee, J. Lee, C. Lee, J. Power Sources 165 (2007) 92;
38. H. Nakahara, T. Manabu, S.-Y. Yoon, S. Nutt, J. Power Sources 160 (2006) 645;
39. W. Xing, A.M. Wilson, G. Zang, J.R. Dahn, Solid State Ionics 93 (1997) 239.
40. A.M. Wilson, G. Zang, K. Eguchi, W. Xing, J.R. Dahn, J. Power Sources, 68 (1997) 195;
41. A.M. Wilson, W. Xing, G. Zang, B. Yates, J.R. Dahn, Solid State Ionics 100 (1997) 259;
42. D. Larcher, C. Mudalige, A.E. George, V. Porter, M. Gharghouri, J.R. Dahn, Solid State Ionics 122 (1999) 71;
43. S.B. Ng, J.Y. Lee, Z.L. Liu, J. Power Sources 94 (2001) 63;
44. Y.S. Jung, K. T. Lee, S.M. Oh, Electrochim. Acta 52 (2007) 7061;
45. J. Xie, G.S. Cao, X.B. Zhao, Mat. Chem. Phys.88 (2004) 295;
46. S. Bourderau, T. Brousse, D.M. Schleich, J. Power Sources 81-82 (1999) 233.

Chapter 9

Mesoporous silica-based nanoparticles as recptors

Izabela Nowak

Faculty of Chemistry, Adam Mickiewicz University, Grunwaldzka 6, 60-780 Poznan, Poland

1. Sensing principle

In the past two decades, the biological, medical and chemical fields have seen great advances in the development of biosensors, biochips and chemical sensors for characterizing and quantifying molecules. A sensor can be generally defined as a device that consists of a recognition system, often called a receptor, and a transducer. The interaction of the receptor with the analyte is designed to produce an outcome measured by the transducer, which converts the information into a measurable effect, such as an electrical signal.

Sensors are classified into four categories as shown in Figure 1, however as the most popular are electrochemical and optical sensors thus only those two sensing principles will be described.

The electrochemical sensing is based on the changes in electrical properties of silica. When the porous layer is infiltrated with different liquids, a change in the baseline capacitance (C) and conductance (G) can be measured in time. The sensor can be modeled as a field effect transistor (FET) in which the metal gate is substituted by the porous layer that acts as a chemical gate. When the surface of the porous layer is exposed to a solution, the liquid/solid interface tends to reach electrostatic equilibrium by modifying the space charge region in the porous silica walls. An electrical double layer is formed between the space charge region (silica) and the Helmholtz layer, which is sensitive to the adsorption/desorption of ions and the components of the

liquid. Changes in the Helmholtz layer lead to a modification of the space charge region in the silica walls as a new electrostatic equilibrium is reached. This change in the electric field distribution of the structure is measured in real time as a change in capacitance (C) and conductance (G) and the device can be modeled with the simplified equivalent electrical circuit shown in Figure 2.

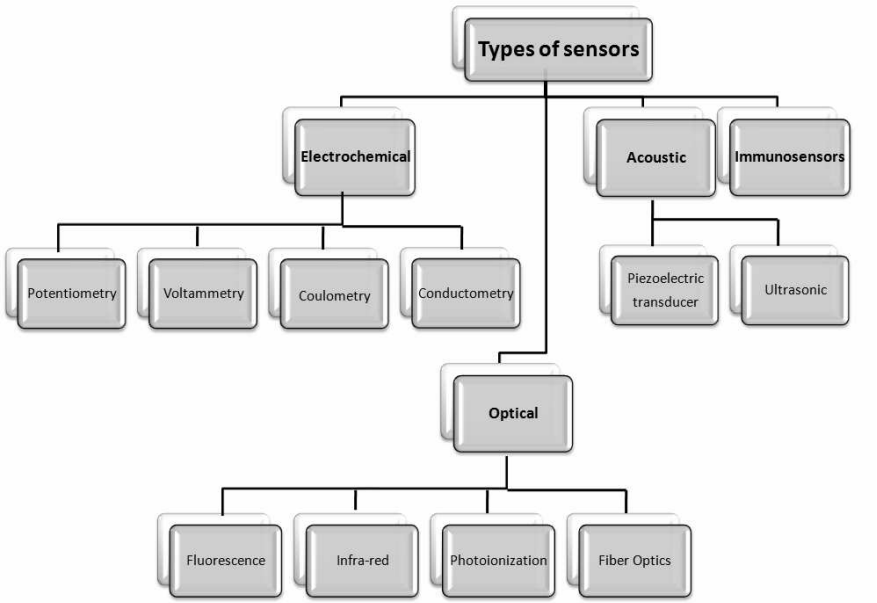

Figure 1. Classification of sensors.

On the other side, silica is a good host material for label-free optical sensing applications because its optical properties (photoluminescence, reflectance) are highly sensitive to the presence of chemical and biological species inside the pores. The capture of biological or chemical molecules inside the pores increases an effective refractive index of the silica structures thus causing a red shift in the photoluminescence or reflectance spectra. The effective dielectric constant of a silica layer is related to its porosity by the Bruggeman effective medium model [1]:

$$(1-P)\frac{\varepsilon_{SiO_2}-\varepsilon_{PSiO_2}}{\varepsilon_{SiO_2}+2\varepsilon_{PSiO_2}}+P\frac{\varepsilon_{pore}-\varepsilon_{PSiO_2}}{\varepsilon_{pore}+2\varepsilon_{PSiO_2}}=0 \quad (1)$$

where P is porosity, ε_{PSiO_2} is the effective dielectric constant of porous silica, ε_{SiO_2} is the dielectric constant of silica, and ε_{pore} is the dielectric constant of the medium inside the pores. The Bruggeman effective medium model shows that the effective refractive index of porous silica ($PSiO_2$) increases as the porosity decreases and as ε_{pore} increases. In sensing applications, ε_{pore} increases due to the binding of targets to the internal surface of the pores. Thus, the overall effective dielectric constant of the porous structure ε_{PSiO_2} increases which causes a red shift in the optical reflectance spectrum of the structure.

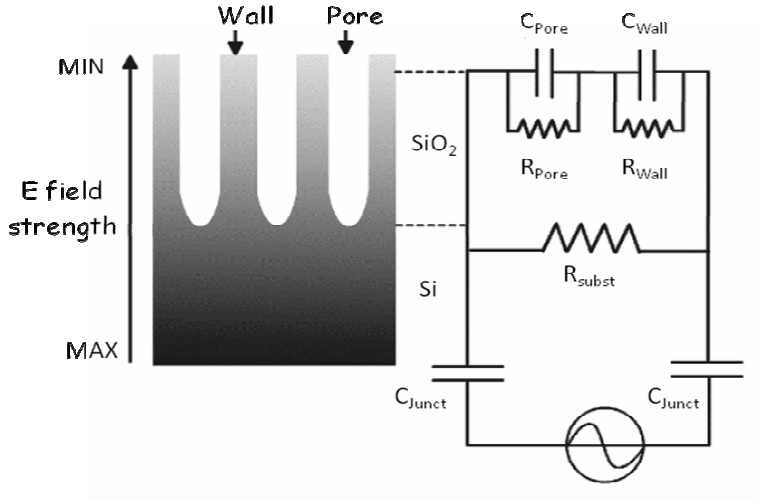

Fig. 2. Schematic representation of the cross section of the silica-based sensor and the electrical equivalent circuit with the associated capacitive and conductive components.

2. Mesoporous molecular sieves - introduction

Prior to a description of coordination chemistry and supramolecular chemistry, fundamental design and preparation methods of mesoporous materials will be briefly summarized. The physico-chemical properties of materials with reduced dimensions demonstrate signs of size dependence and usually exhibit properties different from those of the bulk substances. Enormous number of researches have shown that many nanometer scaled materials exhibit for example: (i) lower melting point [2], (ii) reduced lattice constant [3], (iii) different elasto-plasticity [4], (iv) stability at lower temperatures [5], (v) unique and desirable mechanical characteristic with regard to their flexibility, extensibility, yield strength, adhesion, cyclic fatigue, twisting distortion and control over strain energy storage [6]. With recent state-of-the-art techniques, it is possible to intentionally construct and study nanostructured systems such as nanotubes, nanowires, nanoparticles, nanodots, and nanoporous materials. Progress in the synthesis routes and continuously emerging high-tech technologies has led to the development of various nanostructured materials with remarkable electrical, optical, and mechanical properties promising unique applications. Hence, with bottom-up and/or top-down fabrication approaches, it is feasible to produce a fundamentally and entirely new class of nanomaterials. These materials are initiating development of new devices and sensor designs with unique capabilities [7].

Mesoporous silica is a form of silica with unique properties, distinct from those of crystalline, microcrystalline, or amorphous silica. General synthetic methodologies are summarized in Figure 3. Mesoporous silica materials are prepared essentially using micelle assemblies of surfactants and block-copolymers as soft templates, thus they are the results of using surfactant/block copolymer as a structure directing agent in sol–gel chemistry. They were first prepared in 1992 and since this discovery by Mobil scientists [8], significant research progress has been made in controlling and modifying the properties of mesoporous silica nanoparticles (MSNs). For example, several key structural characteristics of the materials, including the size and morphology of pores [9,10] and particles [11,12] along with their chemical stability can be regulated and moreover further chemically functionalized. MCM-41 (Mobil Composition of Matter), HMS (Hexagonally-ordered Mesoporous Silicas), SBA-15

(Santa Barbara Amorphous) materials are ordered mesoporous materials (OMM) which display a structure of uniform mesoporous (2-30 nm diameter) running through a matrix of amorphous silica. In order to selectively detect targets of interest, the internal surface of SiO_2 needs to be functionalized.

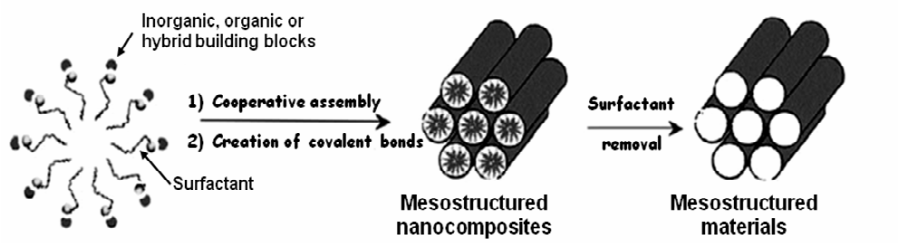

Fig. 3. Surfactant-directed formation of mesoporous materials from inorganic, hybrid, or organic building blocks.

3. Methods of mesoporous molecular sieves functionalization

The surface and structural properties of OMMs, especially silicas can be easily tailored to achieve the high adsorption affinity, desired pore size and pore volume. As it was mentioned in the introduction part, the morphology, porous structure, pore size and pore volume of OMMs, especially ordered mesoporous silicas (OMSs), can be easily tailored by adjusting synthesis conditions and using proper templates. Moreover, since the discovery of these materials various routes of functionalizing their inner surface have been reported to yield hybrid materials with improved adsorption, extraction, ion exchange, or catalytic abilities. Due to their high porosity (pore volume >1.0 cm^3 g^{-1}), concomitant large surface area (>1000 m^2 g^{-1}) as well as their facile synthesis and robustness, OMMs are in principle ideally suited as a support material for sensitive probes. Additionally these materials are obtained from solution, which allows the convenient production of films and bulk materials of any possible shape. Another feature of mesoporous silica materials is their excellent adhesion to glass and other silica substrates due to the covalent linkage that is formed with the silanol groups of the surface.

Selective functionalization of the exterior and interior surface of structurally uniform mesoporous materials with different organic moieties/groups allows precise regulation of the penetration of selective molecules with certain sizes and chemical properties into the mesopores. The high surface area permits doping them with high concentrations of sensitive probes, and the highly uniform porosity allows for facile diffusion making them excellent hosts for sensing molecules or ions [13]. While the aforementioned properties are important in some environmental applications, the major advantage of these materials is the easiness of tailoring their surface properties. This feature makes OMSs very attractive materials for various sensing applications.

The control of framework properties (interior surface) can be achieved by judicious selection of suitable organosilanes and/or their mixing with appropriate amount of tetraethoxysilane (TEOS) (see Table 1). Such materials are called hybrid organic-inorganic materials and have the basic repeating unit of $[RSiO1.5]_n$. Presently these class of materials prepared by the hydrolysis and condensation of organotrialkoxysilanes represent the method of choice for many who wish to introduce organic functionalities into sol-gel processed materials. Surface (exterior) properties can be tailored by using the aforementioned methods, but also there is a vast opportunity for chemical modification of periodic mesoporous organosilicas via reaction with organosilanes. In addition, as shown in the last row of Table 1 organosilanes with bridged and terminal organic groups can undergo co-condensation giving materials with both framework and pendent organic groups [14].

Table 1. Formation of different OMSs by co-condensation of organosilanes in the presence of surfactant and polymeric templates

Type of OMS formed	**Organosilanes used in self-assembly process**
Silica framework 	$Si(\text{-}OR')_4$, e.g. $Si(\text{-}OC_2H_5)_4$ tetraethoxysilane, $Si(\text{-}OCH_3)_4$ tetramethoxysilane

Surface-modified silica 	$Si(\text{-}OR')_4 + R\text{-}Si(\text{-}OR')_3$ 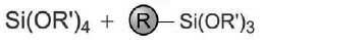 e.g. $Si(\text{-}OC_2H_5)_4 + H_5C_2\text{-}Si(\text{-}OC_2H_5)_3$
Framework-modified silica 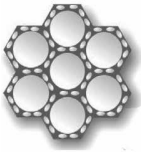	$(R'O\text{-})_3Si\text{-}R\text{-}Si(\text{-}OR')_3$  e.g. $(H_5C_2O\text{-})_3Si\text{-}CH_2\text{-}CH_2\text{-}Si(\text{-}OC_2H_5)_3$
Surface and framework modified silica 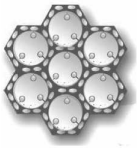	$(R'O\text{-})_3Si\text{-}R\text{-}Si(\text{-}OR')_3 + R''\text{-}Si(\text{-}OR')_3$  e.g. $(H_5C_2O\text{-})_3Si\text{-}CH_2\text{-}CH_2\text{-}Si(\text{-}OC_2H_5)_3 + H_5C_2\text{-}Si(\text{-}OC_2H_5)_3$

R, R', R" denote organic groups in organosilanes.

It is well known that the choice of an suitable support and immobilization procedure is a key step in the fabrication of sensors and will largely determine the characteristics of these devices. Although a great number of immobilization techniques for biological and chemical elements have been developed and evaluated, there is not one general method recommended for all cases. Ideally, the immobilization procedure should led to: (i) an increase in the affinity of the substrate by the biological/chemical receptor, (ii) a broadening of the working pH range, and (iii) a reduction of the microbial/residual chemicals contamination. Methods for immobilization are traditionally classified into two main classes:

- ✓ Physical methods that involve the supporting of a biological/chemical element in any way that is not depending on covalent bond formation (e.g., adsorption, entrapment, microencapsulation). These procedures are simple and in the most cases the support remains unchanged.

- ✓ Chemical methods that involve the formation of at least one covalent bond (e.g., attachment of enzyme to water-insoluble functionalized polymers, intermolecular cross-linking of enzyme molecules using multifunctional reagents). This immobilization is usually irreversible and the biocatalyst is not readily desorbed.

Some of the advantages and disadvantages of the immobilization methods described above are summarized in Table 2.

Table 2. Advantages and disadvantages of the main immobilization methods of the recognition element of sensors

Immobilization method	**Advantages**	**Disadvantages**
Adsorption (physical, ionic binding, chelation)	✓ Simple ✓ Mild binding conditions ✓ Low (bio)molecule changes	✓ Weak binding force ✓ Binding stability highly dependent on pH, solvent and temperature
Entrapment (gel entrapment, microencapsulation)	✓ Mild procedure ✓ Intermediate binding forces ✓ Possible protection from microbiological attack ✓ High stability	✓ Possible loss of biomolecule activity by leakage ✓ Denaturalization by free radicals formed in the process
Cross-linking	✓ High stability ✓ Strong binding force ✓ Used for stabilization of proteins covalently bound to a solid support	✓ Reaction difficult to control ✓ High amounts of (bio)molecules are required ✓ Possible loss of protein activity
Covalent binding	✓ Stable binding ✓ Low leakage ✓ High stability	✓ Time consuming and laborious reactions ✓ Activity losses if the groups required for the biological activity are involved in the binding

Inner surface monofunctionalization or successive inclusion of different organic moieties can be achieved by co-condensation, immobilization (Table 2) or post-synthetic covalent grafting of organic compounds yielding higher-order hybrid materials that can be seen as a first step toward ''biomimetic'', ''enzyme mimicking'' or sensitive nanomaterials [15]. Mesoporous materials can exhibit excellent adsorption properties with large adsorption capacity because of their high surface areas and specificity relying on complexation chemistry of grafted ligands. Use of functionalized mesoporous materials for molecular binding, recognition, and selection is one of the most promising potential applications. Highly selective elements, such as DNA segments and antibodies, can be immobilized on the internal surface of the pores as the bioreceptors or probe molecules. When the sensors are exposed to the target, the probe molecules selectively capture the target molecules. The molecular recognition events are then converted into optical or electrochemical signals via the increase of the refractive index or conductivity.

4. Optically active hybrids

There are the following requisites that are desirable for any support aimed to be used in optical sensing:

- chemical inertness;
- affordability;
- high thermal stability;
- optical transparency;
- low intrinsic fluorescence or absorbance;
- compatibility with the indicator dye;
- homogeneity;
- good mechanical properties (strength);
- flexibility or porous structure to allow fast analyte diffusion;
- permeability to analyte;
- reproducibility of film/bead production;
- controllable film thickness (compromise between sensitivity and response time of the sensor system).

Ordered periodic micro, meso- and macroporous materials allow the assembly of composites incorporating many quest species, such as organic molecules, inorganic ions, semiconductor clusters and polymers. These host/guest materials merge the high stability of the inorganic host, new structure-forming mechanism due to confinement of quest species in well-defined pores and modular composition. The covalent bonding of dye molecules to ordered MCM-41 and MCM-48 (hexagonal and cubic phases of mesoporous silica materials) is a theme that has been a subject of recent interests. The organic molecules/moieties can be dispersed and separated from each other, thus reducing the intermolecular quenching of fluorescent features. Covalently linked chromophores might be used as sensors in separating process to detect the morphologies of molecules located within the channel-like pores of thin membranes of MCM-41 and MCM-48 materials.

From the point of view of engineering optical hybrid materials, microscopic mesoporous siliceous hosts possess the advantage of optical transparency in the visible to UV range, high dye dispersion, mechanical robustness, and high processability [16]. The main differences with sol–gel glasses and amorphous silicas are the ordered sequence of surfactant and block copolymer/silica and holes (pores)/silica on the nanometer scale. Sol–gel synthesis of mesoporous silica with functional templates is very attractive for the fabrication of optoelectronic nanocomposite materials. Applications of these fluorescent mesoporous materials as optical sensing require stability against extraction or leaching of the dye molecules. Therefore dye molecules were covalently anchored to these materials. The goal was first achieved in 1998 by co-condensation of fluorescently-modified triethoxysilyl anchor groups with tetraethoxysilane (TEOS) [17]. After this success many examples have been reported of covalent attachment of functional fluorescent dyes in mesoporous materials either by co-condensation with a fluorescent derivative or attaching the fluorescent dyes to nanoporous molecular sieve surfaces [18]. The first examples of fluorescent mesoporous materials used for optical sensing were reported in 2001 [18]. Mesoporous thin films covalently modified with fluorescein dyes showed a very fast response to pH variations. The response time of the thin films is in the order of 7 s for a 95%

change in the emission intensity. The high porosity of the mesoporous thin film makes possible the fast diffusion of the solution towards the dye molecules.

Brinker and co-workers [19] fabricated first sensors due to the capability of mesoporous materials to form arbitrary functional motifs for directly writing sensor arrays and fluidic or photonic systems (see Fig. 4).

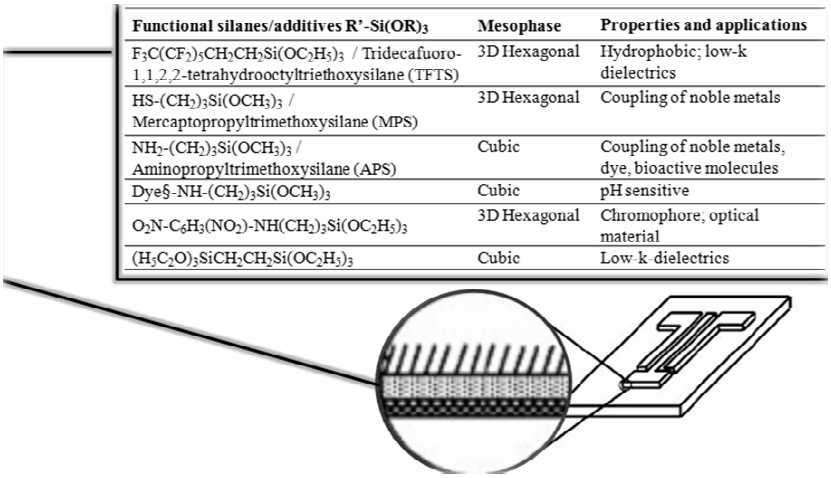

Functional silanes/additives R'-Si(OR)$_3$	Mesophase	Properties and applications
$F_3C(CF_2)_5CH_2CH_2Si(OC_2H_5)_3$ / Tridecafuoro-1,1,2,2-tetrahydrooctyltriethoxysilane (TFTS)	3D Hexagonal	Hydrophobic; low-k dielectrics
$HS-(CH_2)_3Si(OCH_3)_3$ / Mercaptopropyltrimethoxysilane (MPS)	3D Hexagonal	Coupling of noble metals
$NH_2-(CH_2)_3Si(OCH_3)_3$ / Aminopropyltrimethoxysilane (APS)	Cubic	Coupling of noble metals, dye, bioactive molecules
Dye§-NH-$(CH_2)_3Si(OCH_3)_3$	Cubic	pH sensitive
$O_2N-C_6H_3(NO_2)-NH(CH_2)_3Si(OC_2H_5)_3$	3D Hexagonal	Chromophore, optical material
$(H_5C_2O)_3SiCH_2CH_2Si(OC_2H_5)_3$	Cubic	Low-k dielectrics

Figure 4. Scheme of three L-shaped patterns forming typical pads for sensing applications tabulated in Table presented in the top side of the figure.

Such new sensors, for example a fluorescent pH sensor (Fig. 5), were formed by selective de-wetting of self assembled monolayers (SAM)-modified substrates, followed by covalent modification of the mesoporous material with a fluorescent probe to form a microfluidic system for pH sensing.

The use of hybrid materials, such as the fluorescently modified MCM mesoporous solids, for anion-sensing systems was demonstrated in 2002 by Martinez-Manez and co-workers [20]. They showed that the combination of the binding properties of molecular receptors with the structure of the mesoporous materials

results in a enhancement of the anion selectivity and sensing response in water. This micro-sized fluorescent probe was made by grafting aminoanthracene groups onto mesoporous silica materials. The amino groups bind ATP (adenosine triphosphate) anions while the inorganic matrix offers the recognition pocket. Detection limits of 10^{-6} M were obtained. The bulkiness of the grafted group combined with the steric restrictions provided by the pore size of the material led to the ability of the material to respond in different degrees to ATP, ADP, and AMP (adenosine tri-, di-, and monophosphate, respectively). ATP was able to quench the fluorescence of the material to a larger degree than the other two species, and small anions like chloride, bromide, and phosphate did not create any response of the sensor. The answer of the grafted silica mesoporous material was better than that of silica membranes with the same functionalization (a 100-fold improved sensitivity for the MSN-based matrix) [20,21]. The solids exhibit cooperative effects that resulted in an improvement in ATP response with respect to the free probe in solution. This surface effect may arise from the cooperativity of the confined components of the system and the shape of the solid support itself (Fig. 6).

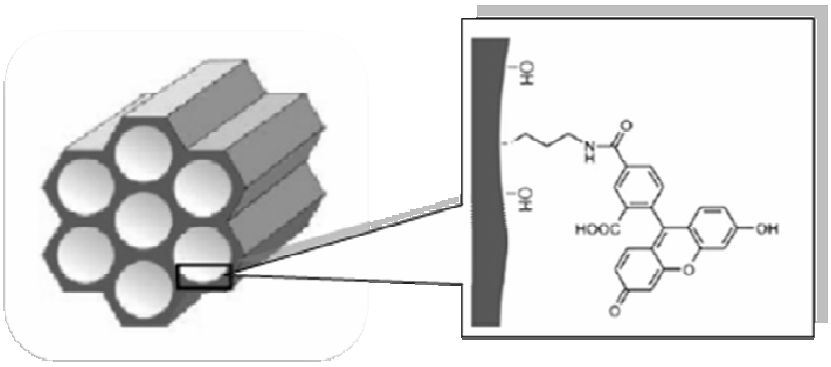

Fig. 5. Schematic chemical structure of the carboxyfluorescein modified mesoporous material

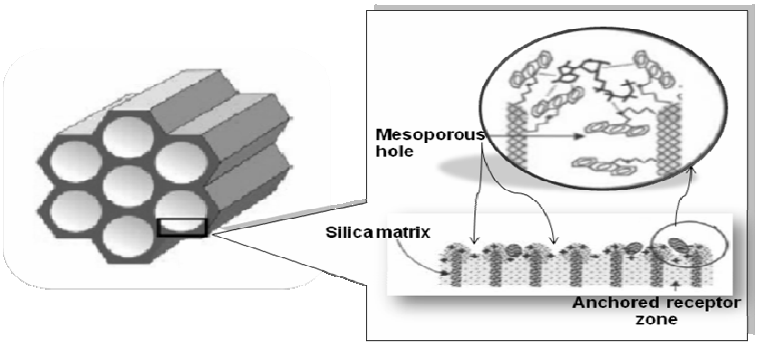

Fig. 6. Schematic view of the surface of a mesoporous material modified with aminoanthracene and interacting with ATP anions.

Lin et al. synthesized a poly(lactic acid) (poly-L-lactic acid, PLA) coated MCM type mesoporous silica nanosphere (MSN) that served as a fluorescent probe for selective detection of amino-containing neurotransmitters under physiological conditions (Fig. 7) [22]. They utilized the PLA layer as a gatekeeper to regulate the penetration (diffusion) of molecules in and out of the nanopores monitoring the molecular recognition between the aminoneurotransmitters (dopamine, tyrosine, and glutamic acid) and a surface-anchored o-phthalic hemithioacetal (OPTA) group. The OPTA is a non-fluorescent moiety which reacts with these neurotransmitters that contain primary amines, forming a fluorescent isoindole derivative. The authors further grafted propyl-, phenyl-, and pentafluorophenyl groups to the OPTA-MSNs to manipulate the properties, such as hydrophobicity, of the mesopores. The largest difference in the fluorescence responses to the two analytes was observed in the case of pentafluorophenyl grafted OPTA–MSN. This difference was attributed to the p–p acceptor–donor interactions taking place between the aromatic ring of the dopamine and the pentafluorophenyl groups. The electrostatic, hydrogen bonding, and dipolar interactions between the neurotransmitters and the poly-L-lactic acid (PLA) layer in pH=7.4 buffer were the dominating factors in regulating the penetration (diffusion) of the neurotransmitters into the mesopores (Fig. 7). In fact, at pH=7.4, dopamine is positively charged (pI = 9.7), whereas tyrosine and glutamic acid are negatively charged (pI < 7.4). It has been reported that PLA has an isoelectric point (pI) lower

than 3.0 and it is negatively charged in pH=7.4 buffer. In the case of those neurotransmitters (dopamine) with electrostatic attraction for PLA, it is understandable why there would be a faster kinetics of entering the pores than those of the other neurotransmitters, such as glutamic acid, with repulsive forces.

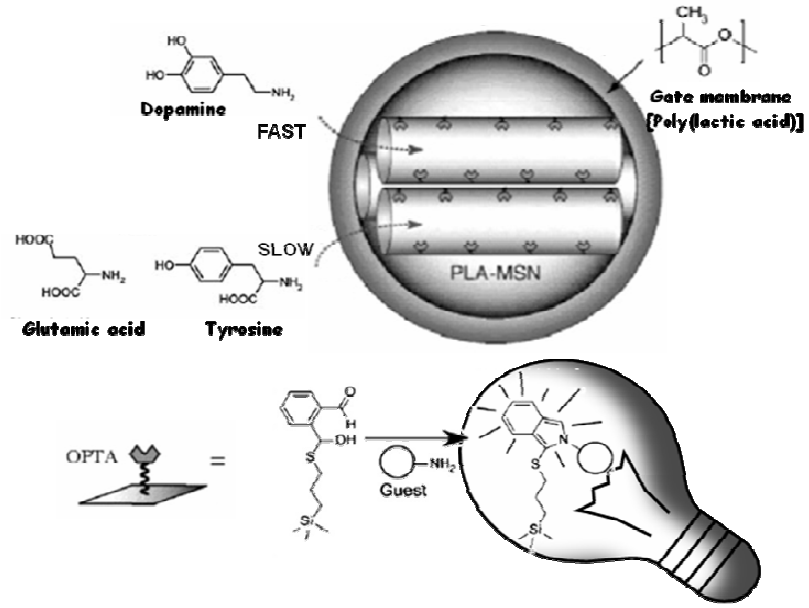

Fig. 7. Schematic representation of the PLA-coated MCM-based fluorescence sensor system for detection of amine-containing neurotransmitters (top) and graphical representation of the functionalized internal walls of the nanopores (bottom).

Rurack and co-workers [23] reported recently the synthesis of hybrid optical chemosensor materials for the detection of long-chain carboxylates – RCOOH. A spacer-substituted 7-urea-phenoxazin-3-one was employed as the signaling moiety and a mesoporous trimethylsilylated MCM-41 type material served as the solid support. The sensor material showed the advantageous features of both modules that is: (i) absorption and emission in the visible spectral range, (ii) fluorescence red-shift and enhancement upon analyte coordination, and (iii) amplification of noncovalent

(binding) and hydrogen-bonding (recognition) interactions in the detection event. The final step of the simplified picture is given in Figure 8 and can be rationalized as the "binding" of the long-chain tail (R) to the hydrophobic walls, whereby the polar head-groups stick to the outside. Presumably due to reduced water content, the hydrogen bond-mediated binding reaction between the probe's receptor group and the carboxylate group is then facilitated and leads to signal generation.

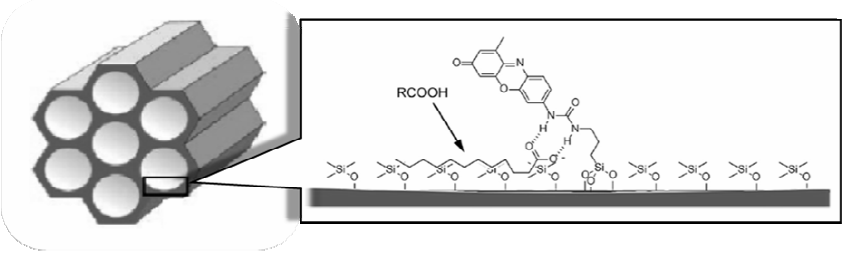

Figure 8. Hydrophobic forces "bind" the tail at the wall (mimicking the "pocket") while hydrogen bonding to the urea group generates the signal.

Li and co-workers [24] grafted 1,10-phenathroline onto mesoporous silica as a second ligand for the $Ru(bpy)_2Cl_2$ (bpy = 2,2-bipyridyl) complex resulting in $[Ru(bpy)_2phen]^{2+}$ groups immobilized at the silicate backbone (see Fig. 9 – square). The mesoporous structures were obtained as bulk xerogels and spin-coated thin films that provided superior optical oxygen sensors with homogeneous distribution and improved sensitivity due to the uniform and nearly parallel porous matrix. Zhang et al. [25] similarly proposed luminescent oxygen sensing materials based on Pt(II)-porphyrin complex: platinum meso-tetrakis(4-N-methylpyridyl)porphyrin ($PtTMPyP^{4+}$) on MCM-41 prepared through simple electrostatic adsorption. Upon increasing oxygen concentration, the emission peak of the Pt(II)-porphyrin/MCM-41 assembly remained at 668 nm and the emission intensity rapidly decreased (see Fig. 9 – circle).

Optical sensing of different gas mixtures has been carried out with mesoporous molecular sieves that have covalently anchored rhodamine dyes. The concentration of SO_2 in a gas can be deduced from the quenching of the fluorescence of the dye [26].

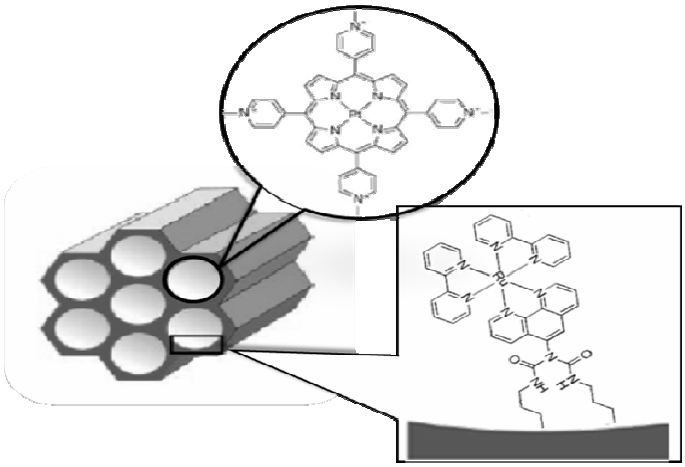

Fig. 9. Oxygen sensing sites immobilized on mesopore.

The use of a mesoporous silica as a support for grafting chromophores also opens new opportunities for efficient optical sensors of heavy metals. Palomares et al. [27] investigated the selectivity and sensitivity of two colorimetric sensors based on the ruthenium complexes N719 [bis(2,2-bipyridyl-4,4-dicarboxylate)ruthenium(II) bis(tetrabutylammonium) bis(thiocyanate)] and N749 [(2,2:6,2-terpyridine-4,4,4-tricarboxylate)ruthenium(II) tris(tetrabutylammonium) tris-(isothiocyanate)] that had been immobilized in mesopore space (Fig. 10). Hg(II) ions can coordinate reversibly to the sulfur atom of the NCS groups, while the sensor molecules can be adsorbed onto high surface area mesoporous oxide films, allowing reversible heterogeneous sensing of mercury ions in aqueous solution. The interaction between Hg(II) ions and the NCS groups of the ruthenium dyes N719 and N749 is responsible for the color change of the corresponding dye. Interestingly, the interaction is selective for Hg(II) even in the presence of much higher concentrations of other potentially competing metal cations such as Pb(II), Cd(II), Zn(II), or Fe(II).

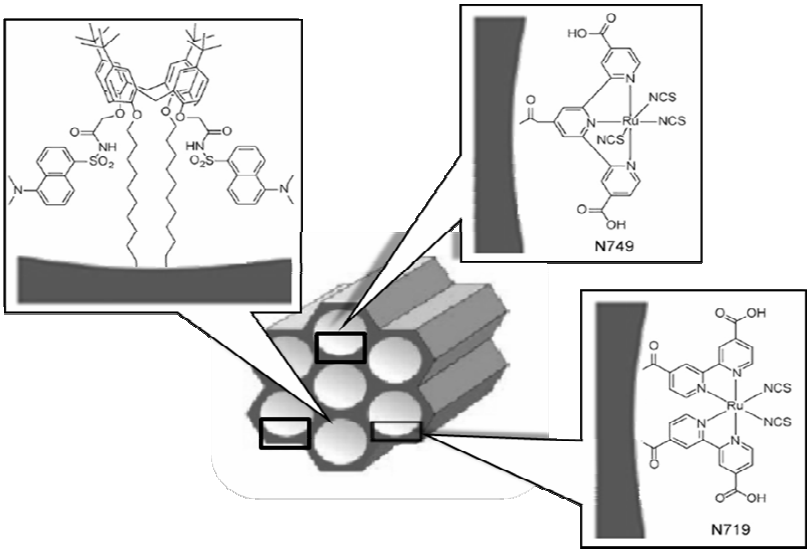

Fig. 10. Binding sites for optical Hg(II) sensing.

Wang and co-workers [28] grafted luminescent Schiff-base groups on the surface of mesoporous material MCM-48 and employed it to sense metal ions. The first step involved the treatment of the MCM-48 (cubic structure) surface with 3-aminopropyl-(trimethoxy)silane followed by condensation between amine groups and 2-hydroxybenzaldehyde. Treatment of suspensions of the Schiff-base-containing MCM-48 with Zn(II) ions in aqueous solution resulted in yellow solids that fluorescence strongly. The fluorescence of the prepared MCM-48 solid with Schiff-base groups could be quenched completely by Cu(II) ions and thus proved suitable for sensing Cu(II) ions in aqueous media. Cu(II) could quench completely the emission of the parent material even in the presence of equimolecular Zn(II), Co(II), Ca(II), Pb(II), Ni(II), Mn(II), or Cd(II) ions.

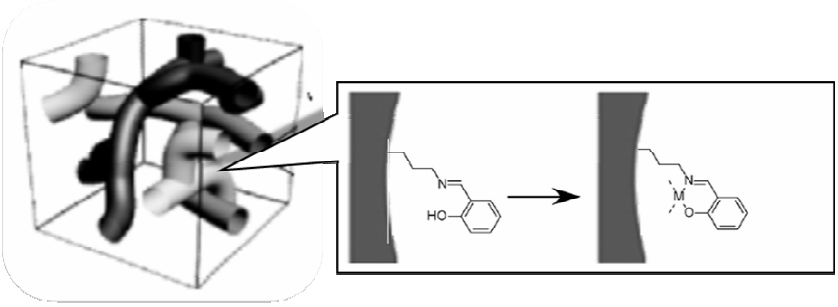

Fig. 11. Binding sites for optical Cu(II) sensing.

Specific ionophores such as calixarenes bearing two dansyl groups have been grafted on large porous silica materials via two long alkyl chains containing triethoxysilane groups to sense Hg(II) in water [29]. The material responded reversibly to the presence of Hg(II) within few seconds and displayed a detection limit close to 10^{-7} M. Functionalized mesoporous solids can act also as binding pockets for anion-recognition in water using displacement colorimetric assays [30]. Citrate and borate were selectively detected in water with a detection limit of 10^{-5} M by this method.

Target analytes are not limited to gaseous substances or metal ions. Garcia-Acosta et al. reported the rational development of sensory materials for the chromo- and fluorogenic detection of biogenic amines in complex liquid samples [31,32]. The probe molecule is a reactive pyrylium chromophore that is anchored into the inner surface of hydrophobic pores of a mesoporous siliceous support (Fig. 12). Although fatty amines are biologically important, they are often silent in some kinds of chromo-fluorogenic tests. The prepared mesoporous materials performed considerable color changes upon binding to fatty amines through formation of the corresponding pyridinium derivatives. Use of mesoporous materials as chromophore supports leads to size discrimination of the guest amines. Amines with a medium-sized alkyl or alkyl-aryl end group exhibit a much faster response than the fatty amines.

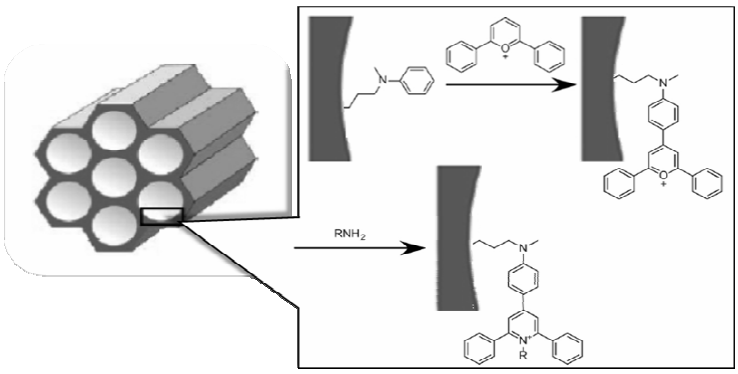

Fig. 12. Sensing site for amine guest.

5. Biologically active hybrids

Research is currently in progress to fabricate nanomaterials by integrating nanofabrication and chemical functionalization, particularly in the case the development of chemosensors. Such sensors will be integrated, for example, into the next-generation ´gene-chips´, especially where detection of less than an atom/molecule, such as amino acids or DNA, is critical. One of the most promising applications of nanostructured materials is biosensing. A biosensor is a device that uses a biological element (e.g., enzyme, antibody, nucleic acid, whole cell, etc.) to monitor the presence of various chemicals on a substrate by enabling highly specific interactions between biological molecules to be detected and utilized. Typically antibodies or enzymes are coupled to microelectronics to enable their interactions with the substances of interest to be monitored. The ability of biomolecules to react with very low concentrations of substances allows biosensors to be used in various applications such as the monitoring of pollutants in water, air, and soil, and in the detection of medically important molecules such as hormones, sugars, and peptides in body fluids.

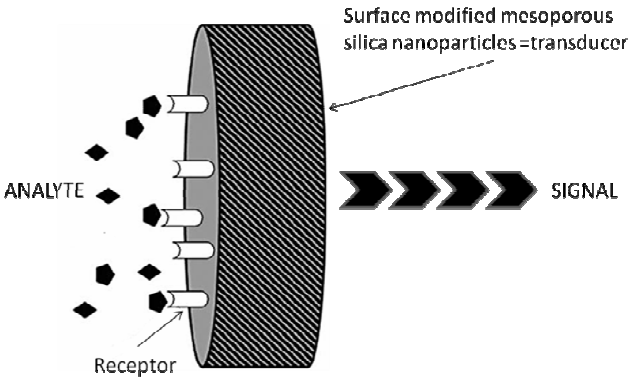

Fig. 13. Scheme of biosensor.

The sensing part of a biosensor consists of a biological element, which is the bio-receptor, having remarkable properties concerning the specific molecular recognition of a target analyte as shown in Figure 13. The biological element is closely associated with a transducer that converts the physicochemical signal occurring during the molecular recognition phenomenon into an electrical signal. In a biosensor, the biological element acts as an extremely selective filter compared to a chemical system. This makes the biosensor a powerful tool when a high selectivity is needed. Examples of biomolecular recognition include antigen-antibody, nucleic acid-DNA and hormone-receptor interactions. Some biomolecules can exhibit two binding sites. Proteins can also be engineered to produce molecules with specific anchoring groups at specific locations on the surface thus increasing the options further.

Biomolecular functionalized nanoparticles required for such devices can be formed through [33]:

(i) Electrostatic interactions, e.g. binding of immoglobulin G (IgG) to gold and silver nanoparticles functionalized with negatively charged citrate ions;

(ii) Chemisorption and covalent binding through bifunctional linkers, e.g. oligopeptide binding to gold nanoparticles previously functionalized with $_{L}$-cysteine through thiol groups on the surfaces of the particles;

(iii) Programmed assembly using specific affinity interactions, e.g. streptavidin (Sav)-functionalized gold nanoparticles have been used for affinity binding

of biotinylated proteins and oligonucleotides as well as to other functionalized nanoparticles. This type of interaction is also feasible for nanoparticle bound antibody-antigen interactions.

For example, glucose oxidase- and horseradish peroxidase(HRP)-loaded mesoporous silica material have been used as a selective sensor for glucose detection [34]. Excellent results were achieved after immobilizing tyrosinase and HRP on a mesoporous matrix [35]. The porous structure of MCM-41 results in a high catalytic activity and fast response rate of the immobilized tyrosinase-HRP. The enhanced sensitivity of the tyrosinase-HRP electrode to phenol is observed compared with tyrosinase and HRP monoenzyme electrodes according to the following equations:

$$\text{Phenol} + \text{tyrosinase } (O_2) \rightarrow \text{catechol} \quad (2)$$

$$\text{Catechol} + \text{tyrosinase } (O_2) \rightarrow \text{o-quinone} + H_2O \quad (3)$$

$$\text{o-quinone} + 2H^+ + 2e^- \rightarrow \text{catechol (at electrode)} \quad (4)$$

This matrix is very efficient for retaining the tyrosinase-HRP activity and preventing their leakage out of the film, which results in a long-term stability and good reproducibility of the sensor. MCM-41 provides an efficient strategy and a new promising platform for the study of the developments of biosensors .

In another study, myoglobin and hemoglobin were immobilized in mesoporous silica-modified electrodes to be used as a sensor for H_2O_2 and NO_2^- [36,37]. Apparently, the reason for using enzymes and proteins as the recognition unit is their high specificity for substrates.

Construction of artificial bionanohybrids nanomaterials including metal and semi-conductor nanoparticles have dimensions on the same length scale (2-20 nm) as biomolecules such as proteins and DNA [33]. The hybrid materials generated from the chemical or physical juxtaposition of these two types of materials generates novel bionanohybrids with a range of properties and functions (Fig. 14). Currently available nanoparticles including metals (e.g. Au, Ag, Pt and Cu) and semiconductors (e.g. PbS, Ag_2S, CdS, CdSe and TiO_2) show unique electronic and photonic properties [34]. Because of their size and versatile chemistry, nanomaterials are gaining interest as

powerful tools for sensing applications. The unique surface properties and the small particle sizes of these nanoparticle-based sensor systems permit for the detection of analytes within individual cells both in vivo and in vitro. In particular, nanoparticles offer several advantages over homogeneous fluorescent and staining dyes. Unlike stains, nanoparticles do not suffer from fluorescent self-quenching and other diffusion-related problems. Furthermore, the ability to functionalize the surface of nanoparticles with large quantities of cell-recognition or other site-directing compounds makes them ideal agents for cell tracing.

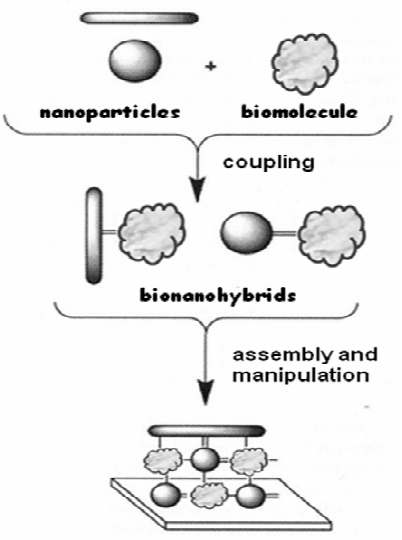

Fig. 14. Schematic of the interactions occurring between nanoparticles and biomolecules.

6. Conclusions and outlook

In contrast to other solid nanoparticle sensors, mesoporous silica provide two important unique advantages: (i) high porosity – the large surface areas and pore volumes allow the encapsulation/immobilization of large amounts of sensing molecules per particle; (ii) optical transparency – this unique feature permits optical detection through layers of the material itself. These features allow for the detection of larger analyte molecules/moieties and the incorporation of a great amount of

receptors/sensors into the porous matrix to achieve a better detection limit. A faster diffusion of the analytes through the mesopores of these materials to the sensor sites also permits a shorter response time. Many specific molecular receptors, for example proteins, dyes, enzymes, etc., have been used to achieve analyte selectivity in many mesoporous silica-based biosensors.

In this short review, a number of different approaches for the development of sensors based on mesoporous silica matrix have been discussed. However, there is still a need of sensors for many different targets. The production of new functional materials able to report continuously and reversibly recognition events plays an important role in the development of sensors since they performance depends very much on the properties of the supporting material.

Acknowledgement

This paper was written with partial support from Polish Ministry of Scientific Research and Information Technology (grant 2006-2008).

Abbreviations:

ADP	adenosine diphosphate
APS	aminopropyltrimethoxysilane
ATP	adenosine triphosphate
HMS	Hexagonally-ordered Mesoporous Silicas
HRP	horseradish peroxidase
MCM	Mobil Composition of Matter
MCM-41	Hexagonally-ordered MCM
MCM-48	MCM with cubic structure
MPS	mercaptopropyltrimethoxysilane
MSNs	Mesoporous Silica Nanoparticles
OPTA	o-phthalic hemithioacetal
PLA	poly(lactic acid)
SAM	Self Assembly Monolayer
SBA-15	Santa Barbara Amorphous

TEOS	tetraethoxysilane
TFTS	tridecafuoro-1,1,2,2-tetrahydrooctyltriethoxysilane

References:

1. W. Theiss, Surf. Sci. Rep., 29 (1997) 91;
2. P. Buffat and J. P. Borel, Phys Review A, 13 (1976) 2287;
3. A.N. Goldestien, C.M. Echer, and A.P. Alivisatos, Science 256, 1425 (1992);
4. T.M. Shaw, S. Trolier-McKinstry, and P.C. McIntyre, Annual Rev. Mater. Sci. 30 (2000) 263;
5. Y. Champion, C. Langlois, S. Guerin-Mailly, P. Langlois, J. Bonnentien, and M. J. Hytch, Science 300 (2003) 310;
6. A. Vaseashta [in:] Functional Properties of Nanostructured Materials, R. Kassing et al. (Eds.), Springer, 2006, 431;
7. A. Vaseashta, J. Materials Science: Materials in Electronics, 14 (2003) 653;
8. J.S. Beck, J.C. Vartuli, W.J. Roth, M.E. Leonowicz, C.T. Kresge, K.D. Schmitt, C.T.W. Chu, D.H. Olson, E.W. Sheppard, S.B. McCullen, J.B. Higgins, and J.L. Schlenker, J. Am. Chem. Soc., 114 (1992) 10834;
9. J.Y. Ying, C.P. Mehnert, and M.S. Wong, Angew. Chem. Int. Ed., 38 (1999) 56;
10. C.T. Kresge, M.E. Leonowicz, W.J. Roth, J.C. Vartuli, and J.S. Beck, Nature, 359 (1992) 710;
11. S. Huh, J.W. Wiench, J.-C. Yoo, M. Pruski, and V.S.Y. Lin, Chem. Mater., 15 (2003) 4247;
12. B.G. Trewyn, C.M. Whitman, and V.S.Y. Lin, Nano Lett., 4 (2004) 2139;
13. J.L. Shi, Z.L. Hua, and L. X. Zhang, J. Mater. Chem., 14 (2004) 795;
14. Q. M. Zhang, K. Ariga, A. Okabe, and T. Aida, J. Am. Chem. Soc., 126 (2004) 988;
15. T. Asefa, M. Kruk, M.J. MacLachlan, N. Coombs, H. Grondey, M. Jaroniec, and G.A. Ozin, J. Am. Chem. Soc., 123 (2001) 8520;
16. B. J. Scott, G. Wirnsberger, and G. D. Stucky, Chem. Mater., 13 (2001) 3140;
17. T. Pellegrino, S. Kudera, T. Liedl, A. M. Javier, L. Manna, and W. J. Parak, Small, 1 (2005) 48;

18. G. Wirnsberger, B.J. Scott, and G.D. Stucky, Chem. Commun., (2001) 119;
19. H.Y. Fan, Y.F. Lu, A. Stump, S.T. Reed, T. Baer, R. Schunk, V. Perez-Luna, G.P. Lopez, and C.J. Brinker, Nature, 405 (2000) 56;
20. A.B. Descalzo, D. Jimenez, M.D. Marcos, R. Martınez-Manez, J. Soto, J.El Haskouri, C. Guillem, D. Beltran, P. Amoros, and M.V. Borrachero, Adv. Mater., 14 (2002) 966;
21. A.B. Descalzo, M. D. Marcos, R. Martınez-Manez, J. Soto, D. Beltran, and P. Amoro, J. Mater. Chem., 15 (2005) 2721;
22. V.S.Y. Lin, C.Y. Lai, J. G. Huang, S. A. Song, and S. Xu, J. Am. Chem. Soc., 123 (2001) 11510;
23. A. B. Descalzo, K. Rurack, H. Weisshoff, R. Martınez-Manez, M. D. Marcos, P. Amoros, K. Hoffmann, and J. Soto, J. Am. Chem. Soc., 127 (2005) 184;
24. B. Lei, B. Li, H. Zhang, S. Lu, Z. Zheng, W. Li, and Y. Wang, Adv. Funct. Mater., 16 (2006) 1883;
25. H. Zhang, Y. Sun, K. Ye, P. Zhang, and Y. Wang, J. Mater. Chem. 15 (2005) 3181;
26. M. Wark, Y. Rohlfing, Y. Altindag, and H. Wellmann, Phys.Chem. Chem. Phys., 5 (2003) 5188;
27. E. Coronado, J.R. Galan-Mascaros, C. Marti-Gastaldo, E. Palomares, J.R. Durrant, R. Vilar, M. Gratzel, and M.K. Nazeeruddin, J. Am. Chem. Soc., 127 (2005) 12351;
28. H. Zhang, P. Zhang, K. Ye, Y. Sun, S. Jiang, Y. Wang, and W. Pang, J. Lumin.,117 (2006) 68;
29. R. Metivier, I. Leray, B. Lebau, and B. Valeur, J. Mater. Chem., 15 (2005) 2965;
30. M. Comes, G. Rodrıguez-Lopez, M. D. Marcos, R. Martınez-Manez, F. Sancenon, J. Soto, L. A. Villaescusa, P. Amoros, and D. Beltran, Angew. Chem., Int. Ed., 44 (2005) 2918;
31. B. Garcia-Acosta, M. Comes, J.L. Bricks, M.A. Kudinova, V.V. Kurdyukov, A.I. Tolmachev, A.B. Descalzo, M.D. Marcos, R. Martinez-Manez, A. Moreno, F. Sancenon, J. Soto, L.A. Villaescusa, K. Rurack, J.M. Barat, I. Escriche, and P. Amoros, Chem. Commun., (2006) 2239;

32. M. Comes, M.D. Marcos, R. Martinez-Manez, M.C. Millan, J.V. Ros-Lis, F. Sancenon, J. Soto, and L.A. Villaescusa, Chem. Eur. J., 12 (2006) 2162;
33. H.A. Currie, S.V. Patwardhan, C.C. Perry, P. Roach, and N.J. Shirtcliffe [in:] Hybrid Materials, G.Kickelbick (Ed), Wiley-VCH 2007, 292;
34. Y. Wei, H. Dong, J. Xu, and Q. Feng, Chem. Phys. Chem., 3 (2002) 802;
35. Z. Dai, X. Xu, L. Wu, and H. Ju, Electroanalysis, 17 (2005) 1571;
36. Z. Dai, S. Liu, H. Ju, and H. Chen, Biosens. Bioelectron., 19 (2004) 861;
37. Z. Dai, X. Xu, and H. Ju, Anal. Biochem., 332 (2004) 23.

Chapter 10

Experimental and theoretical evaluation of vibrational spectra for guest – host systems

Kamilla Małek, Joanna Łojewska, Leonard M. Proniewicz

Faculty of Chemistry, Jagiellonian University, Ingardena 3, 30-060 Kraków

A great deal has been told about vibrational spectroscopy and its application in the structural and mechanistic studies of biosensors [1,2,3-5]. In this chapter, we present only some experimental and theoretical issues connected with their analysis. The choice of the problems depends on the form of sensors, in which an active medium is often spread on surface of a solid matrix or in physiological liquids. Thus, the concern is mainly on analyses of the surfaces of solids and water containing systems. Following this train of though a milestone in understanding supramolecular systems are intermolecular interactions, which occur not only between guest and host but also on surface or between solute and solvent molecules. These interactions in fact determine both the structure and reactivity of biosensors.

In our opinion, the most effective way to resolve the structure and reactivity is the approach based on experiment aided with quantum-chemical calculations. In this approach, the synergy occurs when both an experiment and a model stimulate each other asking and answering the questions. In fact, vibrational spectroscopy can be successfully explained by reasonably composed quantum-chemical models.

From the experimental standpoint, the advances in infrared and Raman spectroscopy in recent years, driven by the development of optical and electronic technologies, has given rise to a considerable increase in sensitivity and precision of instruments opening new horizons of investigations of biomolecules. The progress concerns especially Raman spectroscopy in which each year brings innovative

solutions in optical (diode lasers, holographic notch filters) and detecting systems (diode arrays DA, charge couple devices CCD) [6-9].

A real obstacle is that quantum chemical calculations are carried out for gas phase usually for isolated molecules in contrast to the majority of the experimental measurements. This is one of the sources of the discrepancies between theoretical and experimental spectra. Paving the way to design molecules of desired properties the selectivity of the interactions is simulated using more advanced tools based on density functional theory or any electron correlation methods. In such cases, a quantum-chemical method must be capable to describe ground state, namely equilibrium structure of a molecule and forces (dispersive, charge transfer, π-π stacking, etc.) with environment. In this chapter, some examples of the application of DFT computations serve as an illustration of the problems as these methods allow reproducing vibrational spectra with relatively high quality and reasonable computation time. However, an approach to quantum-chemical evaluation considerably depends on the presence of functional groups of a given character in investigated molecular systems and requires considering various molecular models. The quality of the models, i.e. compatibility of theoretical vibrational spectra with experimental results, prompts for an analysis of the geometrical and energetic factors determining structural interactions present in the studied molecular systems.

Structure of isolated molecules - matrix isolation

An experimental approach to the vibrational spectra of isolated molecules provides the matrix isolation technique. In spite of the fact that this method is restricted to relatively small and covalently bonded molecular systems, it can be used in the studies on structural and flexible moieties of the guest – host complexes.

The technique allows maintaining molecules in an inert medium at very low temperature and is particularly well-suited for preserving reactive species in a solid environment for spectroscopic analyses. The analytical method is especially recommended for hard to distinguish molecular fragments, such as:

- ✓ free radicals that may be important intermediates for chemical transformations in photo induced reactions,

- ✓ weak molecular complexes such as those concentrated around H-bond and charge transfer complexes that may stabilise at low temperatures,
- ✓ molecular ions that are produced for example in plasma discharges or by high-energy radiation

The structure resolving may be much aided by the studies of IR dichroism as for example to distinguish conformers It also makes possible the determination of the energy difference and the barrier height between them [10, 11].

Theoretical evaluation of electronic structures with the continuous increase in computational resources creates new opportunities for high accuracy determination of potential energy surfaces (PES) of medium-size molecules. Hence, it allows performing a detail analysis of their conformational flexibility. Such a geometrical arrangement might have very important dynamical consequences leading to specific effects on an inactive site of a receptor. In the case of the presence of different rotamers, comparison of their zero-point corrected electronic energies gives a deep insight into the relative stability of conformers. Additionally, calculations of the Gibbs free energies allow determining relative abundances of the isomeric structures in a chosen isomer population.

As an example of this approach, the IR spectrum of salicylhydroxamic acid (*sha*) isolated in the argon matrix will be described briefly [12]. The optimization process at B3LYP/6-311++G(d,p) level of theory, yielded nine energy minimized geometries of *sha* (Fig. 1, letters denote *e* - entgegen and *z* – zusammen conformations around the N-O bond). Among them, the most stable is an isomer 1 for which the relative abundance is ~99.5%, so that the occurrence of the other isomers could be negligible. This prediction is confirmed by a very good agreement between calculated and experimental frequencies for this structure (Fig. 2). Moreover, the stretching mode of the hydroxyl group appears at 3341 cm^{-1} and provides support for H-bonding in *sha*.

A detailed analysis of the geometry of the most stable isomer reveals that this conformation enables the formation of two: 5- and 6-membered, pseudo rings stabilized by hydrogen bonding. Furthermore, the most important factor is the presence of the phenolic group in *ortho* arrangement to the hydroxamic fragment that facilitates the formation of the 6-membered ring. The energy of this hydrogen bonding

was calculated as 39 kcal/mol. Stabilization of molecular structure by the presence of the intramolecular hydrogen bonding is also observed for the other isomers, however, all of them possess only one pseudo ring. The matrix isolation studies on L-amino acids as phenylalanine and tryptophan have also showed the importance of hydrogen bonding in stabilisation of conformers structures [13,14]. As it is known, amino acids exist in the zwiterionic form in crystalline state and in solution. However, proteins are built of amino acid residues in their neutral structures. This form is present in the gaseous state only, and since low temperature isolation in inert gases mimics this state, it is possible to investigate the amino acids structures by the IR absorption. An advantage of these studies is that the spatial arrangement of side chains in proteins is governed by minimum energy conformers. In the case of phenylalanine [13], the set of twenty five conformers is defined by rotations around five dihedral angles. It was predicted on the basis of Gibbs free energies found for these structures that eight conformers exist at temperature of sublimation (423 K) but two of them relax to the more stable form due to the low energy barriers. Moreover, a comparison of the weighted calculated spectrum for the six energetically favoured conformers with the experimental one confirms the thermochemical consideration given above. The lowest-energy rotamers of phenylalanine are stabilized by O-H···N intramolecular H-bonding and differ only in the mutual arrangement of the amino group and the phenyl ring. Similar analysis was carried out for the tryptophan molecule [14]. The conformational space of the amino acid consists of 42 minima and as many as 17 of them represent conformers with the relative energy in the range 0 – 17 kJ·mol^{-1}. This time again as for phenylalanine, the DFT calculations of entropic effects reduce this group to the set of twelve structures contributing to the IR spectrum isolated in the noble gases. The analysis of the spectral features allowed distinguishing two groups of conformers. The first group is characterized by the presence of O-H···N bonding, whereas the second - exhibits the N-H···O-H bond and the *cis* conformation of the carboxylic group.

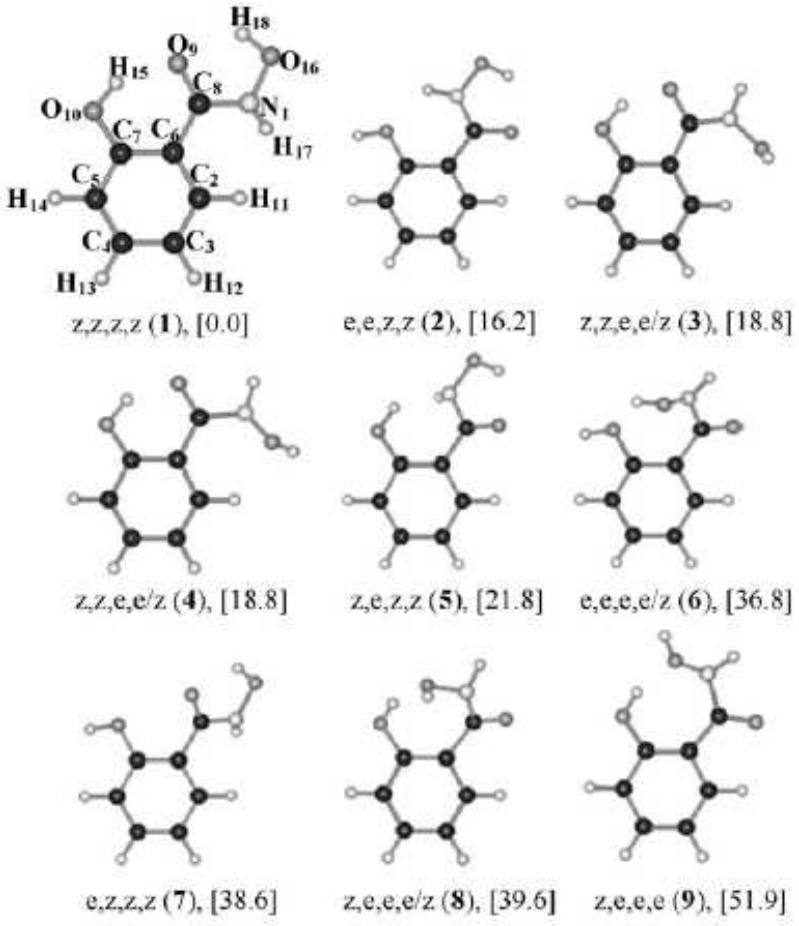

Fig. 1. The geometries of the optimized conformers of sha. The values in square brackets indicate the difference of energies relative to the most stable isomer [kJ/mol] [1].

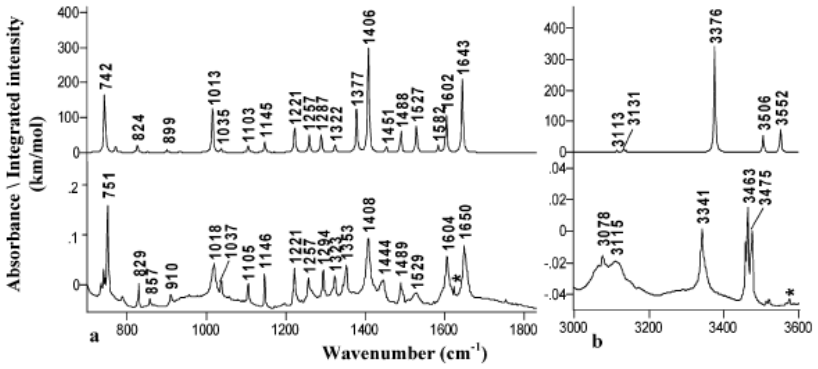

*Figure 2. The experimental (lower) and calculated (upper) spectra of sha in the range of 700-1850 cm^{-1} (a) and 3000-3600 cm-1 (b). Calculations are based on z,z,z,z-keto sha model. *Denotes water vibrations. [1]*

Intermolecular interactions – techniques for solutions and solids

It goes without saying that a successful model should reach beyond the determination of molecular structures at gaseous state. Therefore, both experimental and theoretical investigation of the behaviour of receptor molecules in aqueous solutions, at solid state or more importantly at solid-liquid interfaces is of a particular interest for the researchers. Indubitably, a local potential of a receptor molecule apparently determining its properties is a result of intermolecular interactions mentioned above.

From the experimental point of view, there are a great many techniques available that make possible looking into the changing environment of a reacting guest-host system. It seems that Raman spectroscopy is more useful for biological research or research in aqueous environments than infrared spectroscopy in which very broad bands at 1640 cm^{-1} and ~ 3200 cm^{-1} originating from water molecules bending vibrations eliminate fine the detail of the vibrational spectra. In practice, due to relatively low sensitivity of the signal in Raman spectroscopy the detections limit is for the concentration of solutionscan be set at 0.1 mol/dm^3 [3]. This, however, can be overcome with use of the surface enhanced Raman methods, which will be discussed in the next paragraph. The analyses of water solutions can also be performed in IR [15-

20] but in this case to obtain reliable signal from the solute the length of the pathway of the incident light going through the solution should be very small (of order of several micrometers). An alternative method of the signal enhancement is the application of the ATR multireflection unit [21]. Also, a deuterium exchange offers a reasonable tool for water solution surveys [21,22].

Currently the analysis of solid samples by infrared spectroscopy has slowly resigned from time-consuming sample preparation methods. What is accessible is the detection of reflection by various optical systems as shown in Figure 3, which is achieved by numerous commercially available devises for external total reflection, attenuated total reflection (ATR), diffused reflection (diffuse reflectance infrared Fourier transformed spectroscopy, DRIFT). [3] Except this, photoacustic spectroscopy (PAS) which not only enables the analyses of the samples fully absorbing radiation but also the depth profiling of the samples can be used in detection of infrared spectra [3].

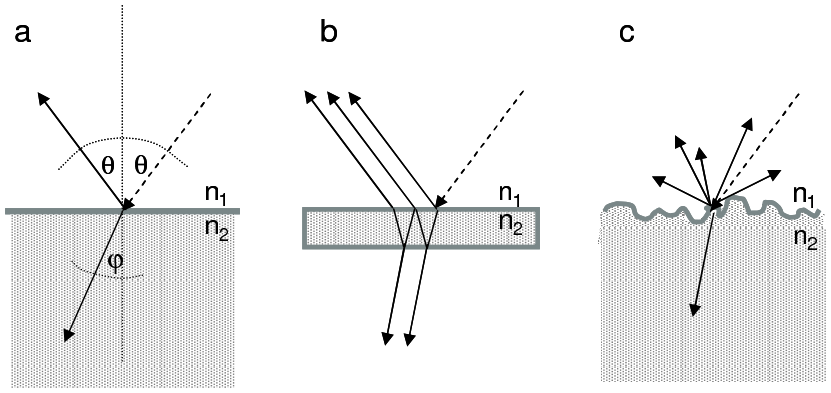

Figure 3. Reflection types for various surfach topology: a) external specular reflection, b) internal total reflection, c) odiffused reflection. Prameters n_1 and n_2 are refraction indexes for two phases.

In order to obtaine spectra with high lateral spatial resolution microscopic methods have been being developed and refined both for infrared and Raman systems.

A comparison between the performance of a classic Fourier transformed Raman spectrometer and a confocal micro-Raman spectrometer is presented in Table 1.

In an attempt to study the dynamics of the receptor systems, time resolved techniques (TRIR) seem of greatest importance. The methods utilise either step-scan devices which are the modification of classic interferometers [23] or laser pulses to observe fluctuation in the system studied [24] providing information on the fate of the excited state of a material. In the case of the step scan technique the time resolution reaches nanoseconds whilst with the help of pulsed lasers, it is possible to study processes, which occur on time scales as short as 10^{-14} seconds. Among other applications, the time resolved technique poses a powerful tool for investigating energy and charge transfer processes, vibrational and conformational relaxation, isomerisation, coupling of electronic and vibrational degrees of freedom, deformation and relaxation in organic fibers and matrices where changes in frequency and intensity can be related to molecular stress, chain orientation and conformational analysis. etc. [24].

Table 1. Comparison of a confocal micro-Raman spectrometer and Fourier transformed Raman spectrometer

	Confocal Raman microscope	FT-Raman
detection range	10- 9000 cm^{-1}	50-3650 cm^{-1}
Sources	UV/VIS/NIR lasers	mainly 1064 nm
Detectors	Si, CCD	Ge, InGaAs
detector sensitivity	high	low for InGaAs
analysis At elevated temperature	Even > 1000°C	< 250°C
analyses of water solutions	yes	difficult for 1064 nm laser
dark samples analysis	yes	emission
resolution	<1 □m	> 5 □m
Fluorescence	Low for 785, 830 nm lasers	low
Signal attenuation (785 nm/1064 nm)	3.5x	1x

In one of our works [25], we investigated *1H,4H*-1,2,4-triazolium cation (the unsubstituted triazolium cation, [TriazoliumH_2]$^+$) and its two derivatives: 1-benzyl-3,4-diphenyl-1,2,4-triazolium chlorate(VII) ([Triazolium(CH_2Ph)(Ph)$_2$]$^+$) and 1-(1-adamantyl)-3-phenyl-4-(4-bromophenyl)-1,2,4-triazolium chlorate(VII) ([Triazolium(BrPh)(Ph)(Ad)]$^+$) (Fig. 4).

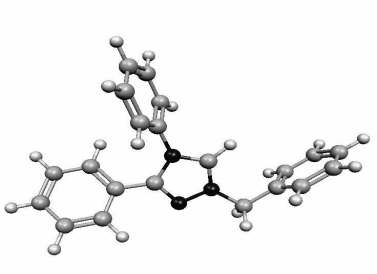

[Triazolium(CH_2Ph)(Ph)$_2$]$^+$

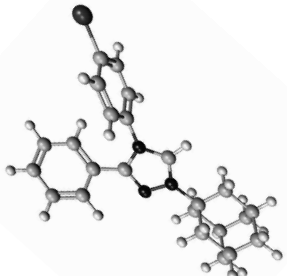

[Triazolium(BrPh)(Ph)(Ad)]$^+$

Figure 4. Structures of the triazolium derivatives.

The aim of this study was to distinguish the spectral features of the triazolium ring and its derivatives, and thus to represent the effect of the various substituents on the heterocyclic ring. In our calculations (B3LYP/6-31+g(d)), we neglected an effect of the anion [chlorate(VII) ion] on the structure of the triazolium cations studied. Thus, the cationic forms are molecular models. Even though these calculations pertain to the gas phase, optimal molecular geometries of the cations are in agreement with the crystal structures of the related compounds published. The geometrical parameters are in very good agreement with those presented previously. The average deviation does not exceed 2.1% and 1.7% for the bond lengths and angles, respectively. Obviously, such small discrepancies result only from the presence of very weak London forces

and of the bulky substituents preventing from the ionic interaction between the oppositely charged species.

A good agreement between theoretical and experimental spectra (rms less than 15 cm^{-1}) confirms the choice of the models (c.f. Fig. 5). Secondly, the detailed assignment of the experimental bands (Potential Energy Distribution of the normal modes) showed that the dominant bands in the spectra originate from the vibrations of the substituents, i.e. the phenyl and adamantyl groups. However, some of them are characteristic of the triazolium moiety and can serve as marker bands, especially, those attributed to stretching vibrations of the bonds of the N-heterocyclic ring.

A more complex problem was encountered in the modelling of vibrational spectra of alkanephosphonic acids. They constitute a class of the analogues of natural amino acids in which the peptide bond is formed between the carboxylic group of an amino acid and the amino group of the phosphonic moiety. Here, we present results obtained for the phosphonic derivatives of glycine (Fig. 6). Our studies focused on the evaluation of an appropriate theoretical model of these compounds for which calculations of IR and Raman spectra would give proper description of the experimental data. As the models for calculations, we took into consideration various rotamers predicted from calculations of potential energy structures with respect to the selected dihedral angles, structures with various deprotonation patterns and models with intra- as well as intermolecular H-bonding. Figure 5 illustrates an exemplary Potential Energy Surface computed by AM1 for one of the derivative with the following R: -CH_3; -CH_3 (G1). The previous studies on these compounds [26-29] have showed that the molecules exist in the zwiterionic form where the amino group is protonated whereas the phosphonic one loses one proton (c.f. Fig. 6). Unfortunately, the unconstrained optimization led to the proton transfer. This fact is not surprising because the non-ionic form is the most stable in gaseous state (black area on the PES). This observation is in agreement with previous findings for amino acids. Therefore, the next models contain the molecules with these dihedral angles that provide the zwitterionic form.

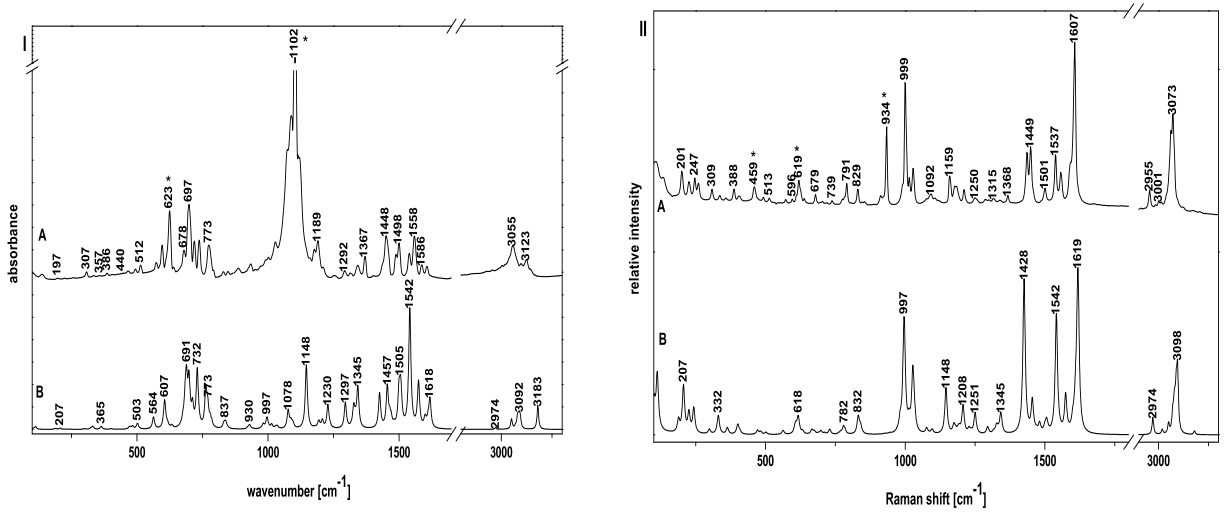

*Figure 5. IR (**I**) and Raman (**II**) spectra of [Triazolium(CH_2Ph)($Ph)_2$]$^+$: A. theoretical, B. experimental, (*denotes ClO_4^-).*

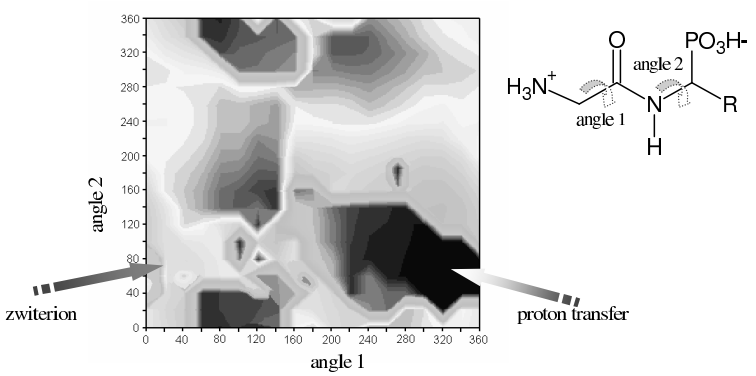

Figure 6. Exemplary PES analysis (AM1) for G1.

Crystallographic data [26-29] of the analogous compounds (glycine, phenyloalanine and leucine derivatives) reveal that this type of molecules are arranged in crystalline lattice as zwitterions surrounding by water molecules and forming complex H-bonding with the neighbouring phosphonic moieties (Fig. 7A). However, such a complex structure cannot be calculated using theoretical methods of high accuracy due to computation cost and limits. Hence, in order to simplify the system we "cut off" the dimeric structure to retain H-bonding and we inserted dihedral angles found in PES to create the zwiterionic form of the molecules present there. Unfortunately, the optimization process for this model is still highly time consuming and it has not yielded a satisfactory reproduction of the experimental spectra. Then, to mimic the water environment in solid state, which plays an important role in stabilization of these phosphonic derivatives, we calculated vibrational spectra by using PCM (Polarizable Continuum Model) for the zwitterions. This approach treats the solvent as a polarizable continuum and places the solute in a cavity within the solvent; in this case for water (ε=78.4). As shown below (Fig. 8), this simple approach brought about the best simulation of the experimental IR and Raman spectra.

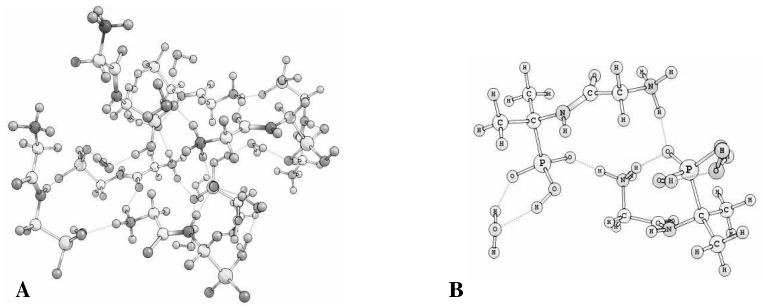

Figure 7. Crystalline arrangement of glycyl-aminomethylphosphonic acid monohydrate (A) [6] and the dimeric form of G1 (B).

Solid surfaces – SERS

With all its flexibility conventional Raman spectroscopy suffers from low signal intensity, compared with fluorescence. Thus, it is not capable to identify minor components of mixtures, which is a frequent requirement in life sciences. To overcome two of the present limitations of the conventional Raman microspectroscopy: spatial resolution and sensitivity, the new technique of Surface Enhanced Raman Scattering (SERS) has been designed and refined. The spatial resolution of Raman microscopy (1 mm) has been increased with confocal optics to the range 1 m which has been shown in the previous paragraph and of near-field approach (Near-Field Scanning Optical Microscopy, NSOM) even to nanometer range. Both resolution and sensitivity are much enhanced by applying the concept of Surface Enhanced Raman scattering. Results dating back over 20 years show that the Raman signal can be enhanced when small metal particles are located in close proximity to molecules being examined. The

enhancement has been shown to be as much as 8 orders of magnitude on Cu, Ag and Au surfaces. Also, a lot of authors have since demonstrated the feasibility of single molecule detection [30].

In the studies of biosensors the utility of the SERS is related to its extreme sensitivity and from the fact that it can operate in an intermittent contact mode with liquid specimens, biological materials in their physiological media can be examined. The SERS measurements can be carried out in a conventional Raman system such as Renishaw Raman microscope, but also using the near-field system based on an atomic force microscope (AFM) controller with a cantilevered fiber optics probe. The substrate for the analyzed molecules can be nanoparticles of the metals mentioned above in colloidal solutions, electrodes or prepared surface nanostructures (metals surfaces coated with polymers or opposite) [30]. Also, the SERS operation can be implemented by the use of a special gold nanoparticle, which is attached to the fiber probe and scanned over the specimen surface. In addition to SERS the NSOM system can be used for the near field spectroscopy and imaging simultaneously with the AFM mapping. Thus, chemical variations in a specimen across an area in the order of 1 □m can be detected with greatly enhanced sensitivity (10^4 enhancement over and above that of the corresponding Raman microscope) and spatial resolution in the order of tens of nanometers.

An interesting application of SERS is the use of immobilized monolayers of bioreceptors (oligonucleotides or antibodies) in medical diagnostics [31,32]. An alluring idea is also implementation of biomolecules, which show SER properties for marking a DNA sequence. Another one is colloidal gold particles anchored with antibodies to detect antigens in solutions.

The theory beyond the observed signal enhancement by SERS is not well established yet [33]. The amplification effect is said to have at least two origins: the first physical connected with the resonance of surface plasmons and the second - chemical coming from increased polarisability of the chemisorbed molecular system on the probe surface.

Herein we present some methods of modelling of SER spectra mostly because it has received considerable attention in the chemical and biomedical fields. For

understanding the action of biochips on receptors, a metal surface may serve as an analogue for the biological interface. Even though the enhancement phenomenon of the Raman signal on the rough metal layer is widely known, its unambiguous physical explanation has not been yet proposed. Therefore, no theoretical description of SER intensities has been given so far. However, some computation studies have been carried out in order to elucidate behaviour of biomolecules at the metal interface [34-38].

The simplest method supporting explanation of SER spectra are just the calculation of normal modes with their potential energy distribution at high level of theory (DFT, *ab initio*). It allows performing the clear-cut assignment of the normal Raman bands, and then on the basis of the comparative studies on the ordinary Raman spectrum and the SERS spectrum, the models of binding orientation are suggested [34-36]. The most sophisticated models include interaction between metal atom or metal cluster (for silver colloid only) and investigated molecules [37,38]. Generally, this type of modelling is carried out after inspection of a molecular structure. The presence of some atoms or groups may suggest binding sites to the silver surface, for example the lone pair electrons of nitrogen, oxygen or sulphur atoms, or the π-electron system of aromatic rings. To determine, from the theoretical point of view, the most probable interaction possibility, DFT calculations (energy, charges, and normal modes) are performed on model compounds including a silver atom attached to these sites. The computed energy value may suggest stability of geometries and those, which are the least stable, are theoretically excluded. Additionally, calculations of the PES for the binding atom–metal bond length provide information on the most favourable energetically distance between these atoms. Furthermore, the comparison of the total atomic charges of oxygen, nitrogen, and sulphur atoms may also indicate the surface enhancement mechanism by considering the fact that an increased negative charge on an atom rises its adsorptive ability. It should be mentioned as well that in the case of aromatic rings two configurations are optional: first with the metal atom below the ring plane and second one with the atom above this plane. In this way, taking into account the predictions of calculations carried out on different SERS complexes and

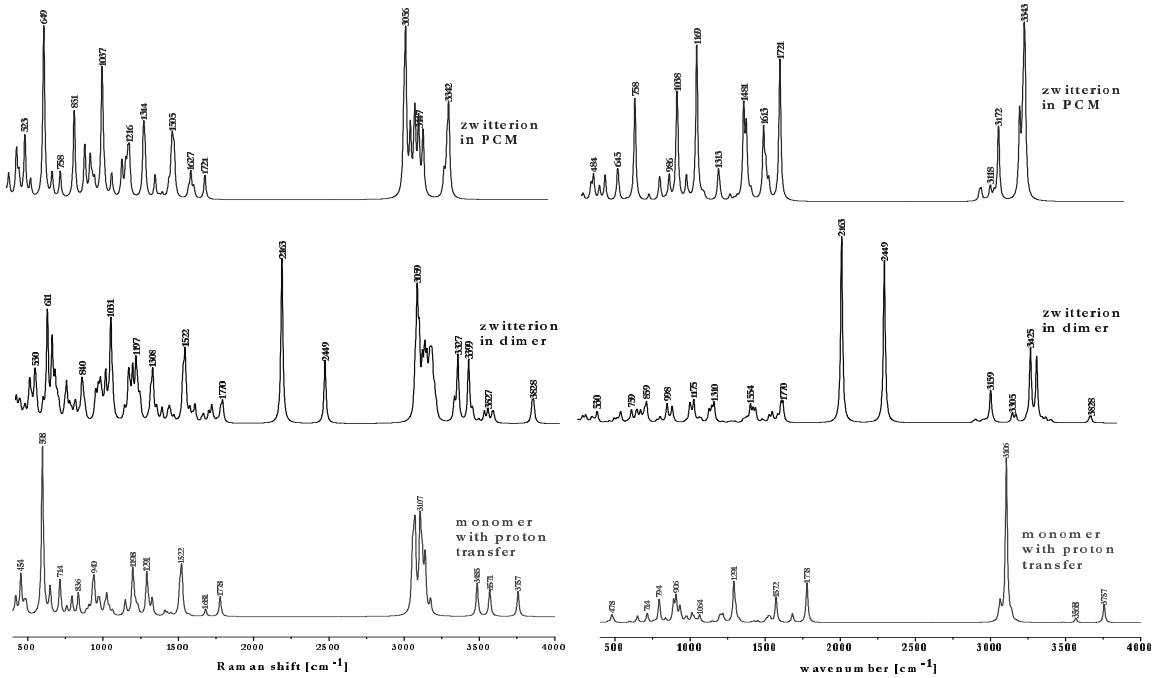

Figure 8. Comparison of experimental and theoretical [B3LYP/6-31+G(d)] spectra of various models of G1.

from the comparison of the corresponding SERS and Raman bands, it can be concluded how molecules are adsorbed on the metal particles.

Acknowledgements

The authors thanks the Polish Ministry of Science and Higher Education for financial support under Grants No. R015 016 01 in the years 2006–2008.

References :

1. D.A. Long, Raman Spectroscopy, McGraw-Hill Intls. Book Co., New York 1977;
2. J.J. Laserna, Modern Techniques in Raman Spectroscopy, John Wiley & Sons Inc., Chichester 1996;
3. M. Chalmers, P.R. Griffiths: Handbook of Vibrational Spectroscopy, John Wiley & Sons Inc., Chichester 2002 vol. 1;
4. D.J. Gardiner, P.R. Graves, Practical Raman Spectroscopy, Springer-Verlag, Berlin 1989;
5. G. Turrell, J. Corset (red.) Raman Microscopy. Developments and Applications, Harcourt Brace and Co., London 1999;
6. E. Smith, G. Dent, Modern Raman Spectroscopy – A Practical Approach, John Wiley & Sons Inc., Chichester 2005;
7. D.A. Long, Raman Spectroscopy, McGraw-Hill Intls. Book Co., New York 1977;
8. J.J. Laserna, Modern Techniques in Raman Spectroscopy, John Wiley & Sons Inc., Chichester 1996;
9. Z. Kęcki, Podstawy spektroskopii molekularnej, PWN, Warszawa 1992;
10. P. Klaeobe, C.J. Nielsen, Analyst, 117 (1992) 335-340;

11. S.P. Wilson, L. Andrews, in M. Chalmers, P.R. Griffiths: Handbook of Vibrational Spectroscopy, John Wiley & Sons Inc., 2002 vol. 32, p. 1342-1351;

12. A. Kaczor, J. Szczepanski, M. Vala, L.M. Proniewicz, Phys. Chem. Chem. Phys., 7 (2005) 1960-1965;

13. A. Kaczor, I.D. Reva, L.M. Proniewicz, R. Fausto, J. Phys. Chem. A, 110 (2006) 2360-2370;

14. A. Kaczor, I.D. Reva, L.M. Proniewicz, R. Fausto, J. Phys. Chem. A, 111 (2007) 2957-2965;

15. M. Lafleur, M. Pigeon, M. Pczolet, J.P. Caill, Raman Spectrum of Water in Biological Systems, J. Phys. Chem. 93 (1989) 1522-1526;

16. M. Purcell, J.F. Neault, H. Malonga, H. Arakawa, R. Carpentier, H.A. Tajmir-Riahi, Biochimica et Biophysica Acta 1548 (2001) 129-138;

17. J. Ramesh a, J. Kapelushnik b, J. Mordehai c, A. Moser b, M. Huleihel d, V. Erukhimovitch, C. Levi a, S. Mordechai, J. Biochem. Biophys. Methods 51 (2002) 251–261;

18. F. Geinguenauda, J.A. Mondragon-Sancheza, J. Liquiera, A.K. Shchyolkinab, R. Klementc, D.J. Arndt-Jovinc, T.M. Jovinc, E. Taillandiera, Spectrochimica Acta Part A 61 (2005) 579–587;

19. Hiromi Kitano, Kohei Takaha, Makoto Gemmei-Ide, Journal of Colloid and Interface Science 283 (2005) 452–458;

20. R. Pouliot, A. Saint-Laurent, C. Chypre, R. Audet, I. Vitte´-Mony, R.C. - Gaudreault, M. Auger, Biochimica et Biophysica Acta 1564 (2002) 317– 324.

21. H. Fabian, Infrared Spectroscopy of Proteins, in M. Chalmers, P.R. Griffiths: Handbook of Vibrational Spectroscopy, John Wiley & Sons Inc., 2002 vol. 5, p. 3399-3426;

22. J. Łojewska, P. Miśkowiec, T. Łojewski, L.M. Proniewicz, , Polym. Deg. Stab., 88 (2005) 512-520;

23. C.J. Manning, Instrumentation for Step-scan FTIR Modulation Spectrometry, in M. Chalmers, P.R. Griffiths: Handbook of Vibrational Spectroscopy, John Wiley & Sons Inc., 2002 vol. 1, p. 283-298;

24. G.D. Smith, R.A. Palmer, Fast Time Resolved Mid-infrared Spectroscopy, in M. Chalmers, P.R. Griffiths: Handbook of Vibrational Spectroscopy, John Wiley & Sons Inc., 2002 vol. 1, p. 625-64;

25. K. Malek, G. Schroeder, L.M. Proniewicz, Vib. Spectr., 44 (2007) 19-29;

26. W. Wang, W. Zheng, X. Pu, N-B. Wong, A. Tian, J. Mol. Struct., 618 (2002) 235-244;

27. M. Cotrait, J. Avignon, J. Pugant, C. Garrigou-Lagrange, J. Mol. Struct., 32 (1976) 45-65;

28. N.M. Blaton, O.M. Peeters, C.J. De Ranter, Acta Crystallogr., Sect. C: Cryst. Struct. Commun., 53 (1997) 1952-1954;

29. P. Hermann, I. Lukeš, P. Vojtíšek, I. Císařová, J. Chem. Soc., Dalton Trans., (1995) 2611-2618;

30. W. Ewen Smith, C. Rodger, Surface Enhanced Raman Scattering, in M. Chalmers, P.R. Griffiths: Handbook of Vibrational Spectroscopy, John Wiley & Sons Inc., 2002 vol. 1, p. 775-785;

31. M. Moskovits, Surface-Enhance Raman spectroscopy: a brief retrospective, J. Raman. Spec., 2005, 36, 485-496;

32. Tuan Vo-Dinh, D.L. Stokes, SERS-based Probes, in M. Chalmers, P.R. Griffiths: Handbook of Vibrational Spectroscopy, John Wiley & Sons Inc., 2002 vol. 2, p. 1303-1342;

33. A. Campion, P. Kambhampati, Surface-enhanced Raman scattering, Chem. Society Rev. 27 (1998) 241-251;

34. B. Giese, D. McNaughton, J. Phys. Chem. B, 106 (2002) 101-112;

35. N. Biswas, S. Kapoor, H.S. Mahal, T. Mukherjee, Chem. Phys. Lett., 444 (2007) 338-345;

36. H.F. Yang, J. Zhu, C. Sheng, X.J. Sun, J.H. Ji, X.L. Ma, J. Raman. Spectr., 38 (2007) 890-895;

37. M. Baia, L. Baia, W. Kiefer, J. Popp, J. Phys. Chem. B, 108 (2004) 17491-17497;

38. M. Muniz-Miranda, G. Cardini, M. Pagliai, V. Schettino, Chem. Phys. Lett., 436 (2007) 179-183.

Видавниче підприємство „Східний видавничий дім”
(Державне свідоцтво № ДК 697 від 30.11. 2001)
Вул. Артема 45, 83086 м. Донецьк, Україна
тел/факс (+380 62) 338-06-97, 337-04-80

Publishing house „Schidnyj wydawnyczyj dim”

ISBN 978-966-317-013-8